

THE EVOLUTION OF POLYCYCLIC AROMATIC HYDROCARBONS
DURING THE PYROLYSIS OF COAL

A Thesis

submitted in partial fulfilment of the
requirements of the degree of

DOCTOR OF PHILOSOPHY

Under the supervision of

Professor Adel F. Sarofim
Department of Chemical Engineering
Massachusetts Institute of Technology
Cambridge, MA., U.S.A.

BY

Amitava Mitra

BIRLA INSTITUTE OF TECHNOLOGY AND SCIENCE
PILANI, INDIA

November, 1984

BIRLA INSTITUTE OF TECHNOLOGY AND SCIENCE
PILANI, INDIA

CERTIFICATE

This is to certify that the thesis entitled "The Evolution of Polycyclic Aromatic Hydrocarbons During the Pyrolysis of Coal" and submitted by Amitava Mitra, ID No. 77S83001 for award of Ph.D. degree of the Institute, embodies original work done by him under my supervision.

Signature in full
of the Supervisor

Name in Capital
block letters

ADEL F. SAROFIM

Date:

Designation

Professor of Chemical
Engineering,
M.I.T.,
Cambridge, MA
U.S.A.

To my
father and mother

ABSTRACT

Polycyclic aromatic hydrocarbons (PAH) are mutagenic and carcinogenic. With the anticipated increase in the use of low-grade fuels such as coal, PAH emissions into the environment are expected to increase, thus aggravating health hazards.

Data was obtained on the evolution of PAH during the pyrolysis of coal in a laminar flow, drop tube furnace. Five coals of different ranks were selected for study, namely, a lignite, a sub-bituminous, a high volatile-A bituminous, a medium volatile bituminous and an anthracite.

Well-defined coal particles (44 to 53 μm , wet-sieved) were heated at rates of about $10,000^{\circ}\text{C/s}$ to peak temperatures ranging from 900K to 1700K. Samples were held at these peak temperatures for times ranging from 75 to 300 ms. Pyrolysis products were analysed for PAH by capillary column gas chromatography and gas chromatography-mass spectrometry. Bioactivities were measured in Salmonella typhimurium so as to determine the mutagenic potential of the PAH evolved and cross-check the trends observed from chemical analysis.

Pyrolysis results indicate that PAH yields peak at about 1300K, regardless of the type of coal being pyrolysed. Specific mutagenicity also peaks in the temperature range of 1300K to 1500K. Soot yields increase with temperature, generally levelling out at temperatures greater than 1300K.

Variations of PAH yield with residence time of the coal particles, appear to follow a first-order type of global behaviour. The peak in PAH evolution shifts to lower residence times as the pyrolysis temperature is increased. Similar trends are observed

for specific mutagenicity as a function of residence time. However, soot yields increase with residence time, levelling out at values greater than 225 ms.

It is observed in literature that PAH and soot evolution increases with the aromaticity of the parent fuel. For the case of coal pyrolysis however, though PAH and soot yields increase with coal rank, they reach a peak for the high volatile bituminous coal (85.71% carbon, dmmf) and decrease as the aromatic carbon fraction in the coal is further increased. PAH yields in decreasing order are as follows: high volatile bituminous > medium volatile bituminous > subbituminous > lignite > anthracite. Specific mutagenicity values show the following order with respect to coal type: high volatile bituminous > medium volatile bituminous > lignite > subbituminous > anthracite. However, the PAH evolved from coals of different ranks are very similar in terms of the number of aromatic rings and types of alkyl substituents. Direct acting mutagens are evolved from all the coals studied. However, those evolved from the low-rank coals exhibit mutagenic activities greater than that shown by the activated form of the mutagen.

A comparison between PAH yields observed during pyrolysis and PAH emissions from field units as reported in literature was also made. This comparison reiterates the approach that pyrolytic conditions are the "worst-case" situation for prediction of the degree of pollution.

ACKNOWLEDGEMENTS

I am grateful to Professor Adel F. Sarofim for his continuous guidance, support and encouragement and for his faith in my abilities. He has been very patient, has given generously of his time and has opened up new vistas for me.

Professors J.B. Howard, J.M. Beer, J.P. Longwell and J.E. Vivian were a regular source of help and advice.

The encouragement and friendship that was offered me by Professor Ashwani Gupta, Dr. Simon Hanson and Dr. Ezra Bar-Ziv and the extensive discussions with them were very fruitful.

I had the good fortune to interact with the following people and in the process learned a good deal about chemical analysis, bioassay techniques and how to make things work: Gilles Prado, Kin-Chiu, Dr. Andy Braun, Barbara Andon, Maged Toqan, Ed Kruzel, Charlie Foshey, Al and the ChE Machine Shop.

I would like to thank Regina Nenniger for allowing me to use her equipment and Tony Modestino for his invaluable help in the downstairs lab.

I am grateful to the Director, B.I.T.S. and to the Dean, R & C Division BITS for granting me permission to conduct my thesis work at M.I.T. under the BITS-MIT linkage.

I also thank Dr. J. Wei, Head, Department of Chemical Engineering, M.I.T. for giving me permission to use all the facilities at M.I.T.

My aunt, Dr. Rita Mitra's help and support were a boon, as were that from Anuradha Mitra-Ghemawat.

The swift, efficient and cheerful typing job by Messrs G.R. Bhomia, H.S. Kulhari, D.R. Sonar, V.S. Srivastava and Sardara Ram Saini kept me on my toes and the production humming. Mr. K.N. Sharma's neat and quick hand churned out drawings as it raced with the typing, while Mr. H.C. Pant and his team of reprographers quickly converted them to photocopies. Mr. Ram Niwas and Mr. Dhura Ram were invaluable during the compiling and collating work. Shambhudassji's sagacious and thoughtful marshalling of the production forces kept me to my deadline.

The PSOC Bank supplied the coals used, together with elemental analysis and other details. The financial support provided by the N.C.E.R.T., India for the first two years and thereafter by the N.I.E.H.S., U.S.A. (under contract # NIEHS 5 P30 ESO2109) is gratefully acknowledged.

To my friends in Cambridge, Pilani and elsewhere — Shambhudassji, Vijuda, Reji, Harriet, Dipanjan "Noname" Dey, Ezra, Maged, Dr. V.K. Tewary, Simon, Ashwani, Maria, Wolfgang, Parimal didi, Toy, Poonam, Anjan, Gil, Daisy, Roberta, Mr. H.C. Mehta — Thanks very much for everything.

My mother, Dr. Sandhya Mitra and my father, Dr. Chitta Ranjan Mitra have been my best friends and critics through this odyssey. They have put up with a lot but have had an unshakable faith in me, something which has given me a deep confidence. From my father I have realised the virtues of planning and organising and how to put things together. Thank you, and here's another "Doc" in the family !

TABLE OF CONTENTS

	<u>Page</u>
Certificate	2
Abstract	4
Acknowledgements	6
List of Figures	10
List of Tables	15
Nomenclature	16
Chapter 1 <u>INTRODUCTION</u>	18
Chapter 2 <u>COAL STRUCTURE AND PYROLYSIS</u>	22
2.1 The Origin of Coal	24
2.2 Structural Parameters for Coal	26
2.3 Models of Coal Structure	33
2.4 Simple Kinetic Models of Coal Pyrolysis	44
Chapter 3 <u>EVOLUTION OF PAH</u>	52
3.1 Mechanisms of Formation of PAH	52
3.2 PAH-soot Interactions	66
3.3 The Influence of Fuel Type	85
Chapter 4 <u>EFFECT OF COMBUSTION CONDITIONS ON THE YIELD OF PAH</u>	96
4.1 Effect of Temperature	96
4.2 Effect of Pressure	101
4.3 Effect of Oxidiser Concentrations	103
4.4 Effect of Mixing	108
4.5 Effect of Residence Time	110

Chapter	5	<u>EXPERIMENTAL SETUP AND PROCEDURES</u>	118
	5.1	Introduction	118
	5.2	Experimental Setup	120
	5.2.1	Pyrolysis Furnace System	120
	5.2.2	Sample Collection Train	124
	5.3	Experimental Procedures	129
	5.3.1	Coal Preparation	130
	5.3.2	Pretreatment of Sampling Equipment	130
	5.3.3	Furnace Operation	132
	5.3.4	Sample Processing	134
	5.3.5	Sample Analysis	135
	5.3.6	Mutagenic Assays	136
Chapter	6	<u>RESULTS AND DISCUSSION</u>	140
	6.1	Effect of Pyrolysis Conditions	140
	6.2	Effect of Coal Type	152
	6.3	Mutagenic Activity	170
	6.4	Comparison with Field Studies	189
Chapter	7	<u>CONCLUSIONS AND RECOMMENDATIONS</u>	195
Appendix	A	CHEMICAL STRUCTURES OF PAH IDENTIFIED FROM COAL PYROLYSIS	199
Appendix	B	AN ASSESSMENT OF ENVIRONMENTAL SOURCES OF PAH	209
References			218

LIST OF FIGURES

<u>Figure No.</u>		<u>Page</u>
1.1	Smoke formation in a JT8D combustor	20
2.1	A schematic representation of packing of locally flat regions of the buckled layers	29
2.2	Aromaticity versus coal rank	29
2.3	Model structure for coal (Fuchs and Sandhoff, 1942)	34
2.4	Model structure for coal (Given, 1960)	35
2.5	Model structure for coal (Hill and Lyon, 1962)	37
2.6	Model structure for coal (Mazumdar, 1962)	38
2.7	Model structure for coal (Van Krevelen, 1963)	39
2.8	Model structure for coal (Wender, 1975)	41
2.9	Model structure for coal (Wiser, 1975)	42
2.10	Model structure for coal (Heredy and Wender, 1979)	43
2.11	Model structure for coal (Solomon, 1984)	45
2.12	Cracking of hypothetical coal structure during pyrolysis	49
2.13	Schematic of coal pyrolysis	51
3.1	Formation of PAH during pyrolysis	55
3.2	Reaction scheme for the formation of PAH in rich premixed flames	55
3.3	Free radical addition scheme for PAH formation	62
3.4	Relative signal intensities versus distance from burner	62

<u>Figure No.</u>		<u>Page</u>
3.5	Pathways for soot formation	69
3.6	PAH and soot fluxes in a premixed C_2H_2/O_2 flat flame	69
3.7	PAH, soot, carbonaceous residue and chloroform soluble material in a $C_2H_4/O_2/N_2$ diffusion flame	71
3.8	Carbon black and tar yields during the thermal decomposition of benzene	71
3.9	PAH and soot yields from an atmospheric pressure premixed CH_4/O_2 flame	73
3.10	PAH and soot yields in turbulent kerosene and benzene diffusion flames	73
3.11	PAH and soot production in a 1MW unstaged turbulent combustor burning SRC-II	75
3.12	Pyrolysis of n-tetradecane: PAH and soot evolution	75
3.13	Growth of soot aggregates with ionic species as nucleating agents	77
3.14	Effect of the number of carbon atoms in hydrocarbon fuels on their sooting tendencies	77
3.15	Effect of H/C ratio on soot production in a turbulent diffusion flame	93
3.16	Threshold sooting index versus number of carbon atoms in alkene, alkane and aromatic fuels	93
3.17	Threshold sooting index versus C/H ratio - premixed flames	95
3.18	Comparison of sooting indices for diffusion and premixed flames	95
4.1	Temperature profile in a C_2H_2/O_2 flat flame	97
4.2	Mole fractions of naphthalene, indene and styrene from acetylene pyrolysis	97
4.3	The fractional conversion of aromatic species to soot in a shock tube	102

<u>Figure No.</u>		<u>Page</u>
4.4	PAH flux at different O_2/C_2H_2 ratios	102
4.5	Effect of mixing on PAH yields in a turbulent kerosene diffusion flame	109
4.6	Effect of mixing on soot yields in a turbulent kerosene diffusion flame	109
4.7	Soot yields in well-stirred reactors	111
4.8	PAH yields from an $n-C_7H_{16}/O_2/N_2$ flame in a vertical flow reactor	111
4.9	PAH and perinaphthenyl radical (PN) concentrations in a vertical flow reactor	113
4.10	PAH concentrations in a vertical flow reactor	113
4.11	Ratios of two-seven ring PAH to pyrene in premixed CH_4/O_2 flames	115
4.12	PAH and soot yields in a CH_4/O_2 flat flame	115
4.13	Yields of three-seven ring PAH in an atmospheric pressure, premixed CH_4/O_2 flat flame	116
4.14	Pyrolytic conversion of benzene to diphenyl	116
4.15	Growth of soot in flat flames	117
4.16	Concentration profiles of soot, ions and precursors in premixed flames	117
5.1	Schematic of laminar flow pyrolysis furnace system	123
5.2	Fluidized coal feeder	125
5.3	Collection probe schematic	127
5.4	Particulate collection system for pyrolysis furnace	128
6.1	Pyrolysis of hvAb coal (900K)	141
6.2	Pyrolysis of hvAb coal (1100K)	142
6.3	Pyrolysis of hvAb coal (1300K)	143

Figure No. Page

6.4	Pyrolysis of hvAb coal (1500K)	144
6.5	Pyrolysis of hvAb coal (1700K)	145
6.6	Pyrolysis of lignite coal (300 ms)	147
6.7	Pyrolysis of sub-bituminous coal (300 ms)	148
6.8	Pyrolysis of medium volatile bituminous coal (300 ms)	149
6.9	Pyrolysis of high volatile bituminous coal (300 ms)	150
6.10	Pyrolysis of anthracite coal (300 ms)	151
6.11	Variation of \bar{N} with rank	154
6.12	Ring condensation index versus rank	156
6.13	Variation of aliphatic and phenolic hydrogen with rank	157
6.14	Hydroaromatic hydrogen content versus rank	159
6.15	Methylene hydrogen content versus rank	160
6.16	Methyl hydrogen content versus rank	160
6.17	Hydroxyl oxygen content versus rank	161
6.18	Carboxylic oxygen content versus rank	161
6.19	PAH yields versus rank (300 ms)	165
6.20	Soot yields versus rank (300 ms)	166
6.21	GC spectra: coal pyrolysis at 1100K, 300 ms	168
6.22	PAH mutagenicity per mg tar for Montana lignite coal	176
6.23	PAH mutagenicity per mg tar for Montana Rosebud subbituminous coal	177
6.24	PAH mutagenicity per mg tar for Pittsburgh high volatile-A bituminous coal	178
6.25	PAH mutagenicity per mg tar for Pocahontas medium volatile bituminous coal	179

<u>Figure No.</u>		<u>Page</u>
6.26	PAH mutagenicity per mg tar for Primrose anthracite coal	180
6.27	PAH mutagenicity per g coal for Montana lignite coal	181
6.28	PAH mutagenicity per g coal for Montana Rosebud subbituminous coal	182
6.29	PAH mutagenicity per g coal for Pittsburgh high volatile-A bituminous coal	183
6.30	PAH mutagenicity per g coal for Pocahontas medium volatile bituminous coal	184
6.31	PAH mutagenicity per g coal for Primrose anthracite coal	185
6.32	Molecular weight distribution of PAH in the gas phase and deposited on soot	190
6.33	Stratification of PAH deposited on soot and in the gas phase	191
7.1	Schematic diagram of PAH emission during the series of processes in coal combustion	197

LIST OF TABLES

<u>Table No.</u>		<u>Page</u>
2.1	Average yields of Fischer assay of various coals	23
3.1	Thermally "Reactive" PNA	80
3.2	Thermally "Unreactive" PNA	81
5.1	Characterization of the coals studied	121
5.2	Polycyclic aromatic hydrocarbons identified from coal pyrolysis	137
6.1	Structural parameters for coals studied	162
6.2	Polycyclic aromatic hydrocarbons evolved (mg/g coal) during coal pyrolysis at 1250K, 300 ms	167
6.3	Mutagenicity of polycyclic aromatic hydrocarbons evolved during the pyrolysis of Montana lignite coal (1250K)	171
6.4	Mutagenicity of polycyclic aromatic hydrocarbons evolved during the pyrolysis of Montana lignite coal (1500K)	172
6.5	Mutagenicity of polycyclic aromatic hydrocarbons evolved during the pyrolysis of Primrose anthracite coal (1250K)	174
6.6	Comparison of PNA evolved during the pyrolysis of Montana lignite and Pittsburgh high volatile-A bituminous coals with that emitted by various sources	193
6.7	Comparison of PNA evolved during the pyrolysis of some liquid fuels with that emitted by field sources	194
B.1	Emission factors for benzo(a) pyrene and total PAH emitted by a variety of environmental sources in U.S.A.	210
B.2	Estimates of annual POM emissions by source type	213

NOMENCLATURE

an	anthracite coal
amu	atomic mass unit
BaP	benzo (a) pyrene
BeP	benzo (e) pyrene
d	diameter
daf	dry ash free
dmmf	dry mineral matter free
EPA	Environmental Protection Agency
ESR	electron spin resonance spectroscopy
ϕ	fuel equivalence ratio
	$= \frac{(\text{fuel/air})_{\text{actual}}}{(\text{fuel/air})_{\text{stoichiometric}}}$
f_a	aromaticity
F_r	free valence at atom 'r' in an aromatic structure
FTIR	Fourier transform infra-red spectroscopy
hvb	high volatile bituminous coal
hvAb	high volatile-A bituminous coal
I.D.	internal diameter
I.P.	ionization potential
IR	infra-red spectroscopy
J	Joule
lig	lignite coal
lvb	low volatile bituminous coal
mvb	medium volatile bituminous coal
ma_{coal}	PAH mutagenicity per g coal
ma_{tar}	PAH mutagenicity per mg tar

M.A.	methyl affinity
Me	methyl
M.L.	Montana lignite coal
MM	mineral matter
M.R.	Montana Rosebud coal
NMR	nuclear magnetic resonance spectroscopy
Ph	phenyl
PAH	polycyclic aromatic hydrocarbon(s)
N-PAH	nitrogen containing polycyclic aromatic hydrocarbon(s)
S-PAH	sulphur containing polycyclic aromatic hydrocarbon(s)
PNA	polynuclear aromatic hydrocarbon(s)
POM	polycyclic organic matter
PMR	proton magnetic resonance spectroscopy
PMS	post mitochondrial supernatant
RCI	ring condensation index
Sm	standard metre
SRC-II	solvent refined coal
Sub-b	sub bituminous coal
τ	residence time
TSI	threshold sooting index
TSP	total suspended particulates
$\mu\text{g}/\text{bb1}$	micrograms per barrel
μm	micron
UV	ultra violet spectroscopy
VM	volatile matter
XAD-2	styrene-divinyl benzene copolymer
XRD	X-ray diffraction spectroscopy
z,Z	height above burner surface

CHAPTER 1
INTRODUCTION

Polycyclic aromatic hydrocarbons (PAH) and soot are found throughout the environment and are formed as a result of incomplete combustion of organic materials. There is considerable evidence that PAH induce mutations in bacterial systems and are carcinogenic to experimental animals. Epidemiological observations suggest that they have similar effects in humans (Skopek et al, 1979).

PAH in the environment are usually associated with combustion generated soot and flyash, which act as carriers for their transport (NAS, 1972). Particulate collection strategies for these particles in the respirable size range of 0.1 to 5 μm are especially difficult, due to their small diameters. Furthermore, techniques for reducing emissions of pollutants like NO_x , such as staged combustion incorporating a fuel-rich step, often result in increased emissions of PAH and soot.

There is a large data base on the evolution of PAH and soot in relatively simple flames of vapourizable fuels such as methane, benzene, toluene etc. However, there has not been much systematic study on the pattern of PAH evolution during the combustion of industrial fuels such as coal, partly because of difficulties in clearly defining coal structure and also in product analysis.

Nevertheless, there has always been a historical awareness that coal combustion results in emission of species

which are detrimental to health. This resulted in proclamations banning the use of coal as early as 1306 (Evelyn, 1661; Lodge, 1969). By the eighteenth century, Pott (1775) recognised a relationship between cancer of the scrotum and occupational exposure by chimney sweeps to coal-generated soot and related chemicals.

With the dwindling of petroleum resources, a shift to coal and coal-derived fuels is strongly indicated. This would further aggravate environmental problems, since coal is expected to evolve greater quantities of PAH and soot than conventional petroleum-derived fuels. This is illustrated in Figure 1.1 .

It is well-known that in developing countries and non-industrial societies, the burning of coal for cooking and heating purposes is the single most important source of smoke and other pollutants. In industrialised nations, a substantial amount of coal is still burned inefficiently in utility boilers and home heating units. In the future, operations involving coal-based combustors, coal liquefaction and gasification and coal-oil slurries are expected to become increasingly important. It would be desirable to minimise the evolution of PAH and soot during these coal processing and handling operations. It is in this context that it would be useful to have a data base on the evolution of PAH and soot during pyrolysis.

From the point of view of formation of PAH, the primary variables of interest are pyrolysis temperature and fuel residence time. It has been established that even small

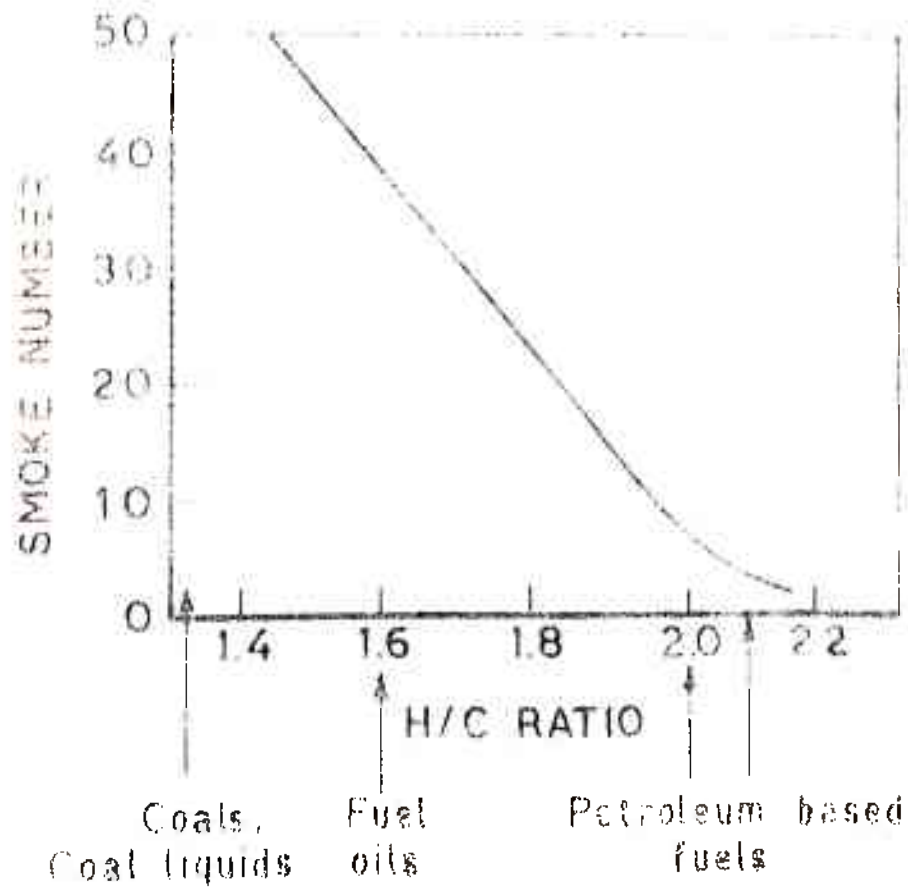


FIGURE 1.1 SMOKE FORMATION IN A JTBD COMBUSTOR

concentrations of oxygen in the combustor atmosphere drastically reduce PAH yields. Similarly, backmixing or turbulent flow conditions are also expected to decrease PAH formation. Thus it was decided to select pyrolytic, laminar flow conditions, to simulate "worst-case" situations, where PAH yields are expected to be maximised. Pressure variations have not been considered as they are not expected to significantly influence the evolution of PAH. It was also decided to observe the effect of these primary variables on the evolution of PAH from different grades of coals.

PAH evolved were analysed by capillary column gas chromatography, confirmatory analysis being performed by gas chromatography-mass spectrometry. Bioassays were performed on the PAH evolved, not only to obtain data on their mutagenic activity, but to also serve as an independent check of the chemical analysis.

Before describing the experimental setup and discussing the results, it would be informative to set the background by examining the state-of-the-art in literature, specifically with reference to current thinking on coal structure, mechanisms of formation of PAH in flames and the effect of combustion conditions. These are presented in the next three chapters.

TABLE 2.1

Average yields of Fischer Assay of various coals
(as-received basis: maximum temperature, 500 C.)

Rank of coal*	Coke, %		Tar, gal/ton		Light oil, gal/ton		Gas, cuft/ton		Water, %	
	Average		Average		Average		Average		Average	
Sa	-		0.7		0.03		-		-	
Lvb	89.7		8.6		1.02		1,760		3.2	
Mvb	83.3		18.9		1.67		1,940		4.1	
Hvab	75.5		30.9		2.29		1,970		6.0	
Hvbb	70.4		30.3		2.18		2,010		11.1	
Hvcb	67.1		27.0		1.88		1,800		15.9	
Hvcb or Suba	59.1		20.5		1.65		2,660		23.4	
Suba	-		17.8		1.35		-		-	
Subb	57.6		15.4		1.33		2,260		27.8	
Lignite	36.5		15.2		1.19		2,100		44.0	

*Sa, semianthracite; Lvb, low-volatile bituminous;
Mvb, medium-volatile bituminous; Hvab, high-volatile A bituminous;
Hvbb, high-volatile B bituminous; Hvcb, high-volatile C bituminous;
Suba, subbituminous A; Subb, subbituminous B.
(from Tsai, 1982)

after all other constituents have been experimentally determined.

Ideally, the mineral matter content should be determined from detailed equations such as the following derived by Padia (1976) and improved by Suuberg (1977):

$$\begin{aligned}
 \text{MM} = & \text{Ash} + 0.625 (S_{\text{pyrite}}) + 0.833 \left[S_{\text{sulphate coal}} \right. \\
 & \left. - S_{\text{ash sulphate}} \times \frac{\text{Ash}}{100} \right] \\
 & + \frac{\text{Ash}}{100} \left[0.354 (Al_2O_3)_{\text{ash}} \right. \\
 & \left. + 0.79 (CaO)_{\text{ash}} + 1.1 (MgO)_{\text{ash}} \right] \quad (2.1)
 \end{aligned}$$

However, in this study, detailed mineral matter analysis of two coals is not available, and in any case determination of oxygen content is not critical. Hence, mineral matter is estimated from the Parr formula:

$$\begin{aligned}
 \text{MM (wt. \%)} = & 1.08 \times \text{Ash (wt. \%)} + 0.55 \\
 & \times \text{Sulphur (wt. \%)} \quad (2.2)
 \end{aligned}$$

2.1 The Origin of Coal

There is considerable evidence that coal is formed from plant substances which have been preserved from complete decay in a favourable environment and have been altered chemically and physically by various environmental effects.

The conversion of plant debris to peat deposits is essentially a biochemical process. The basic starting materials include cellulose, lignin, resins, waxes and fats. Peat formation is favoured by anaerobic fermentation during which

cellulose is a source of oxygen for micro organisms. Aerobic fermentation on the other hand, decomposes cellulose into carbon dioxide and water, and lignins to humic acids. Lignins, fats, waxes and resins are quite resistant to anaerobic attack. Thus it can be visualised that coals of widely varying compositions may be produced, depending on the mode of attack on coal precursors such as plant deposits and peat.

Definitions of coal rank are always controversial. By the very nature of coal, it is difficult to precisely quantify any one property which bears correlation with the maximum number of relevant coal characteristics. However, rank, in terms of carbon fraction, generally reflects the progression in coal metamorphosis. Lignites are nearest in composition to peats, after which coalification increases through subbituminous, high volatile bituminous, medium volatile bituminous, low volatile bituminous, semianthracite, anthracite to metaanthracite which is very similar to graphite. Anthracites with the highest heating values are the least abundant. Low rank coals such as lignite and sub-bituminous are found in greater quantities than bituminous, which are of great utility because of their coking characteristics (also see Table 2.1).

Coals are heterogeneous in appearance as well as in composition. Most coals are made up of strata easily distinguishable by the eye. The science of coal petrography deals with the description of what is seen in the coals by microscopic observations. Usually thin sections of 5/15 ^{to} μm are prepared and observed in transmitted light, a procedure

developed by Thiessen et al (1920, 1938). They observed that coals were composed of different amounts of distinct petrographic entities, subsequently defined as macerals.

Macerals are of three broad categories and are known as vitrinites, exinites and inertinites. These vary in composition and chemical properties. In general, it has been found that exinites have the highest hydrogen content, volatile yields and heating value. Inertinites have the greatest density, refractive index, surface area and aromaticity, whereas properties of vitrinites, by far the major component in most coals, lie somewhere in between. Exinites also evolve more tars than the other macerals.

2.2 Structural Parameters for Coal

One of the major problems concerning the study of evolution of PAH and soot from coal is that coal structure is not clearly understood. Advances in analytical techniques have enabled identification of various species evolved during coal pyrolysis, though it should be stated that product analysis of hydrocarbons and compounds containing oxygen, nitrogen and sulphur is still a delicate and 'messy' procedure. However, these pale into insignificance when one attempts to probe the chemical nature of coal.

Coal is a complex polymeric solid with no repeating monomeric units. It is composed of substituted condensed polynuclear systems. These "monomers" comprise PNA and hydrogenated PNA and increase in terms of number of aromatic rings with coal rank. Primary substituents are short-chain

alkyl and cyclic groups. The relative proportions of the substituents and the PNA groups vary with maceral composition.

Probably the most significant parameter representative of coal chemical structure is aromaticity (f_a), defined as the ratio of aromatic carbon to total carbon present. Other important structural parameters are molecular weight, aromatic and aliphatic hydrogen and functional groups. Various physical and chemical methods have been used to characterize these and other parameters.

Chemical methods in general are inadequate in resolving molecular structures. The chemical reactions involved are: alkylation, acylation, aromatic interchange, reductive alkylation, oxidation, liquefaction and hydrolytic reactions. All these reactions are useful in solubilizing or liquefying the coal. Detailed analysis, such as by GC-MS, is possible of such samples produced in solution. However, such analyses are not particularly useful in determining the structure of the original coal, because degradation of the original coal structure is severe and secondary reactions certainly take place. Furthermore, coal is never completely soluble under conditions which are likely to preserve its basic structure. Increased solubility is gained at the expense of degradation of the functional groups and aromatic species originally present.

However, chemical analyses provide some corroborative information. For example, Chakrabartty and Berkowitz (1974) observe ^{to} 2/5 ring PAH in pyridine extracts of an hvAb coal, indicating that some of the "monomers" contain 5 ring species. Kessler et al (1969) from high resolution GC-MS of pyridine

extracts of a reduced and an unreduced Pittsburgh hvAb find a variety of phenols in the reduced coal fraction, indicating that ether linkages exist in the parent coal and are ruptured under reducing conditions. The presence of eight times as much organic sulphur in the unreduced fraction also indicates sulphur linkages.

Fischer assay yields of low rank coals which give only water, carbon monoxide and carbon dioxide as products, imply that esters, anhydrides and alkoxides are present in these coals. Low yields of these gases from bituminous coals indicate the absence, or very low concentrations of the above groups. Further, the observation that for a bituminous coal, the maximum evolution of oxygen is at much higher temperature than that of volatile matter indicates the presence of ether linkages.

Physical methods of analysis of coal structure include X-ray diffraction (XRD), electron microscopy and spectroscopic techniques like infra-red (IR), fourier-transform infra-red (FTIR), nuclear magnetic resonance (NMR), proton magnetic resonance (PMR) and electron spin resonance (ESR). These provide more reliable information than chemical methods, as they do not disturb the basic chemical structure of coal.

From XRD studies, Hirsch (1954) has observed that coals have lamellae of condensed aromatic rings. The number of such rings per lamella increases with coal rank, being 1 to 3 for low rank vitrains and 2 to 5 for vitrains with 90% carbon. The aromatic lamellae in groups of two or more form larger, imperfect sheets stacked as shown in Figure 2.1 . The average number of lamellae in these stacked sheets increases with

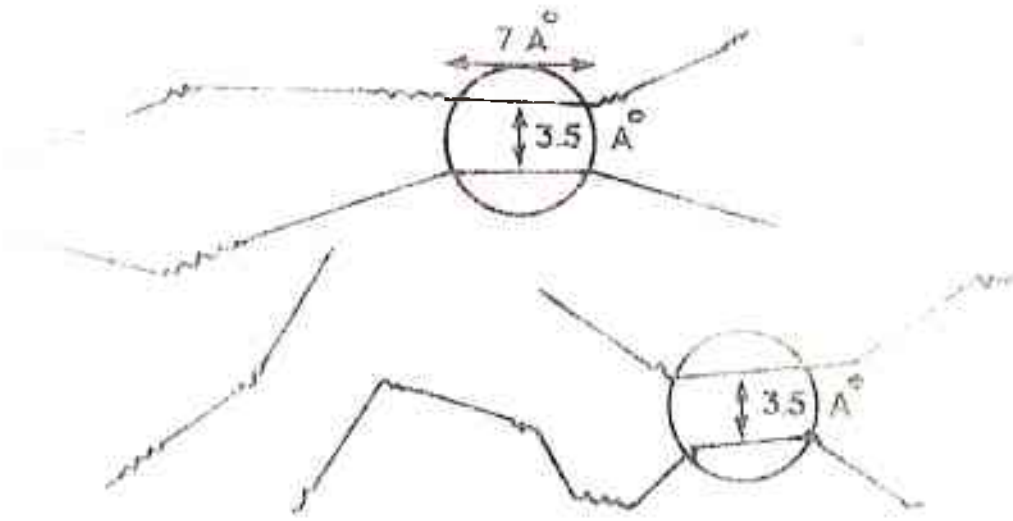


FIGURE 2.1 A SCHEMATIC REPRESENTATION OF PACKING OF LOCALLY FLAT REGIONS OF THE BUCKLED LAYERS (TSAI, 1982)

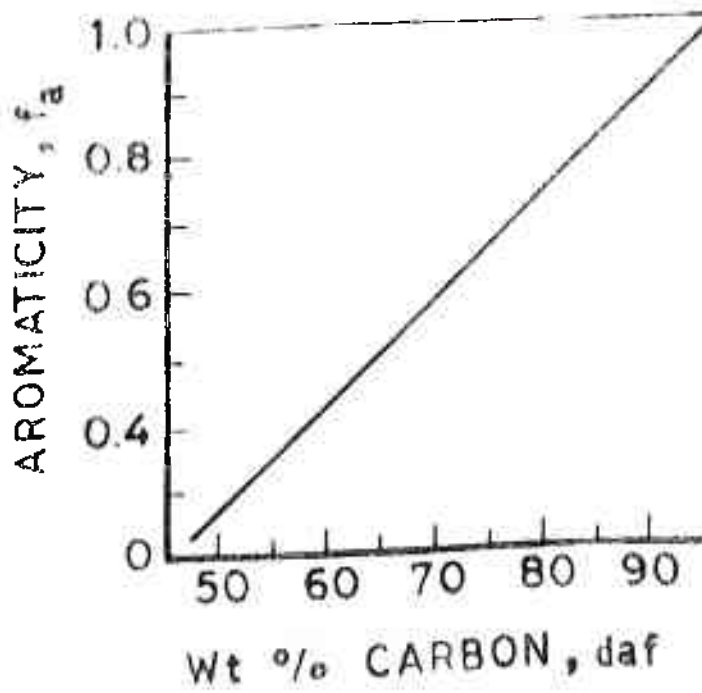


FIGURE 2.2 AROMATICITY VERSUS COAL RANK (TSAI, 1982)

carbon aromaticity (rank), with coals of highest rank such as metaanthracites approaching graphitic structures. XRD provides data on the size of these aromatic lamellae, the average distance between lamellae ($\sim 3.5 \overset{\circ}{\text{Å}}$) and mean bond lengths. Since the mean distance between lamellae is less than the distance of approach of aliphatic chains ($\sim 4 \overset{\circ}{\text{Å}}$ to $5 \overset{\circ}{\text{Å}}$), it follows that some cross links are of the C-C type rather than in the form of aliphatic bridges. The aliphatic side chains and other substituents constitute the amorphous material in the XRD pattern. These decrease in quantity with rank, from about 34% at 78% carbon content to about 12% at 94% carbon content.

High resolution NMR spectra of coals, obtained through the use of magic angle spinning (Bartuska et al, 1976) and cross polarization (Pines et al, 1973, 1978) offers a very powerful analytical techniques. Aromaticity (f_a) is obtainable directly and exhibits the trend shown in Figure 2.2.

^{13}C NMR spectra of an hvb coal clearly indicates that the aromatic carbon is mainly in substituted forms (Zilm et al, 1979). The aliphatic carbon exists largely in the form of aromatic methyl, β -methylene and methylene such as $\text{R-CH}_2\text{-R}'$, where R and R' are aromatic groups. It was also found (Wender et al, 1981) that about one-third of the hydrogen in a high rank lvb coal occurs in aliphatic and dicyclic structures, whereas in a lignite, this fraction is about two-thirds.

The ^{13}C NMR spectra of the hvb coal and its 493°C hydrogenation product (Zilm et al, 1979) have been found to be strikingly similar. The only difference is that the peak corresponding to the methylene groups joining two aromatic rings

is absent in the liquefaction product spectrum, indicating the presence of $-CH_2-$ bridge groups in the coal. Presence of such bridges have been postulated earlier by Heredy et al, 1965 . The cross-polarization and magic angle spinning NMR techniques are far more powerful than the low resolution NMR probing discussed by Suuberg (1977), who discounted evidence obtained by the latter method in elucidating coal structure.

IR can be used to identify specific functional groups such as CH, C=O and OH. Thus, quantitative ratios of aromatic hydrogen to aliphatic hydrogen have been obtained from their respective C-H stretching bands in the IR spectra (Brown, 1955). This ratio is observed to increase with rank. A bituminous coal has been found to contain aliphatic CH, CH_2 and CH_3 groups as well as aromatic rings. It also contains C-O-, C-O-C and associated -OH/-NH bonds (Speight, 1971; Dryden, 1963; Retcofsky, 1968). Depp et al (1957) have observed no carbonyl groups. Further, bands due to isolated C=C, $C\equiv C$ or long aliphatic chains are not observed. Relative intensities of three bands in the region from 900 to 700 cm^{-1} indicate the degree of condensation and substitution of the aromatic lamellae. The 900 to 700 cm^{-1} out-of-plane bending vibrations have been used to estimate f_a .

FTIR offers another powerful quantitative tool for estimation of various parameters, such as, numerical concentrations of the hydroxyl, aliphatic and aromatic hydrogen (Solomon, 1979) and of aliphatic (hydroaromatic) and aromatic carbon (Solomon, 1980). Qualitative information has also been obtained, about the types of ether linkages, the

distribution of aromatic hydrogen, mineral concentrations (Painter et al, 1978) and the forms of aliphatic hydrogen (methyl or methylene).

ESR measures the number of unpaired electrons. These are generally associated with PAH structures in coal. The g-values from spin-orbit coupling have been measured and are found to decrease with an increase in coal rank, indicating the growth of aromatic structures which have more mobile unpaired electrons. The unusually high g-values of low rank coals indicate the presence of oxygen radicals.

From the previous discussion, the following broad conclusions may be drawn:

(a) The basic structure of coal is aromatic. The average number of condensed aromatic rings is two to four, primarily of the phenanthrene and fluorene type, except for very high rank coals which approach graphitic structures. The aromaticity increases with rank.

(b) The aromatic rings form lamellae, which in groups of two or more form ring clusters. The number of aromatic rings per lamella increases with coal rank: one to two rings for low rank and three to five for coals with 90% carbon content (dmmf). The fraction of aromatic lamellae per cluster also increases with rank.

(c) The main bridges linking the ring clusters are:

(i) short aliphatic chains such as methylene and ethylene, with methylene predominant in lignites and ethylene in bituminous coals, (ii) ether, (iii) sulfide and, (iv) biphenyl type aryl-aryl linkages. Hetero atoms such as oxygen,

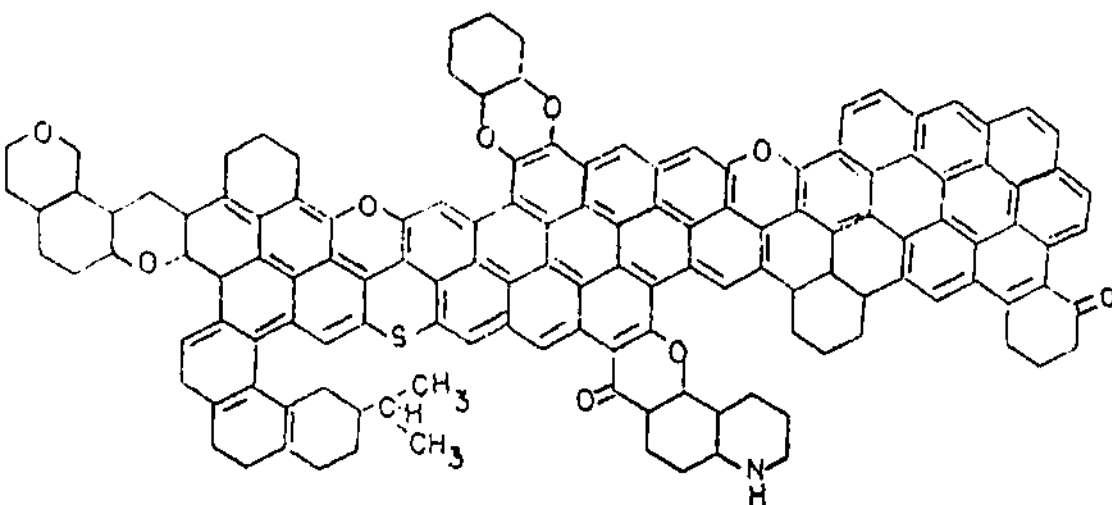
sulphur and nitrogen are present in the following forms: quinones, furans, xanthenes, dioxins, thiophenes, pyridines, quinolines and carbazoles.

2.3 Models of Coal Structure

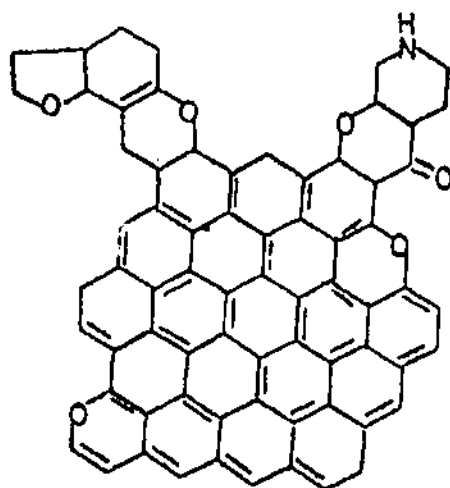
The structural parameters discussed in Chapter 2.2 may be used to evaluate various models proposed in the literature to represent coal.

Fuchs and Sandhoff (1942) have proposed the "chicken-wire" model shown in Figure 2.3 . It is clear that the number of condensed rings is too large as also are the dimensions proposed for the model structures. Moreover, routes for pyrolysis based on these structures would involve a large-scale rupture of aromatic rings which appears to be unlikely. Values of f_a calculated from such structures are much higher than those observed from NMR studies of coals with similar carbon contents.

An average coal molecule of repeating 9, 10 - dihydroanthracene units has been postulated by Given (1960) for a coal containing 82.3% carbon (daf). Though this (Figure 2.4) is a better representation of coal than that shown in Figure 2.3 , there are still some questions. IR spectra of coals with similar carbon contents do not indicate the presence of carbonyl groups, though Given's model postulates the presence of chelated quinonoid carbonyl groups. Thus, there should be more ether linkages. There is no sulphur present though in a later study, Given (1976) says that based on the molecular weight range there would be



$C_{135} H_{97} O_9 NS$
 (47.0 x 22.5 x 9.0 Å)



$C_{70} H_{41} O_6 N$
 (16.5 x 19.5 x 6.0 Å)

FIGURE 2.3 MODEL STRUCTURE FOR COAL (FUCHS AND SANDHOFF, 1942)

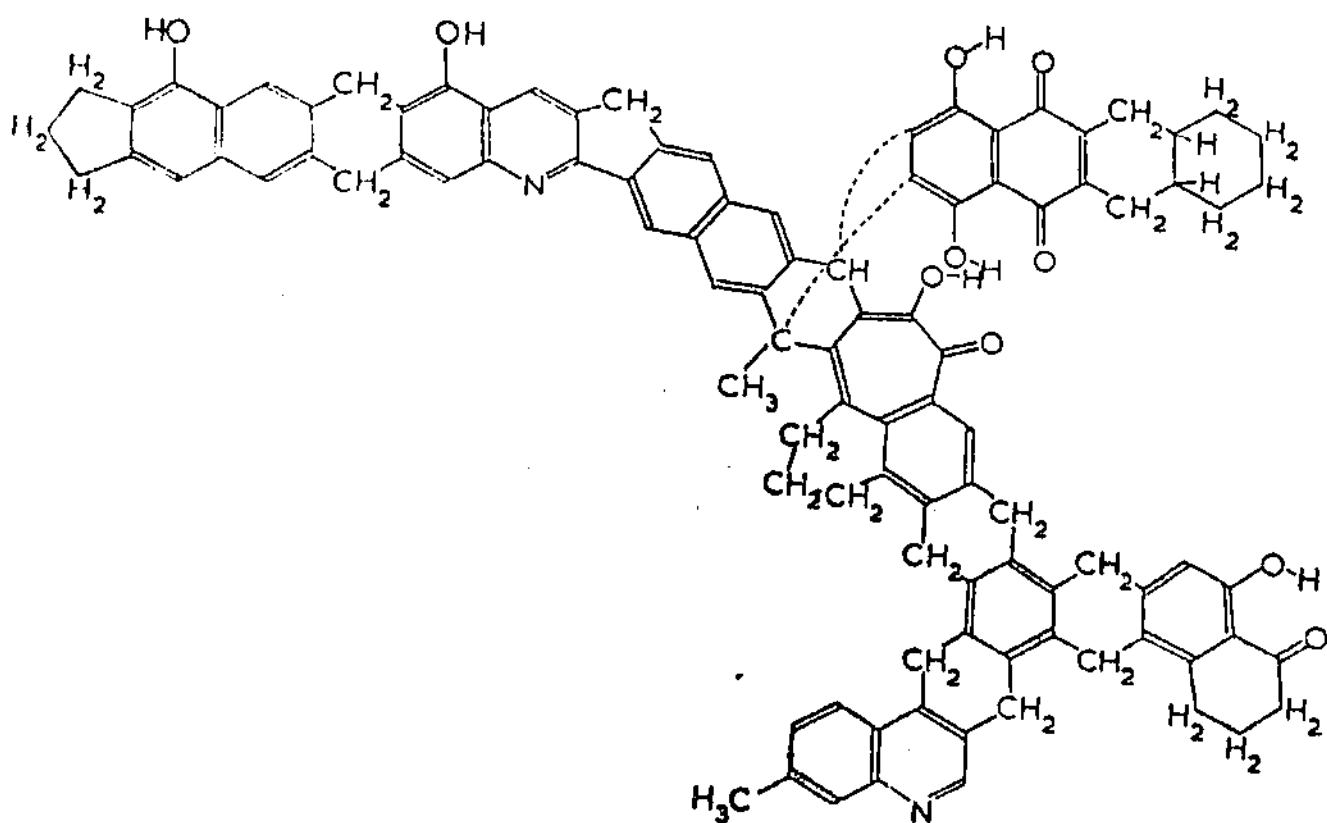


FIGURE 2.4 MODEL STRUCTURE FOR COAL (GIVEN, 1960)

less than one S atom. However, this does not explain the absence of sulfide bridges, which have been observed experimentally. Aromaticity values are less than expected implying that there should be more rings in each condensed structure unit. As a corollary, the average number of inter-cluster linkages appears to be high. Given's model can give qualitative yields of various species on pyrolysis. The stereo-chemistry which causes buckling is introduced by the small group attached to the centre of his model molecule.

The model proposed by Hill and Lyon (1962), shown in Figure 2.5 has many inconsistencies. No average structure has been defined, there should be more hydroaromatic hydrogens, it is unlikely that there would be 6-carbon alkyl bridges, and the carboxylic groups shown have not been found in spectroscopic studies. The aromaticity of the structure is lower than expected. Further, the large number of OH groups shown are highly unlikely.

Mazumdar et al (1962) proposed that coals are mixtures of macerals of various ranks. Thus, a bituminous coal would contain varying proportions of I, II and III (Figure 2.6). While this is an attractive approach, the structure I, with a carbon content in the lignite range should have one-two rings at most. Further, no hetero atoms such as S and N have been shown. Van Krevelen (1963) has also proposed model structures (Figure 2.7) which are more representative of intermediate steps in coalification than of coal. Mazumdar's (1962) representation appears to give a better picture.

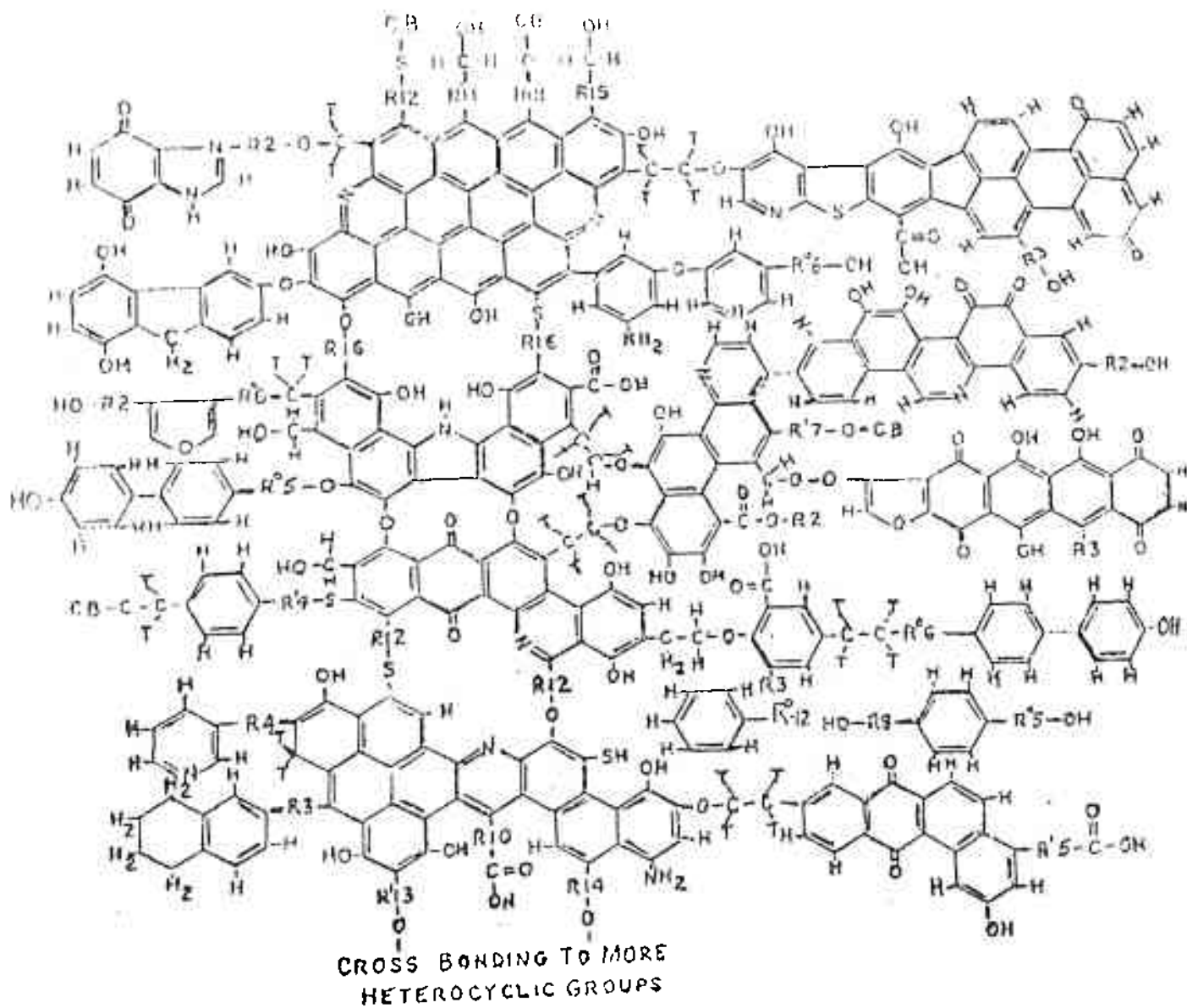


FIGURE 2.5 MODEL STRUCTURE FOR COAL (HILL AND LYON, 1962)

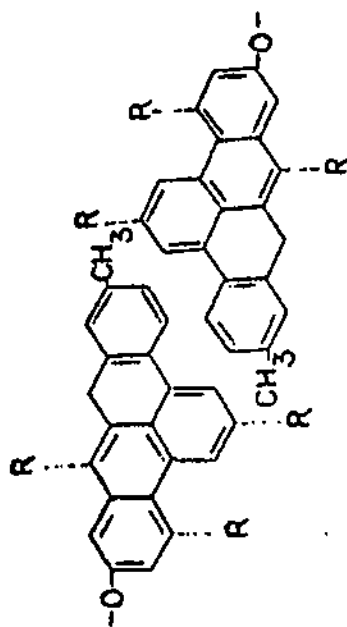
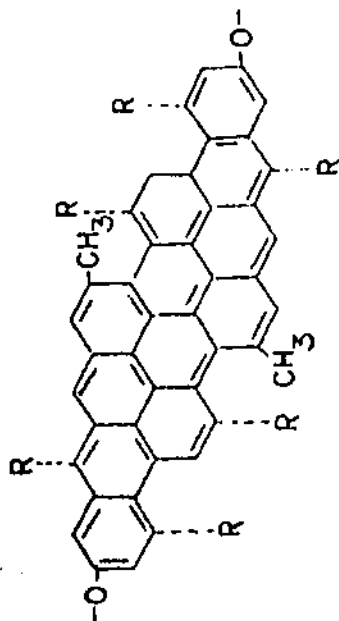
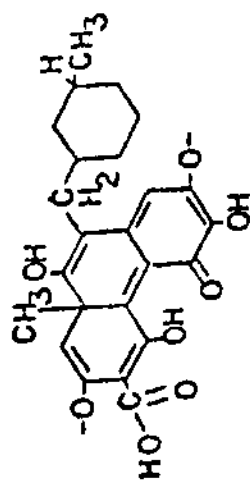
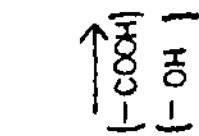
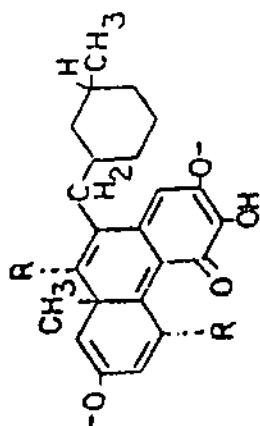
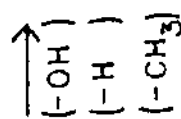
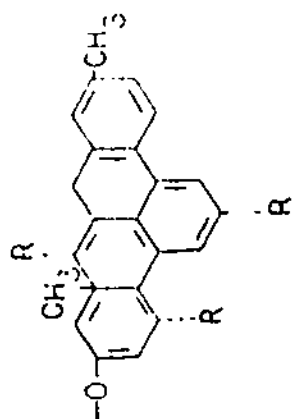


FIGURE 2.6 MODEL STRUCTURE FOR COAL (MAZUMDAR, 1962)

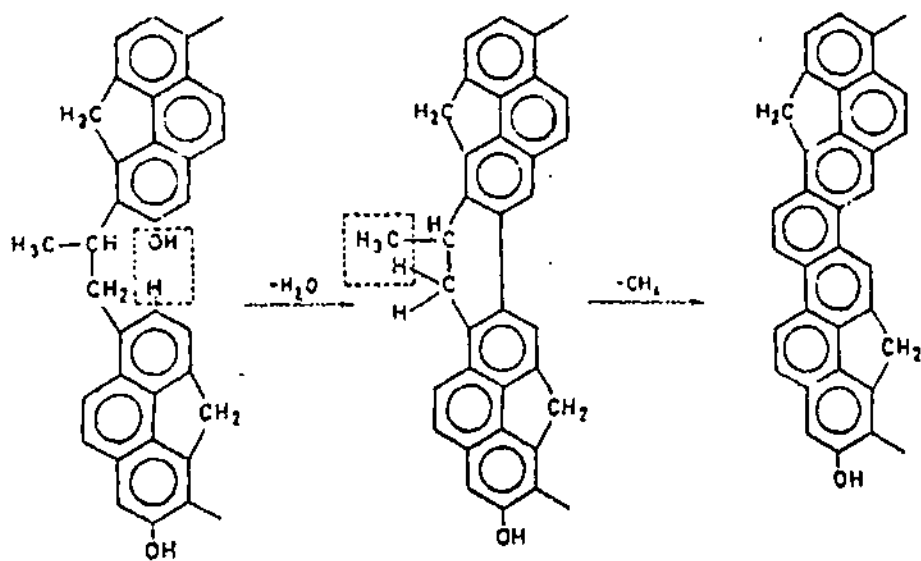
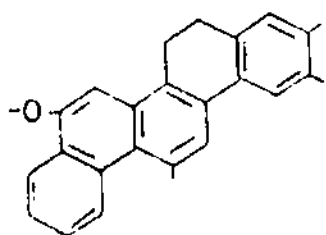


FIGURE 2.7 MODEL STRUCTURE FOR COAL
(VAN KREVELEN, 1963)

Wender (1975) uses the structures shown in Figure 2.8 as a convenient way of understanding the reactions of various kinds of coals. The structures for the hvAb and the lvb are in accordance with the parameters discussed in Chapter 2.2. However, there is no sulphur or nitrogen and the subbituminous coal appears to have a greater aromaticity than usually observed (~ 0.7). The lignite model is quite different from others proposed, but could fit much of the experimental data.

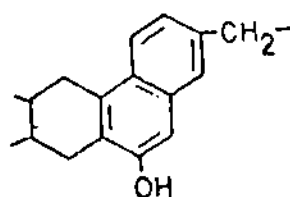
Wiser's (1975) structure (Figure 2.9) incorporates many features such as sulphide bridges, aliphatic and aromatic nitrogen and different forms of oxygen, though again carboxylic groups are unlikely as are the C=O groups. However, this gives a good qualitative picture of various experimental findings and as can be seen, cleavage of methylene bridges should provide the desired range of PAH and tars. The propylene bridge shown is not likely to be present.

Heredy and Wender's (1979) model incorporates carbon aromaticities derived by CP-MAS NMR, and spectroscopically determined oxygen distributions amongst various functional groups (Figure 2.10). Observed linkages between condensed ring systems such as biphenyl, heteroatom (aromatic ether) and methylene are also included. The expected behaviour of the model molecule is compared with the behaviour of hvb coals of similar carbon contents, for reactions such as catalytic dehydrogenation, reduction with lithium-ethylene diamine, phenol-BF₃ - catalyzed depolymerization and reactions to give carboxylic acids. Good agreements are obtained between the experimentally obtained and expected product distributions. Though visual inspection of the



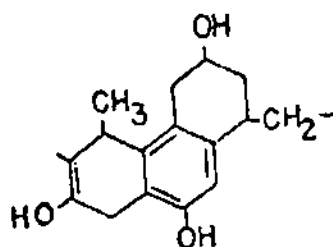
Pocahontas No. 3 Bed, W.Va. (LVB)

	<u>% MAF</u>
C	90.7
H	4.6
O	2.8
N	1.3
S	0.6
VM	18.7



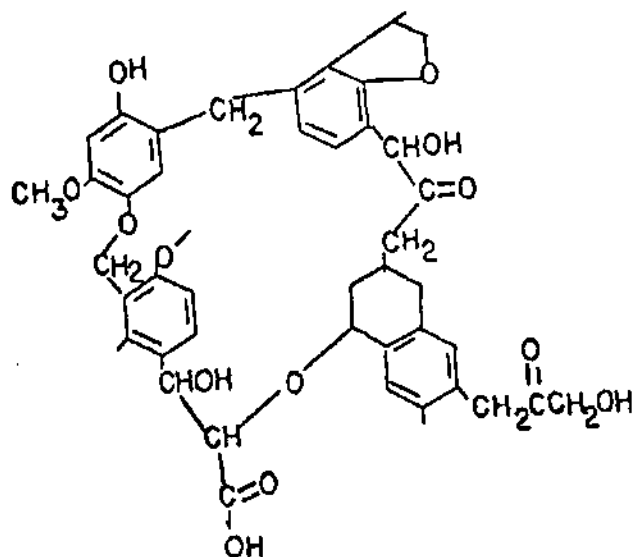
Pittsburgh Bed (HVAB)

	<u>% MAF</u>
C	84.2
H	5.6
O	6.9
N	1.6
S	1.7
VM	39.9



Mammoth Bed, Wyo. (Subbituminous A)

	<u>% MAF</u>
C	76.7
H	5.6
O	15.5
N	1.3
S	0.9
VM	43.6



Beulah Zap Bed, N.D. (Lignite)

	<u>% MAF</u>
C	72.6
H	4.9
O	20.2
N	1.1
S	1.2
VM	45.9

FIGURE 2.8 MODEL STRUCTURE FOR COAL
(WENDER, 1975)

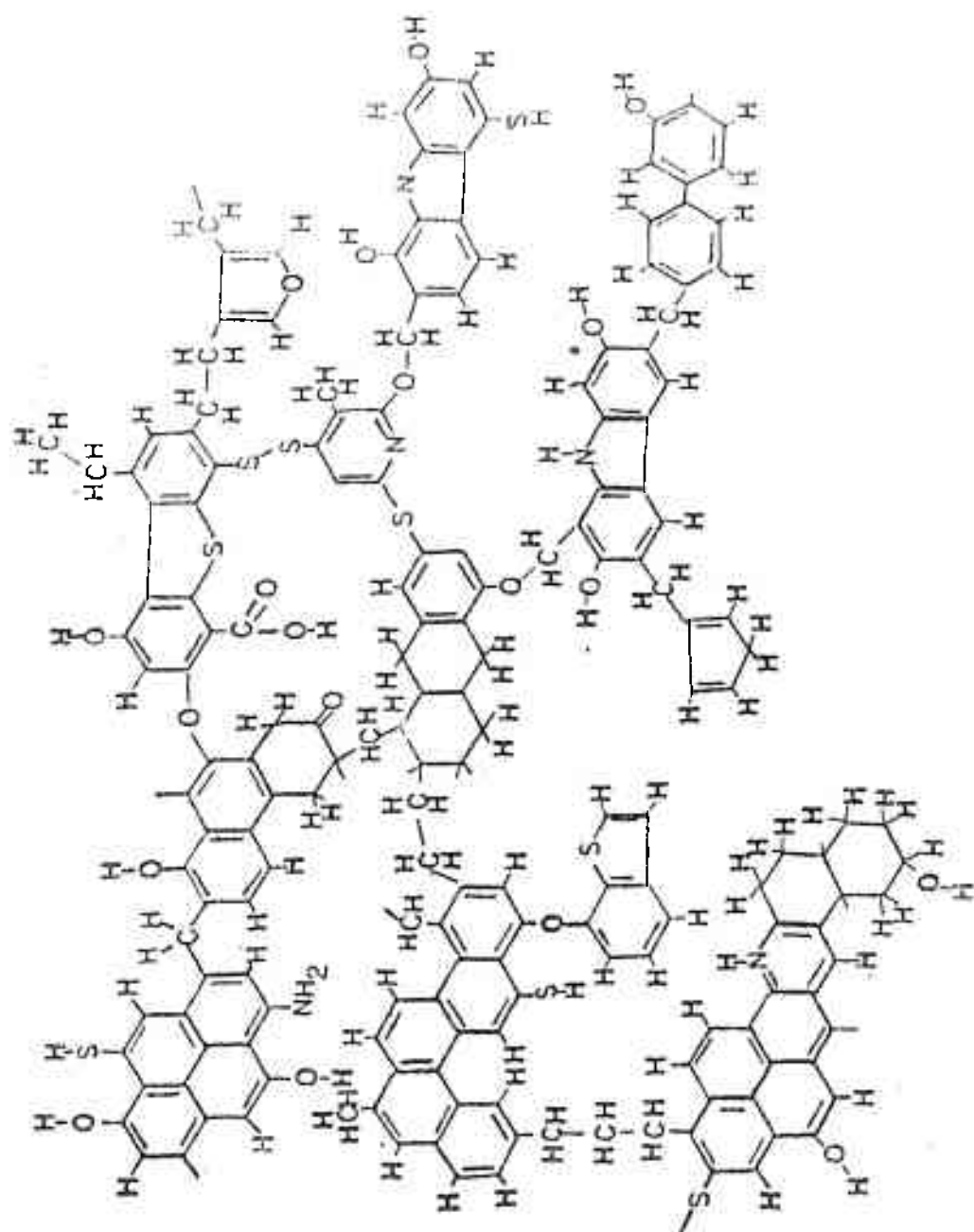
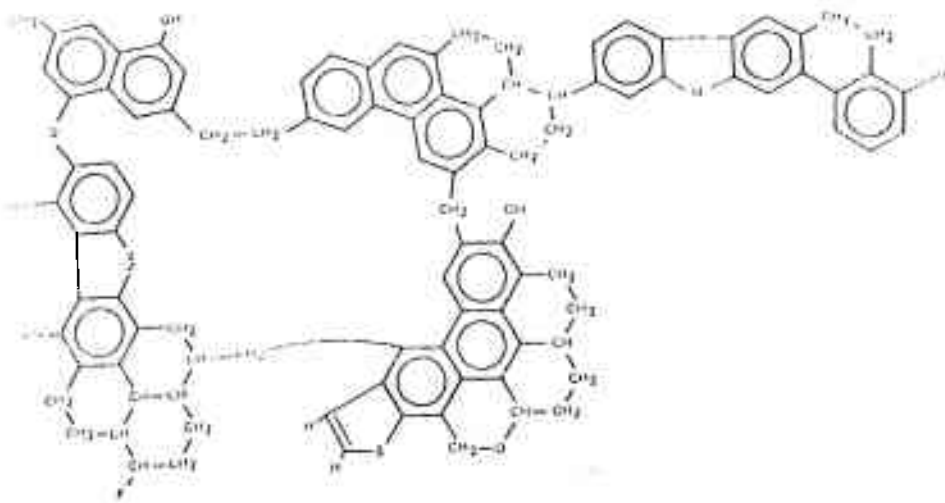


FIGURE 2.9 MODEL STRUCTURE FOR COAL (WISER, 1975)



Proposed Structure of the Model Coal Molecule

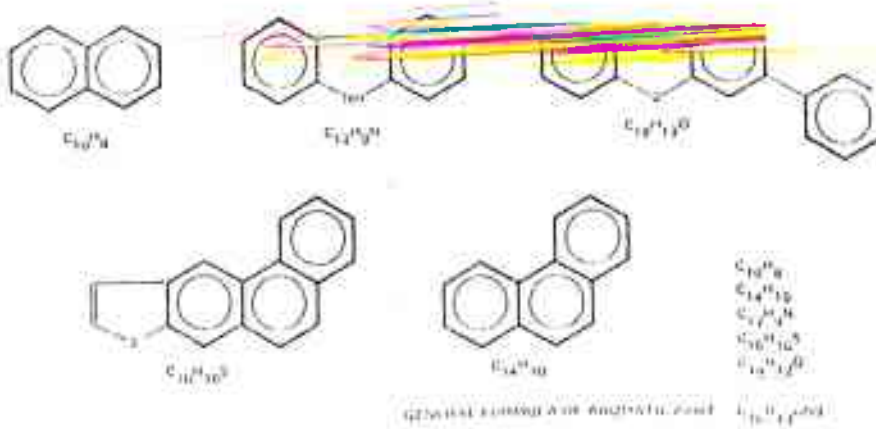


FIGURE 2.10 MODEL STRUCTURE FOR COAL (HEREDY AND WENDER, 1979)

expected behaviour under pyrolysis would appear to give good results (for example : from cleavage of the bridges shown and dehydrogenation of the $C_{18}H_{10}S$ structure, one to six ring PAHs should be evolved), it would be instructive to compare computed and experimentally observed tar yields.

Finally, Solomon (1984) has proposed the model shown in Figure 2.11 for PSOC 170, a high volatile bituminous coal. It needs to be emphasized that this configuration should not be considered as a representation of the actual coal structure but as a device for summarising research results.

The model is very similar to that presented by Heredy and Wender (1979). The major difference is in the use of parametric information derived from FTIR in addition to ^{13}C NMR (CP-MAS) used by Heredy and Wender, for determining aromaticity. An innovation is the inclusion of hydrogen bonding as indicated by FTIR spectra. The aromaticity values are higher than those obtained by Heredy and there are less hydrogenated ring structures. Thermal decomposition experiments have been performed so as to obtain information on the relative bond strengths. There is a very good agreement between the structural parameters of the model and the measured parameters for PSOC 170.

2.4 Simple Kinetic Models of Coal Pyrolysis

Volatile matter significantly higher than that indicated by the proximate analysis can be obtained from coal by rapid heating at rates greater than 10^4 °C/s. This would lead to greater yields of species of interest such

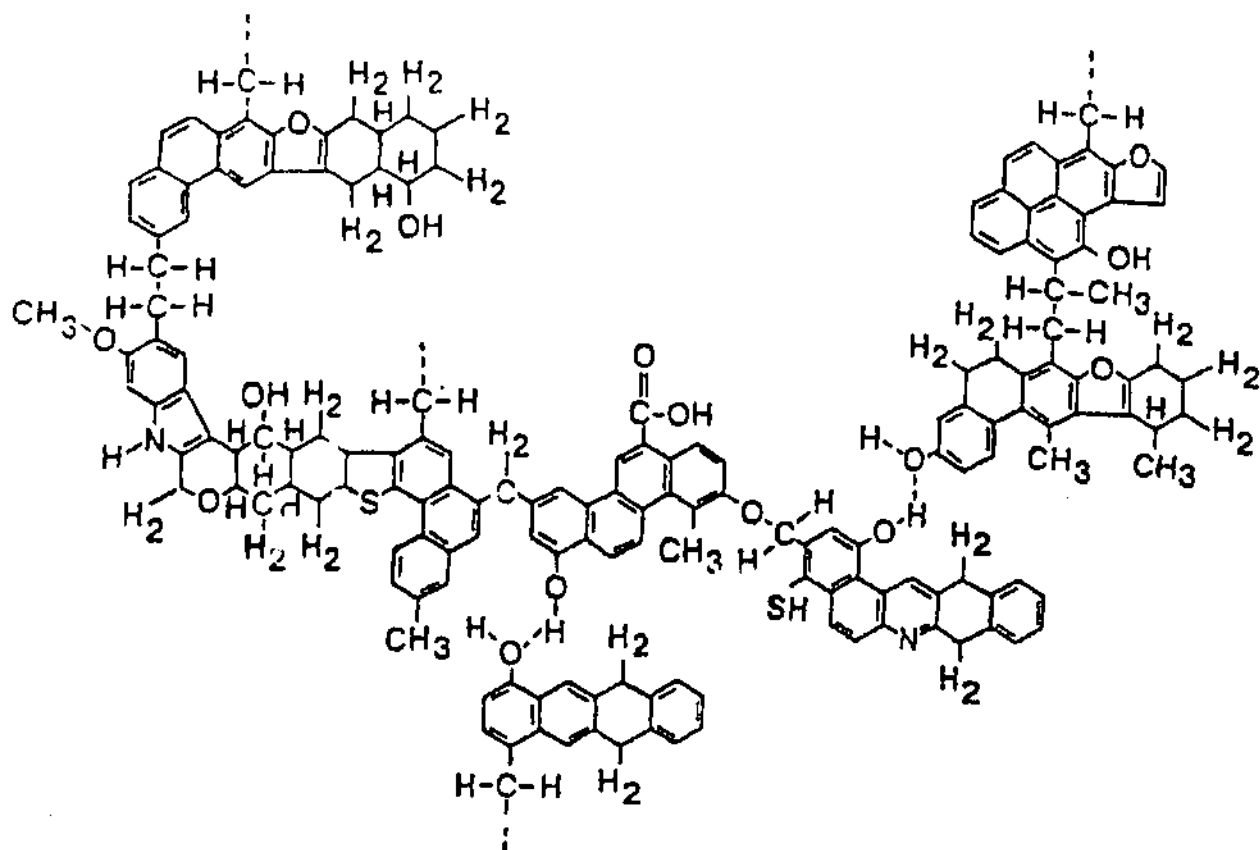
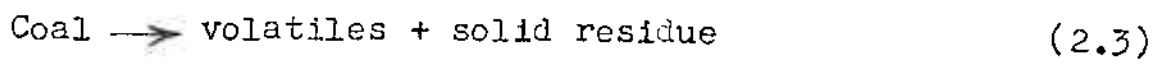


FIGURE 2.11 MODEL STRUCTURE FOR COAL
(SOLOMON, 1984)

as PAH. In this section some simple kinetic models for pyrolysis of coal are discussed, from the point of view of prediction of tar yields.

The simplest approach is to model the overall process as a first-order decomposition reaction of the following general type:



If V = volatile matter remaining in the coal at time t, expressed as a fraction of the initial mass of the coal

V_∞ = volatile content as t → ∞

then dV/dt = k (V_∞ - V) (2.4)

where the rate constant k has the usual Arrhenius form,

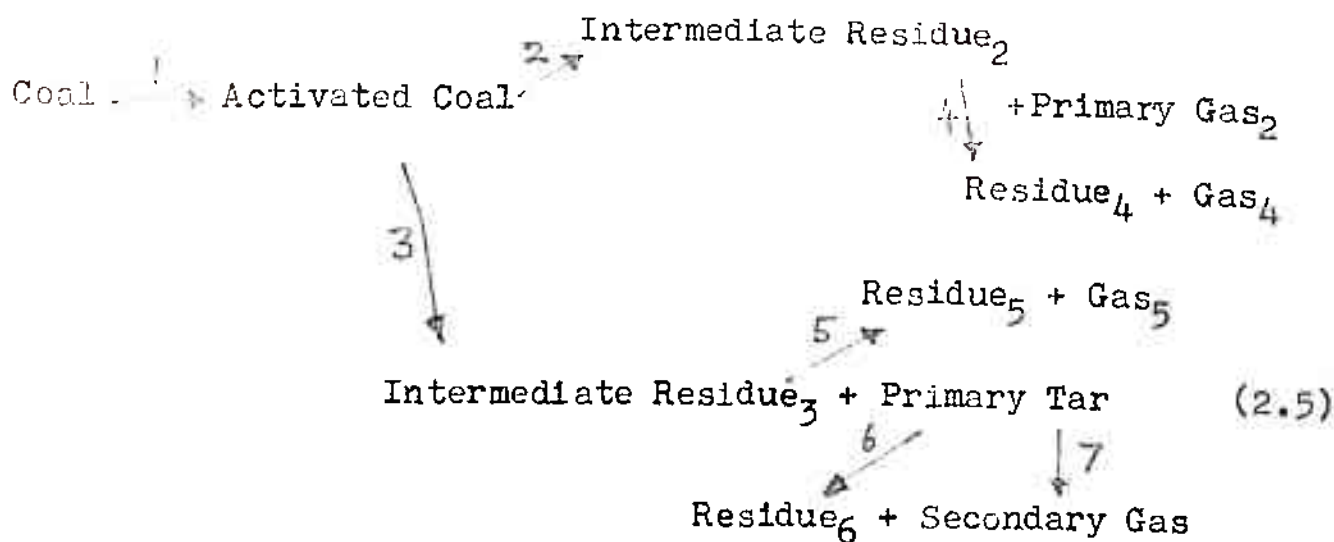
k = k₀ e^{-E/RT}

Thus, by experimentally determining temperature-time histories and V_∞, various workers have chosen values for the pre-exponential factor k₀ and activation energy E to fit the weight-loss data. Values of k₀ from less than 10⁻² to 10¹¹ sec⁻¹ and of E from 1 to 45 kcal/mole have been proposed.

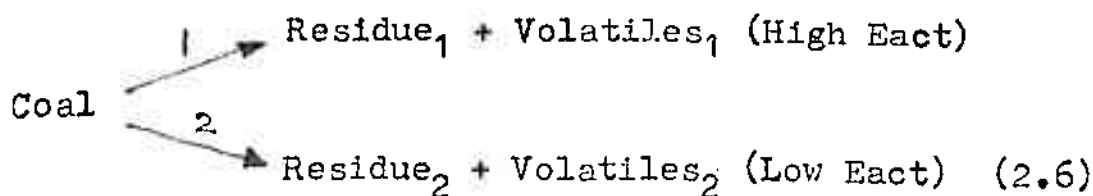
The kinetic models proposed are summarised below:

- (a) Jüntgen and Van Heek (1968); for evolution of various gaseous species, use an equation similar to Equation 2.4 with a different k, and E for each species.
(b) Anthony et al (1975) consider an infinite set of parallel independent decomposition reactions having the form of Equation 2.4 with the same k₀ but with a Gaussian distribution of activation energies.
(c) Reidelbach and Summerfield (1975) postulate a multi-step

series competition model of the following type:

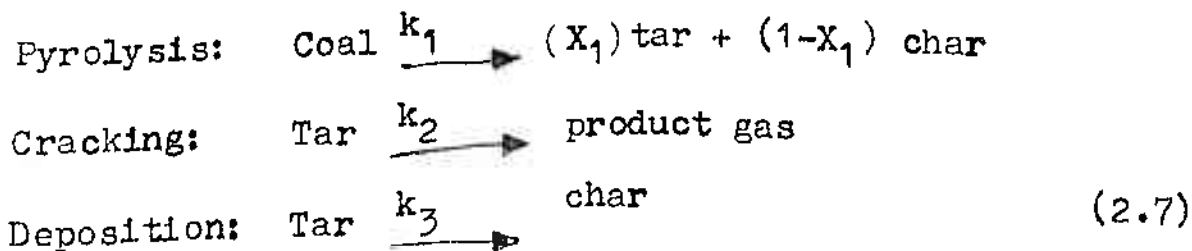


(d) Kobayashi et al (1977) propose a simpler model containing two competing reactions.



(e) Suuberg et al (1978) present a semi-empirical model where the appearance of key species (such as tar) are described by $1/3$ ^{to} parallel reactions, each with different k_0 and E values.

(f) Wen and Chen (1979) have proposed the following reactions:



(g) Sprouse and Schuman (1981) have compared the multiple Parallel reaction model of Anthony et al (1975) with the two-competing reaction model for predicting the devolatilization

characteristics of a lignite. They find that the multiple parallel reaction model has a better fit for the high-temperature data.

All the models cited above show reasonably good agreement with certain experimental data for the proper choice of parameters, with Anthony's (1975) possibly offering the most realistic description of the coal devolatilization process using the fewest (four) number of modelling parameters. However, they do not provide much insight into the mechanistics of the process and are better regarded as provisional hypotheses that are convenient for correlating the experimental data. They do not bring us any nearer to answering the question - "Given the complete chemical analysis of a coal, is it possible to predict the evolution of tars, PAH and soot?".

Recently, a mathematical model has been proposed by Solomon (1984) for the thermal decomposition of coal, based on data from vacuum pyrolysis experiments. This fits the general behaviour of the coal model discussed in Chapter 2.3 and its behaviour under pyrolytic conditions, as depicted schematically in Figure 2.12. At sufficiently high temperatures, the weak links, such as the middle of the ethylene bridge are ruptured. Bonds between oxygen and an aliphatic carbon are also likely to break. The ring clusters which are released are observed in the form of coal tar. PAH would then be evolved from the tars via further thermal decomposition reactions.

Coal pyrolysis has been modelled via two routes. The coal is depicted as a two dimensional map with X and Y

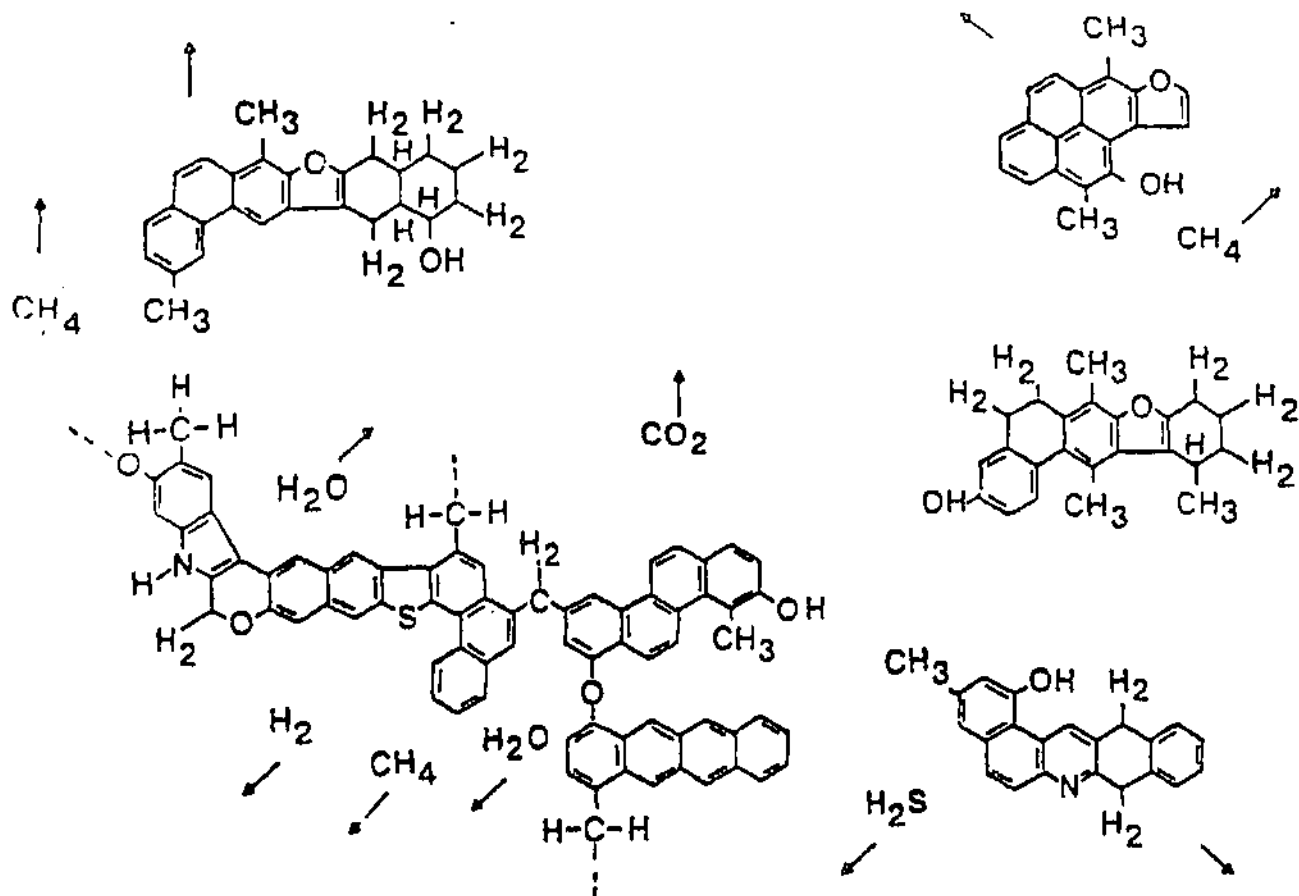


FIGURE 2.12 CRACKING OF HYPOTHETICAL COAL STRUCTURE DURING PYROLYSIS (SOLOMON, 1984)

dimensions (Figure 2.13). The evolution of each component into the gaseous form is represented by the following first order reaction for depletion of the Y(i) species:

$$Y(i) = Y^0(i) e^{-k_i t} \quad (2.8)$$

The X dimension comprises a potential tar forming fraction X^0 and a non-tar forming component $(1-X^0)$ with the evolution of the tar represented by a first order diminishing of the X dimension:

$$X = X^0 \cdot e^{-k_x t} \quad (2.9)$$

Comparison of experimental results with those obtained from the model are quite good. More important, they allow detailed predictions of species evolution under conditions of vacuum pyrolysis, and provide an understanding of the thermal decomposition process using a single set of rate parameters which vary with volatile species but are independent of coal rank.

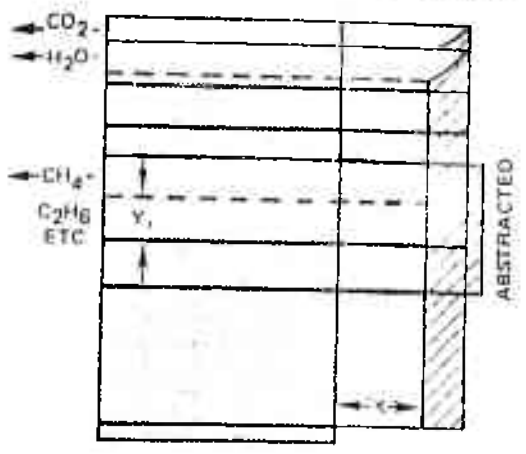


a) FUNCTIONAL GROUP COMPOSITION OF COAL

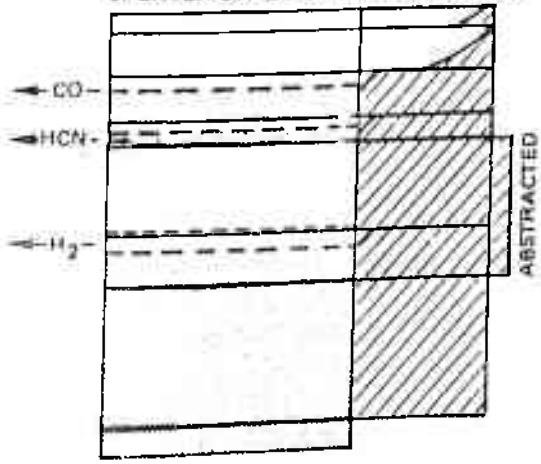
CARBOXYL	
HYDROXYL	
ETHER	
NITROGEN	
ALIPHATIC	
AROMATIC	
NONVOLATILE CARBON	

NON-TAR FORMING FRACTION $(1-x^0)$ TAR FORMING FRACTION x^0

b) INITIAL STAGE OF DECOMPOSITION



c) LATER STAGE OF DECOMPOSITION



d) COMPLETION OF DECOMPOSITION

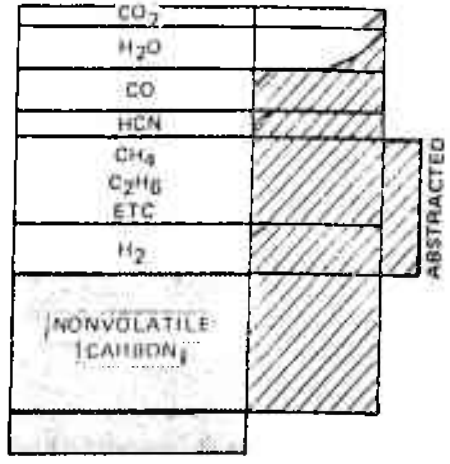


FIGURE 2.13 SCHEMATIC OF COAL PYROLYSIS (SOLOMON, 1984)

CHAPTER 3

EVOLUTION OF PAH

A variety of theories have been proposed in literature to explain the steps leading to the formation of PAH. Flames and pyrolysis regimes utilising simple fuels such as acetylene, methane, 1,3-butadiene, benzene, toluene etc. have been examined in detail. However, most of the hypotheses are of a phenomenological type. The starting fuels and end-products are known, as are many of the intermediate reactive and unreactive species, and different mechanisms have been fitted to these fixed coordinates.

PAH found in the environment are often associated with soot. Soot may act as a carrier or as a reaction site. PAH may be directly involved in soot formation processes, or may be stable byproducts of such reactions. It is in this context that PAH-soot interactions are of interest.

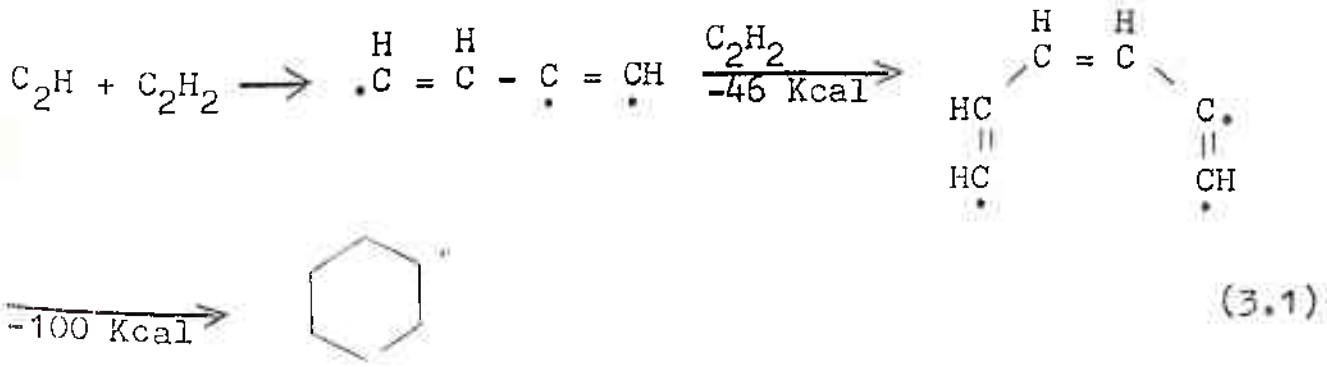
The type of fuel being pyrolysed or burnt is expected to influence PAH and soot evolution. The influence of fuel type is discussed in the last section.

3.1 Mechanisms of Formation of PAH

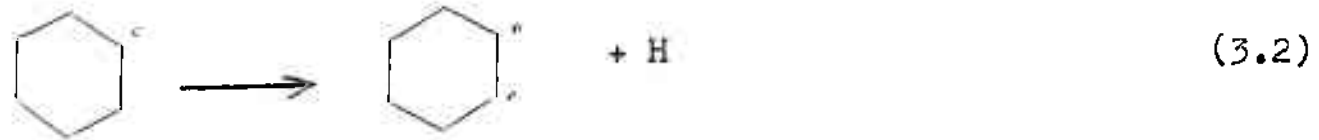
Burgoyne (1940) observed the presence of PAH from the combustion of benzene, toluene and ethylbenzene. The addition of a side chain to benzene appeared to facilitate oxidation. A mechanism involving degradation of the side chain, attack on the aromatic ring, and ring rupture was proposed. Later studies indicate however that ring rupture is unlikely to occur

in Burgoyne's temperature range (300° - 500°C). From premixed flames burning a range of n-alkanes, Street & Thomas (1955), imply that fuel molecules may undergo dehydrogenation, polymerization and cyclization to form C₆-C₂₀ aromatic intermediates, which then polymerize to particles containing PAH.

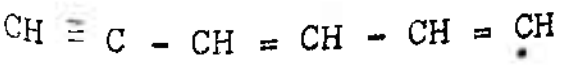
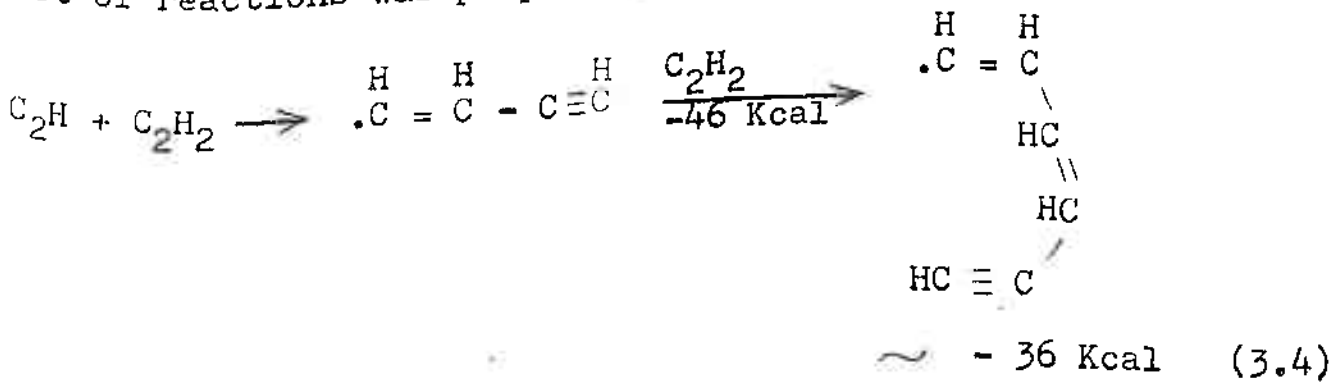
Flames propagating in acetylene in straight tubes were examined by Stehling et al (1957), and the following types of free radical reactions were postulated:

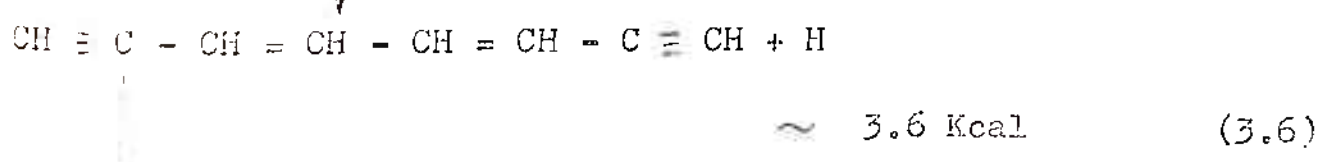
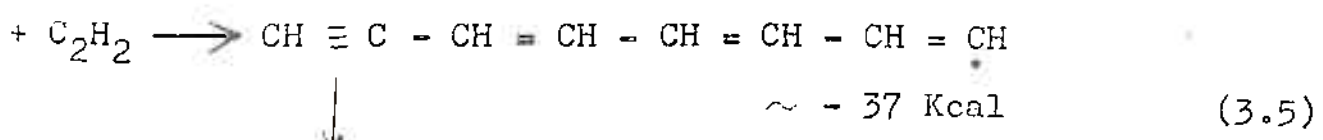


This could release sufficient energy so that reactions 3.2 and 3.3 could proceed as follows:



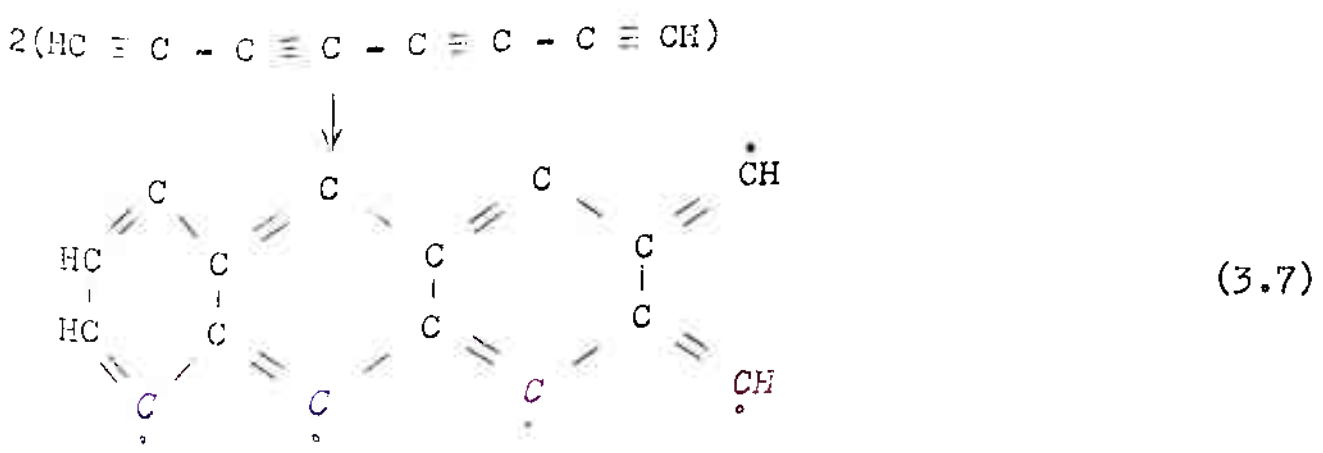
However benzene was not found to be very reactive and another set of reactions was proposed:





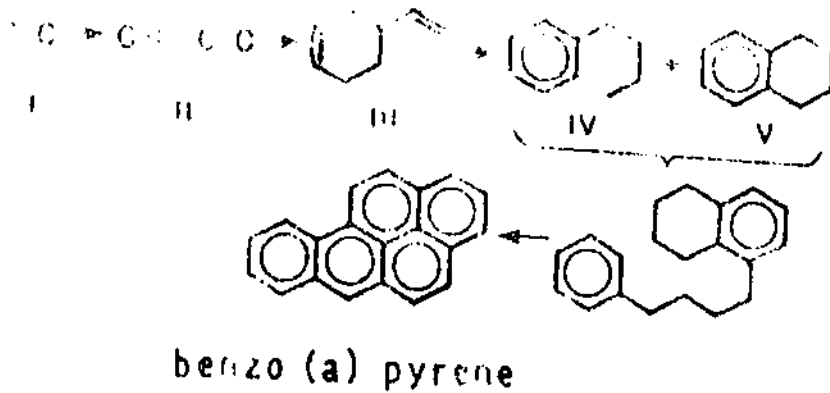
Octatriynes

Octatriynes may recombine as follows:



Such reactions could occur more rapidly than a simple condensation of aromatic species to larger PAHs.

In their classical studies on pyrolysis, Badger and coworkers (1962, 1960, 1960a, 1960b, 1960c) suggested that PAH were formed by free radical mechanisms which involve substitutions by aryl radicals, followed by cyclodehydrogenations. They proposed the scheme shown in Figure 3.1, for the formation of benzo (a) pyrene. Primary radicals could be evolved at high temperatures via C-H and C-C bond fission. Thus, pyrolysis of toluene would give the benzyl radical, since the C-H bond in the methyl group has a lower bond dissociation energy (78 Kcal/mole) than the C-C bond in C₆H₅ - CH₃ (89 Kcal/mole). These radicals would then



Possible structures for the intermediates are

- I. Ethylene / Acetylene
- II. Butadiene / Vinylacetylene
- III. Styrene / Ethylbenzene
- IV.] Tetralin / Phenyl butadiene
- V.]
- VI. Benzo (a) pyrene

FIGURE 3.1 FORMATION OF PAH DURING PYROLYSIS (BADGER, 1962)

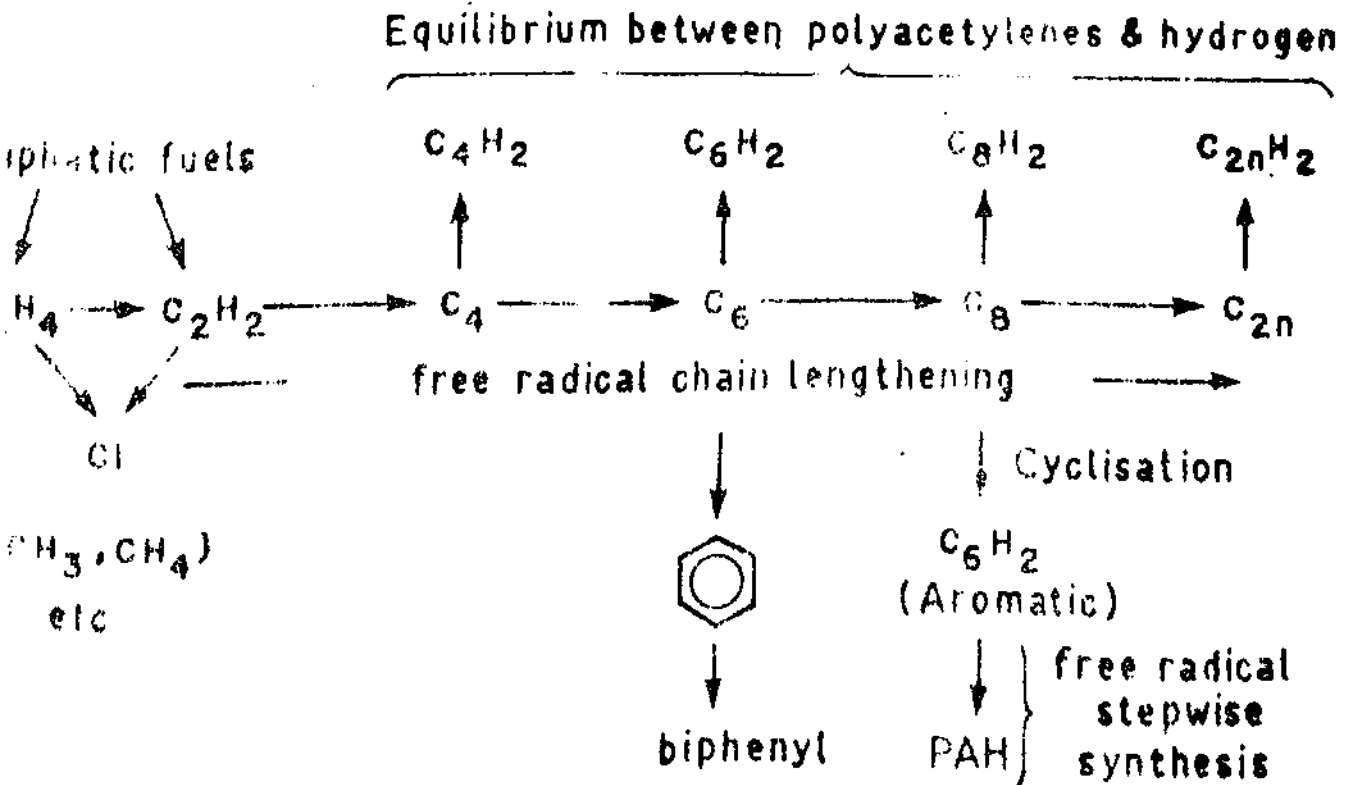


FIGURE 3.2 REACTION SCHEME FOR THE FORMATION OF PAH IN RICH PREMIXED FLAMES (CRITTENDEN AND LONG, 1973a)

recombine to give products which were highly condensed. Thus, through a series of addition and chain-lengthening reactions PAH were synthesized. The presence of high concentrations of methane at the exit appeared to confirm the free radical nature of the reactions which would presumably involve methyl radicals. Using labelled (α C ¹⁴) ethylbenzene, Badger also proposed routes for the formation of toluene, naphthalene, phenanthrene and 3,4-benzofluoranthene.

As further evidence for Badger's route (Figure 3.1), Stehling et al (1962) observed an increase in the concentration of naphthalene, when styrene (structure III in Figure 3.1) was an additive during acetylene pyrolysis. Key aromatic species with the C₆-C₂ structure (structure III) have also been pointed out as precursors of PAH by Crittenden /^{and} Long (1973a), who observed the presence of styrene and phenylacetylene in rich premixed acetylene and ethylene flames in both the oxidation and burned gas zones.

Crittenden (1973a) postulated the thermal breakdown of ethylene to acetylene which then proceeded via a series of free-radical chain lengthening reactions to a variety of end products. This sequence is depicted schematically in Figure 3.2.

Oro and Han (1967) investigated the thermal degradation of methane and observed a wide range of PAH species with a yield of about 15%. The route could also be as in Figure 3.2.

Zaghini et al (1972) from studies on n-C₇H₁₆/O₂/N₂ in a vertical flow reactor advanced the hypothesis, that PAH formation is essentially occurring via Badger's (1962) route in pyrolysis zones within the flame. Various species such as vinylacetylene, benzene, toluene, xylenes etc. were detected, all of which could

be regarded as intermediates in the formation of PAH.

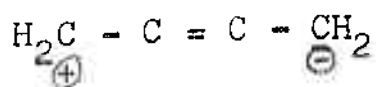
The high temperatures available in the oxidation zones of rich premixed hydrocarbon flames could lead to decomposition of ethylene to acetylene, which would proceed via Badger's (1962) pyrolysis route to form PAH. Kozlov and Knorre (1962) observed that at high temperatures, the rate of acetylene decomposition was appreciably higher than that for ethylene. Further, ethylene concentrations declined to zero very rapidly while there was a considerable formation of acetylene in a rich premixed oxy-ethylene flame (Homann et al, 1963).

Pasternak et al (1981, 1982) postulated similar mechanisms of PAH formation in polymer and hydrocarbon flames, after the initial thermal degradation of polymers to simpler hydrocarbon fragments. By addition of C_2 or C_4 units to ring structures, reactive aromatic radicals could be produced successively. It was postulated that any PAH observed were stable byproducts of the reactions (also vide Bonne, Homann & Wagner, 1965; Thomas, 1965; Homann, 1967; Longwell, 1982; Beér et al, 1983).

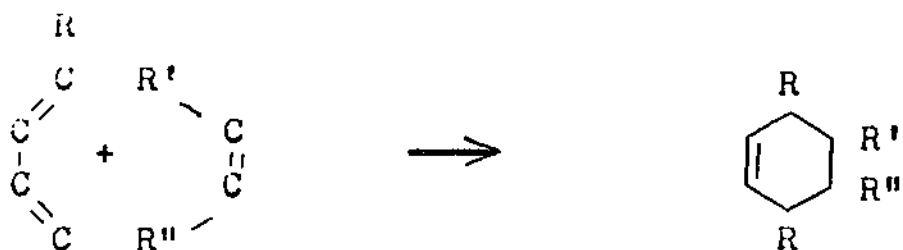
PAH of two-three rings decreased rapidly relative to pyrene, whereas there was almost no effect on five-seven ring species (Di Lorenzo et al, 1981), in a premixed CH_4/O_2 flat flame. Buildup of ring size appears to be occurring via free radical routes. Tompkins and Long (1969) observe a similar behaviour in a premixed H_2/O_2 flat flame. With increasing height above the burner, there is a rapid decline in ratios of 2/3 ring PAH to pyrene and an increase in this ratio for higher molecular weight PAHs.

As further evidence of the essentially free radical nature of the PAH formation reactions Franceschi et al (1976) find that increasing the concentration of chain reaction inhibitors such as nitric oxide and methanol decreases PAH yields. Conversely, the presence of benzenic and methyl radicals promotes the formation of PAH and perinaphthenyl radicals (proposed as a precursor for larger PAH). Similar effects of nitric oxide (Thomas, 1965) and methyl radicals (Asaba and Fujii, 1971) have also been observed.

It had been proposed that PAH could be formed by successive Diels - Alder type additions of 1,3-butadiene (structure II in Figure 3.1) to hydrocarbons. This however is unlikely, since adding 1,3-butadiene to pyrene resulted in very little increase in yield of larger PAHs (vide Badger & Spotswood, 1960a). Cypres and Bredael (1980) have also proposed the diene as an intermediate, based on studies of flash pyrolysis of cyclohexane and cyclohexene. Cole (1983) was able to account for benzene production rates within an order of magnitude while assuming the 1,3-butadienyl radical to be a benzene precursor. However, Crittenden and Long (1973a) find no evidence of the diene as a precursor in fuel rich premixed flat flames, and Vranos and Liscinsky (1984) find no 1,3-butadiene present during the formation of a wide range of PAHs. A more interesting possibility is the polar diene form, proposed by Glassman (1979):



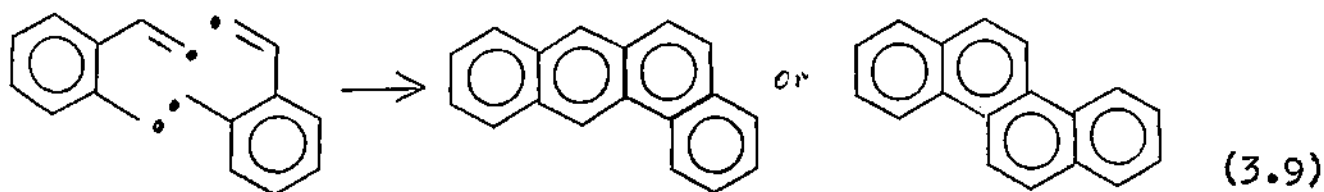
The importance of conjugated free radicals in PAH and soot formation has also been stressed by Thomas (1965). Conjugated species could undergo the following type of Diels-Alder condensation reactions:



Davies and Scully (1966) outlined possible routes for PAH formation from indene, involving 2-3b bond scission:

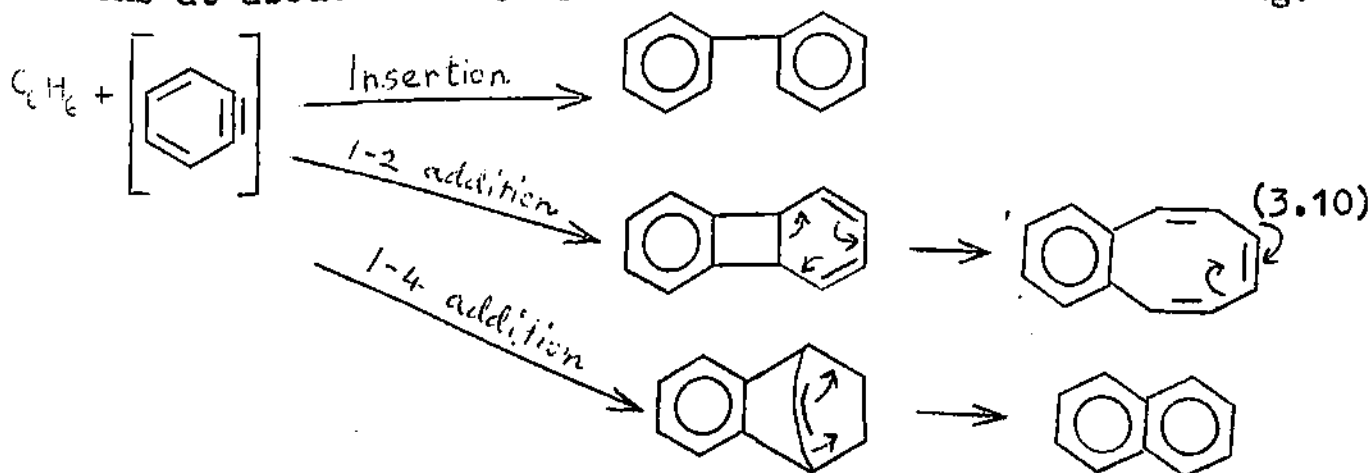


Polymerization of two such diradicals would give:

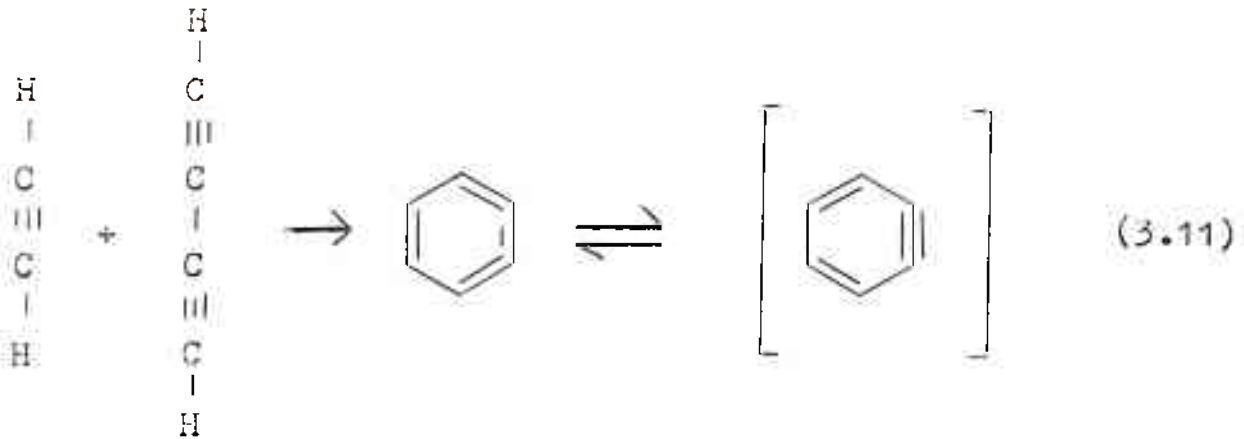


Bond scission of C-C in cyclic rings was also observed by Cypr s and Bredael (1980) during the pyrolysis of decalin and tetralin. The cracking of the ring structures in decalin resulted in a wide range of PAH being evolved.

Aromatic species such as benzene and perinaphthenyl radical have also been proposed as precursors of PAH. Fields and Meyerson (1969), from studies on the pyrolysis of aromatic hydrocarbons at about 1000K proposed schemes such as the following:



Benzynes are formed in aromatic fuel systems as universally as acetylene is in the pyrolysis of aliphatic fuels, and may result from the cyclo-addition of acetylene to diacetylene:



Justification for the perinaphthenyl (PN) radical as an intermediate for PAH is offered by Franceschi et al (1976). PN is stable in solution, is a non-ionic radical with a polycyclic aromatic structure and on pyrolysis evolves higher molecular weight PAHs. A correlation has been shown between PN concentrations and those of high molecular weight PAH in heptane flames stabilised in a vertical reactor. However the steps leading to the formation of the PN radical have ^{not} been delineated.

Bittner and Howard (1980, 1981) in their pioneering work, have obtained mole fraction profiles of fiftyone species by using a molecular beam mass spectrometer system to study a near-sooting flat, low pressure benzene/oxygen/argon flame. It is postulated that C₂-C₅ species are initially evolved as a result of reactions between benzene and oxygen atoms. Radicals are formed by the addition of these non-aromatic hydrogenated species to aromatic compounds. The formation of such stable adducts which can cyclize subsequently, would appear to be the rate-limiting step in the evolution of PAH. Mass addition is

by species such as C_2H_2 , C_4H_4 , C_4H_3 etc. and not by polyacetylenes (Homann and Wagner, 1967, 1968). Heats of various reactions have been computed to determine the relative importance of initial addition steps, steps to stabilise the adduct by the formation of six-membered rings and stabilisation without ring formation. An example of possible free radical addition reactions is shown in Figure 3.3. Further corroboration of free radical mechanisms in the formation of high mass species of molecular weight greater than 700 amu ($M > 700$) is provided by the observation that relatively high mole fractions of benzene, monocyclic aromatics and low molecular weight PAH are found in a region of rapid growth of $M > 700$ species. Smith (1979, 1979a) from shock tube studies on toluene, also observed peak concentrations of phenyl radical, C_4H_4 , C_3H_3 , C_3H_4 etc. (all species which can add mass to radicals) in a region where high molecular weight PAH had maximum concentrations. Further, the sharp decrease of $M > 700$ is accompanied by the disappearance of C_6H_6 and low molecular weight PAHs. Thus, it would appear that the production of monocyclic aromatics such as benzene, toluene, phenyl radical etc. is a controlling factor, and a good mix of these and non-aromatic species such as C_2H_2 , C_4H_4 , C_4H_3 etc. would lead to a rapid growth of PAH. Two mechanisms of growth of PAH have been postulated. In the oxidation zone, where radical concentrations are high, growth is via free radical reactions. However, in the post-flame zone, radical concentrations are substantially reduced, implying that heterogeneous mechanisms on soot surfaces or molecular mechanisms are more likely.

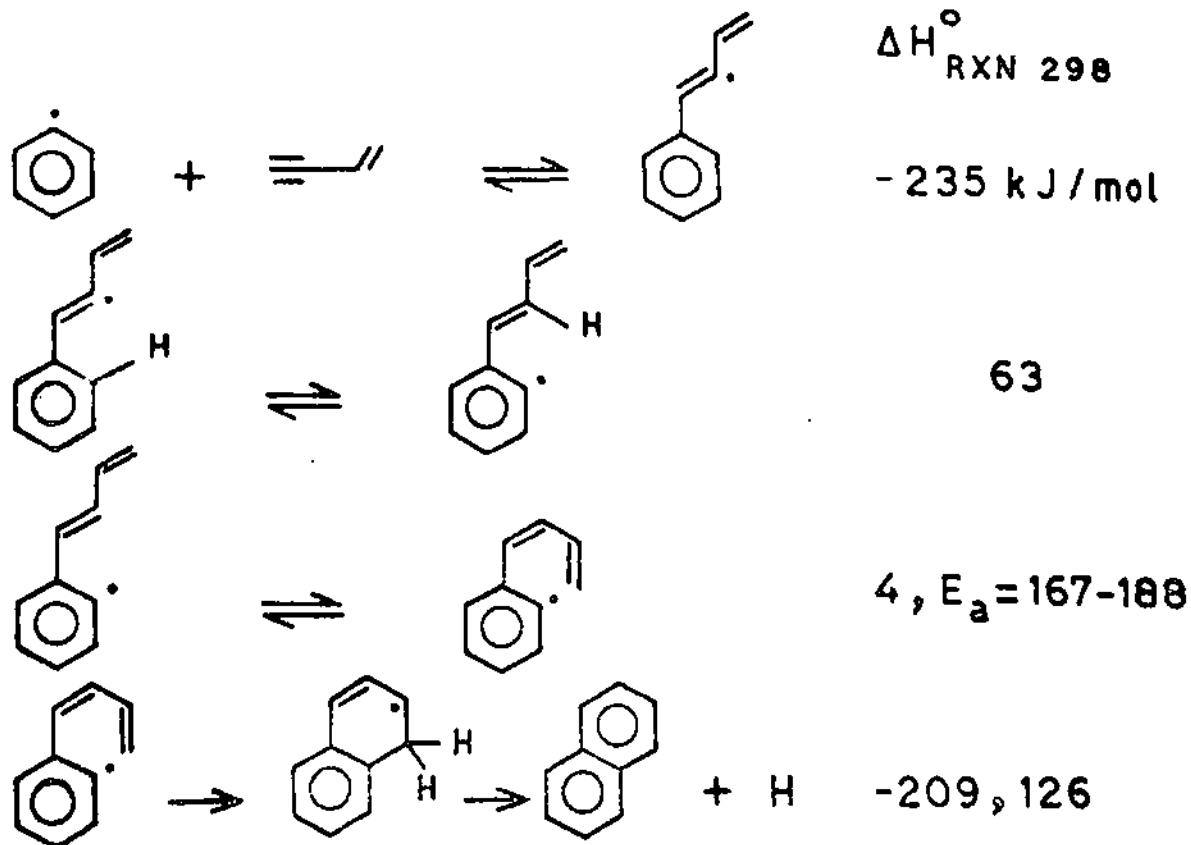


FIGURE 3.3 FREE RADICAL ADDITION SCHEME FOR PAH FORMATION (BITTNER AND HOWARD, 1981)

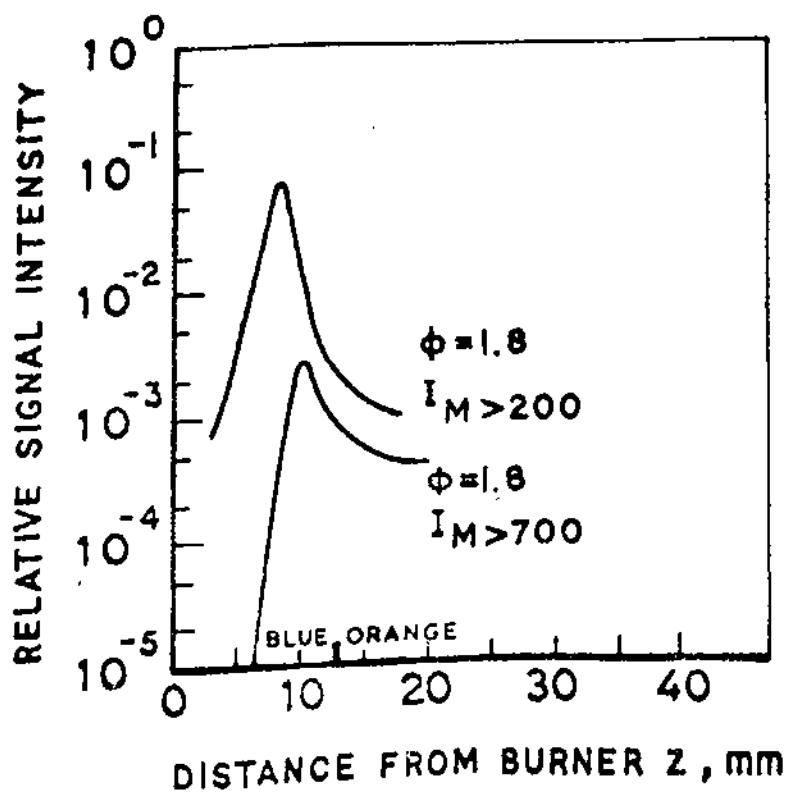
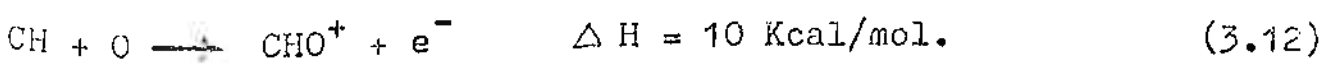


FIGURE 3.4 RELATIVE SIGNAL INTENSITIES VERSUS DISTANCE FROM BURNER (BITTNER AND HOWARD, 1981)

A progression in the maxima of PAH in the mass range 100-200 amu, from 8 to 9 mm above the flame has been observed. There is also a shift in the mass distribution of the 200 to 700 amu species from 8 to 10 mm (Figure 3.4). These observations suggest a sequential growth from smaller aromatic species through PAH of 120-210 amu to heavier species.

Ionic mechanisms have also been proposed for the formation of PAH in flames. Concentrations and mass distributions of charged species have been measured in a premixed sooting C₂H₂/O₂ flat flame at 20 mm mercury (Wersborg et al, 1975). Observed species include heavy hydrocarbon ions and charged soot particles. A sequential growth of high mass charged species is indicated.

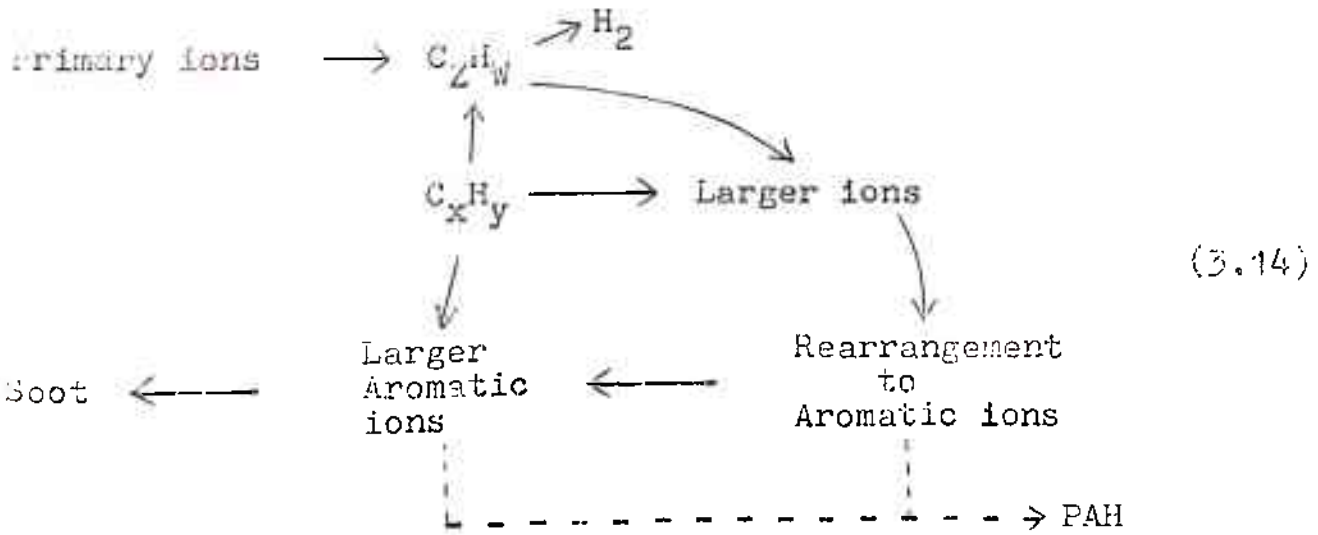
Ions in flames are formed through chemi-ionization and not via thermal processes (Feugier, 1970; Calcote, 1962). The main mechanism could be the formation of CHO⁺ by:



Other ions would be formed by reactions between an ion and a molecule (Lahaye and Prado, 1978), for e.g.

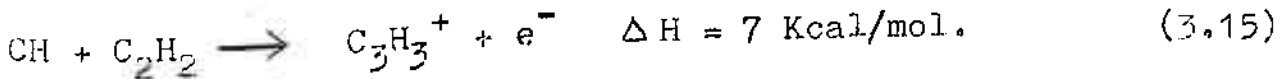


Evidence of the importance of ionic species has been obtained by many investigators such as Wersborg et al, 1973; Calcote, 1978; Haynes et al, 1979; Glassman, 1979; Calcote, 1981; Michaud et al, 1981; Olson and Calcote, 1981; and Smyth et al, 1982. Calcote (1981) suggests the following scheme:

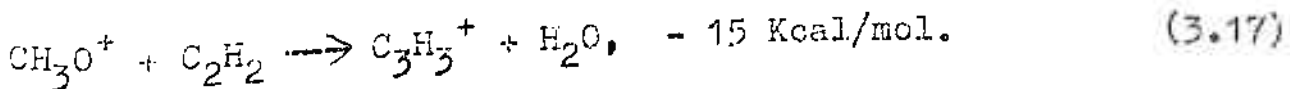
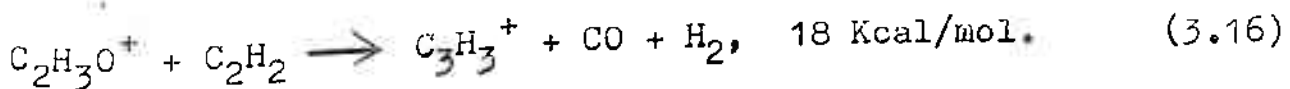


PAH could be formed by neutralization of larger aromatic ions.

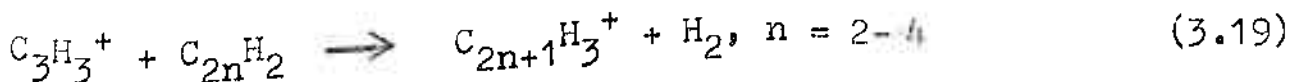
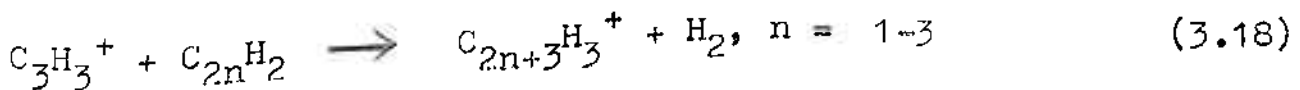
$C_3H_3^+$ has been found to be one of the most abundant ions in a variety of systems (Lahaye & Prado, 1978). This could form by the following reactions in rich flames:



Another possibility is charge transfer in lean flames via:

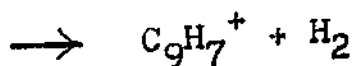
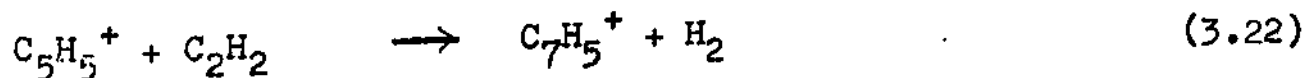
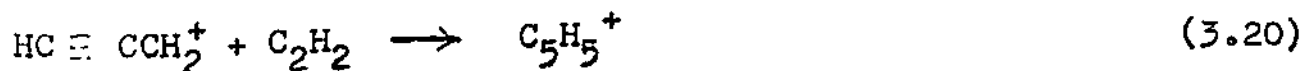


Michaud et al (1981) find that over 80% of the signal by flame ions is due to $C_3H_3^+$. Reactions such as the following could occur:



Smyth et al (1982) confirm the abundance of $C_3H_3^+$ and suggest two structures for it: a cyclopropenium ion which

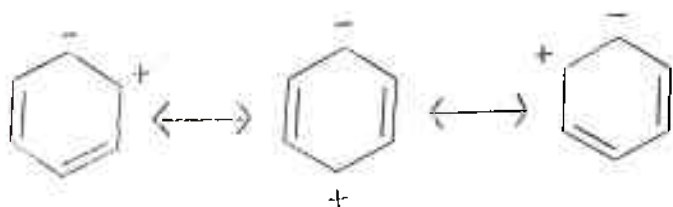
is less reactive, and the more reactive linear propargyl ion. The cyclic $C_3H_3^+$ is found to react with a wide variety of unsaturated hydrocarbons at flame temperatures leading to the rapid production of large PAH molecular ions. Further, the linear $C_3H_3^+$ condenses with acetylene and benzene forming larger PAH ions (some of which could neutralize and form neutral PAH):



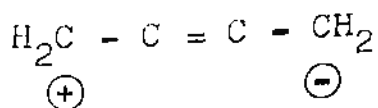
Ionic mechanisms for PAH formation are attractive since isomerization and initial reaction rates are expected to be very fast. In general, free radical reaction rates are slower and rearrangement of linear hydrocarbon chains to aromatic species has a very high activation energy. However, in flame regions, concentrations of ionic species are much lower than free radical species (Homann, 1967, 1968; Olson and Calcote, 1981a; Calcote, 1981). In the post flame zone, ion concentrations are still low compared to neutral reactive species, though in some cases, the ion concentration can exceed

the number concentration of soot (Longwell, 1982). Further, ionic mechanisms cannot explain the tendency in diffusion flames of isomers to soot differently.

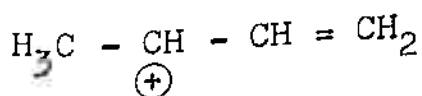
A role for both free radical and ionic mechanisms has been suggested by Glassman (1979). The stability necessary for PAH and soot precursors at high flame temperature is inherent in aromatic species and multiple bond aliphatics which are conjugated and have resonance structures. Some of these resonance structures are polar and can undergo rapid reactions with each other and with other ions and neutral species. For example, the polar resonance structures of benzene are:



1,3-butadiene, earlier postulated as an intermediate in the formation of PAH has the following polar resonance structure:



By addition of hydrogen, 1,3-butadiene can readily form a reactive carbonium ion:



C_2H_2 is unlikely to be a precursor to PAH since it is not polar or conjugated. Diacetylene and vinylacetylene satisfy these requirements.

3.2 PAH - soot Interactions

The interactions of soot with PAH is of considerable interest (Mitra et al, 1982). PAH from combustion sources

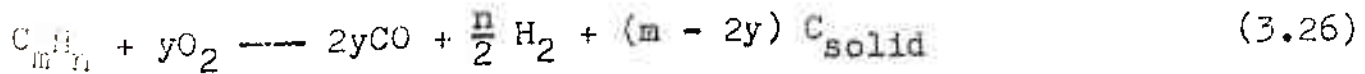
are usually associated with soot, which may play multiple roles — reactant, condensation site, catalyst and transport vehicle. Condensation of PAH onto soot during sampling procedures has an impact on adverse health effects, since PAH laden soot persists in the atmosphere and is subsequently ingested into humans via respiration. Soot surfaces also provide reaction sites on which the oxidation reactions which transform PAH into more potent mutagens may take place. Further, it is probable that PAH may be a precursor to soot formation, that in the hot reaction zones of industrial combustors, PAH may decompose to form soot or react with soot already present.

Soot generated in such processes is not a uniquely defined substance. It contains carbon (greater than 90% by weight), upto 10% (W/W) hydrogen and traces of other elements. A large fraction of the hydrogen can be extracted by organic solvents where it appears mainly in condensed aromatic species. Thomas (1965) has postulated that soot probably consists of highly condensed polybenzenoid structures similar to circum-anthracene. Soot particles collected during their growth show much stronger ESR signals than those of fully developed particles (Wagner, 1979), thus demonstrating the radical character of soot.

Visible soot flocculates comprise agglomerate chains of elementary particles which are nearly spherical and have mean diameters of 100 - 300 Å, corresponding to about 10^6 carbon atoms. The density of these particles is of the order of 2g/cm^3 .

Soot formation, at temperatures ranging from 1000K to 2800K, is usually accompanied or preceded by the formation of

unsaturated hydrocarbons, especially acetylenes and condensed unsaturated ring systems such as PAH. These hydrocarbons are chemically stable as compared to olefins or paraffins. The general tendency of this process can be seen in Figure 3.5 (Wagner, 1979). As can be seen, the growth line of PAH does not lead to soot directly. As Wagner states — "What would be necessary is a condensation of species of the right hydrogen content, a condensation of species with higher hydrogen content and consecutive dehydrogenation, or a combination of both". From a thermodynamic point of view, the formation of soot should start when 'm' in



becomes equal to or larger than 2y, that is when the C/O ratio exceeds one. However, experimentally, soot is observed to occur at C/O ratios as low as 0.5.

Of a large variety of the "right" kind of species, PAH radicals have most of the necessary properties to be soot precursors. They can survive the high flame temperatures, are very stable due to resonance, can accommodate considerable energy (thermal and chemical) without dissociating, and can undergo fast free radical reactions and Diels-Alder type condensations (Thomas, 1965).

Direct evidence from experimental systems shows that in a variety of cases, PAH or PAH type substances peak in concentration prior to the buildup of soot, implying that PAH are important in the soot formation mechanisms.

Concentration profiles of PAH run through maxima and decrease when carbon is formed in benzene-oxygen flames (Homann

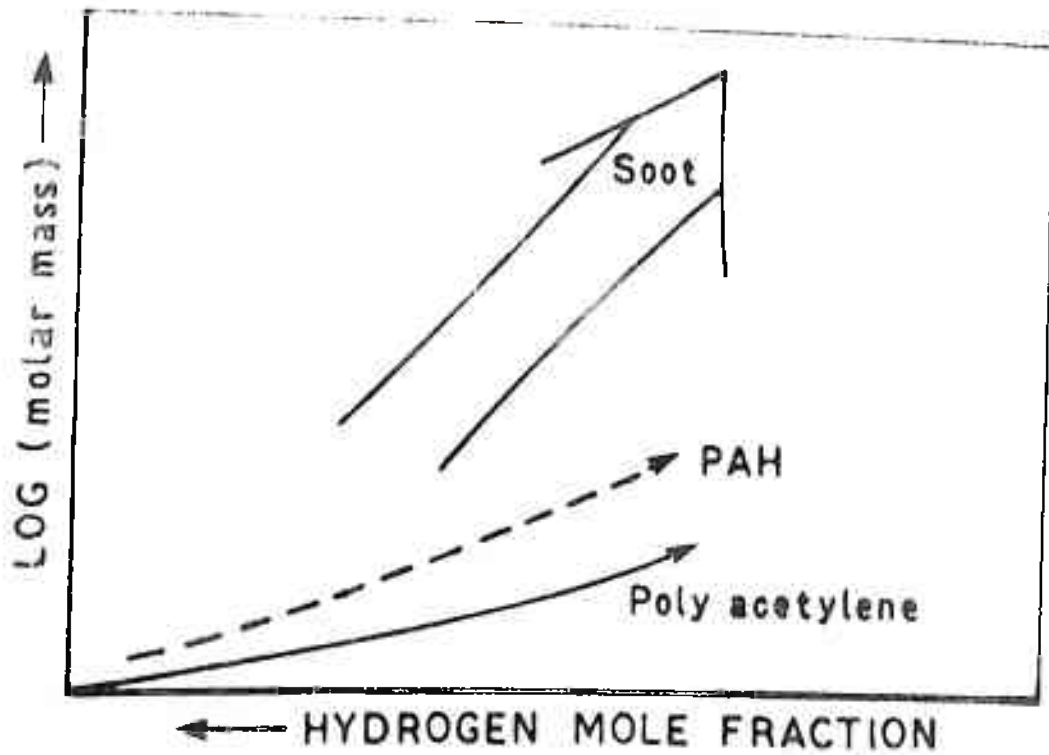


FIGURE 3.5 PATHWAYS FOR SOOT FORMATION
(WAGNER, 1979)

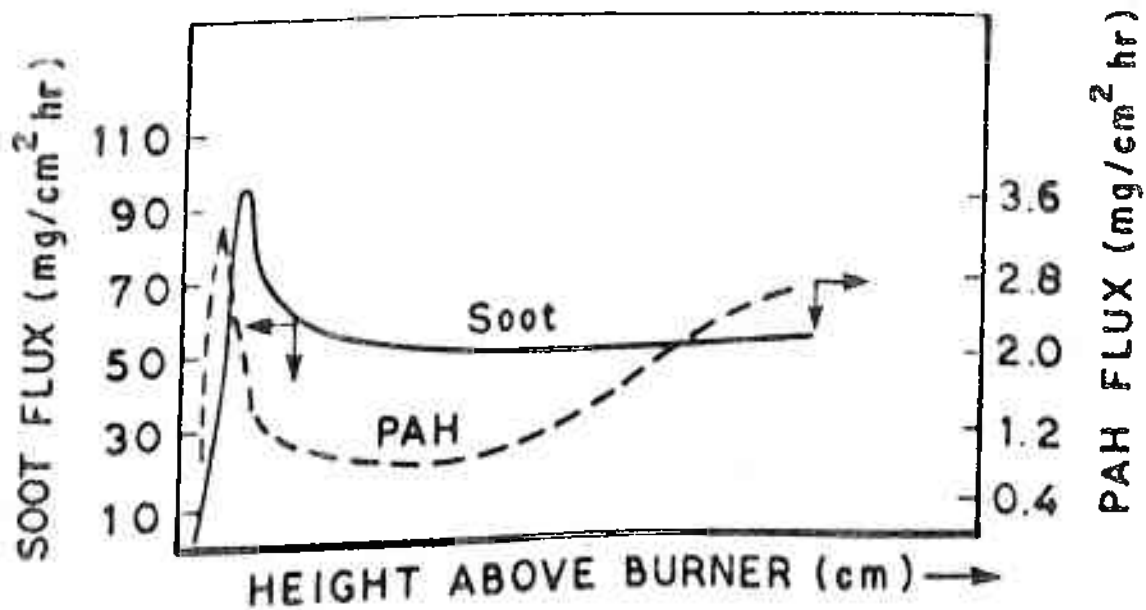


FIGURE 3.6 PAH AND SOOT FLUXES IN A PREMIXED
 C_2H_2/O_2 FLAT FLAMES (TOMPKINS AND LONG,
1969)

and Wagner, 1967). The PAH are already formed in the oxidation zone which mainly contains C_6 species and PAH.

Tompkins and Long (1968) observe that in their premixed C_2H_2/O_2 flat flames, total PAH concentrations reach a maxima 0.5 cm prior to the soot maxima. These maxima are early in the flame just beyond the blue-green zone, and just after the peak flame temperature of about 1600K (Figure 3.6).

As oxygen mole fractions are increased from 0.18 to 0.26 in a $C_2H_4/O_2/N_2$ diffusion flame (Chakraborty and Long, 1968), soot concentrations increase by about 16%, carbonaceous residue (CR) by 100%, whereas PAH and chloroform soluble materials (CSM) decrease to zero (Figure 3.7). As the oxygen concentration increases, temperatures increase and due to enhanced pyrolysis, soot formation should increase initially. However, as the concentration of oxygen gas increases that of the oxidisers O, OH also rise in concentration and thus rates of reactions with soot precursors should also be enhanced leading to a decrease in soot formation. These two competing routes balance at an oxygen mole fraction of 0.26, subsequent to which increased diffusion of OH into the pyrolysis zone essentially consumes all the PAH and combustion of soot takes over.

While studying the thermal decomposition of benzene, Prado (1972) measured the yields of carbon black, pyrolytic carbon and tars. Fuel concentrations were 2% molal benzene in nitrogen and the pyrolysis temperature was about 1400K (Figure 3.8).

Tars, obtained by benzene extraction of carbon black, consist primarily of PAH (Palmer et al, 1968; Ray and Long, 1964, 1968) and are seen to peak and then decrease as soot formation

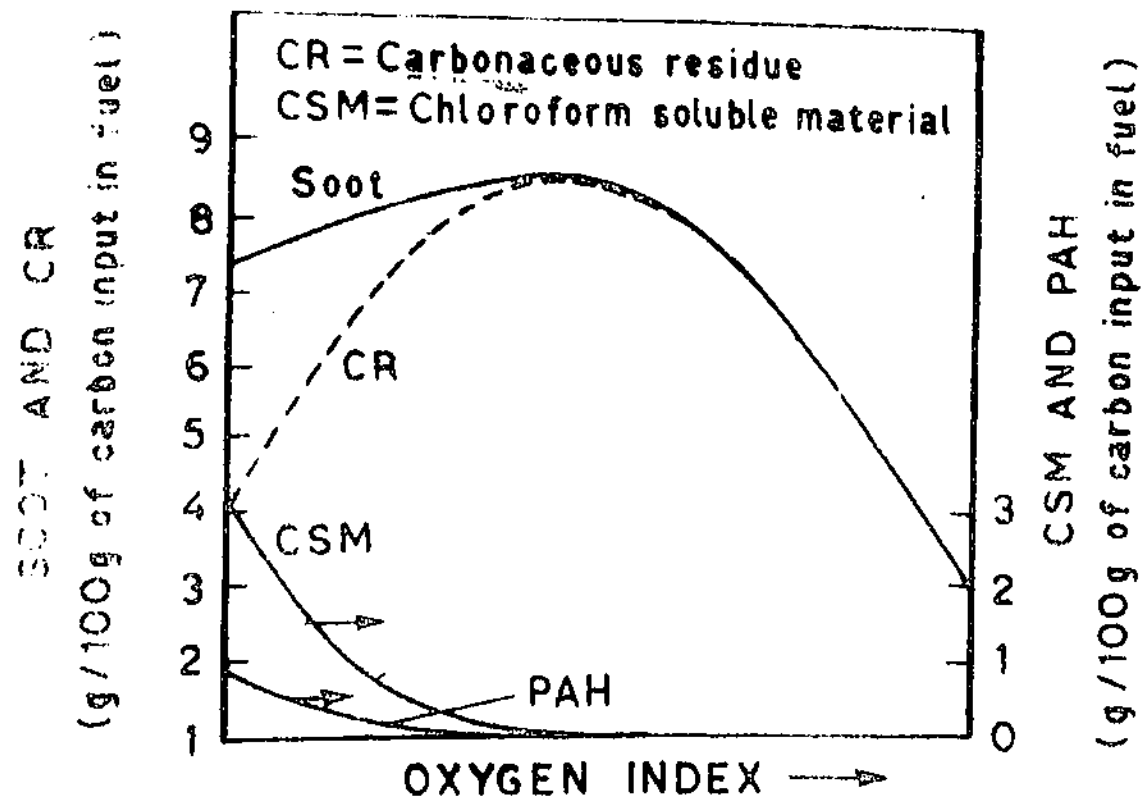


FIGURE 3.7 PAH, SOOT, CARBONACEOUS RESIDUE AND CHLOROFORM SOLUBLE MATERIAL IN A $C_2H_4/O_2/N_2$ DIFFUSION FLAME (CHAKRABORTY AND LONG, 1968)

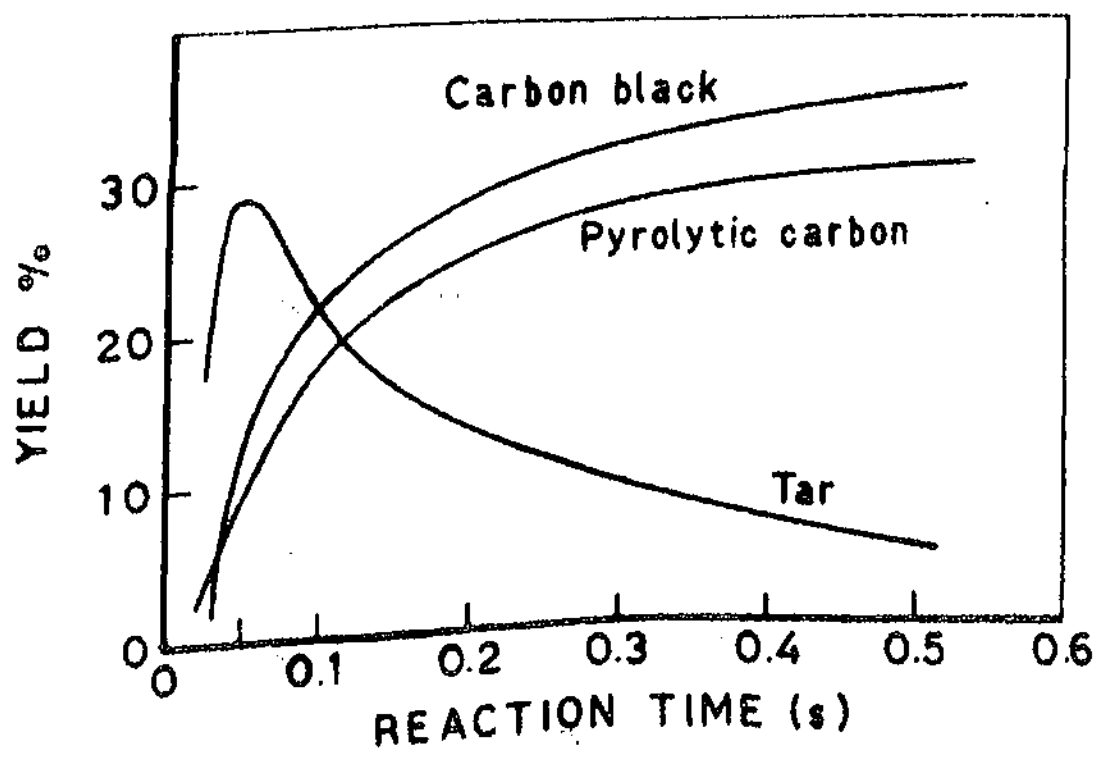


FIGURE 3.8 CARBON BLACK AND TAR YIELDS DURING THE THERMAL DECOMPOSITION OF BENZENE (PRADO, 1972)

reaches asymptotic values. Zaghini et al. (1972) also observe that the size of soot agglomerates increases after the yellow flame, in a region corresponding to the maximum concentration of PAH.

The 'reactive' PAH are found to peak prior to soot formation (Figure 3.9) in atmospheric premixed CH_4/O_2 flames (D'Alessio et al., 1975); however, the 'unreactive PAH' increase in concentration with height above the flame. The above authors deduce that though the reactive PAH are precursors in the soot formation route, their contribution would be only of the order of 2 to 3% of the soot formed.

Profiles of PAH exhibit a maximum just upstream of the soot maximum in turbulent benzene/air and kerosene/air flames studied by Prado et al. (1977). The decrease in PAH concentration is more drastic than for soot (Figure 3.10), strongly indicating that PAH are intermediates of soot formation. Though the authors speculate that this could also be possible if PAH burnout were faster than that of soot, local turbulent mixing conditions would indicate that this is less likely. Further, the rate of decrease in PAH concentration is faster for benzene flames than that for kerosene flames, though the mass loading for the former, more aromatic fuel is over three times as much as the latter. This again implies that PAH are precursors of soot. They are observed to be present in greater concentrations in the aromatic flame and would form soot faster (and hence decay faster) than in the kerosene flame.

It was generally found that long chain alkylated PAH in fuels such as Solvent Refined Coal (SRC-II) either disappeared or were present in the effluent in very low concentrations, during

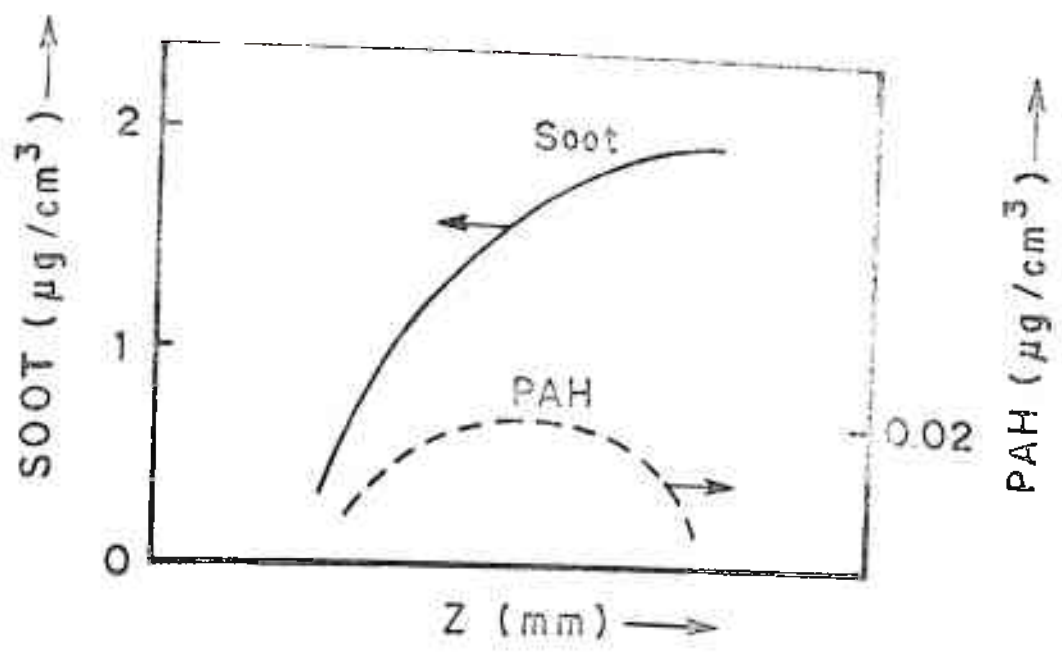


FIGURE 3.9 PAH AND SOOT YIELDS FROM AN ATMOSPHERIC PRESSURE PREMIXED CH₄/O₂ FLAME (D'ALESSIO et al, 1975)

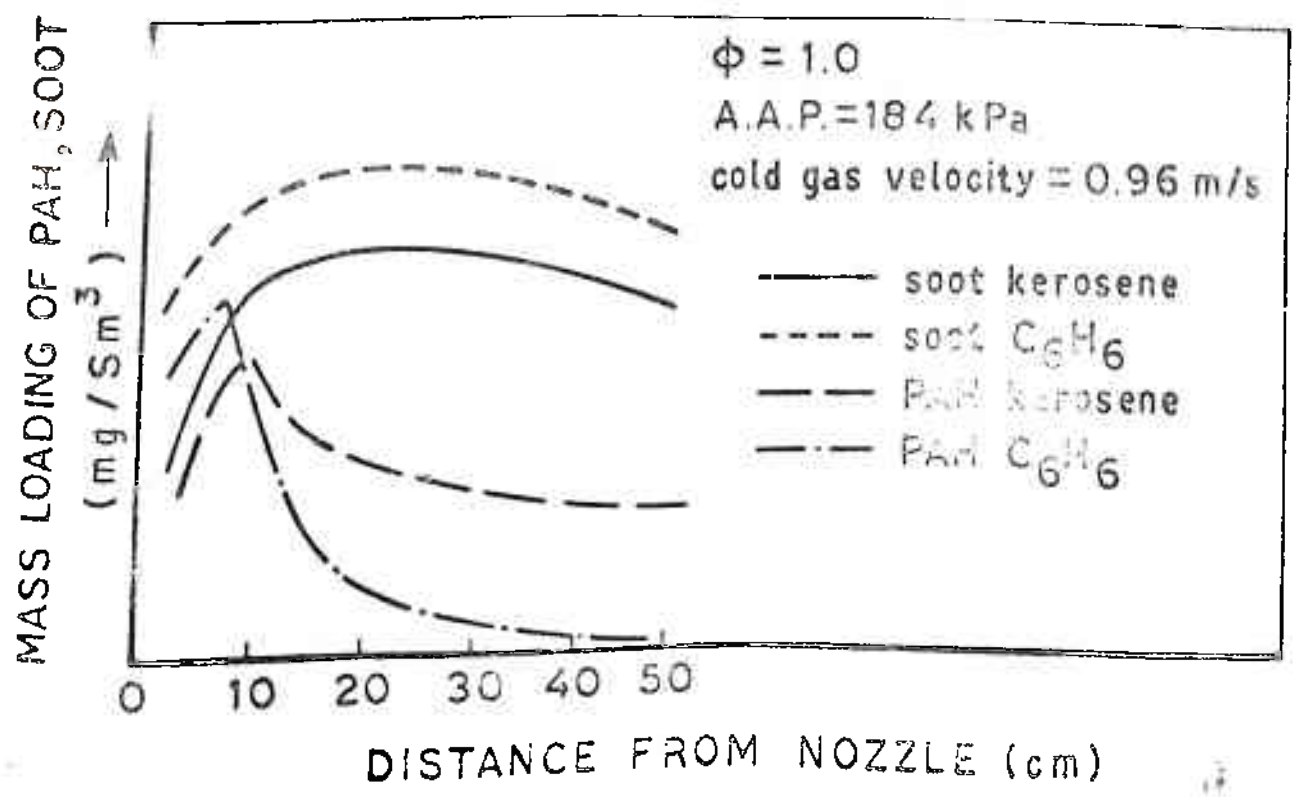


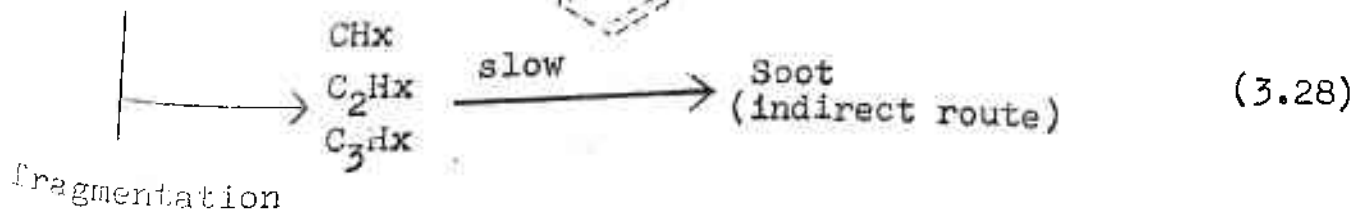
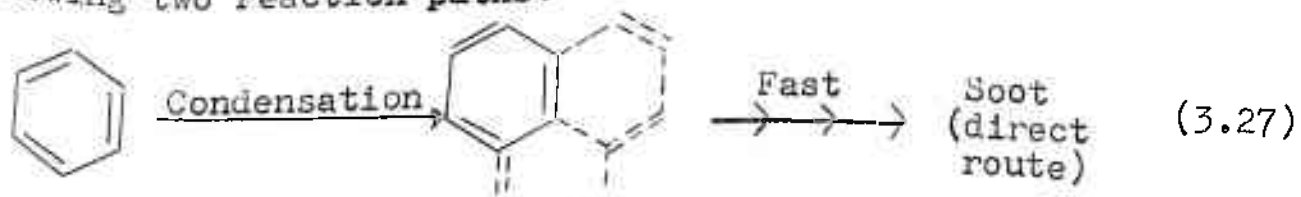
FIGURE 3.10 PAH AND SOOT YIELDS IN TURBULENT KEROSENE AND BENZENE DIFFUSION FLAMES (PRADO et al, 1977)

combustion in staged and unstaged 1MW turbulent combustors (Bicer et al, 1982). Compounds such as acenaphthalene or naphthalene were pyrosynthesized, whereas unreactive (Lewis ^{and} Edstrom, 1963) PAHs such as pyrene, fluoranthene, phenanthrene and anthracene were quite resilient to burnout. Various PAH decreased sharply in concentration along axial distances, as soot formation increased to peak values in an SRC-II heavy distillate flame under unstaged combustion (Figure 3.11). Similar trends were observed during staged combustion, suggesting that PAH were consumed by the soot formation process, leaving only stable ^{to} 3/5 ring species.

Vranos and Liscinsky (1983), from pyrolysis of n-tetradecane in free droplet vapourization, observed that PAH attained a maximum level of about 1400K before appreciable soot production commenced (Figure 3.12). The majority of the PAH identified contained four rings or less. Maximum PAH levels shifted to higher temperatures at reduced residence times.

Graham et al (1975) have observed two regions of soot formation in their shock tube studies on aromatic hydrocarbons; at temperatures below 1750K, the rate of soot formation increases very rapidly, whereas at higher temperatures, soot yield is drastically reduced. This suggests a competition between the

following two reaction paths:



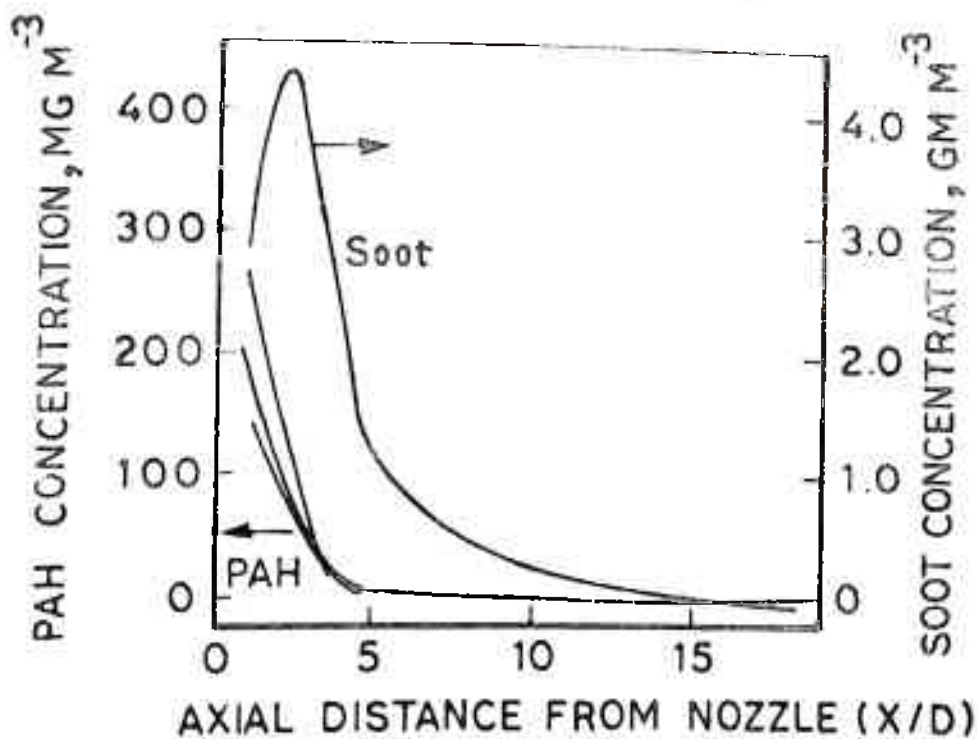


FIGURE 3.11 PAH AND SOOT PRODUCTION IN A 1MW UNSTAGED UNSTAGED TURBULENT COMBUSTOR BURNING SRC-II (BEER et al, 1983)

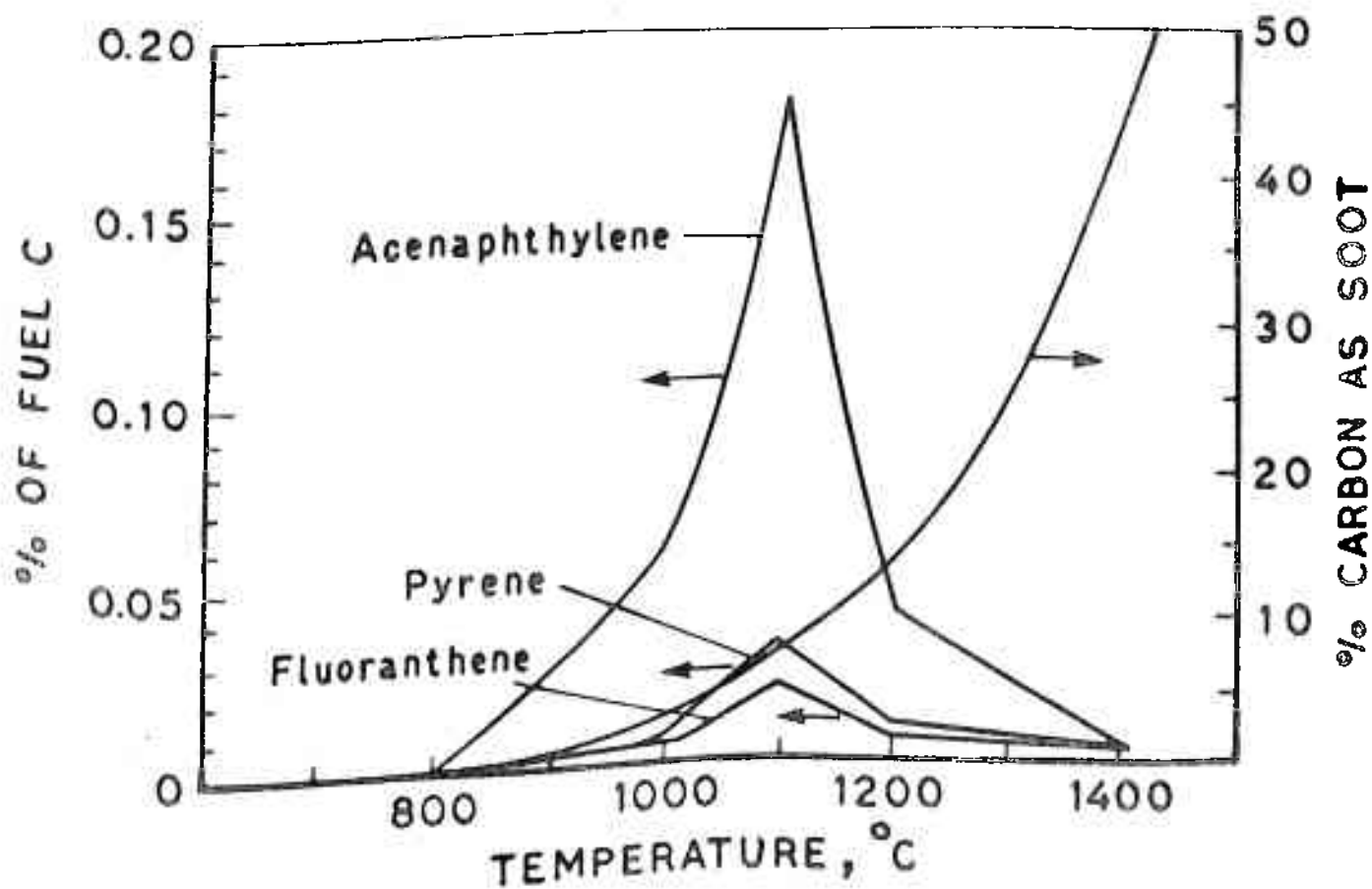


FIGURE 3.12 PYROLYSIS OF n-TETRADECANE: PAH AND SOOT EVOLUTION (VRANOS AND LISINSKY, 1983)

By the direct route aromatics undergo condensation reactions, proceeding via intact PAH to soot. Graham (1977), Marsh (1975) and Bonnet et al (1974) have also suggested that soot may be formed by polymerization/dehydrogenation of the sub-microscopic liquid crystalline droplets of molecular PAH, produced during gas phase pyrolysis at low temperatures by reaction 3.27.

Macromolecules of polycyclic character could be synthesized during gas phase reactions of hydrocarbons at 1100°C and a residence time of about 1s (Lahaye / Prado, 1978). The partial pressure of these macromolecules would increase with time till supersaturation would cause physical condensation into droplets, at which point, no further formation of liquid nuclei would be likely. The macromolecules still present would maintain nuclei growth formation and would ultimately crack thermally to produce solid soot. Albright and Yu (1979) have suggested a similar mechanism for coke formation from the pyrolysis of acetylene, butadiene and benzene in tubular reactors. Physical condensation of PAH and heavy hydrocarbon molecules (produced in the gas phase) could take place in the form of liquids on the reactor walls, where they would subsequently decompose to coke and other products.

Calcote (1981) in his review of mechanisms of soot nucleation processes in flames, has proposed an overall process from primary molecular species to soot aggregates, assuming ions as the nucleating agent (Figure 3.13). Various polycyclic aromatic ions have been observed in sooting C₂H₂/O₂ flames, ranging up to C₁₉H₁₁⁺, a five ring PAH ion. Other details on PAH ions and their formation have already been discussed in Chapter 3.1.

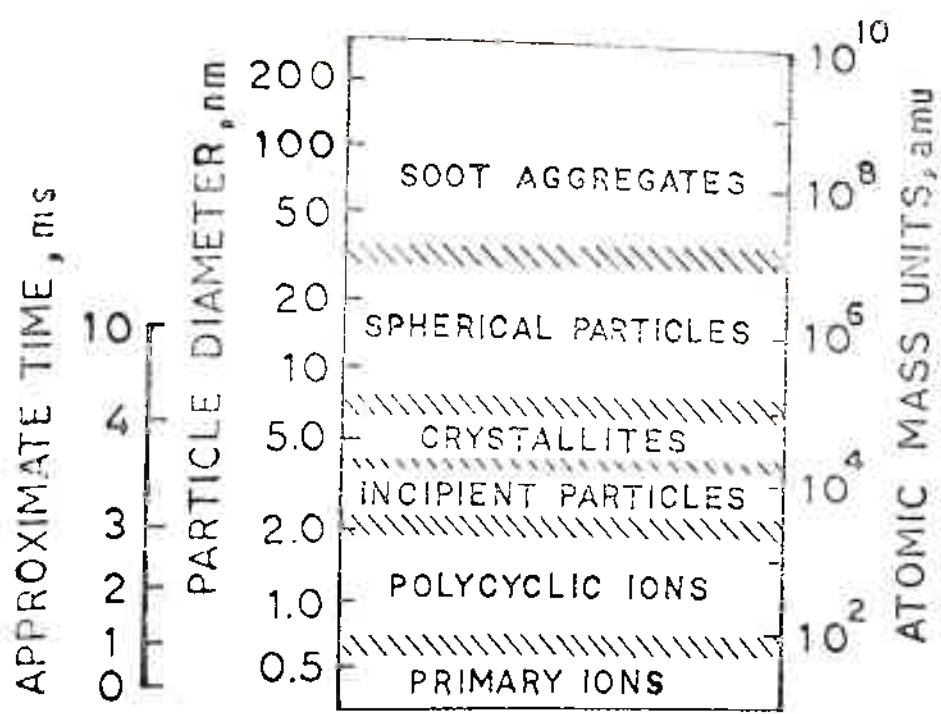


FIGURE 3.13 GROWTH OF SOOT AGGREGATES WITH IONIC SPECIES AS NUCLEATING AGENTS (CALCOTE, 1981)

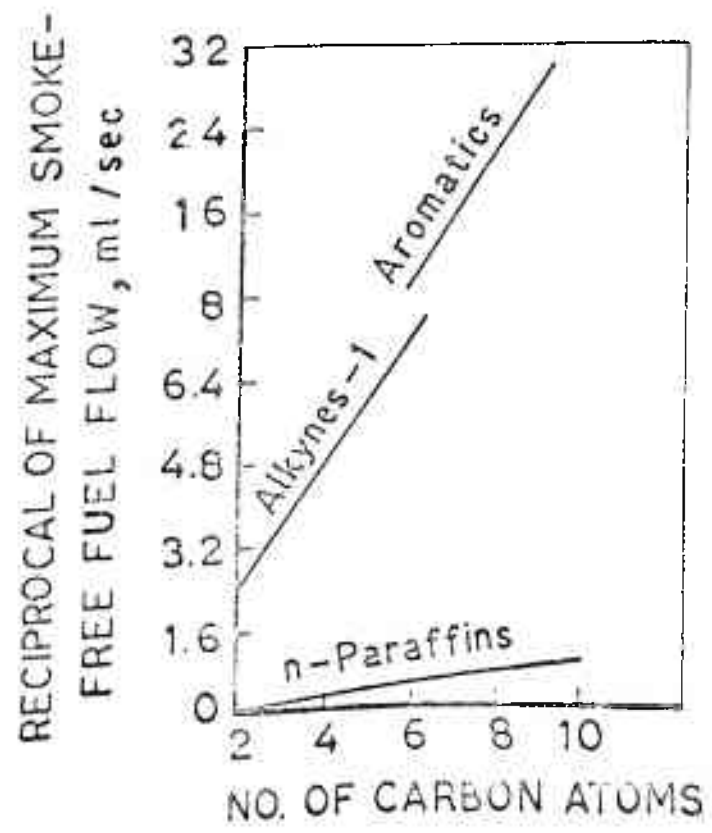
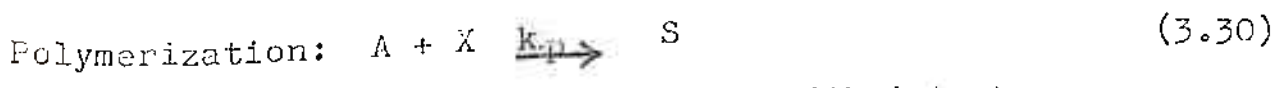
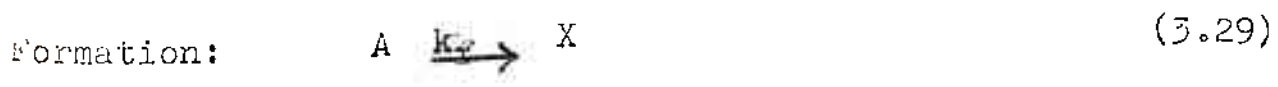


FIGURE 3.14 EFFECT OF THE NUMBER OF CARBON ATOMS IN HYDROCARBON FUELS IN THEIR SOOTING TENDENCIES (SCHALLA AND McDONALD, 1953)

Frenklach et al (1983) have investigated soot formation in toluene-argon mixtures behind reflected shock waves. S-shaped curves were generated for soot yields as a function of residence time, a shape very characteristic of autocatalytic reactions. They suggest that soot formation from aromatic hydrocarbons is controlled more by kinetic, rather than equilibrium considerations since the maximum in soot yield is found to depend on factors such as observation time, pressure and the wavelength used in measurement. The following kinetic skeleton is suggested:



- where A = aromatic species with intact rings
- X = fragmented ring species
- S = soot

The computed profiles of soot yield are very similar to actual data on soot yield versus temperature. The reactions 3.29 and 3.30 also explain the autocatalytic trends observed. These similarities can be explained only if $A \rightarrow X$ is the decomposition of the parent aromatic hydrocarbon to its fragments. The attack of X on A is similar to reactions of C_2H_2 type species with an aromatic ring, postulated by Bittner and Howard (1981).

It has also been suggested that PAH isolated from most combustion systems do not participate directly in soot formation processes. They may be stable byproducts of premature chain termination reactions and consist primarily

of non-substituted PAH (Thomas, 1965; Bonne et al, 1965; Homann, 1967; Pasternak et al, 1981; Longwell, 1982; Beer et al, 1982). Lewis and Edstrom (1963) have defined two classes of PAH, thermally 'reactive' and thermally 'unreactive' (see Tables 3.1, 3.2). The former class forms tars under pyrolysis at temperatures of about 1000K, whereas the latter distill in the absence of any reaction. The PAH isolated from flames have generally been observed to be of the unreactive type. Yokono et al (1979) corroborate Lewis and Edstrom (1963) by computing free valences (Fr) of atoms in PAHs, where Fr is a measure of the free radical tendency of a PAH. Brown (1950) calculates the reactivities of various species to Diels-Alder addition reactions. The 'unreactive' PAH show very little reactivity. Thus, PAH species which could be intermediates in soot formation are the 'reactive' kind, PAH radicals, large polycyclic ions, and substituted PAH containing alkyl side chains, known to be very reactive in chain propagation reactions.

Various investigators have also concluded that PAH cannot function as intermediates in soot formation mechanisms.

Parker and Wolfhard (1950) found no absorption bands for naphthalene or anthracene in benzene flames. However, these species may be stable enough to escape and other polycyclic species have been found by other workers in such flat flames. They also proposed a mechanism involving polymerization, followed by 'graphitization' of large polymers. A major objection to this scheme is that if these polymers are not polycyclic in nature, steric hindrance to the liberation of hydrogen atoms from large polymers would preclude such a mechanism.

TABLE 3.1Thermally "Reactive" PNA

No.	PNA	M.A. (1)	I.P. (2)	Fr(max) (3)
1.	Pentacene	-	6.23	0.540
2.	Dibenzo (a,i) pentacene	-	6.40	0.536
3.	9,10 Benzylanthracene	-	7.07	0.534
4.	Dibenzo (def, mno) chrysene	-	6.86	0.531
5.	Dibenzo (a,i) pyrene	-	7.07	0.531
6.	Naphthacene	9250	6.64	0.530
7.	Dibenzo (b,k) chrysene*	-	6.95	0.517*
8.	Tribenzo (a,e,i) pyrene*	-	7.16*	0.513*
9.	9,9' - dianthranyl	-	-	-
10.	9,9' - difluorenyl	-	-	-
11.	9,9' - bifluorylidene	1370	-	-
12.	Decacyclene	-	-	-
13.	Acenaphthylene	1030	-	-

Criteria for "Reactive" PNA:

- (1) M.A. > 950 (Lewis and Edstrom, 1963)
 (2) I.P. < 7.10 eV (Lewis and Edstrom, 1963a)
 (3) Fr (max) > 0.530 (Yokono et al, 1979)

* = Exceptions

TABLE 3.2

Thermally "Unreactive" PNA

No.	PNA	M.A. ⁽¹⁾	I.P. ⁽²⁾	Fr(max) ⁽³⁾
1.	Benzene	1	10.00	0.399
2.	Diphenyl ether	2.5	-	-
3.	Pyridine	3	-	-
4.	Biphenyl	5	8.69	0.436
5.	Triphenylene	-	-	0.439
6.	Acenaphthene	11	-	-
7.	Naphthalene	22	8.12	0.452
8.	Phenanthrene	27	8.03	0.451
9.	3,4 - benzophenanthrene	-	-	0.451
10.	Fluoranthene	-	-	-
11.	Quinoline	29	-	-
12.	Isoquinoline	36	-	-
13.	Chrysene	57.5	7.72	0.457
14.	Picene	-	7.62	0.457
15.	Benzo (e) pyrene	-	7.60	0.464
16.	Pyrene	125	7.56	0.469
17.	Perylene*	-	6.84*	0.477
18.	Fluorene	300	-	-
19.	Acridine	430	-	-
20.	Dibenz (a,h) anthracene	-	7.42	0.498
21.	Dibenz (a,c) anthracene	-	7.43	0.499
22.	Dibenz (a,j) anthracene	-	-	0.510
23.	Dibenzo (a,e) pyrene	-	7.23	0.512
24.	Benzo (a) anthracene	515	7.35	0.514

TABLE 3.2 (contd.)

No.	PNA	M.A. (1)	I.P. (2)	Fr(max) (3)
25.	Anthracene	820	7.22	0.520
26.	9-phenylanthracene	-	-	-
27.	1-1' binaphthyl	-	-	-
28.	Dibenzo (a,1) pyrene*	-	7.05*	0.526
29.	Benzo (a) pyrene	-	7.31	0.529
30.	Coronene	-	7.50	0.437

Criteria for Thermally "Unreactive" PNA,

(1) Methyl Affinity, M.A. < 950
(Lewis and Edstrom, 1963)

(2) Ionization Potential, I.P. > 7.10 ev
(Lewis and Edstrom, 1965a)

(3) Free Valence at atom r, Fr(max) < 0.530
(Yokono et al, 1979)

* = Exceptions

Garner et al (1953) did not find any diphenyl in sooting paraffinic or naphthenic fuels and concluded that PAH were unlikely to be intermediates. Here again it must be stressed that other PAH could be present as intermediates but were not identified by these workers.

Schalla and McDonald (1955) state that a breakdown to smaller products must occur rather than a growth to aromatic ring structures in diffusion flames. Smoke formation would then occur through a simultaneous polymerization and dehydrogenation of small molecules such as acetylene and hydrocarbon fragments.

Stehling et al (1962) suggest that since aromatic hydrocarbons such as benzene and naphthalene are less reactive than acetylene or vinylacetylene under pyrolytic conditions, it is unlikely that in general soot is formed by polymerization of C_2H_2 to PAH followed by dehydrogenation/condensation. Reactions such as $Ar - H + H - Ar \rightarrow Ar - Ar + H_2$ are thermodynamically feasible but are not self-propagating. Further, orientation and entropy factors from successive steps to produce condensed ring structures from simpler aromatics would imply reactions too slow for the soot formation time scales observed.

That PAH type macromolecules are byproducts of thermal decomposition of hydrocarbons, was stated by Johnson and Anderson (1962). They concluded that large amounts of polymers are obtained in situations where no soot appears, that soot and polymers are formed by two competing reactions in the gas phase and that the "continued increase in the size and number of solid particles under conditions where liquid polymer is not produced provides additional evidence contradicting the theory of carbon formation from polymers".

As discussed earlier, Lewis and Edstrom (1963) observed that there existed a large class of unreactive PAHs which would distill and not form soot under low temperature pyrolytic conditions.

Bonne et al (1965), Homann and Wagner (1967) and Homann (1967) observe that in premixed C_2H_2 flames, PAH evaporated from soot sampled beyond the oxidation zone and PAH sampled in the gas phase by a molecular beam system are identical. Thus, they infer that PAH condense with soot during sampling procedures. PAH are formed later than polyacetylenes which reach a maximum at the end of the reaction zone, in a region where nuclei for carbon particles are formed. Further, total PAH concentrations are of the order of 10^{-2} mole % of the burned gas, and their concentration increases steadily behind the oxidation zone without passing through a maxima. From these observations, they infer that PAH cannot be important intermediates for soot formation. D'Alessio et al (1975) also conclude that unreactive PAH are byproducts of soot formation reactions and that reactive PAH contribute at most 2/3% to total soot mass loadings.

Lahaye and Prado (1978) confirm that it is possible to obtain PAH in the absence of soot. Under conditions such as low residence times and low molal fractions of initial hydrocarbon, the vapour pressure of PAH type macromolecules would be insufficient to induce nucleation in the bulk of the reactor. At the reactor exit, where temperatures would be lower than under reactor conditions, condensation of these macromolecules could occur without their transformation into carbon black particles. Longwell (1982) observed that for toluene, increasing ϕ from

very little effect on the evolution of PAH. In an n-heptane flame an intermediate quantity of soot was formed, though PAH production was larger. Thus, adjustment of a rich mixture flame to reduce soot formation will not automatically reduce PAH.

3.3 The Influence of Fuel Type

Projected shifts to lower grade fuels increase the possibility of adverse health effects due to higher production of mutagenic and carcinogenic species. Fuels themselves contain widely varying amounts of PAH (Longwell, 1982). Gasoline may contain small amounts of naphthalene and alkyl naphthalenes in its high boiling fractions. Automotive diesel fuel and No. 2 residential heating oil can contain many higher molecular weight polycyclics such as the mutagenic alkyl phenanthrenes and alkyl anthracenes. Such liquid fuels, vapourized and mixed with hot combustion products can pyrolyze and oxidise. Mutagenic and carcinogenic species so formed may bypass the flame zone and condense on to soot and other particulates in the effluent. Significant fractions of unburned fuels and pyrolysis produced tars may escape to the atmosphere when burning synthetic fuels such as H-coal and in the case of domestic stoves and fireplaces. Gross (1972) observes that as the PNA content of commercial gasoline is increased during combustion in automobile engines, PNA emissions are correspondingly higher. Detailed analysis of light fuel oil and of the emissions from a domestic oil oven demonstrate that the emitted aromatics can be unburned residues from the fuel charge (Herlan, 1978). Large quantities of

oxygenated polyaromatics are detected in the exhaust gas, some of which are direct acting mutagens and need no activation. Sources of PAH emissions are evaluated in Appendix B.

It is thus clear that it is necessary to examine the effect of fuel type on sooting and emissions of PAH during combustion. This section discusses some qualitative trends observed in a variety of combustion systems.

The most important distinction may be made between aromatic and aliphatic fuels. Franceschi et al (1976) observe that total PAH in the exhaust of a vertical flow reactor is strongly linked to the aromaticity of the fuel. Thus, ratios of PAH to that produced while burning the aliphatic n-heptane are as follows:

(n-heptane + 10% toluene) : (n-heptane + 10% mesitylene) :
(n-heptane + benzene) : (n-heptane)

17.5 : 10.5 : 5.7 : 1.0

benzene fuel evolves over three times as much PAH and soot as mesitylene in a turbulent diffusion flame (Prado et al, 1977). For example, at a sampling location of 4 cm above the burner, the values for PAH are 802 mg/Sm³ and 75 mg/Sm³ respectively. Further, in the aromatic flame, PAH (and soot) are generated earlier implying faster reactions mechanisms. Pasternak et al (1981) however observe that an aliphatic polymer, polypropylene evolves more PAH than polystyrene, in both flaming and non-flaming modes. In another investigation though (Jagoda et al, 1980) polystyrene evolves PAH in greater quantities than polypropylene, for which no PAH is observed in the pyrolysis zone. PAH is observed in the former in both the pyrolysis zone and the flame front but only in the flame front in the latter. Whereas

the concentration of polycyclics in the burned gas from a premixed H_2 flame is roughly 10^{-2} mole percent, that of benzene is of the order of 1.0 mole percent, for the same C/O ratio (Homann and Wagner, 1967).

Sooting tendencies of fuels are generally as above for PAH aromatic fuels produce greater quantities than aliphatics under similar conditions (Thorp et al, 1951; Calcote and Manos, 1953). When plotted as a function of the number of carbon atoms, it is clear that aromatics have the greatest tendency to soot (figure 3.14). Various workers have reported sooting propensity in diverse fuel systems. For premixed flames, Street and Thomas (1955) and Schalla et al (1957, 1959) observe the following sooting propensity to soot:

naphthalenes > benzenes > alkanes > alkenes > acetylenes

in diffusion flames, Clark et al (1946) and Schalla and Donald (1955) report the following sooting order:

naphthalenes > benzenes > alkynes > alkenes > alkanes

However, such general categorizations could be misleading since they ignore flame parameters such as temperature, oxygen concentration (discussed in Chapter 4) and detailed fuel structures.

Quantitative soot yields are provided by Davies and Scully (1956) from a premixed flame; whereas indene (53%) and ethylbenzene (21%) yields are high, that for acetylene is only 4%.

Further, the critical equivalence ratio for soot formation, ϕ_c , is found to increase from aromatic to aliphatic hydrocarbons:

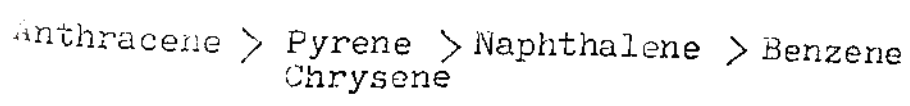
Fuel	ϕ_c	
Oxylene	1.45	
Toluene	1.46	
Benzene	1.54	
Cumene	1.56	
Octane	1.73	
Hexane	1.75	
Propane	1.73	(from Miller and
Cyclo-hexane	1.74	Calcote, 1977:
Acetylene	2.00	Meker burner)

Thus, greater quantities of oxygen are required to burn the same fuel if it is aromatic rather than aliphatic. Glassman and Yaccarino (1981) explain this by stating that at a given stoichiometry, an aromatic is "richer" than an aliphatic mixture, presumably because two / ^{carbon} atoms in the ring form carboxyl groups and thus the oxygen demand is greater. Bittner and Howard (1980, 1981) note that the initial aromatic structure has the ability to undergo substitution reactions readily, and thus has a propensity for forming PAH and soot. Glassman (1979) also speculates that those fuels such as aromatics which have a greater ability to form multibonded radicals with polar resonance structures, should have the greater tendency to soot.

Various trends are observed within the class of aromatic fuels with respect to tendency to evolve PAH and soot. In general, increasing the number of rings leads to an increase in PAH and soot formation. Thus, Pasternak et al (1981) report the following values for the yields of PAH (mg/g of combusted material):

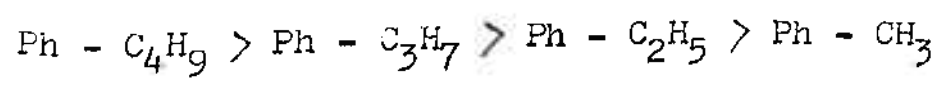
Benzene	7.2
Naphthalene	15.0
Anthracene	32.5
Pyrene	36.6

A similar trend was observed for soot yields. Kinney and DelBel (1954) report the following trend with respect to ease of conversion to soot during pyrolysis:



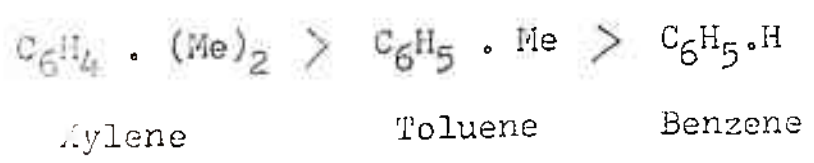
It should be noted that for PAH of larger than three rings, orientation factors could cause steric hindrance and thus reduce soot yields.

Alkyl substitution at carbon atoms on the aromatic ring and markedly increases PAH and soot yields (Davies / Scully, 1956). Frazee and Anderson (1959) observe that substitution by a methyl group has more effect than increasing the number of rings; thus toluene has greater sooting tendencies than naphthalene. As the length of the side chain and the number of side chains increases, PAH and soot production is usually higher. From pyrolysis studies, Badger et al (1960, 1960a) observe that PAH evolution is in the following order:



As the length of the side-chain is increased the PAH mass distribution shifts to those of higher molecular weight. Calcote and Manos (1983) however note that in premixed and diffusion flames, though sooting increases with sidechain substitutions in aromatics, increasing the length of the sidechain results in reductions in soot yields. An increase in polymerization

during carbon black manufacture results in higher yields (Scully & Davies, 1965) as the number of methyl substituents increases, namely:



Similar trends are observed by Hunt (1953) and Nakanishi et al (1981). Hetero-atoms within aromatic rings provide sites for ring rupture, as carbon—hetero atom bonds are usually weaker. This also leads to reduced soot yields.

Certain trends are also observed within the group of aliphatic fuels. Smoke point is found to decrease in the following order (Hunt, 1953):

Straight chain alkanes < Branched chain alkanes < Highly branched cycloalkanes.

Branching in n-paraffins and an increase in the ring size of cycloparaffins results in higher soot yields (Schalla and McDonald, 1953). Calcote and Manos (1983) show that the threshold sooting index (TSI) of n-alkanes and n-alkenes increases with the number of carbon atoms, with the alkanes having higher TSI values at a specific carbon number.

The effect on PAH and soot yields of doping fuels with small amounts of aromatics is not clear. Stehling et al (1957) observe that though benzene additive (upto 10%) in C₂H₂ flames in a flow reactor acts essentially as a diluent, toluene, naphthalene and anthracene at only 2 to 4% promote soot formation. However, there is very little difference in PAH and soot yield between a benzene turbulent diffusion flame and one doped with 1% anthracene (Prado et al, 1977). No significant effect is

observed as regards soot yield, on doping a C_6H_6/CH_4 premixed flame with 1% by weight (of N_2 in fuel) of pyrrole, pyridine and thiophene (Kausch et al, 1981). By analysing the nitrogen containing PAH thus evolved, and noting that substitution of argon shield gas by nitrogen had no effect on yields of nitrogen containing PAH, the authors conclude that the nitrogen source is from the fuel and not from the atmosphere.

Various workers have tried to obtain correlations between fuel properties and the tendency to produce soot and PAH. In an early investigation, Schalla and McDonald (1953) found no correlation between parameters such as diffusion coefficient, boiling point, density, rate of pyrolysis and rate of polymerization and the smoking tendency of 108 hydrocarbons burning in wick and tube diffusion flames. However, they did observe that a qualitative linkage appeared to exist between smoking tendency and the total carbon-carbon bond strength (Kcal/mole) of many hydrocarbon species. Bond strengths are of the following magnitude:

- C - C 80 Kcal/mole
- C = C 150 Kcal/mole
- C ≡ C 200 Kcal/mole
- C - H 100 Kcal/mole

Thus, as the stability of the compound increases, there is a greater chance of the C-H bond being broken. This implies that the dehydrogenated carbon skeletons formed would polymerize to form soot. Thus, there is a strong relationship between the ease of removal of hydrogen and smoking characteristics of a hydrocarbon fuel.

Various workers (Beer et al, 1982; Shirmer, 1971; Butze and Ehlers, 1975; Blazowski, 1977) have observed correlations between the H/C ratio (atomic) of a fuel and its ability to soot. Fuels covered include JP-4, JP-5, SRC-II (heavy) and SRC-II (2.9:1). The trend observed is that soot emissions increase as H/C ratio decreases. Data from Holliday (1955) is presented in Figure 3.15 to illustrate this point. However, Schug et al (1980) from plots of sooting height versus C/H ratio of acetylene — fuel mixtures burning in diffusion flames, observe that though C/H ratio is not a major factor in the sooting tendency (all mixtures overlap over a wide range of C/H ratios), at a given C/H, the mixtures soot at different heights. They conclude that flame temperature and fuel molecular structures are more important than H/C ratio. In an attempt to arrive at a common index for evaluating the onset of soot formation in both premixed and diffusion flames, Calcote and Manos (1983) have defined a Threshold Sooting Index (TSI) that is independent of individual experimental apparatus. TSI is analogous to the octane number for petroleum derived fuels and is defined as follows:

Premixed flames,
$$TSI = a - b \phi_c \tag{3.31}$$

Diffusion flames, i)
$$TSI = a \left(\frac{MW}{h} \right) + b$$

 ii)
$$TSI = a \left(\frac{MW}{V} \right) + b \tag{3.32}$$

- where ϕ_c = Critical equivalence ratio for sooting
- h = Critical height of flame for the onset of sooting
- V = Critical volumetric flow rate for the onset of sooting
- a, b = Constants calculated from existing soot formation data to make TSI self-consistent

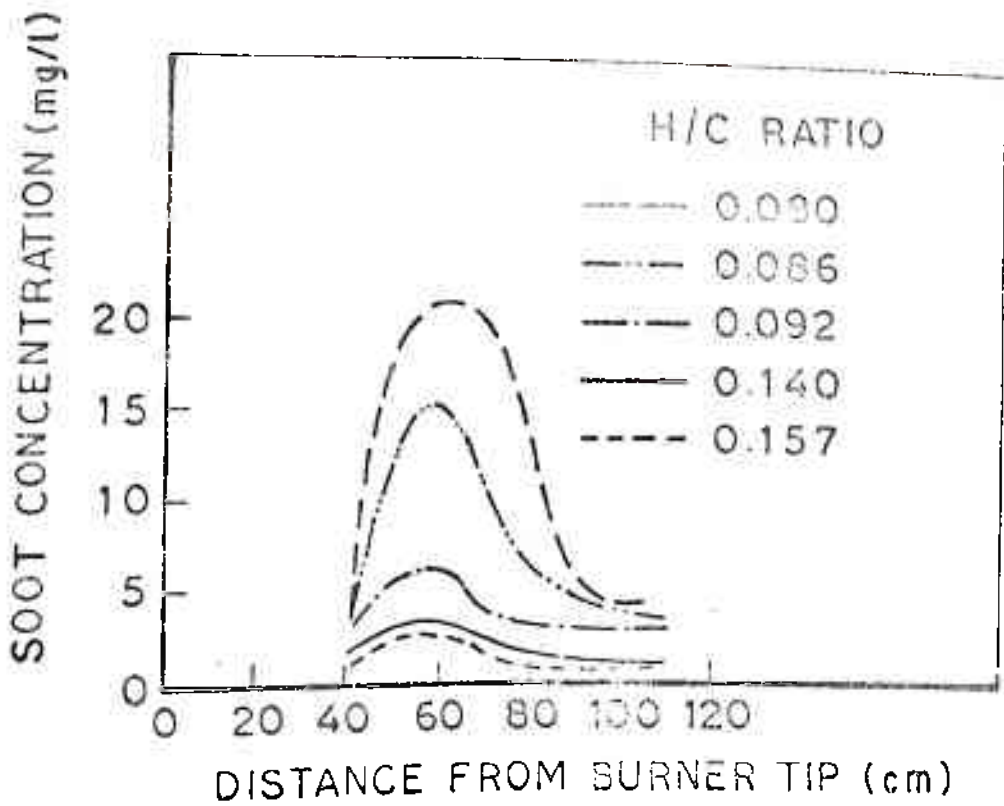


FIGURE 3.15 EFFECT OF H/C RATIO ON SOOT PRODUCTION IN A TURBULENT DIFFUSION FLAME (HOLLIDAY, 1955)

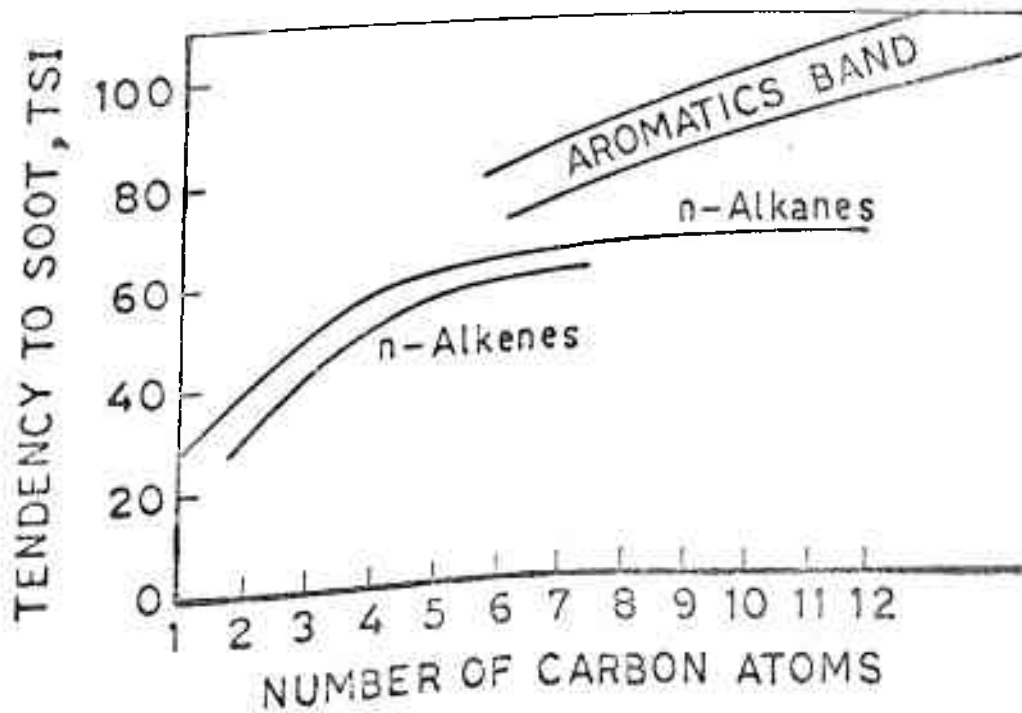


FIGURE 3.16 THRESHHOLD SOOTING INDEX VERSUS NUMBER OF CARBON ATOMS IN ALKENE, ALKANE AND AROMATIC FUELS (CALCOTE AND MANOS, 1983)

TSI is normalised to a range of 0 to 100, where arbitrary values of 2.0 and 100.0 have been assigned to n-hexane and 1-methyl naphthalene respectively, two compounds with the lowest and highest observed sooting tendencies. TSI is plotted as a function of the number of carbon atoms and C/H ratio in Figures 3.16 and 3.17 for premixed flames. TSI for diffusion and premixed flames are compared in Figure 3.18. It is clear from the above figures that the greater the aromatic character of a fuel, the greater is its propensity to form soot. This effect is more pronounced in diffusion flames than in premixed flames.

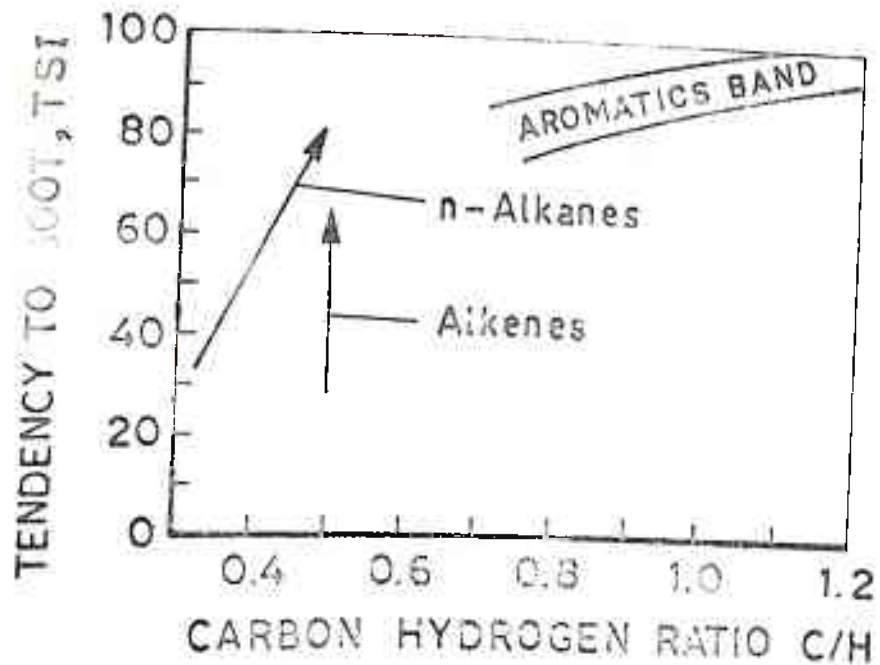


FIGURE 3.17 THRESHOLD SOOTING INDEX VERSUS C/H RATIO-PREMIXED FLAMES (CALCOTE AND MANOS, 1983)

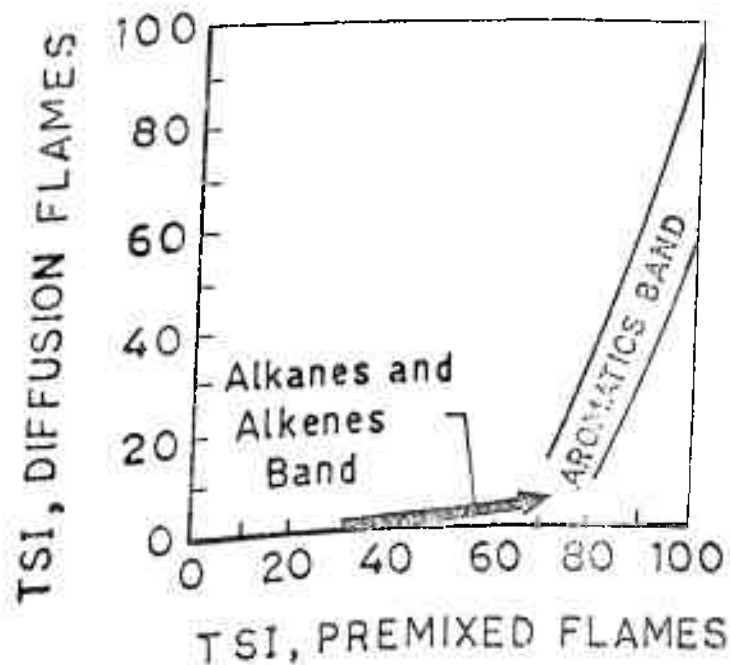


FIGURE 3.18 COMPARISON OF SOOTING INDICES FOR DIFFUSION AND PREMIXED FLAMES (CALCOTE AND MANOS, 1983)

EFFECT OF COMBUSTION CONDITIONS ON THE YIELD OF PAH

The primary variables that are expected to affect the formation of PAH and soot in combustion systems are temperature, ambient oxygen concentrations, fuel equivalence ratios, residence time, pressure and mixing conditions. These effects are interdependent. For example, increasing oxygen concentrations would also increase adiabatic flame temperatures in premixed flames, and variations in temperature in flow systems could affect gas flow rates which would alter fuel residence times. However, in order to identify the effects of these combustion parameters and as an aid in the design of experiments, it is instructive to study these variables separately.

4.1 Effect of Temperature

Studies of the effect of temperature on pyrolysis, PAH and soot formation and thermodynamic stability indicate that PAH production goes through a maximum with increasing temperature.

Badger et al (1960, 1960a, 1960b, 1960c, 1962) observed from pyrolysis studies of simple fuels such as acetylene, toluene and alkyl benzenes that the optimum temperature range for PAH formation was 930 K to 1010 K.

The work of Tompkins and Long (1968) also shows that PAH formation rates are very high till about 1500K, after which they decline rapidly (Figure 4.1). Since these results were obtained from a C_2H_2/O_2 flat flame, where residence times are less than those in Badger's (1962) pyrolysis studies, it is not surprising that the optimum temperature range should extend to higher temperatures.

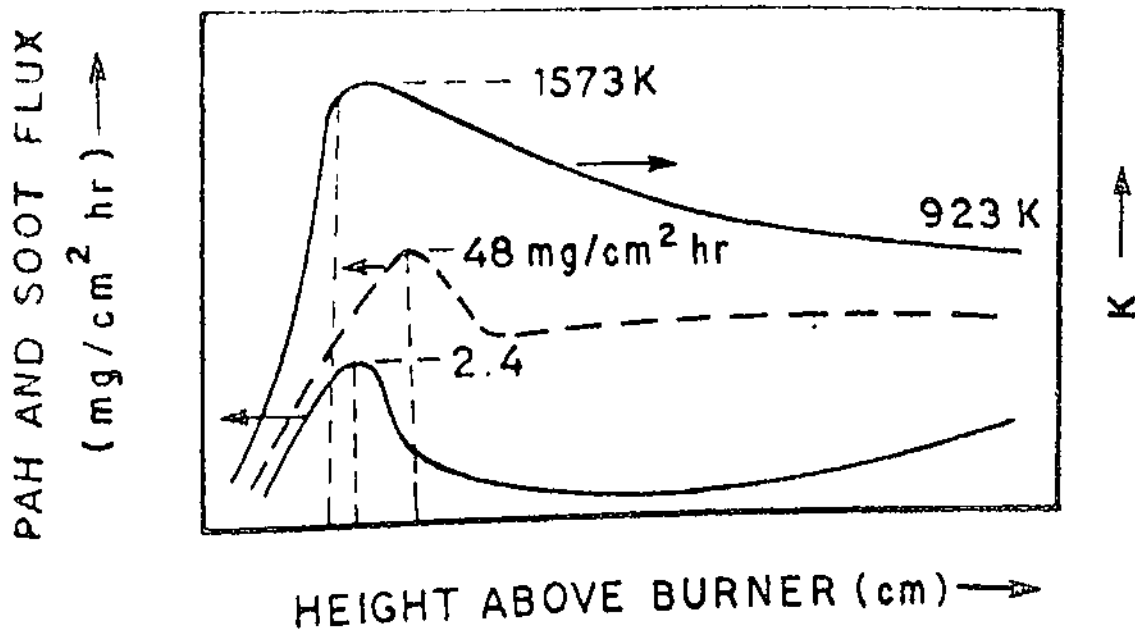


FIGURE 4.1 TEMPERATURE PROFILE IN A C_2H_2/O_2 FLAT FLAME (TOMPKINS AND LONG, 1968)

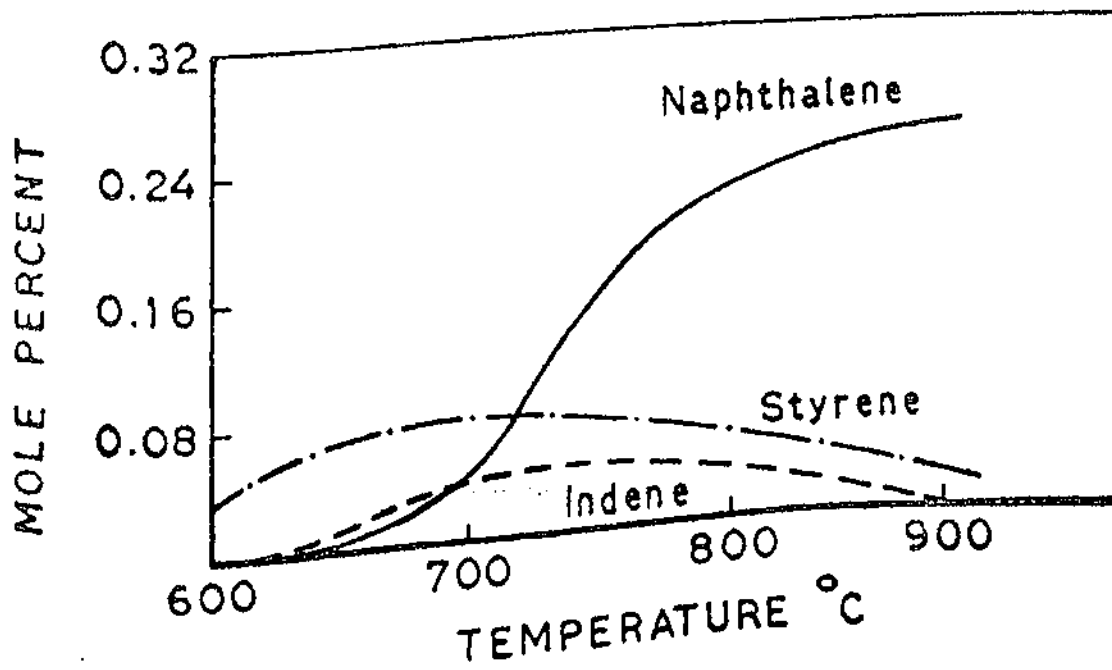


FIGURE 4.2 MOLE PERCENT OF NAPHTHALENE, INDENE AND STYRENE FROM ACETYLENE PYROLYSIS (STEHLING et al, 1962)

Another region of formation of PAH was observed high in the post flame region, corresponding to a temperature range of 1173 K to 923 K. Johnson and Anderson (1962) also observe that at $T < 1073$ K, a liquid polymeric material was obtained from acetylene pyrolysis, whereas at $T > 1273$ K, soot was predominant. Presumably, the polymeric material was composed of tars which would contain PAH. An optimum temperature of 1000 K was also indicated by Chakraborty and Long (1968, 1968a) for the maximum evolution of PAH from a $C_2H_2/O_2/N_2$ diffusion flame. These workers also observed that as the oxygen concentration increased, the flame temperatures also increased. However, Wang et al (1981) indicate that for very fuel rich mixtures the presence of oxygen does not cause a major change in the temperature for maximum soot production. When nitrogen was replaced by argon, soot production was observed to be less, due to the higher adiabatic flame temperature of the $C_2H_2/O_2/Ar$ system.

Zaghini et al (1972) were able to characterize three zones in a premixed $n-C_7H_{16}/O_2/N_2$ flame held in a vertical reactor.

These were:

- | | | | |
|-----------------|-----------|---|--------|
| a) Cool flame | T_{max} | ~ | 773 K |
| b) Blue flame | T_{max} | ~ | 973 K |
| c) Yellow flame | T_{max} | ~ | 1173 K |

They observed however, that though high molecular weight PAH went through a maximum ($T_{max} \sim 1200$ K) as the temperature increased, PAH of low molecular weight continued to increase.

Two routes of formation of particulates were discussed by Pasternak et al (1981, 1982) based on the combustion of polyethylene, polymethylmethacrylate, polypropylene and polystyrene.

In the flaming, or high temperature mode, particulate formation was via chemical reactions, whereas in the nonflaming (smoldering) mode, it was through condensation schemes.

The work of Smith (1979a, 1979b) at 10^{-2} torr shows that production of PAH by toluene pyrolysis maximises at 1300 K to 1400 K. The amount produced decreases by a factor of ten for a 200 K increase in temperature beyond the maximum. Soot production, at higher pressures is also maximised at 1700 K to 1750 K.

Stein (1977, 1978) has published equilibrium concentration calculations for the following reaction:



A calculation for 0.1 atm of acetylene and 1.0 atm of hydrogen pressure shows that growth is not favoured above a certain temperature. For the conversion of benzene to naphthalene, this temperature is about 1650 K. This temperature corresponding to thermodynamic stability, is in the same range as that observed for maximum PAH production.

Bittner and Howard (1980, 1981) have estimated heats of formation of intermediates in the growth of benzene to naphthalene via addition of acetylenic species. They indicate that at flame temperatures, the lifetime of the intermediates proposed is a limiting consideration. Higher temperatures would severely limit free radical pathways for PAH growth.

PAH such as indene, styrene etc. were observed to peak at about 1000 K (Figure 4.2), whereas benzene yield was a maximum at about 1100 K, during the pyrolysis of acetylene

in a flow reactor (Stehling et al, 1962). Though the naphthalene mole percentage did not exhibit a maximum in the temperature range studied it would appear to peak at higher temperatures.

Flame temperature is also a dominant factor in determining the tendency to soot. Changes which increase the flame zone temperature, such as reducing inert diluent concentrations, decreasing diluent heat capacity, preheating the fuel and changing the fuel type, tend to reduce the yields of soot in the presence of oxidisers. This has been observed in premixed flames, diffusion flames, combustion of single droplets etc.; Schalla & McDonald (1955), Street & Thomas (1955), Stehling et al (1957), Homann (1967), Prado et al (1981), Calcote and Olson (1982). Further, the first two groups of workers observed that preheating the fuel over a temperature range of upto 400°C, had little effect on sooting tendency and ϕ_c in premixed flames. Peaks in soot yield were also observed (Nakanishi et al, 1981) as a function of air temperature. The extinction velocity, defined as the air velocity at which a transition was observed from an envelope flame (diffusion) to a wake flame (premixed), also increased with temperature.

Under pyrolytic conditions however, soot yields increase with temperature, usually reaching a plateau at high temperatures (Vranos & Liscinsky, 1983). This explains the observation by Macfarlane et al (1964) that soot formation increased with temperature in their premixed flames. Pyrolytic conditions were probably prevalent.

Thus it would appear that there are two competing pathways, by one of which soot is formed during pyrolysis, soot oxidation occurring via the other. Temperature increases would promote pyrolysis and also increase oxidation rates. It should be noted that Milliken (1962) postulated that soot appears in premixed flames when the following relationship is satisfied:

$$\frac{[C_2H_2]}{[OH]} > \frac{k_{ox}}{k_f} \quad \text{where} \quad (4.1)$$

k_{ox} = oxidation of precursor by OH
 k_f = formation of precursor from C_2H_2

The fractional conversion of various hydrocarbons into soot (after 2.5 ms) in a shock tube is shown in Figure 4.3 (from Graham et al, 1975a) as a function of temperature. This illustrates the competition between rapid chemical growth reactions via polymerization and thermal dissociation reactions which start to compete at higher temperatures.

4.2 Effect of Pressure

There has been little work on the effect of pressure on the evolution of PAH. However, inferences may be drawn from pressure effects observed in sooting flames.

In general, as the system pressure increases, sooting tendency is observed to increase. Schalla and McDonald (1955) note that for combustion of alkenes, aromatics and JP-4 (aviation fuel) in diffusion flames, pressure variations of

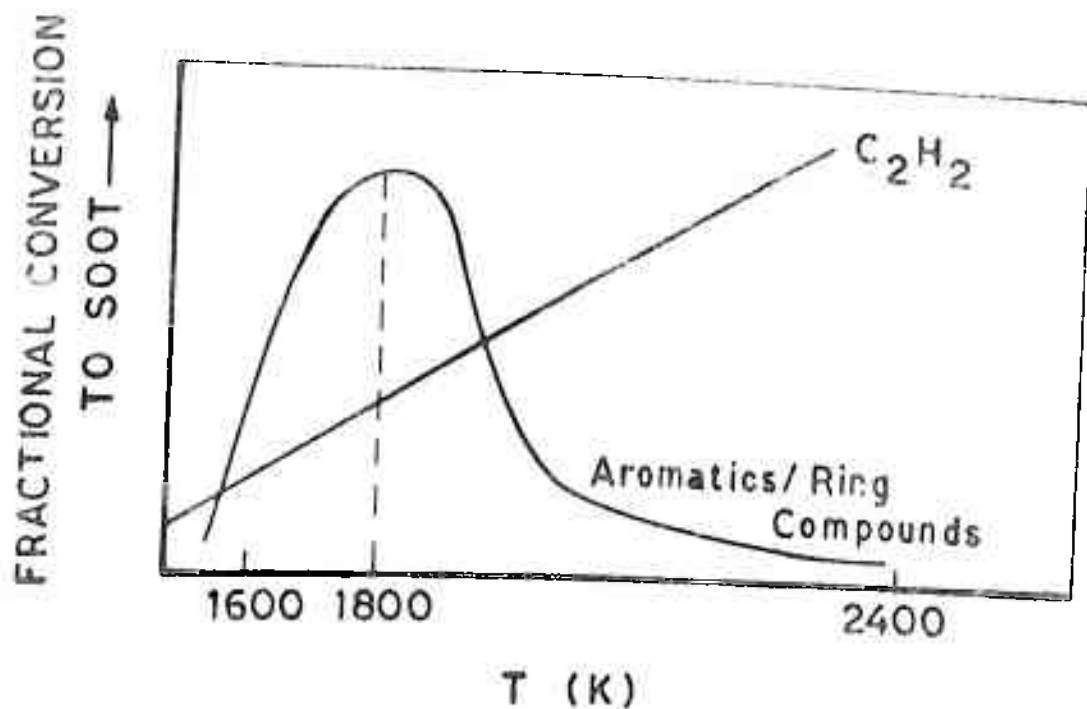


FIGURE 4.3 THE FRACTIONAL CONVERSION OF AROMATIC SPECIES TO SOOT IN A SHOCK TUBE (GRAHAM et al, 1975a)

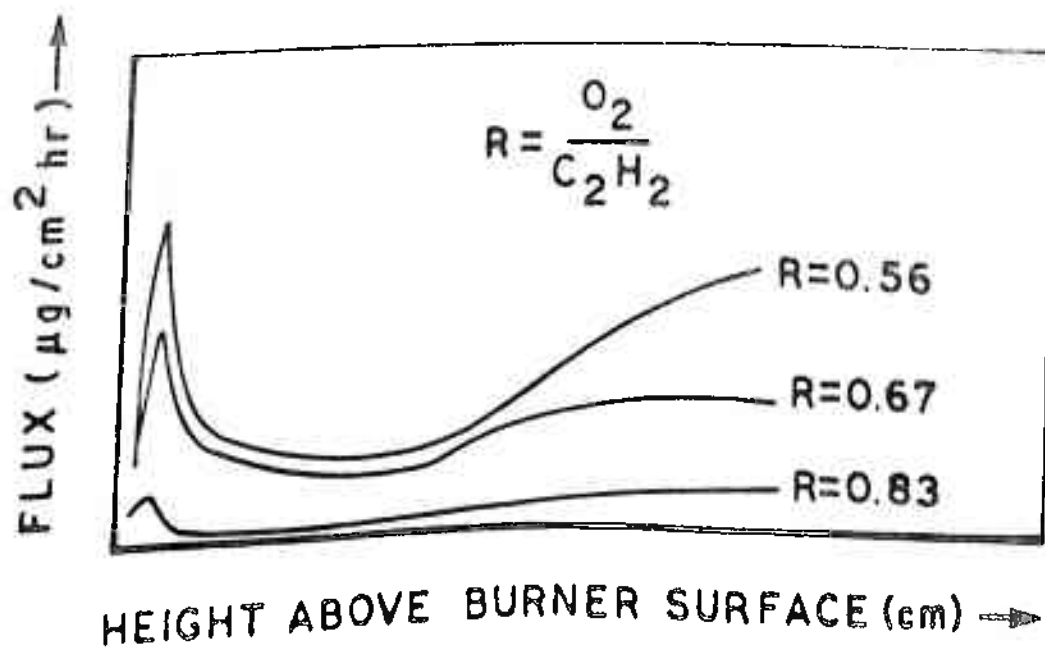


FIGURE 4.4 PAH FLUX AT DIFFERENT O_2/C_2H_2 RATIOS (TOMPKINS AND LONG, 1968)

0.5 atm to 12 atm increased smoke formation. It would appear that pressure directly influences the rate of diffusion of fuel into the oxidation zone. The critical pressure at which soot just appears in premixed flames increases as the mixture is made lean (Fenimore et al, 1957). Soot formation ratio varies directly as $P^{2.5}$ or P^3 upto a maximum value of P (pressure). The critical fuel equivalence ratio however is affected very little by pressure variations in premixed flames ; vide Macfarlane and Coworkers (1964), Miller and Calcote (1977). Studies in well-stirred reactors (Wright, 1970) also show the same effects. Wang et al (1981) observe two types of behaviour from shock tube studies on toluene/oxygen mixtures. At temperatures below 1800K, the influence of pressure is similar to the trends discussed. However at higher temperatures, soot yields decrease with ascending pressure.

From the above it may be deduced that at constant ϕ , the mole fraction of PAH should increase with pressure. Bittner and Howard's (1980, 1981) nonsooting $\phi = 1.8$, 20 torr benzene flame gave naphthalene concentrations below the detection limits of 10^{-6} mole fraction. On the other hand a mildly sooting, $\phi = 1.63$, atmospheric pressure toluene flame gave measurable amounts of PAH (Longwell, 1982). Most flame systems have been investigated at sub-atmospheric pressures, primarily because a longer reaction zone is obtainable. At atmospheric pressures it is difficult to resolve concentration distributions of PAH species.

4.3 Effect of Oxidiser Concentrations

Pyrolysis regimes result in high yields of PAH (Longwell, 1982; Mitra et al, 1982, 1983). Lahaye and Prado (1978)

report upto 30% conversion to tar (containing PAH) for *Pyrolysis of benzene-oxygen mixtures at very short residence times*. Similar results were reported by Scully and Davies (1965) in investigations where aromatic hydrocarbons were injected into the post-flame oxygen-deficient zone of a rich toluene gas flame. Badger et al (1960, 1960a, 1960b, 1960c, 1962) also observed very high yields of PAH from the thermal cracking of a variety of aliphatic and aromatic hydrocarbons.

In general it has been observed that an increase in oxidizer concentrations in systems such as premixed flames, turbulent flames, shock tubes, stirred reactors and flow systems, results in lower yields of soot and PAH.

Tompkins and Long (1968) report that the flux of PAH is lower at increased ratios of O_2/C_2H_2 (Figure 4.4). The observed increase in PAH formation at $Z > 18$ cm is probably due to increased pyrolysis of C_2H_2 in these oxygen-deficient post-flame zones. Similar results are also obtained by Crittenden and Long (1973), who also observe sharp increases in PAH formation rates in the blue zone where oxygen concentrations are high but decrease very rapidly.

Macfarlane (from Thomas, 1965) reports that the net yields of various 3 to 7 ring PAHs in a turbulent premixed flame of C_6H_6/O_2 increase with ϕ . Hydroxyl radicals (OH) are observed to inhibit the formation of the 3-ring perinaphthenyl radical and reduce total yields of PAH in rich heptane/oxygen flames (Franceschi et al, 1976). The authors conclude that

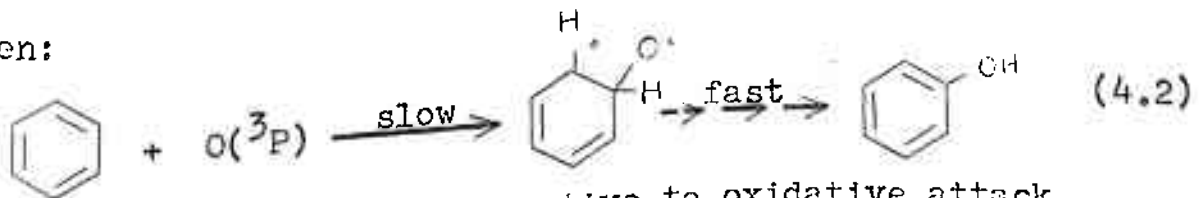
similar phenomena would occur if compounds producing oxygen containing radicals were introduced into the flame. Concentrations of cyclopenta (c d) pyrene increase as ϕ increases in a turbulent C_6H_6 diffusion flame. Soot yields also increase dramatically from 96 mg/sm^3 to 410 mg/sm^3 as ϕ is raised from 0.8 to 1.2 (Prado et al, 1977). An increase in the ratio of O_2/CH_4 from 0.79 to 0.91, produces a four-fold reduction in PAH yields in an atmospheric pressure flat flame (Dilorenzo et al, 1981). Studies conducted in a vertical flow reactor (Zaghini et al, 1972) using n-heptane as the fuel also show that PAH concentrations are highest in the yellow flame, a region of very low oxygen concentrations. At increased ratios of $\frac{O_2}{C_2H_4}$ in a diffusion flame, a range of PAH from acenaphthylene⁴ to benzo (ghi) perylene decline rapidly in concentration, though soot yield remains at near its maximum value (Chakraborty and Long, 1968).

Ionic PAH exhibit similar behaviour patterns. Heavier polyaromatic species such as $C_{10}H_7^+$ (naphthenylium) and $C_{13}H_9^+$ (fluorenylium) appear only as ϕ is increased past sooting limits (Miller and Calcote, 1977). A strong increase in the number of charged species with molecular weights greater than 300 amu per unit volume is observed by Wersborg and coworkers (1975) as ϕ is raised from 2 to about 3 in acetylene flames. Though total ion concentrations remain nearly constant, a dramatic shift to higher molecular weight ions is observed (Michaud et al, 1981; Olson and Calcote, 1981) at the expense of smaller polyaromatic ions (amu < 300), for enhanced ϕ .

Soot concentrations in premixed flames and other systems which provide mixing of fuel and oxidiser are also reduced at enhanced oxidiser levels (Street and Thomas, 1955; Stehling et al, 1957, 1962; Fenimore & Jones, 1968; Wright, 1975; Prado et al, 1981; Blazowski, 1980; Wang et al, 1981). Hydroxyl radicals and atomic oxygen have been proposed as the primary oxidising species. Doping C_2H_2/O_2 flames with hydrogen chloride increases the soot yield (Fenimore and Jones 1968), probably because O and OH species are consumed as follows:



The chloride radical produced is less efficient oxidant. Davies and Scully (1966) note that oxidisers inhibit the soot promoting tendency of methyl groups attached to aromatic rings. Grovenstein and Mosher (1970) have studied the oxidation of aromatic compounds and postulate attack by ground state atomic oxygen $O(^3P)$, and not by molecular oxygen:



A substrate which was less reactive to oxidative attack produced ten times as much tar, implying that oxidation reduced tar yields in the case of benzene. Wright (1975) also speculates that at high temperatures and low equivalence ratios, oxidation by atomic oxygen would become important, that is, in the region of adiabatic flame temperatures and stoichiometric mixtures. From his gravimetric investigations

of oxidation of soot he infers that in low temperature, fuel-rich regimes, oxidation is more likely by OH radicals.

The situation is qualitatively different in diffusion flames, where there is no intimate mixing of the fuel and oxidiser species (Sjogren, 1973; Glassman and Yaccarino, 1980, 1981; Santoro and Glassman, 1979; Chakraborty and Long, 1968; Schug et al, 1980). Here in general, increasing oxygen concentrations also increase soot yields, though PAH destruction rates are enhanced.

For premixed flames, sooting is determined by a competition between the rate of pyrolysis and growth of soot precursors such as PAH, and the rate of oxidative attack on these precursors. Thus as the concentration of oxidisers is increased, the rate of oxidative attack increases resulting in lower PAH and soot yields.

Under diffusion controlled conditions, there is no oxidative attack on the precursors. However increasing the oxygen concentration results in higher adiabatic flame temperatures, correspondingly higher pyrolysis rates and thus a greater tendency to soot. Indeed, small amounts of oxygen diffusing through the flame front could homogeneously catalyse fuel pyrolysis, again increasing sooting. Two mechanisms have been observed in sooting diffusion flames (Glassman and Yaccarino, 1980). At low oxygen mole fractions of upto about 0.24 an increase in the oxygen concentration results in greater particle burnout rates, and a decrease in sooting. However, at higher oxygen concentrations, the

increase in flame temperature and thus pyrolysis rates offsets the increase in particle burnout rates, resulting in greater soot yields. This explains the apparently anomalous results of Chakraborty and Long (1968). In all cases, increased flame temperatures would result in higher destruction of PAH.

4.4 Effect of Mixing

There have been few studies on the effect of mixing intensity on PAH production.

One of the most detailed investigations is that of Prado et al (1977) on turbulent kerosene and benzene diffusion flames. The non-uniform distribution of the fuel in air was represented by pockets of gas or eddies of varying fuel/air ratios. Thus some eddies were fuel rich and the rest fuel lean. PAH and soot production would then occur in the fuel rich eddies, insufficient residence times accounting for their survival. Prado et al observed that higher atomizing air pressures (better mixing) drastically reduced both PAH and soot yields (Figures 4.5 and 4.6). However, when the throughput of the burner was increased, i.e. the superficial velocity was increased from 0.96 m/s to 2.67 m/s, increases in the atomizing air pressure resulted in decreased peak soot yields, but increased ultimate soot yields, possibly because the flame was quenched at higher throughput.

Studies at high Reynolds numbers indicate that the soot concentration field is essentially mixing controlled (Becker and Yamazaki, 1977). Holden and Thring (1959) observed that

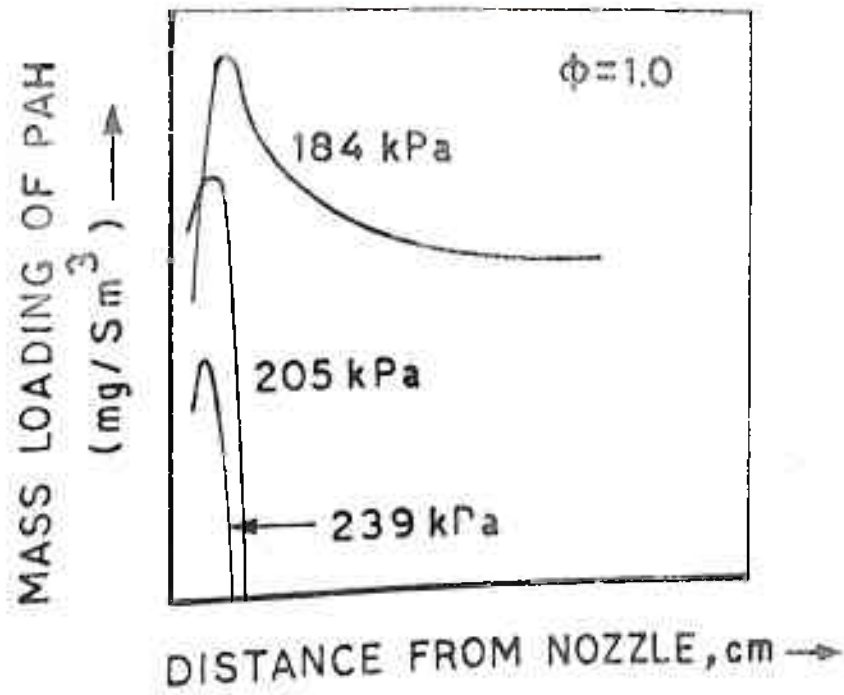


FIGURE 4.5 EFFECT OF MIXING ON PAH YIELDS IN A TURBULENT KEROSENE DIFFUSION FLAME (PRADO et al, 1977)

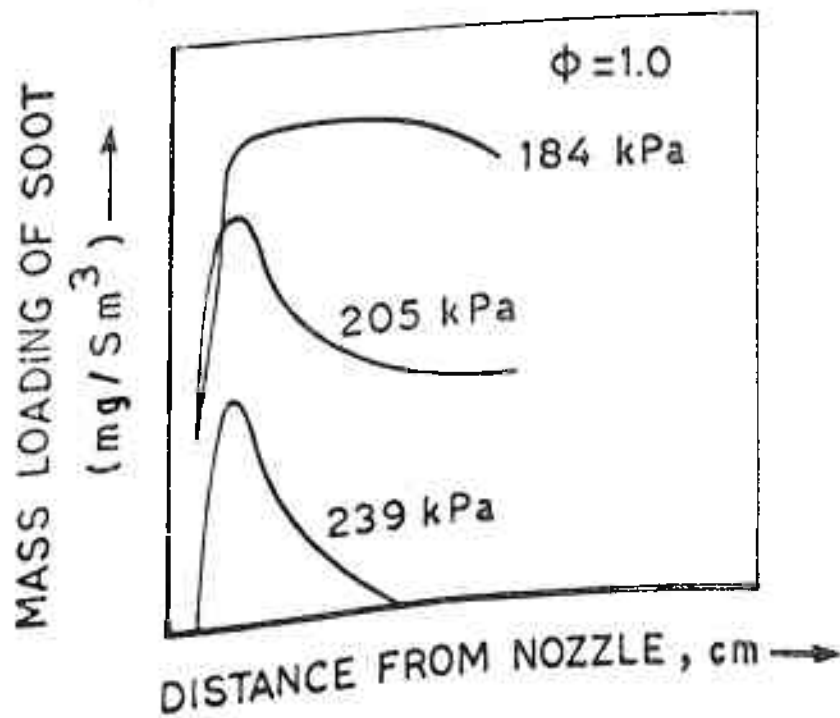


FIGURE 4.6 EFFECT OF MIXING ON SOOT YIELDS IN A TURBULENT KEROSENE DIFFUSION FLAME (PRADO et al, 1977)

soot formation increased as mixing ratios were decreased. Turbulence around a smoking diffusion flame (Schalla and McDonald, 1955) induced by increasing air flow velocities, resulted in a reduction in smoking tendency.

Backmixing or recirculation has also been found to reduce soot concentrations (Macfarlane, 1964; Sjogren, 1973; Chakraborty and Long, 1968) in laboratory flames and industrial burners. Beer et al (1982) discuss the strong effect of an increase in jet momentum on the decay of soot in jet flames. In a review on soot formation in combustion, Wagner (1979) reports a steep increase in the maximum amount of soot present (in turbulent diffusion flames) as a function of the Richardson number Ri (the ratio of buoyant to momentum forces). Finally, Wright (1969, 1970) and Blazowski (1980) note that in well-stirred reactors, soot free combustion of richer mixtures is achieved than is possible in premixed flames. Reductions of over 90% in soot yields are observed for fuels such as ethylene, propene, 1,3-butadiene, benzene and toluene. Results from toluene combustion are presented in Figure 4.7.

4.5 Effect of Residence Time

The time required for the initial appearance of soot is very short, of the order of one ms in premixed flames and about 10 ms in diffusion flames. Figure 3.13 gives the dimensions of the time scales involved. The residence time of the fuel in the reaction zone of a combustor is an important factor in determining PAH and soot yields. This section

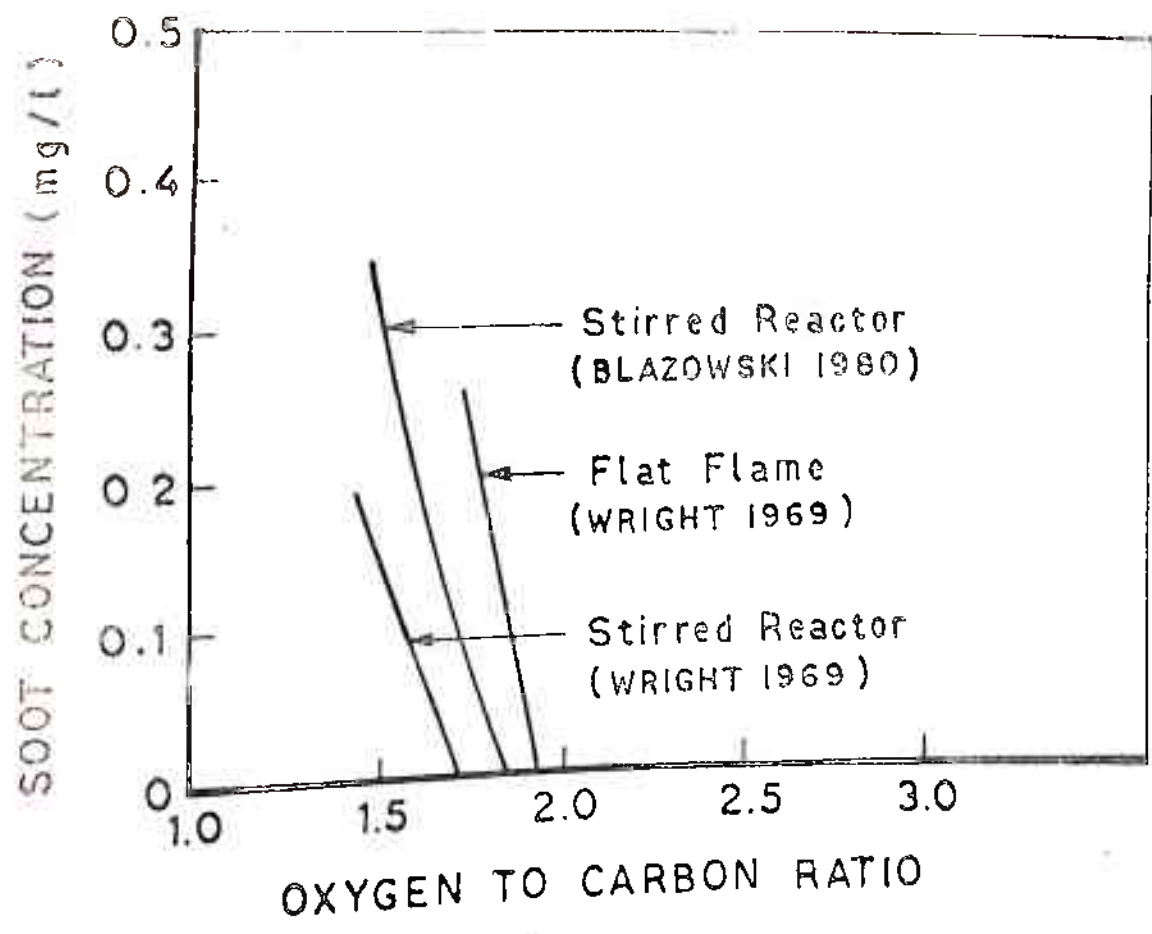


FIGURE 4.7 SOOT YIELDS IN WELL-STIRRED REACTORS (BLAZOWSKI, 1980; WRIGHT, 1969)

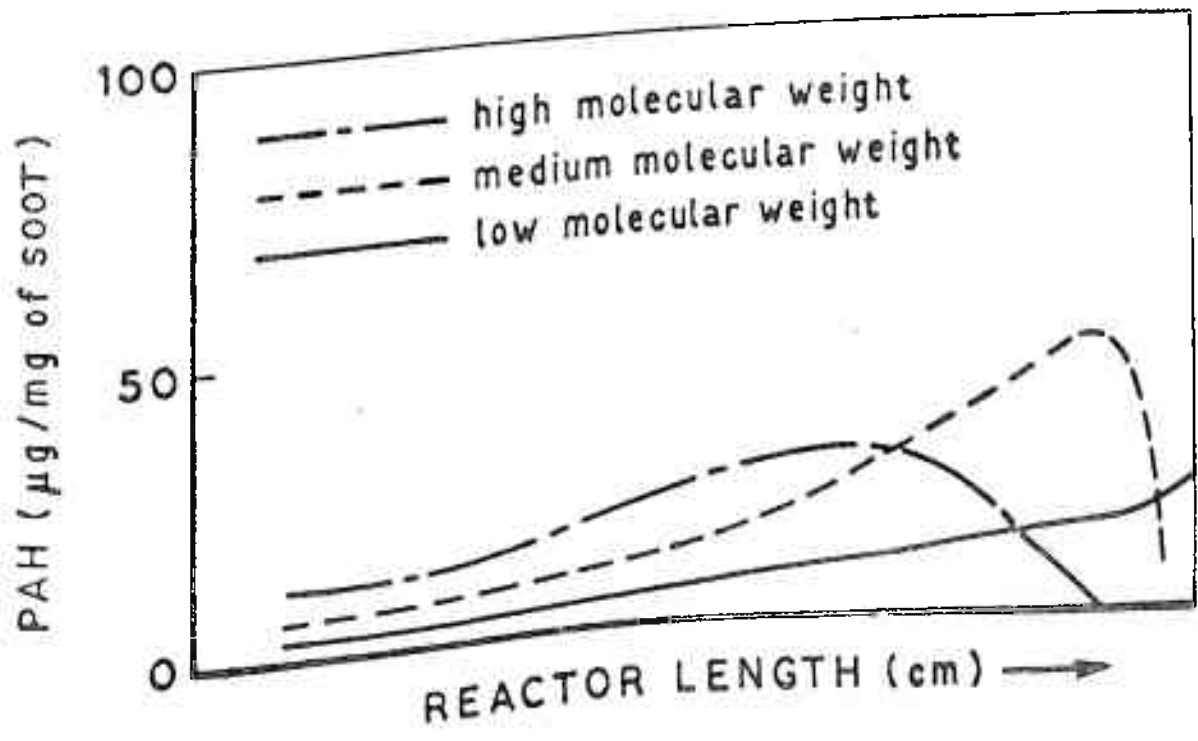


FIGURE 4.8 PAH YIELDS FROM AN $n-C_7H_{16}/O_2/N_2$ FLAME IN A VERTICAL FLOW REACTOR (ZAGHINI et al, 1972)

discusses data obtained from various flame systems, where the height above the burner is taken as a measure of residence time.

Tompkins and Long (1968) observed that as the height above the flat flame burner surface increased, yields of PAH and soot peaked and then decreased.

A first order type of behaviour can be seen from PAH yields in an $nC_7H_{16}/O_2/N_2$ system (Figure 4.8). The flame which was premixed was held in a vertical flow reactor (Zaghini et al, 1972).

Peaks of formation of a range of PAH were observed at higher residence times, as the shift was made from C_2H_2 to C_2H_4 premixed flames (Crittenden and Long, 1973a). In both cases, oxygen concentrations were near zero in the flue zone, the region of maximum PAH formation.

PAH and perinaphthenyl radical both went through a maximum with increasing residence time, in an $(n-C_7H_{16} + 10\% C_6H_6)/O_2$ flame (Franceschi et al, 1976) as in Figure 4.9. Though the low molecular weight (LMW) PAH were observed to decrease with an increase in reactor length, the high molecular weight (HMW) PAH were found to increase, Chrysene and benz(a) anthracene exhibited aberrant behaviour (Figure 4.10).

Prado et al (1977) also observed an enrichment of high molecular weight PAH with residence time. The rate of disappearance of the more reactive PAH, that is, those containing methyl or phenyl groups or a saturated carbon (such as fluorene), was considerably faster than that of more stable PAH.

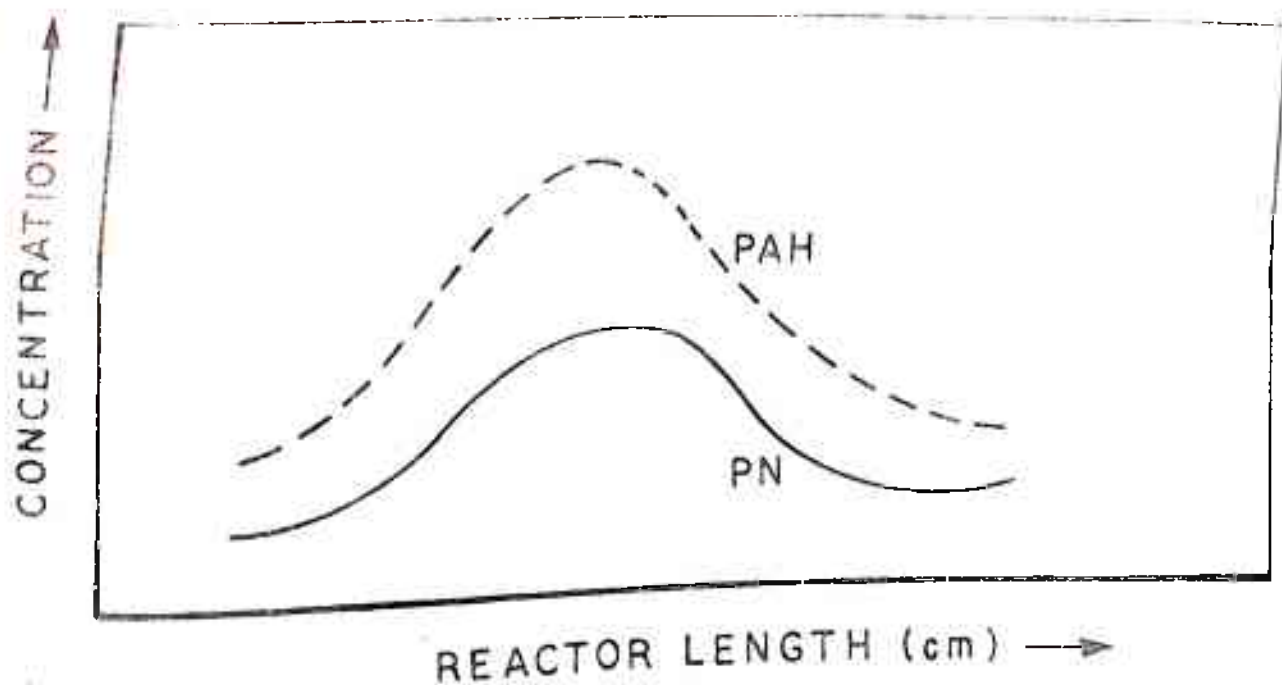


FIGURE 4.9 PAH AND PERINAPHTHENYL RADICAL (PN) CONCENTRATIONS IN A VERTICAL FLOW REACTOR (FRANCESCHI et al, 1976)

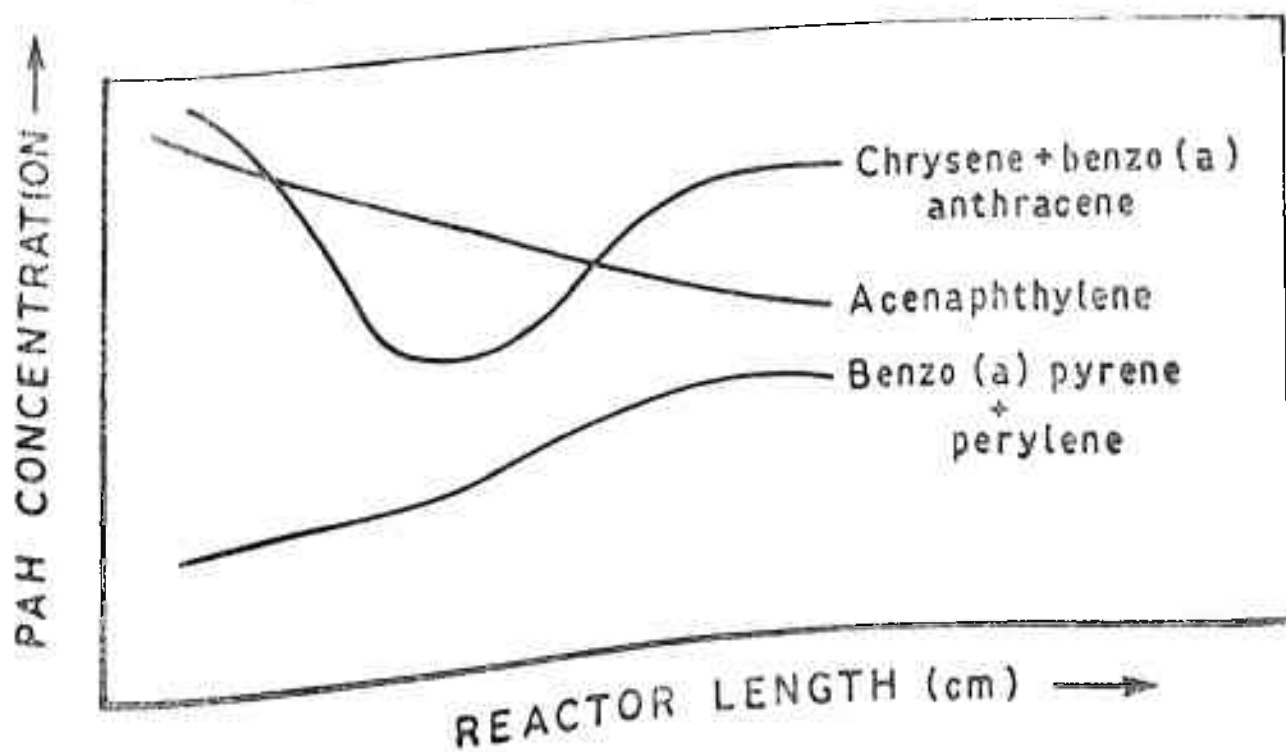


FIGURE 4.10 PAH CONCENTRATIONS IN A VERTICAL FLOW REACTOR (FRANCESCHI et al, 1976)

PAH yields were observed to increase with residence time in a CH_4/O_2 premixed flat flame (Dilorenzo et al, 1981). However ratios of both 2-3 ring and 5-7 ring PAH to a 4 ring PAH (pyrene) decreased (Figure 4.11). The increase in total PAH yields can only be explained by assuming that the bulk of monocyclic aromatic species increased with \bar{t} . No peaking of PAH yields were observed, probably because sampling was not conducted at greater heights above the burner surface.

Kausch et al (1981) noted however that in a CH_4/C_6H_6 flame (1.5 molar ratio), both N-PAH and soot yields approached asymptotic values with increasing height above the burner. PAH concentrations were about 5% of corresponding soot values. PAH and soot both increase with height above the burner (Figure 4.12) in a flat flame system (D'Alessio et al, 1975), subsequent to the oxidation zone. However trends in the behaviour of individual PAH are somewhat different (Figure 4.13). The pyrolytic conversion of benzene to diphenyl (Figure 4.14) shows a first order type of behaviour (Kinney and Del Bel, 1954). The growth of soot through a flame is illustrated graphically in Figure 4.15. Concentration profiles of the major hydrocarbon species are shown in Figure 4.16. The precursors shown in Figure 4.16 are a group of reactive PAH with side chains and are in the mass range of 150 to 550 amu. They contain more hydrogen atoms than PAH such as $C_{14}H_8$, which lie in the mass range of 78 to 300 amu.

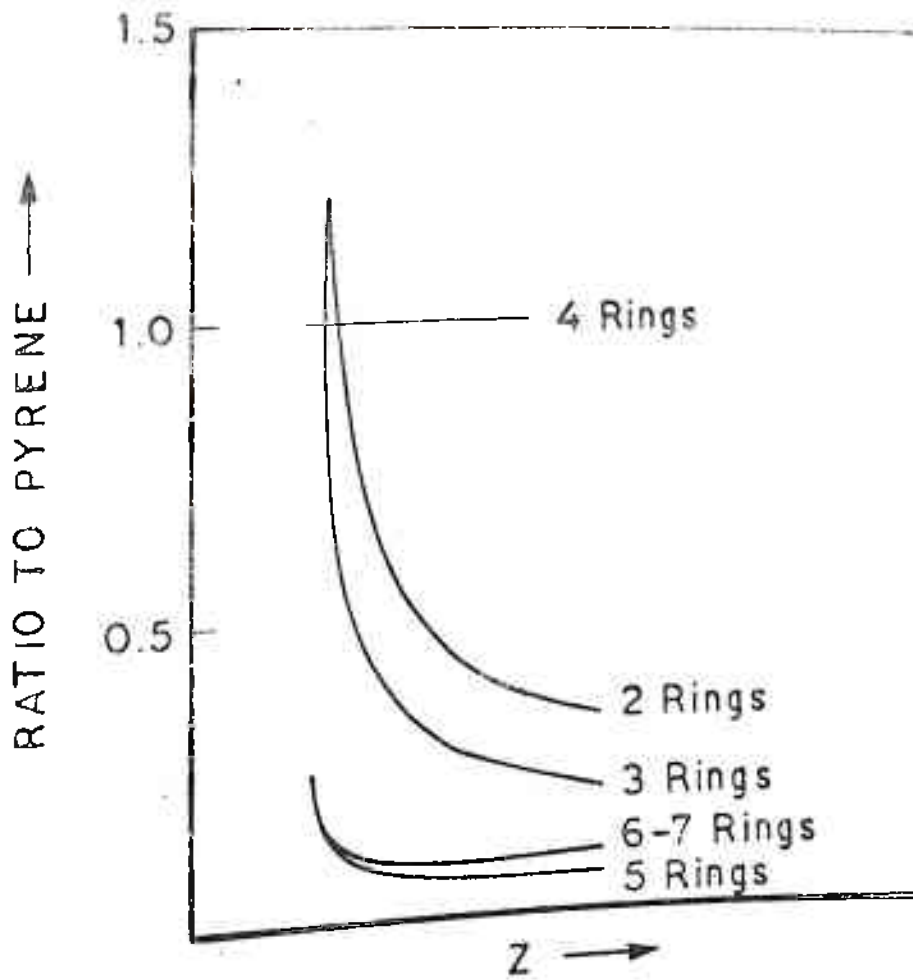


FIGURE 4.11 RATIO OF 2-7 RING PAH TO PYRENE IN PREMIXED CH_4/O_2 FLAMES (D'LORENZO et al, 1981)

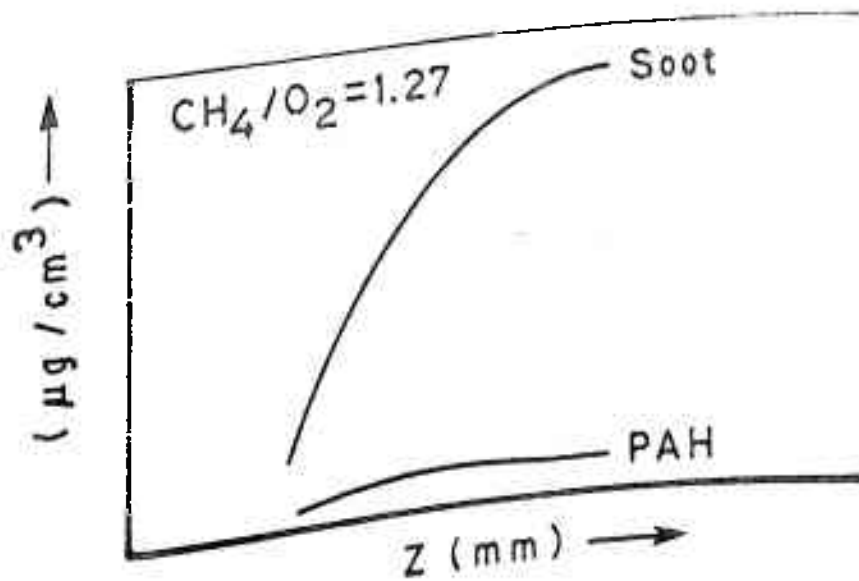


FIGURE 4.12 PAH AND SOOT YIELDS IN A CH_4/O_2 FLAT FLAME (D'ALESSIO et al, 1975)

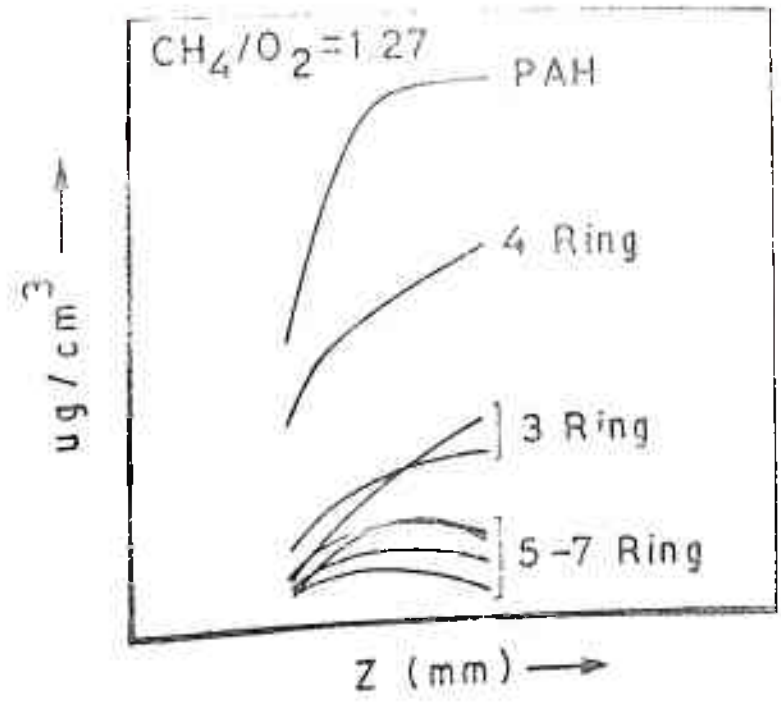


FIGURE 4.13 YIELDS OF 3-7 RING PAH IN AN ATMOSPHERIC PRESSURE PREMIXED CH₄/O₂ FLAT FLAME (D'ALESSIO et al, 1975)

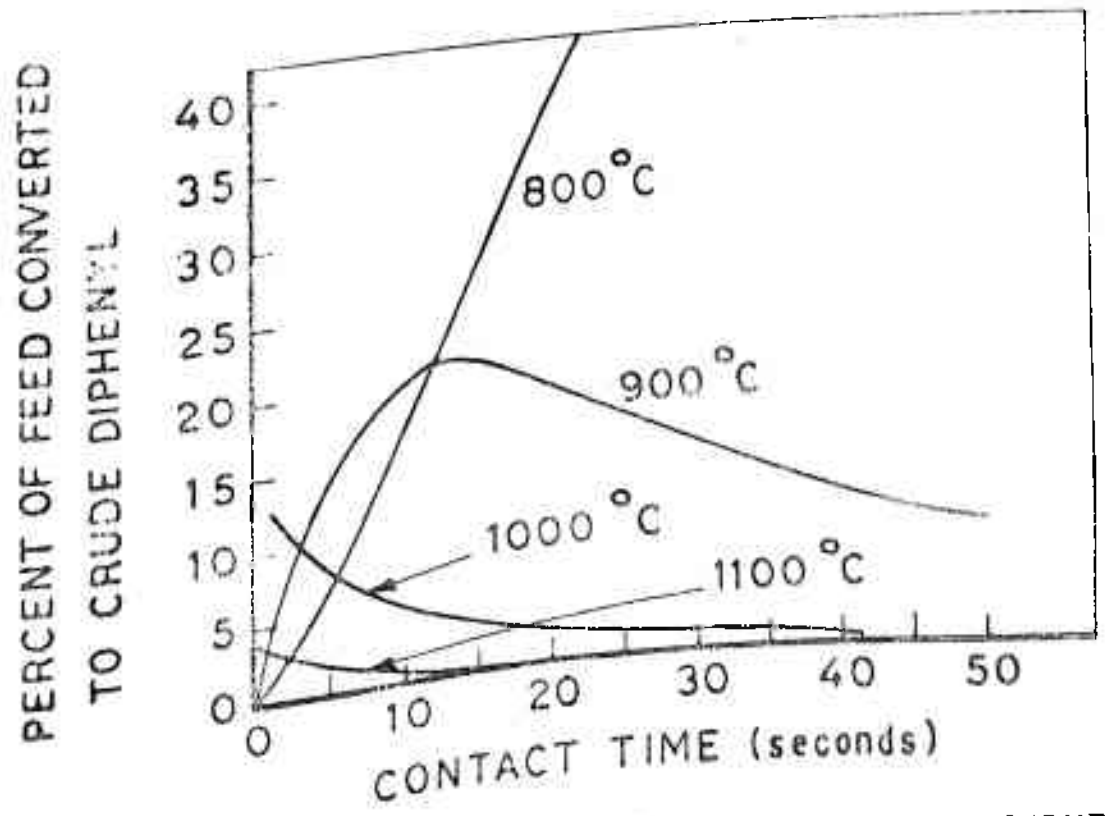


FIGURE 4.14 PYROLYTIC CONVERSION OF BENZENE TO DIPHENYL (KINNEY AND DEL BEL, 1954)

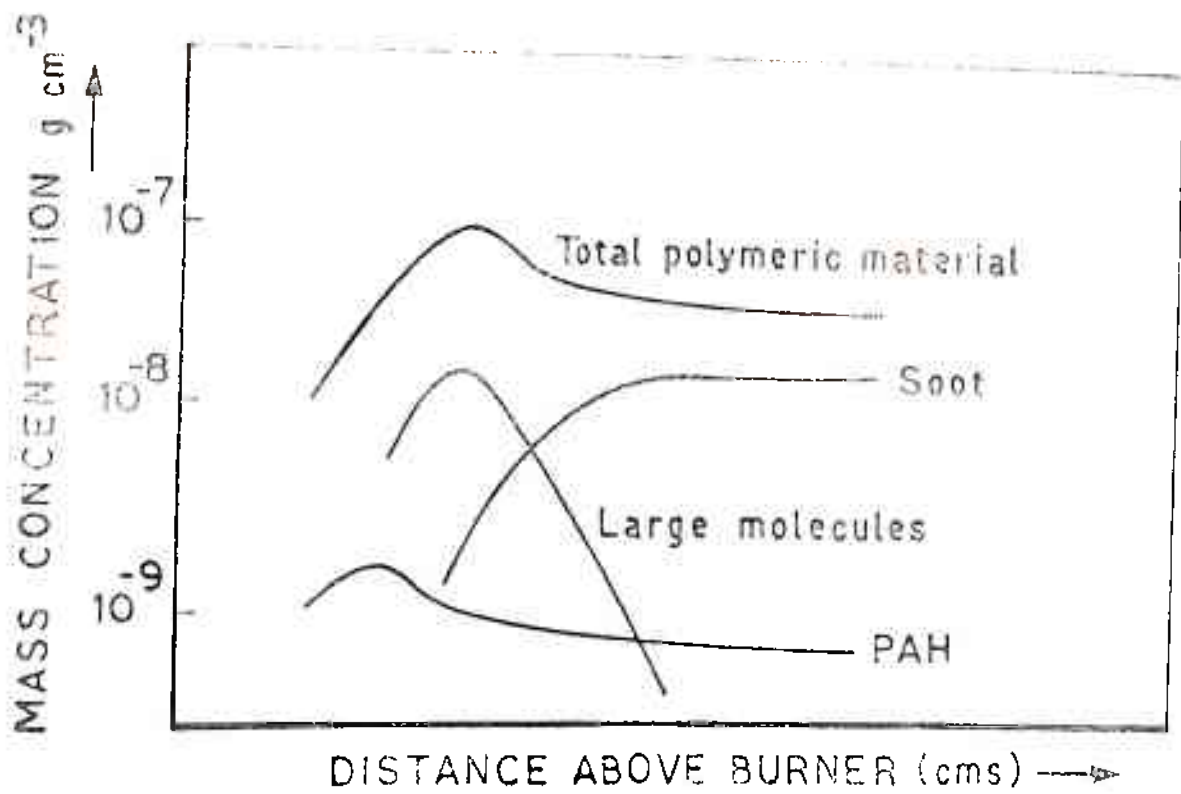


FIGURE 4.15 GROWTH OF SOOT IN FLAT FLAMES (BONNE et al, 1965; TOMPKINS AND LONG, 1968; WERSBORG et al, 1975)

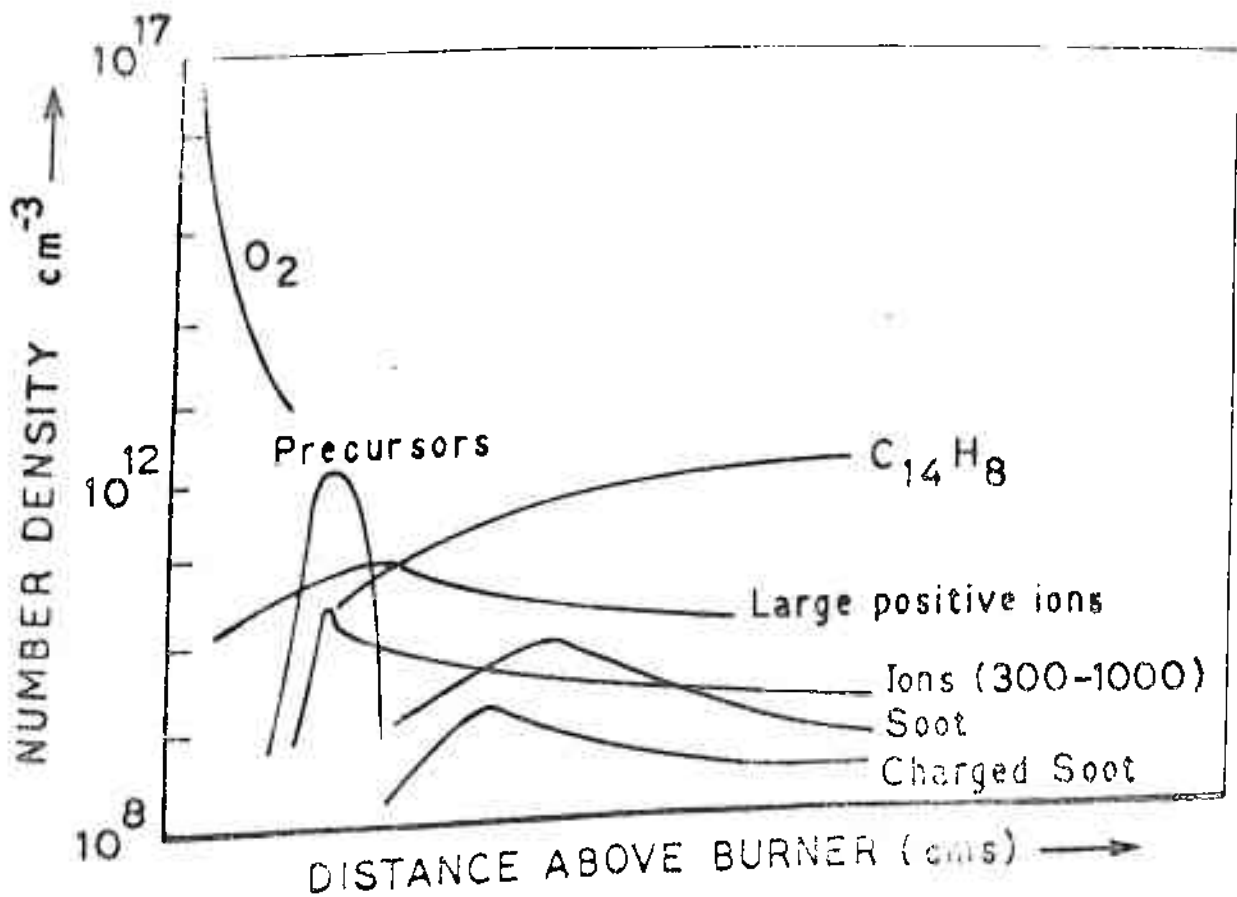


FIGURE 4.16 CONCENTRATION PROFILES OF SOOT IONS AND PRECURSORS IN PREMIXED FLAMES (HOMANN AND WAGNER, 1967, 1968; PRADO AND HOWARD, 1978; OLSON AND CALCOTE, 1981; BONNE et al, 1965; WERSBORG et al, 1975)

CHAPTER 5

EXPERIMENTAL SETUP AND PROCEDURES

5.1 Introduction

The coal pyrolysis experiments were designed so as to obtain the highest possible yields of volatile species, a condition which should result in the maximum evolution of PAH. It is already known (Loison and Chauvin, 1964; Kimber and Gray, 1967; Kobayashi, 1976) that under conditions of rapid heating, that is for heating rates greater than 10^4 °C/s, the evolution of volatiles is upto 50% higher than that obtained in the ASTM proximate yields of volatile matter.

Rapid pyrolysis is possible in both entrained particle and captive particle experiments. The former involves fine ground particles which are carried into a reactor on a stream of hot gas (Badzioch and Hawksley, 1970; Kobayashi, 1976; Anthony and Howard, 1976), where the reactor is usually an electrically heated refractory tube with the carrier gas and coal in plug flow. Captive particle experiments in which high heating rates are desired usually employ fine ground particles (50-70 µm) trapped in the folds of a fine wire mesh (Anthony, 1974; Suuberg, 1977). However, entrained flow experiments have certain major advantages over wire mesh techniques. The particulate density is lower, and thus there are less interactive effects and no external carbon capture. As a result higher yields of volatile matter are obtained. Furthermore, instantaneous heating rates are readily achieved, and isothermal pyrolysis conditions can be easily maintained. The primary disadvantage is that maximum particle residence time are

only of the order of 1s, though such short heating times are representative of industrial processes of coal combustion.

The other major advantage of rapid pyrolysis lies in the fact that the coal devolatilizes without much change in the original structure. At lower heating rates, extensive decomposition and repolymerization reactions could occur, leading to reordering or crystallization of the coal structure. Such chemical processes could bind material that would be otherwise evolved during pyrolysis.

Yields, product distributions and the duration of decomposition reactions are also drastically affected by the coal particle diameter(d) and sample sizes chosen. Though in general the rate of volatile release is dependent on temperature and residence time, this rate is proportional to d^2 for particles larger than $100 \mu\text{m}$ in diameter. The rate of evolution of volatiles is independent of d , for $d < 60 \mu\text{m}$ (Essenhigh in Wen and Lee, 1979). Temperature gradients are also induced within larger particles which together with an increase in the residence time of primary volatile decomposition products within such particles, could lead to increased rates of secondary decomposition reactions. It is also observed that for particle diameters of less than $50 \mu\text{m}$, there is minimal internal soot capture within the pores during thermal cracking and that particles larger than $65 \mu\text{m}$ are screened by the volatile flux from evolving volatile species (Howard and Essenhigh, 1967). Finally, particles smaller than $100 \mu\text{m}$ can be heated rapidly to desired reaction temperatures

For the reasons stated above, an entrained flow reactor has been chosen for the coal pyrolysis experiments. An optimum coal particle size range of 44-53 μm has been selected; the advantages of going down to smaller particle sizes are more than counter-balanced by the difficulties in obtaining well-defined particle sizes under wet-sieved conditions (discussed in Chapter 5.3.1).

The coals chosen in this study are a Montana lignite (ML), a Montana Rosebud subbituminous (MR), a Pittsburgh high volatile-A bituminous (hvAb), a Pocahontas No.3 medium volatile bituminous (mvb) and a Primrose anthracite (an). Elemental compositions and other properties are presented in Table 5.1. The entire range of carbon ranks is covered, including representatives of the three broad types of coal. The medium and high volatile coals have ultimate analyses corresponding to two coals for which Wender(1975) has proposed model structures (see Figure 2.8). The lignite and subbituminous have high oxygen contents and may evolve heterocyclic oxygen-containing PAH. Some of these may be direct-acting mutagens, that is, they would not require activation by PMS in bacterial systems.

5.2 Experimental Setup

The major components of the system are: a laminar flow-temperature controlled drop tube furnace, a fluidized coal particle feeder, a multi-phase sampling probe and a sampling train.

5.2.1 Pyrolysis Furnace System

The coal pyrolysis experiments were conducted in an Astro Model 1000 temperature controlled and electrically heated furnace

Characterization of coals studied

No.	COAL	% C (1)	% H (1)	% N (1)	% S (2)	% O (1)	% VM (3)	H/C (4)	O/C (4)	Heating value (5)
1.	Montana Lignite	69.97	6.36	1.13	1.08	22.54	36.20	1.091	.242	8,809
2.	Montana Rosebud Subbituminous	77.63	4.88	1.27	1.12	16.22	35.16	.754	.157	-
3.	Pittsburgh hvAb (PSOC 997)	85.86	5.97	1.89	1.72	6.22	36.98	.836	.054	15,303
4.	Pocahontas # 3 (PSOC 130)	91.37	4.33	1.13	.56	3.17	21.15	.569	.026	15,630
5.	Primrose Anthra- cite (PSOC 869)	95.73	1.77	.79	.54	1.69	3.32	.222	.013	14,703

N.B. (1) dmmf basis

(2) daf basis

(3) VM - as received

(4) O/C, H/C (Parr, atomic)

(5) Btu/lb, dmmf (Parr)

(Figure 5.1). Heating is accomplished by a graphite resistance element, and a 50 mm I.D. graphite muffle tube is used to maintain a 150 mm long uniformly heated zone. This isothermal zone provides residence times of upto 0.5 s in suspension, adequate for purposes of simulating processes occurring in pulverized coal flames. Longer residence times simulating processes occurring in stokers and fluidized bed combustors, may be achieved by collecting the solids in a porcelain crucible in the hot zone of the furnace.

The temperature is controlled by a graphite/boronated graphite thermocouple located just outside of the heating element in the centre of the furnace. Three quartz observation ports, 12 mm in diameter and located along the vertical axis of the furnace at intervals of 37 mm provide optical access to the reaction zone. A radiation pyrometer of the "disappearing filament" type is used to determine actual furnace temperatures. The instrument is a Micro Optical Pyrometer M6714 (Pyrometer Instrument Co., Bergenfield, N.J.).

0.3 to 0.4 g of size graded coal particles (44-53 μm , wet-sieved) in an argon carrier gas (0.1 l/min STP) are injected into the reaction zone through a water-cooled stainless steel tube along the centre line of the furnace. A uniform feed rate is ensured by using a fluidized coal feeder, that is, by elution from a vibrated bed of coal contained in a glass vial. The coal feed rate is controlled by varying the rate of displacement of the glass vial using a variable speed motor to displace the platform on which the vial is mounted. A Sage Instruments Model 341A Syringe Infusion Pump (Orion Inc., Cambridge, MA) is utilised for

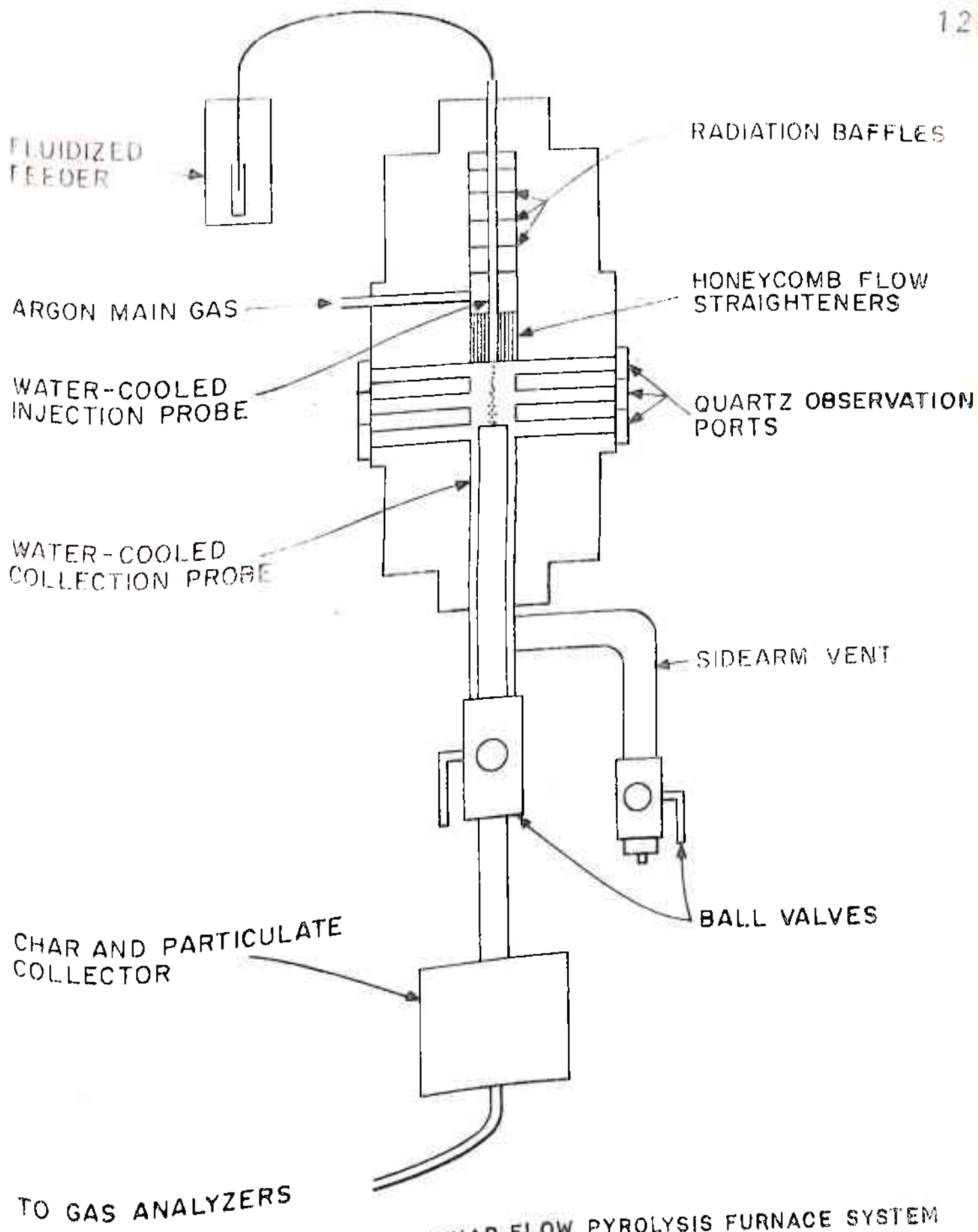


FIGURE 5.1 SCHEMATIC OF LAMINAR FLOW PYROLYSIS FURNACE SYSTEM

this purpose. The coal is fed through an 18 gauge hypodermic tube, placed within the water-cooled stainless steel tube (Figure 5.2). Feed rates of about 2.4 g/hr are used for most of the runs. It is also important to ensure that the total amount of coal fed does not vary by more than 30%, since quantitative yields of PAH and soot cannot then be normalised.

The composition in the furnace is controlled by a flow of 6 l(STP)/min of a gas stream which is preheated to furnace temperatures in a honeycomb flow straightener surrounding the water-cooled injection tube. Argon is used for maintaining an inert atmosphere. Oxygen may be mixed in with the inert gas for combustion or partial combustion studies. Uniform flow around the coal feed stream is achieved by means of the alumina flow straightener. The narrow stream of coal particles exiting the feeder are rapidly heated by the surrounding carrier gas and by radiation from the walls. Particle heating rates have been estimated to be 10^4 to 10^5 K/s.

The products, solid and gaseous are quenched at a specified distance in the furnace by drawing them through a water-cooled probe. Further details are provided in Nenniger (1984), Mitra et al (1980, 1981, 1982, 1983).

5.2.2 Sample Collection Train

The sampling and collection train comprises: a stainless steel porous wall water-cooled probe; a centripeter for on-line aerodynamic separation of the residual char from the solid pyrolysis products (soot and condensed PAH), a modified Anderson 200 cascade impactor for inertial separation and size gradation of the solid species, an XAD-2 polymer trap for collection of gas-

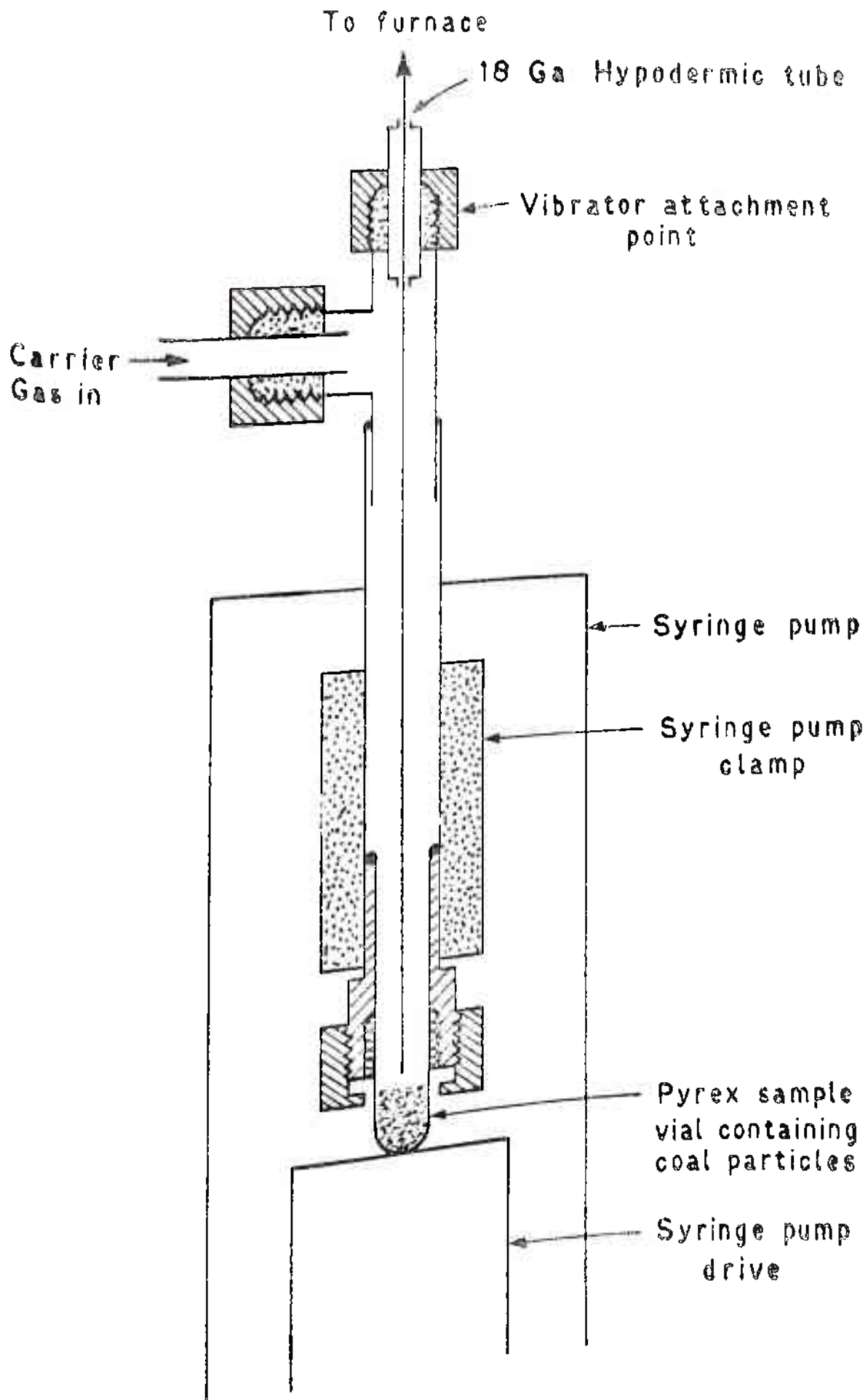


FIGURE 5.2 FLUIDIZED COAL FEEDER

phase PAH and a vacuum system. The train was designed to cocurrently recover a mixture of char, condensible PAH, soot and gaseous products, with minimal interaction between the phases.

Pyrolysis products are drawn into the sampling probe positioned coaxially with the coal feed stream and the main gas flow (Figure 5.3). The outer shell of the probe contains a porous, sintered stainless steel liner through which inert gas is transpired at 6 l (STP)/min. Products are rapidly quenched at the probe mouth by radial injection of 20 l (STP)/min of argon gas. The axially transpiring gas serves to quench reactions and also to prevent deposition of particulates and condensed PAH on the inner wall of the probe. An injection gas velocity of 3 mm/s at the probe wall is sufficient to overcome the thermophoretic drift velocity.

The products from the furnace usually consist of agglomerated char, upto 100 μm in diameter, soot and condensed PAH with characteristic sizes of 100 to 1000 \AA and gas-borne species. The char is separated from soot and condensed PAH by aerodynamic means, by employing a centripeter designed for a cut-off point of about 2.5 μm (Figure 5.4). The soot-char separation is checked qualitatively by scanning electron microscopy. Separation efficiency was excellent for the anthracite, lignite and medium volatile bituminous coals. Some soot was observed in the char fraction of the high volatile bituminous coal and could be attributed to higher soot loading, soot-char coagulation in the sampling probe and possible soot formation internal to the char particle. Particle bounce, which would be manifested by char appearing in

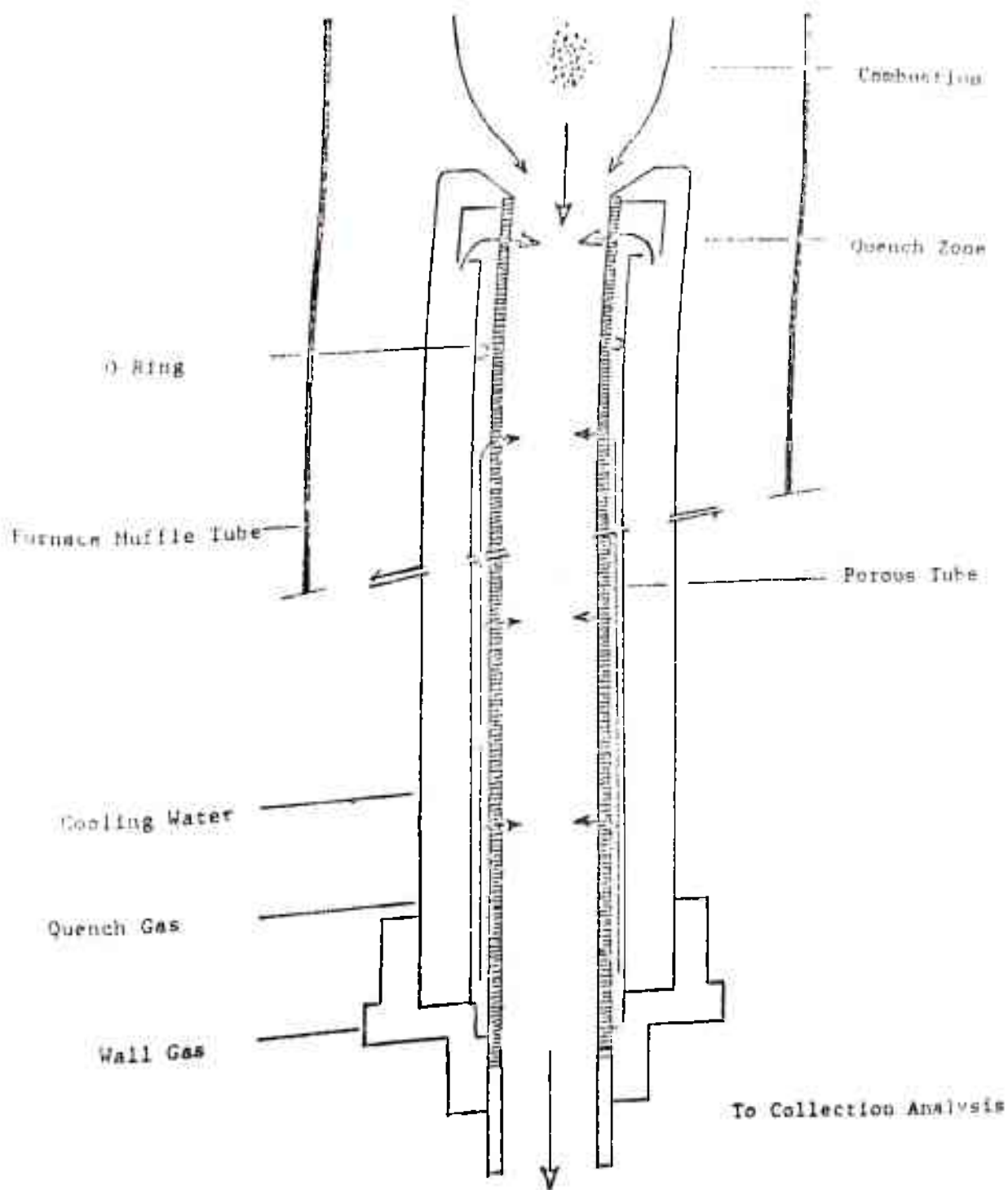


FIGURE 5.3 COLLECTION PROBE SCHEMATIC

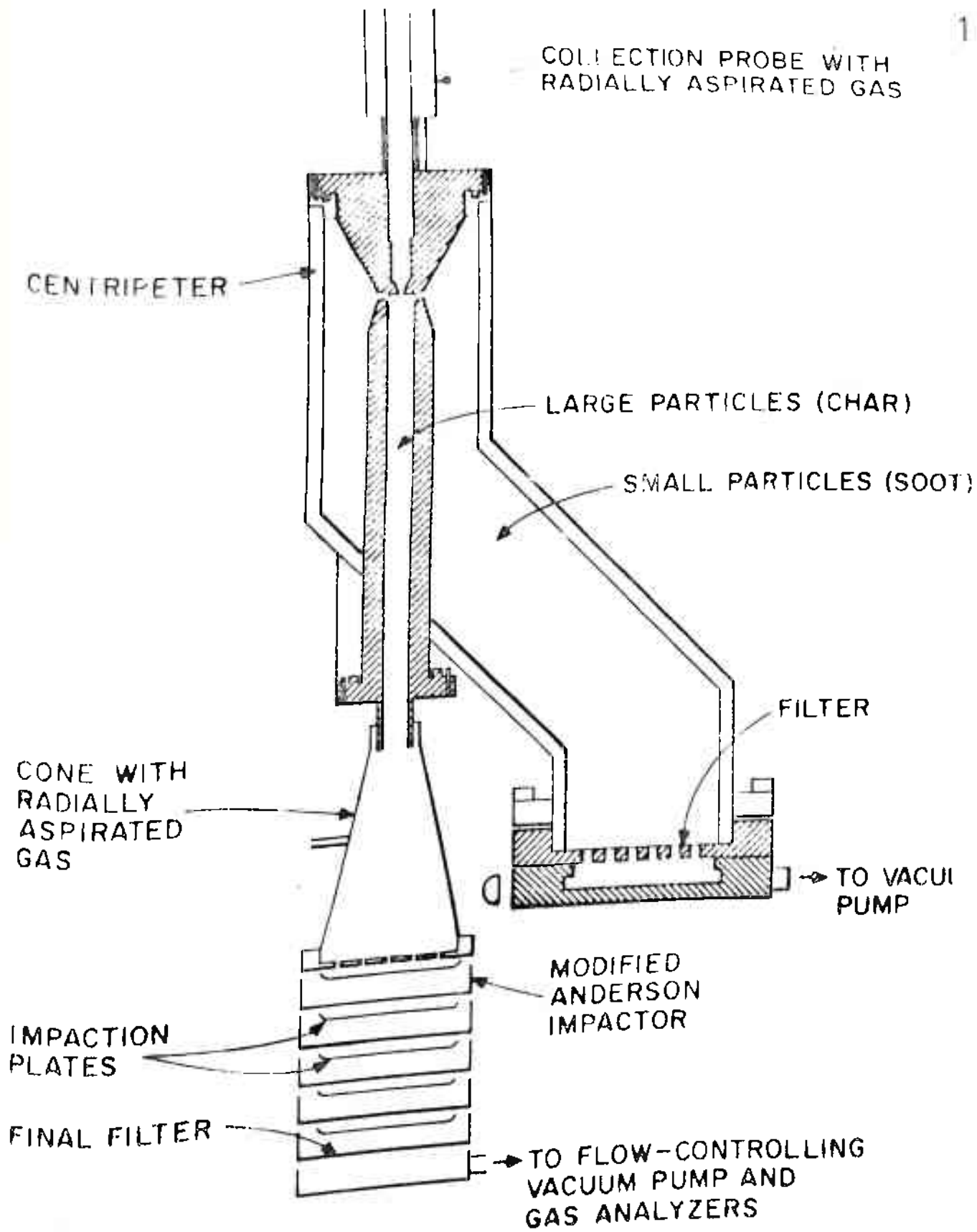


FIGURE 5.4 PARTICULATE COLLECTION SYSTEM FOR PYROLYSIS FURNACE

the soot fraction, was minimal and was observed only for the anthracite coal.

The char is collected on precleaned glass fibre filters on the top two stages of the four stage impactor (Figure 5.4). Soot particulates were collected from the bottom two impactor stages and the exit filters of 0.22 μm pore size (teflon) on the centriper and impactor. Argon at 4 l (STP)/min was injected into the centriper and at 6 l (STP)/min into the impactor, so as to minimize any sample loss through deposition on the inner walls. About 10% of the flow containing the char particles is removed through the centre tube. The remaining 90%, containing most of the finer particles and gas-borne compounds is removed through a side arm and fed to the impactor.

Gas-phase PAH are captured downstream by a water-cooled trap containing XAD-2, a commercial styrene-divinylbenzene copolymer (Rohm & Haas) of 20 to 60 mesh particle size. It is important to ensure that the temperature of the XAD-2 does not exceed about 90°F, since otherwise collection efficiencies are reduced. The efficiency of collection and extraction was evaluated by injecting alumina particles and glass beads (40-70 μm) impregnated with known amounts of PAH into the furnace; 80 to 100% recovery was obtained with the lower yields attributed to loss of the more volatile species by evaporation. The weights of soot and associated PAH are determined by weighing the collection filters in a dry-box, before and after sampling.

5.3 Experimental Procedures

Briefly, the experimental techniques consist of size grading coal, precleaning and passivation of sampling equipment,

furnace pyrolysis runs, sample processing and sample analysis.

5.3.1 Coal Preparation

Coal is obtained in the form of 1/4 inch briquettes from the Pennsylvania Coal Bank (University of Pennsylvania). The briquettes are pulverized in a rolling mill and then size graded in a Testing Sieve Shaker (W.S. Tyler and Co.). Coal particles obtained in the size range of 44-75 µm are then dry sieved by shaking them on a 300 mesh stainless steel screen and simultaneously sucking out the fines through the screen by means of a vacuum pump. However, it has been found that fines still tend to adhere to the 44-53 µm size grade of coal particle thus obtained. To obviate this, the coal particles are subsequently wet-sieved. This consists of taking 1 to 2 g weights of coal, and washing them with distilled water on a 300 mesh stainless screen, till the effluent is clear of any fines. To prevent flocculation caused by the wet sieving process, the coal slurry is then ultrasonicated in a cell disruptor (Ultrasonics Sonnicator Model W-225R) for an hour at moderate pulse speeds. The coal particles are then dried in an oven swept with argon gas, at about 35°C for at least twelve hours and then stored in a dessiccator. Prior to an experiment, the required quantity of coal particles are dried for twelve hours in a drying oven.

5.3.2 Pretreatment of Sampling Equipment

To offer minimum opportunity for sample contamination or loss, all apparatus that come in direct contact with PAH and soot are constructed such that the contact surfaces are made of glass, type 304 or 316 stainless steel or teflon. It is particularly

important that materials such as plastics (for example tygon tubing) should not be in contact with samples, since this leads to very serious background contamination.

Since photochemical degradation of PAH can also occur, sample storage and transfer containers are made of amber coloured glass, or are covered with an opaque material such as aluminium foil. Sample processing laboratories are equipped with gold bulbs, which exhibit no significant emission of light at wavelengths below 350 nm.

All solvents which are used are of ultra-high purity, such as the "Nanograde" variety of Mallinckrodt Chemical Company. These are periodically spot checked by gas chromatography to ensure minimum background.

Stainless steel surfaces coming into direct contact with

samples are cleaned and passified as follows:

- (1) Standing contact for one hour with a 1:1 volume mixture of concentrated nitric acid and distilled water
- (2) Successive washes of distilled water, isopropyl alcohol and small quantities of ultra-pure methylene chloride
- (3) Drying in an oven at 35°C and sweeping the oven with prepurified nitrogen gas at a low flow rate.

Glass surfaces are pretreated as follows:

- (1) Successive washes with a 2:1 mixture of Alconox and tap water, tap water rinse, 1:1 mix of concentrated sulphuric and nitric acids, three successive rinses of distilled water, acetone to remove any water and finally two rinses with ultra-pure methylene chloride.
- (2) Drying in an oven at 35°C and sweeping with prepurified nitrogen gas at low flow rates.

- (3) Passification by successive rinses of dilute hydrochloric acid, formic acid and deionized water.

Teflon surfaces are cleaned as above for glass.

Glass fibre filters, teflon filters and XAD-2 polymer which are used for collection of condensed PAH and soot and gas-phase PAH are cleaned as follows:

- (1) Soxhlet extraction for 24 hours with a 1:1 (vol) mixture of methylene chloride and methanol.
- (2) Subsequent drying in an oven swept with prepurified nitrogen gas at 35°C.

Sampling lines etc. are cleaned down by rinsing with acetone, followed by methylene chloride.

All cleaned surfaces are protected from atmospheric contamination by covering exposed surfaces with clean aluminium foil. Precleaned filters are stored in dessiccators, whereas XAD-2 is preserved in a slurry of methanol.

5.3.3 Furnace Operation

The furnace, which is kept under 10 psig of inert pressure, to prevent any oxygen bleeding in is first vented to the hood. The cooling water supplies to the furnace and the collection probe are turned on, as are the quench gases to the sampling train. The collection probe is checked to ensure that there are no leaks around the cap and that the quench gas flow is uniform. Simultaneously, the furnace is brought up to desired temperature, the final setting being checked by an optical pyrometer.

The sampling train, that is, the centripeter, cascade impactor and XAD-2 trap are assembled, after weighing all filters

in a dry box. Main gas flow is increased to 6 l /min , the collection probe is inserted into the furnace to the desired height and the main vacuum pump is switched on.

Coal to be fed is weighed in a precleaned glass vial and is then carefully evacuated down to a vacuum of about 22 in. of mercury. Care must be taken to ensure that no coal particles escape into the vacuum system. Carrier gas flow is then turned on and adjusted to the desired value.

The sampling train is then attached to the probe and gas flows to the centripeter and impactor switched on. The furnace pressure is adjusted to atmospheric and all gas flows allowed to stabilise so that the system reaches steady state.

Once steady state is achieved, the syringe pump and vibrator are turned on and coal is fed into the reaction zone of the furnace, until 0.3 to 0.4 g of coal has been injected. During the run, furnace pressure is maintained at atmospheric, and the feeder carefully watched for signs of plugging. This is manifested by pressure rise in the feeder vial and a drop in the carrier gas flow-rate.

After 0.3 to 0.4 g of coal has been fed, the run is terminated by shutting off the coal feeder. The coal vial is immediately removed and kept in the dry box. The sampling train is disassembled and all filters and XAD-2 stored in the drybox for subsequent weighing. The probe is removed from the furnace and the seal checked for leakage. Teflon lines connecting the centripeter and the XAD-2 trap are washed down with methylene chloride, the wash being stored in amber glass bottles. The furnace vent to the hood is closed to prevent any oxygen from

entering. The furnace temperature is checked during the run by means of an optical pyrometer through each of the three quartz observation ports.

5.3.4 Sample Processing

The amounts of char, soot and associated PAH are determined by difference in filter weight before and after each run. The XAD-2 and the filters are then extracted for 30 hours in a soxhlet apparatus with nanograde methylene chloride. The line wash with methylene chloride is added to the XAD-2 extract and the total volume of about 400 to 500 ml of soot (filter) extract and gas-phase PAH (XAD-2) extract are separately distilled down to about 2 to 5 ml in an 82 cms long distillation column. From model compound studies, it has been estimated that the recovery of lighter molecular weight PAH (two ring or less) is of the order of 85% whereas that of the heavier species was higher than 95%. It should be emphasized that distillation to concentrate the PAH in solution, though a lengthier process, is far more efficient than the more common vacuum rotary evaporation technique where losses of naphthalene have been estimated to be as high as 50%. Methylene chloride was chosen as the extraction solvent since studies (Donovan, 1978; Grosjean, 1975) have shown that the largest amounts of extracted material are thus obtained. However, recent studies also indicate that for polar compounds and for those with a molecular weight larger than that of coronene, methanol may be a more suitable extraction solvent. It is also important that methylene chloride be handled with care, since inhalation of its vapours or skin contact can lead to health hazards. While handling

all samples, thin plastic gloves are used.

5.3.5 Sample Analysis

The distilled samples are stored in centrifuge tubes equipped with teflon cap liners in the freezer of an unlit refrigerator. It has been estimated that sample integrity is retained for periods of upto two months under such storage conditions.

Capillary gas-chromatographic analysis is performed on the methylene chloride extracts, to separate and identify individual compounds including many PAH isomers. A fused silica capillary column, coated with an SE-52 methyl phenyl silicone stationary phase is utilised for the separation, in a Perkin-Elmer Sigma I Gas chromatograph. The 15 m column is programmed as follows: 45°C (held for 4 min) to 280°C at 10°C/min (held for 13 min at 280°C). An external standard solution containing 24 PAH compounds ranging from tetralin (2-ring) to coronene (7-ring) is used to determine response factors, α_i defined as:

$$\alpha_i = \frac{\text{Mass of compound 'i' injected}}{\text{area recorded by the GC}}, \quad i \in [1, 24]$$

The response factors are then fitted to the retention times of the standard compounds by a 4th-order polynomial, from which α_i of unknown PAH present in the pyrolysis sample can be determined. The concentration, C_i of an unknown PAH would then be:

$$C_i \left(\frac{\text{mg PAH}_i}{\text{g coal fed-dmmf}} \right)$$

$$= \alpha_i \times \left(\frac{\text{Area recorded for PAH}_i}{\text{sample volume injected into GC}} \right) \times \left(\frac{\text{Total sample volume}}{\text{g coal fed-dmmf}} \right)$$

The identification of individual PAH species is performed as follows:

- (1) As a first approximation, the GC of the 24-compound standard is compared with that of the unknown sample and prominent peaks are correlated.
- (2) Detailed gas chromatograph - mass spectrometric identification is carried out on samples containing the widest range of PAHs, after an initial screening has been undertaken by capillary GC.
- (3) Individual structures are assigned by correlating mass spectral data and information from the capillary GC analysis by calculating retention indices (Lee et al, 1979) for each peak in the GC of the pyrolysis sample.

A list of the types of compounds which have been identified by the above procedure is shown in Table 5.2.

5.3.6 Mutagenic Assays

Genetic testing is performed with a bacterial forward mutation assay in *Salmonella typhimurium*, using resistance to the purine analog 8-azaguanine as a genetic marker (Kaden et al, 1979). PAH are not direct-acting mutagens. Rat liver post-mitochondrial supernatant (PMS) is added to PAH to allow metabolism of promutagens to their active forms. The mutagenic metabolites are epoxide forms of PAH.

TABLE 5.2

Polycyclic aromatic hydrocarbons identified from coal pyrolysis

	Primary species	Mutagenic species	N-PAH	S-PAH
1. Indene				
2. Methylphenol				
3. Methylindene	P			
4. Tetralin	P			
5. Naphthalene	P			S
6. Benzo(b)thiophene			N	
7. Indole		M	N	
8. Quinoline	P			
9. 2-methylnaphthalene				
10. 2-methylbenzo(b)thiophene	P	M		
11. 1-methylnaphthalene				
12. Methylquinoline	P			
13. Biphenyl				
14. 2-ethylnaphthalene	P			
15. 1-ethylnaphthalene				
16. Methylindole				
17. 2,6-dimethylnaphthalene				
18. 2,7-dimethylnaphthalene	P			
19. 1,3-dimethylnaphthalene				
20. 1,7-dimethylnaphthalene				
21. 1,6-dimethylnaphthalene				
22. 2,3-dimethylnaphthalene				
23. 1,4-dimethylnaphthalene				
24. 1,5-dimethylnaphthalene	P	M		
25. Acenaphthylene				
26. 1,2-dimethylnaphthalene				
27. 1,8-dimethylnaphthalene				
28. 4-methylbiphenyl	P			
29. Dibenzofuran	P	M		
30. Acenaphthene	P			
31. C3-naphthene	P			
32. Fluorene				
33. 9-methylfluorene	P			
34. C2-biphenyl				
35. 9-ethylfluorene				
36. 2-methylfluorene				
37. 9-fluorenone	P			S
38. Dibenzothiophene	P			
39. Phenanthrene	P			
40. Anthracene			N	
41. Carbazole				
42. 1-phenylnaphthalene				
43. 3-methylphenanthrene	P	M		
44. 2-methylphenanthrene				

TABLE 5.2 (contd.)

	Primary species	Mutagenic species	N-PAH	S-PAH
45. 2-methylanthracene				M
46. 4H-cyclopenta(def)phenanthrene	P			
47. 9-methylphenanthrene				
48. 1-methylanthracene	P	M		
49. 1-methylphenanthrene				
50. 2-phenylnaphthalene				
51. 2-ethylphenanthrene	P	M		
52. Fluoranthene	P			
53. Benz(j)acenaphthylene	F	M		
54. Pyrene				
55. Benzo(a)fluorene		M		
56. Benzo(b)fluorene				
57. 2-methylpyrene	P	M		
58. Cyclopenta(cd)pyrene	P	M		
59. Benz(a)anthracene	P	M		
60. Chrysene	P	M		
61. Triphenylene				
62. Methylchrysene				
63. Benzo(j)fluoranthene		M		
64. Benzo(e)pyrene		M		
65. Benzo(a)pyrene		M		
66. 3-methylcholanthrene		M		
67. Libenz(a,c)anthracene		M		
68. Libenz(a,h)anthracene		M		
69. Benzo(ghi)perylene				
70. Coronene				

A distinction needs to be made between the toxicity and mutagenicity of the pyrolysis products, since in many cases, bacteria are lost due to toxic conditions. The assay is thus corrected for the toxicity of the test sample. Testing is performed in the presence and absence of PMS, so as to determine whether direct-acting mutagens are present.

Mutagenic screening is also complicated by the fact that pyrolysis products contain a complex mixture of PAH. Since the dose-response curves for individual PAH are not linear, it is possible that the mutagenic activity of the mixture would not be represented by the mutagenic activities of individual species.

CHAPTER 6

RESULTS AND DISCUSSION

6.1 Effect of Pyrolysis Conditions

Preliminary experiments were conducted under oxidising conditions, so as to ascertain PAH emission levels. Oxidative pyrolysis of Montana lignite and Pittsburgh high volatile-A bituminous coals in an atmosphere containing as low as 6 percent oxygen produced undetectable quantities of PAH (Chow, 1979). Similar experiments utilising shale oil and solvent refined coal (SRC-II) at temperatures upto 1300 K also resulted in negligible levels of PAH (Mitra et al, 1980). It appears that any PAH initially evolved were immediately oxidised, or that the PAH precursors were consumed.

Data from time-resolved studies on PAH and soot evolution is presented in Figures 6.1 to 6.5. The distance between the coal feed point and the position at which pyrolysis products are quenched and sampled is taken as a measure of residence time. A distance of 6.0 inches corresponds roughly to a residence time of 300 ms for coal particles in the isothermal zone of the furnace.

At temperatures upto 1300 K, the yield of PAH (mg /g dmmf coal fed) increases as the residence time increases. At higher temperatures however, PAH concentrations pass through a maximum at intermediate residence times. The global evolution of PAH thus appears to follow a first-order type of dependance. It is interesting to note that the temperature-time history of soot yields appears to be independent of the pyrolysis temperature. The implication is that PAH are not the primary precursors for soot

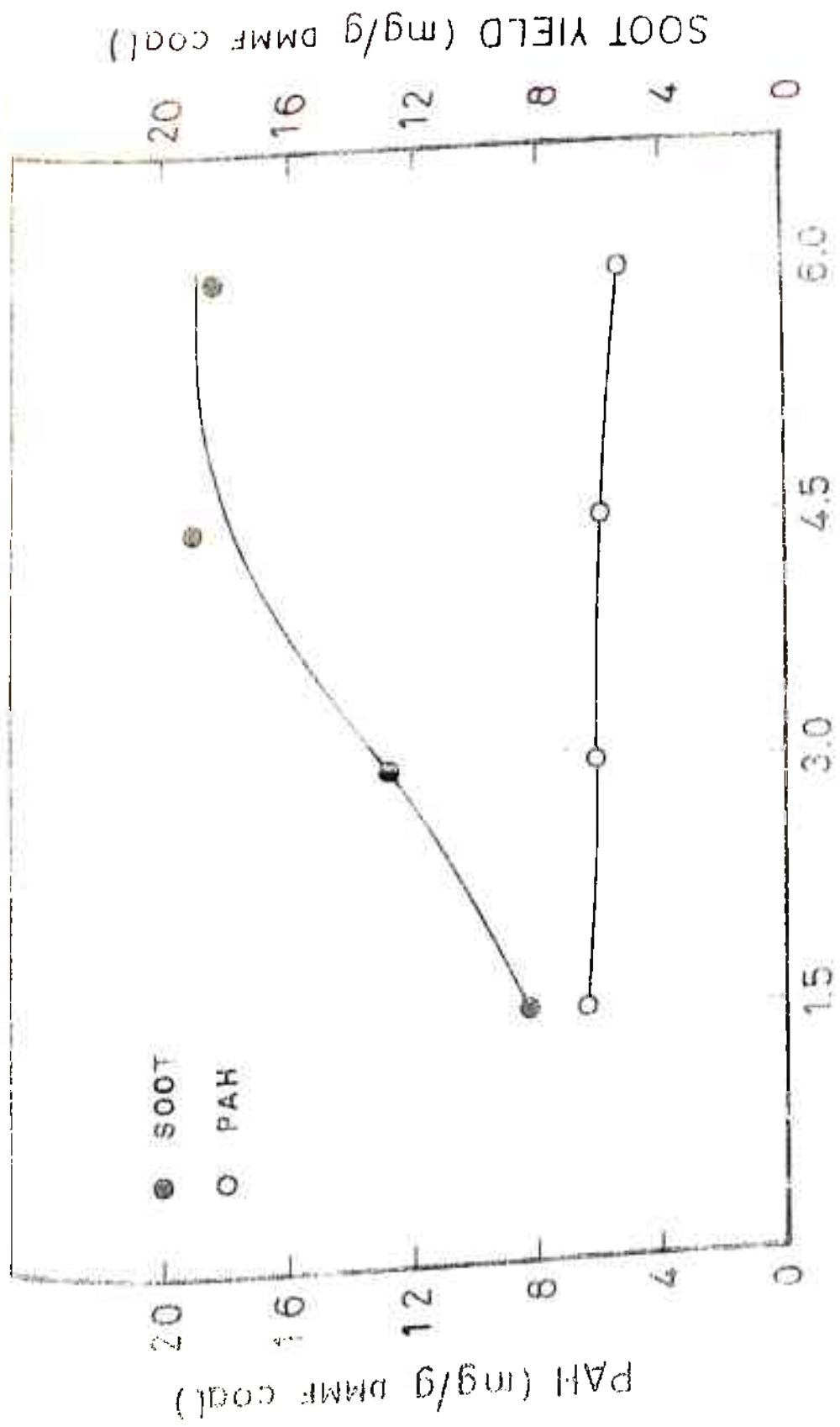
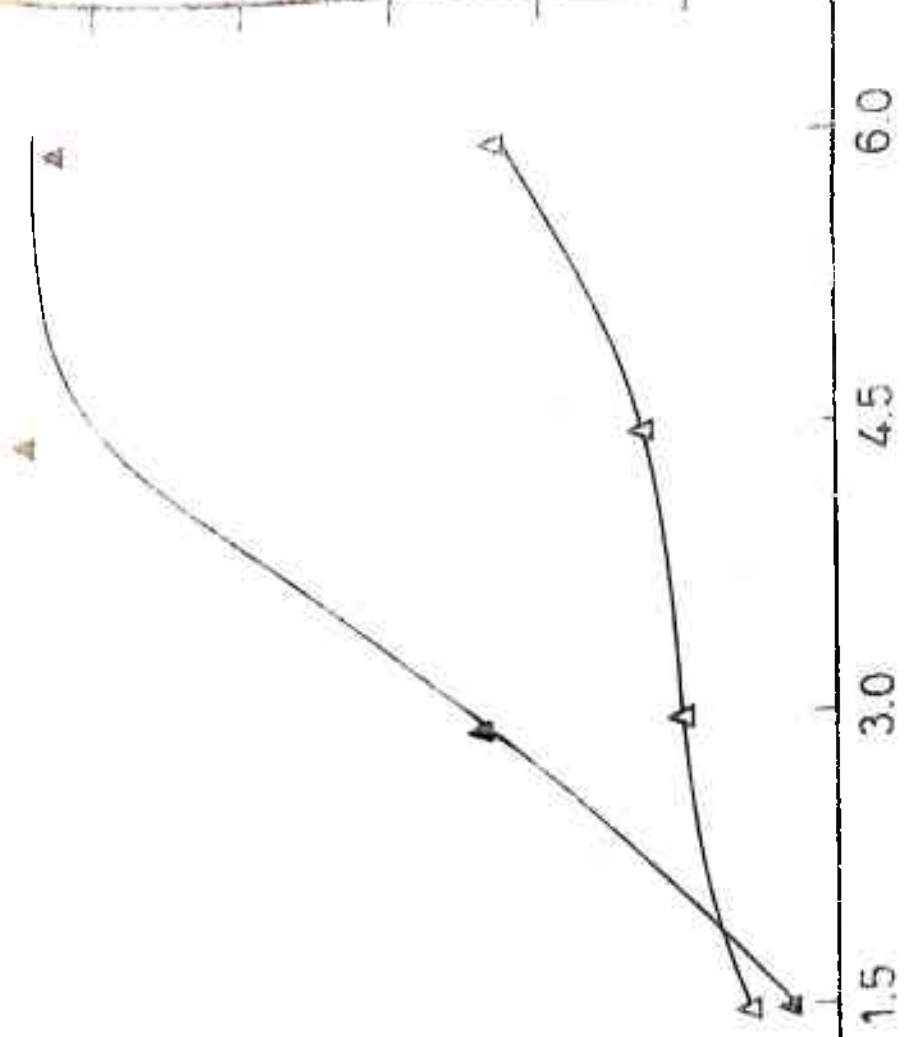


FIGURE 6.1 PYROLYSIS OF HVAD COAL (900 K)

FIGURE 6.1 PYROLYSIS OF HVAD COAL (900 K)

SOOT YIELD (mg/g DMF coal)

200
160
120
80
40
0



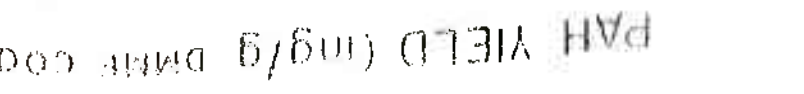
DISTANCE FROM COAL FEED POINT (in)

FIGURE 6.2 PYROLYSIS OF hvab COAL (1100K)

PAH YIELD (ng/g DMF coal)

20
16
12
8
4
0

▲ SOOT
▲ PAH



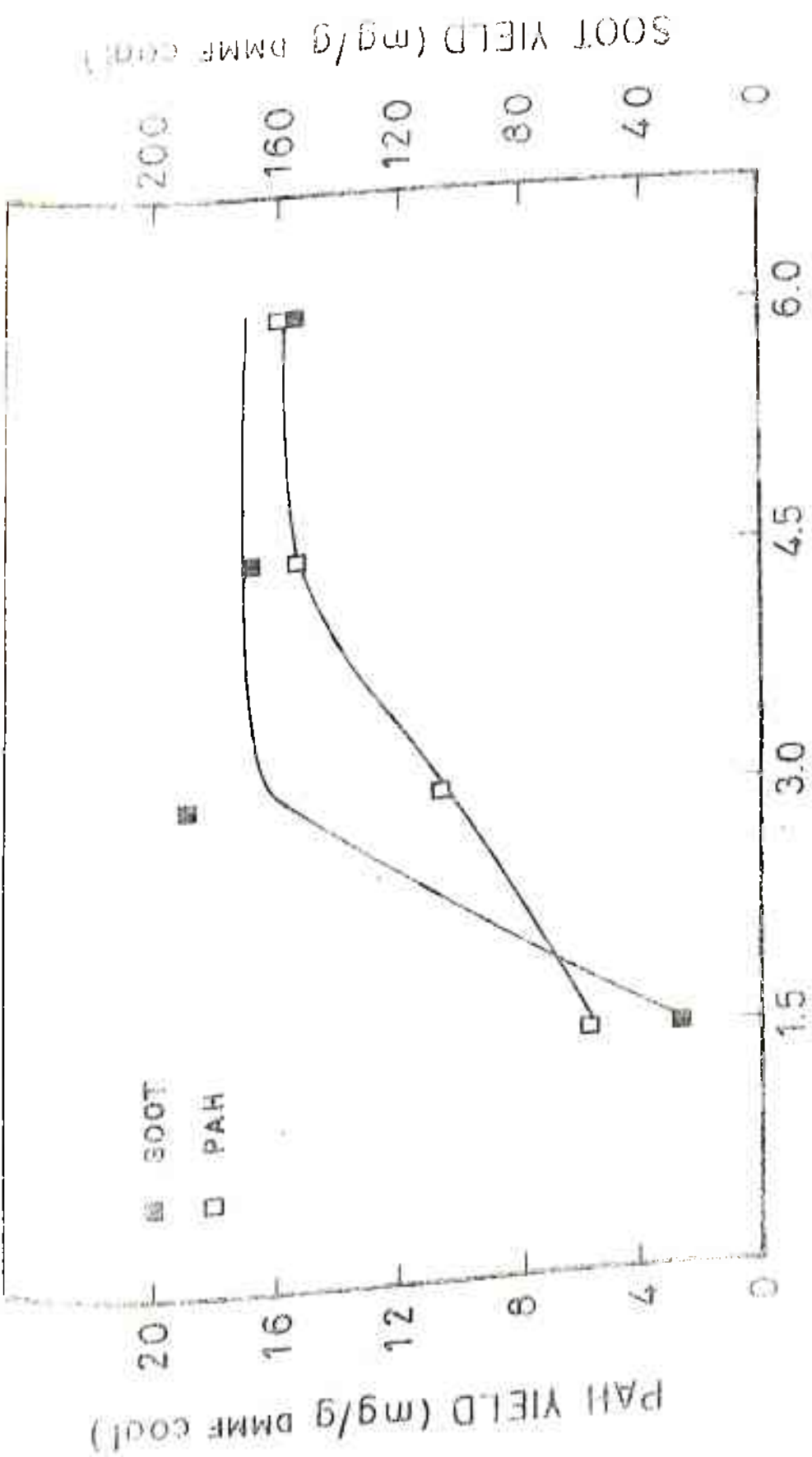


FIGURE 6.3 PYROLYSIS OF NVA6 COAL (1300K)

FIGURE 6.3 PYROLYSIS OF NVA6 COAL (1300K)

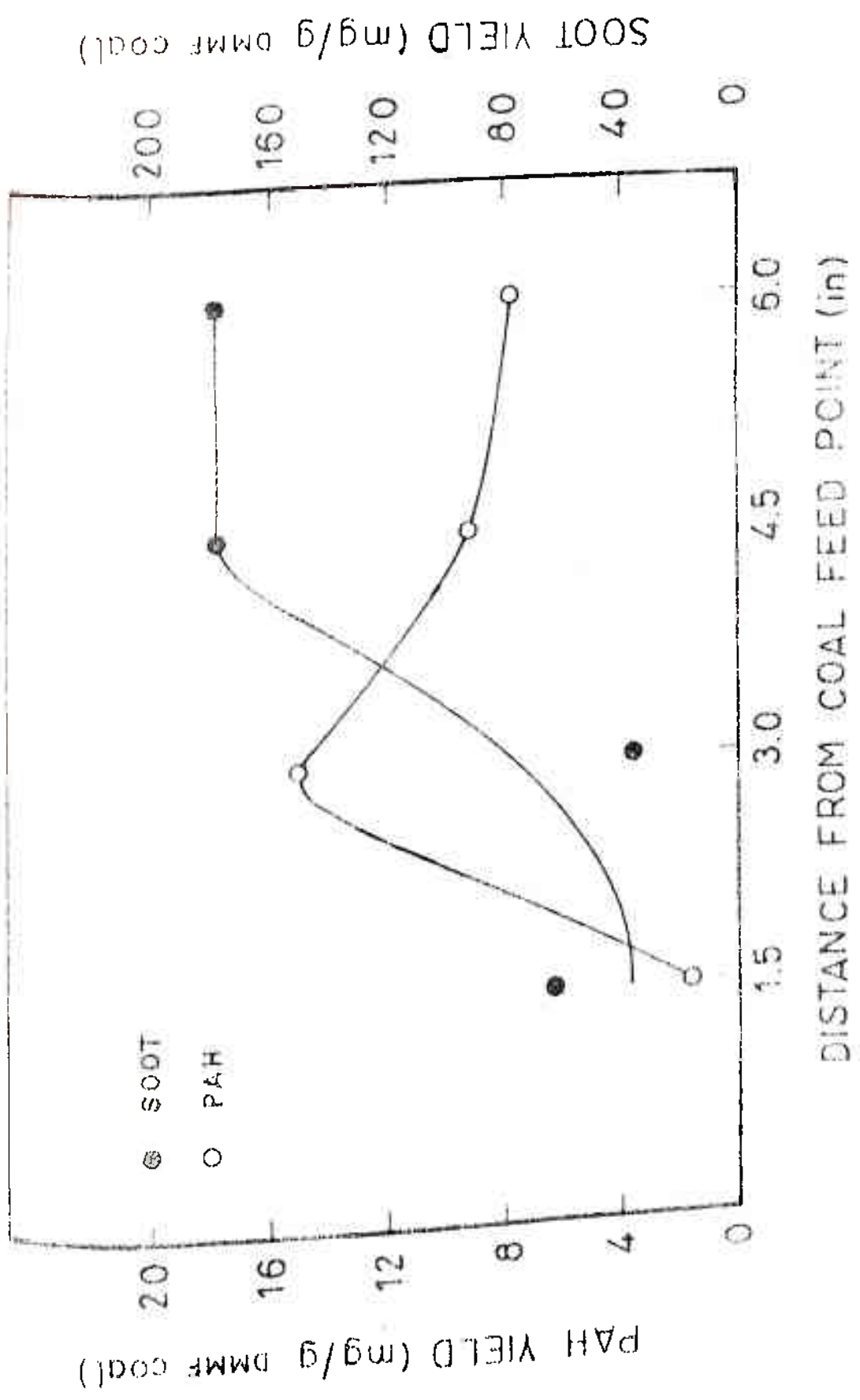


FIGURE 5.4 PYROLYSIS OF hvab COAL (1500K)

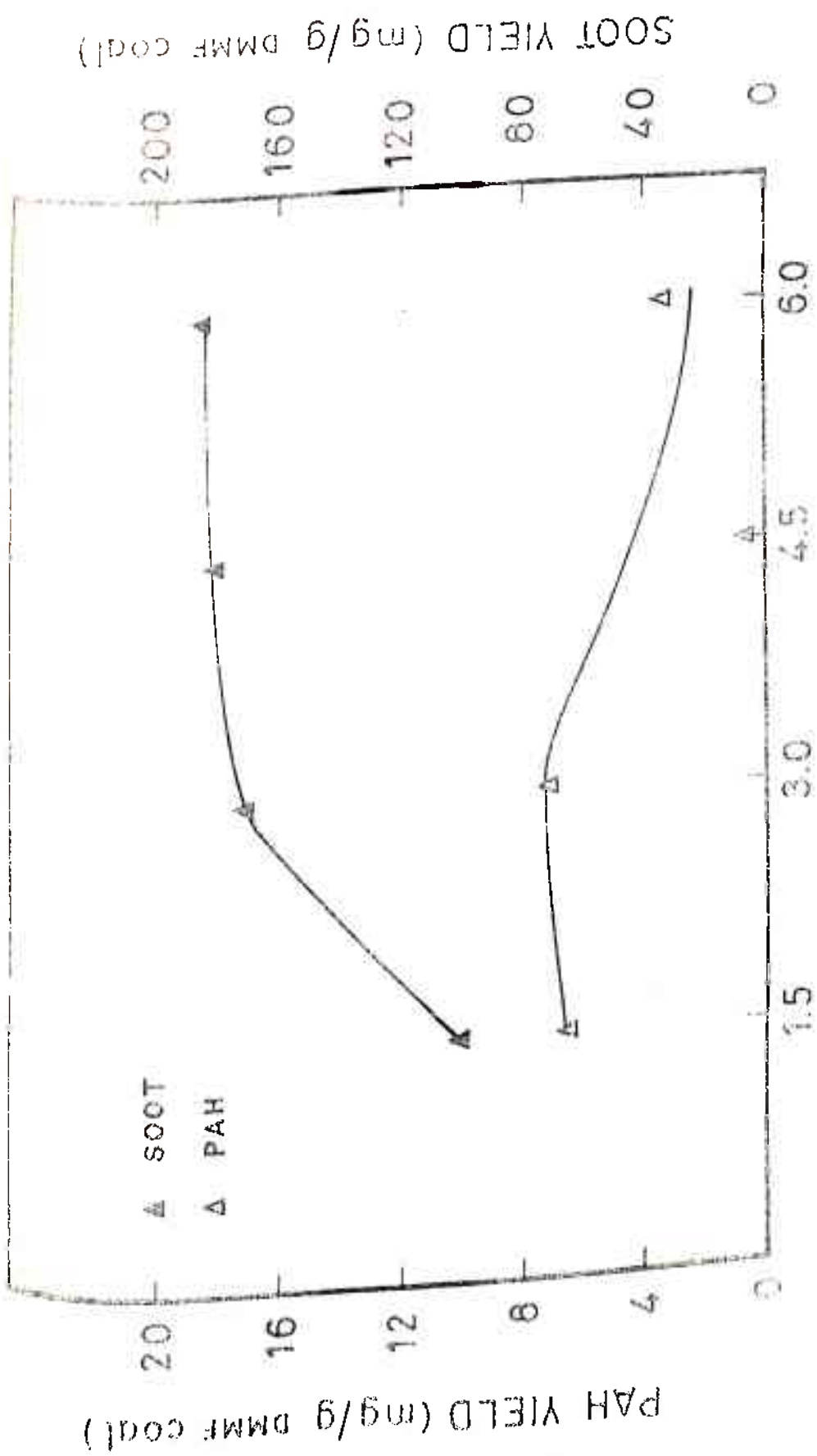


FIGURE 6.5 PYROLYSIS OF hvab COAL (1700K)

FIGURE 6.5 PYROLYSIS OF hvab COAL (1700K)

formation. Moreover, except for the case of pyrolysis at 1500 K, PAH concentrations are at most 10% of soot concentrations at the same residence time.

The evolution pattern of PAH could be explained if one postulates the existence of two parallel reactions of differing activation energies. At temperatures below 1500 K, primary pyrolysis, defined as the reaction with the lower activation energy, is the dominant route. PAH are evolved mainly via thermal cracking of the coal structure, though synthesis from smaller molecular fragments is also occurring. At higher temperatures, destruction of PAH formed initially occurs in the gas phase, via the route defined as secondary pyrolysis.

The competition between evolution and destruction is further illustrated in Figures 6.6 to 6.10, where PAH and soot yields are plotted versus furnace temperature, at a residence time of about 300 ms. For the wide range of coals studied, PAH yields follow the same trend. There is a peak in PAH evolution at 1300 K. In most cases, the decline in PAH concentration lies in a region where soot yields approach asymptotic values. The trends reported here are similar to that from studies on pyrolysis of n-tetradecane in free droplet vapourization (Vranos and Liscinsky, 1983). Here also, PAH formation was observed to peak at about 1400 K. PAH attained a maximum concentration before appreciable soot formation occurred. Tar yields from a variety of coals show a similar temperature dependence (Freihaut et al, 1983).

PAH may be divided into two broad categories: thermally reactive and thermally unreactive (vide Chapter 4.1 and Lewis and Edstrom, 1963). The peak in PAH evolution at 1300 K could then be explained if it is assumed that the thermally unreactive

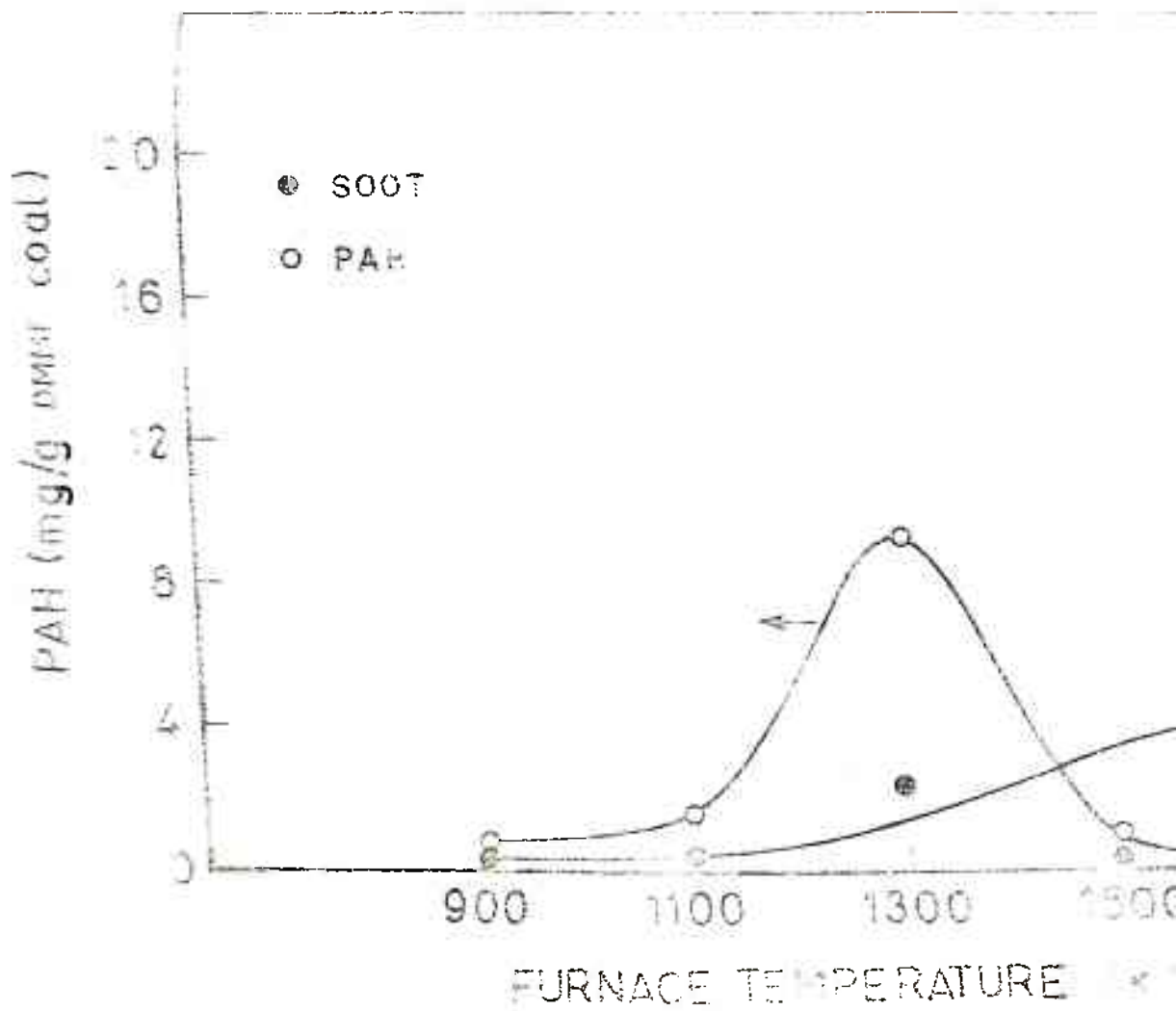
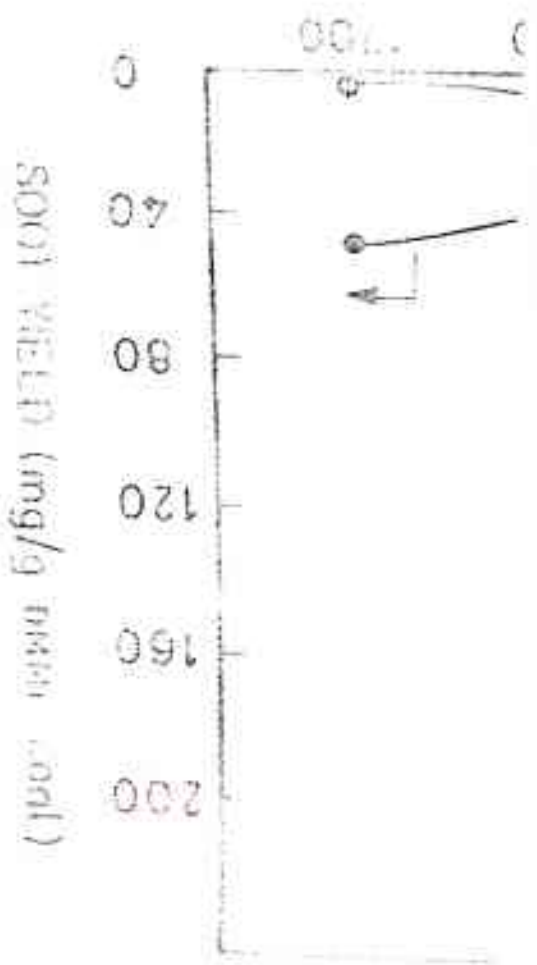


FIGURE 6.6 ANALYSIS OF LIGNITE COAL



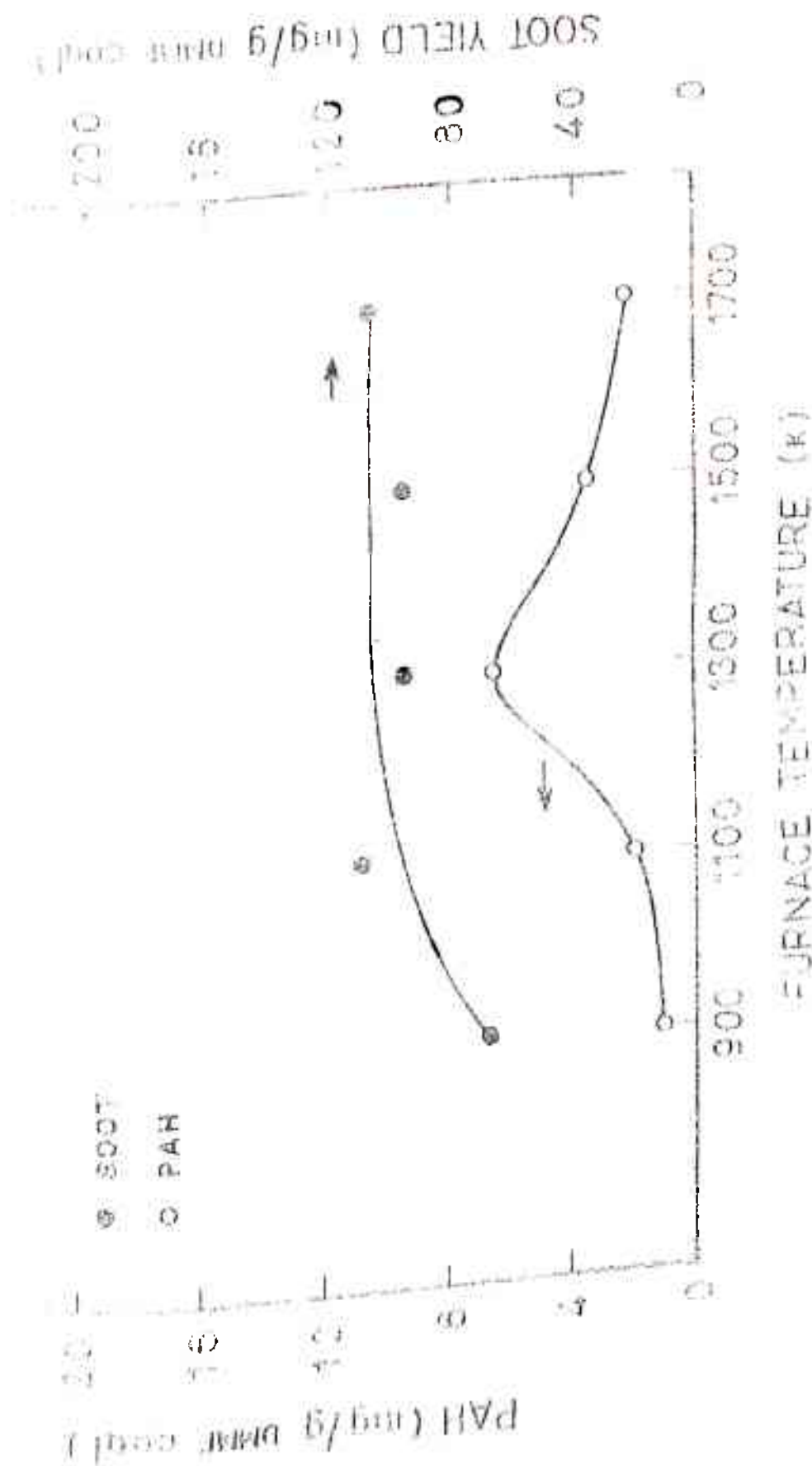


FIGURE 67. PYROLYSIS OF SUB-BITUMINOUS COAL (SOOMS)

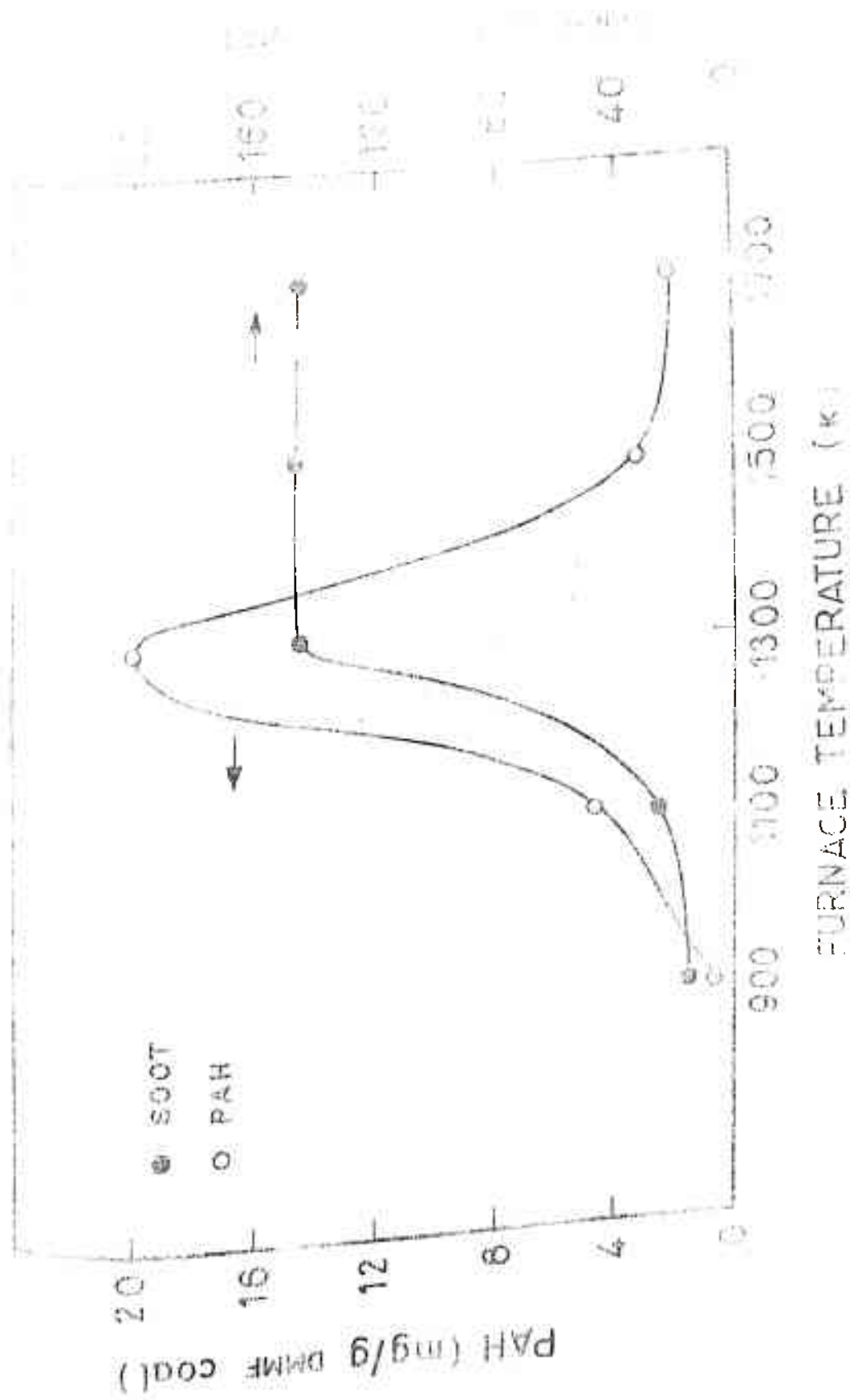


FIGURE 6.6 PYROLYSIS OF MEDIUM VOLATILE BITUMINOUS COAL (3000°F)

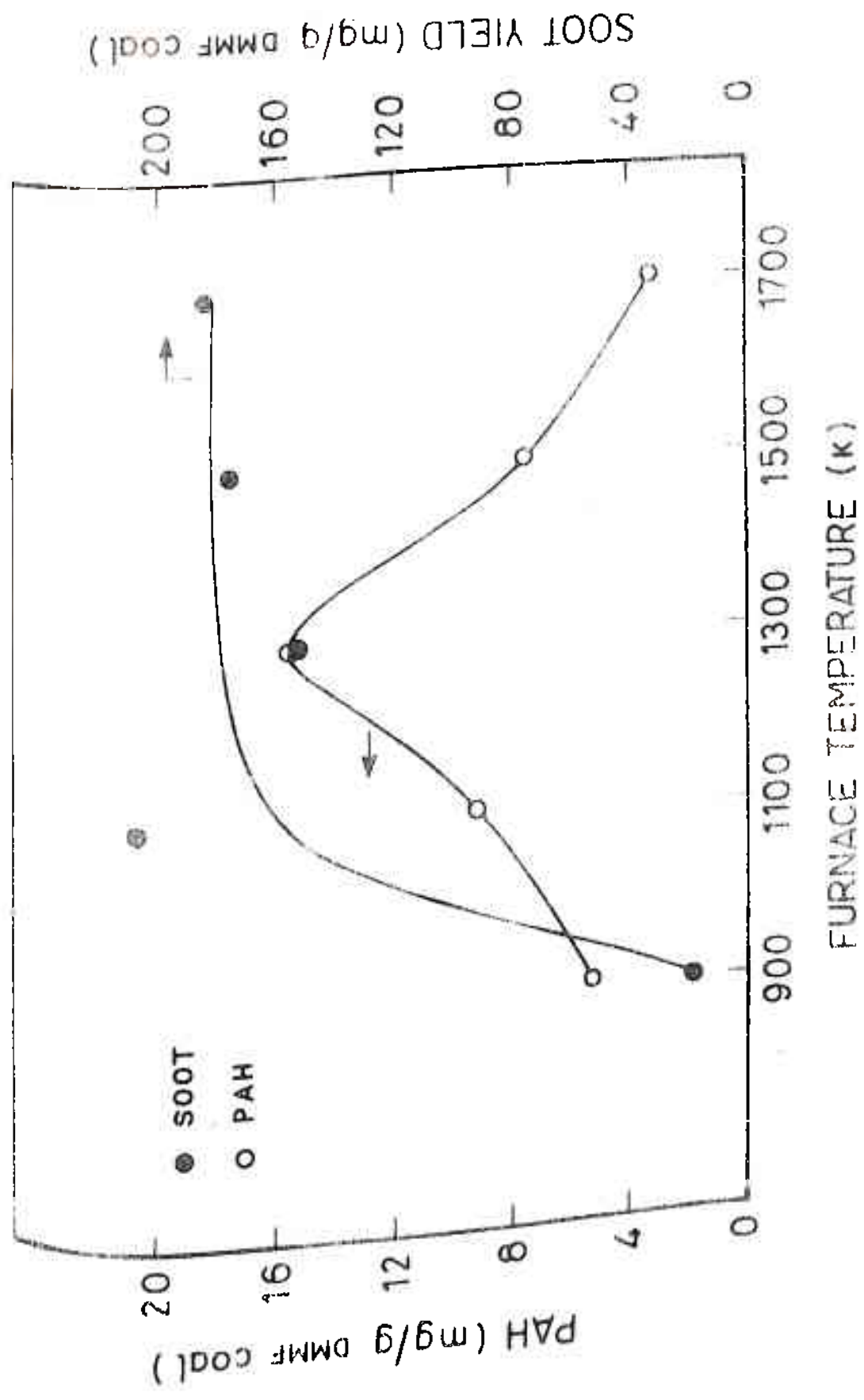


FIGURE 6.9 PYROLYSIS OF HIGH VOLATILE BITUMINOUS COAL (300 MS)

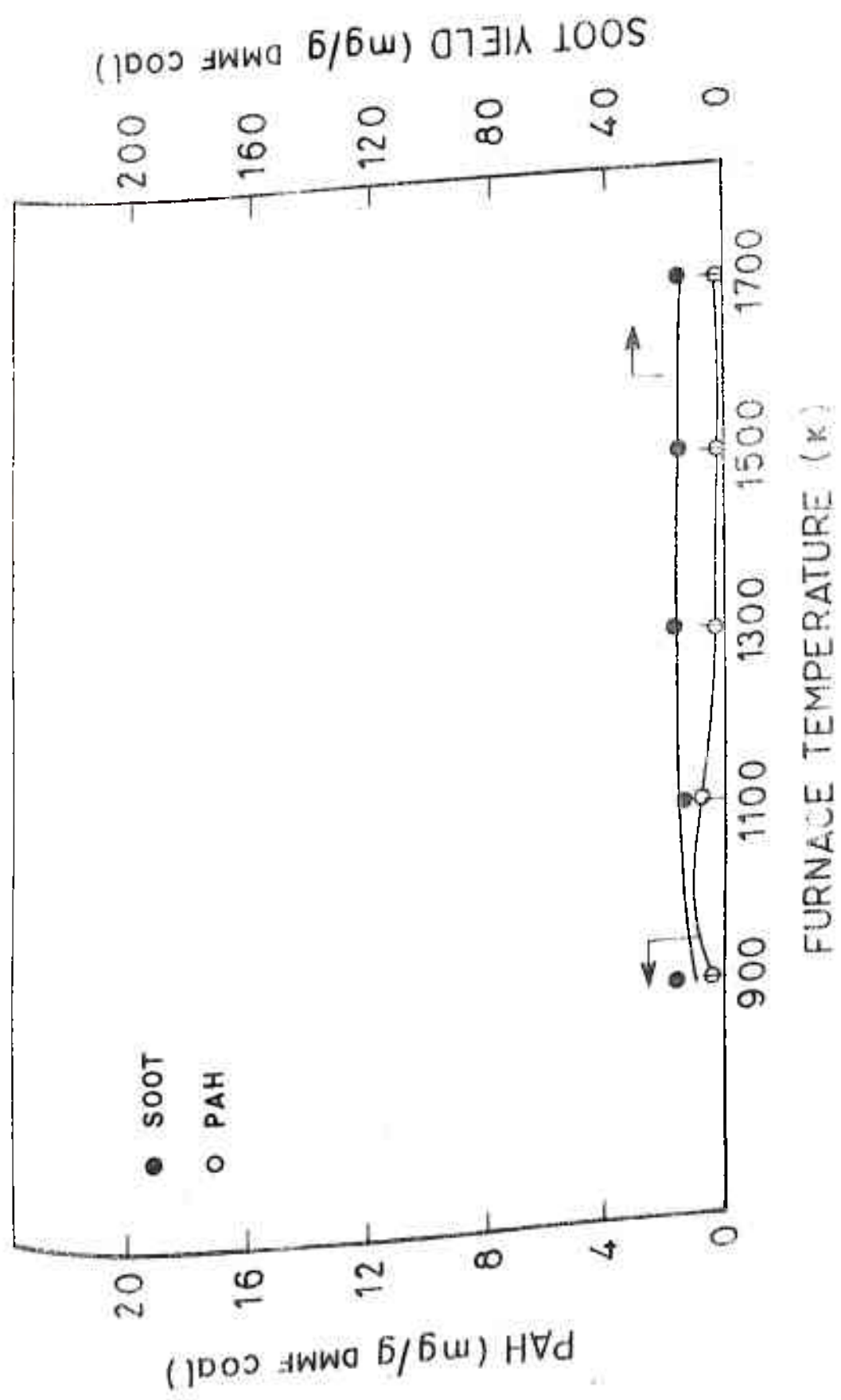


FIGURE 6.10 PYROLYSIS OF ANTHRACITE COAL (300MS)

Certain structural parameters may be calculated for the coals studied in this work, based on elemental analyses of the coals and on the above model structure. These include aromaticity, the number of aromatic rings per average structural unit and the types of aliphatic hydrogen present. The protocol for these calculations is based on the method followed by Suuberg (1977), and is outlined below for the case of the Pittsburgh high volatile-A bituminous coal.

From Figure 2.2, the aromaticity of the high volatile bituminous coal, corresponding to a carbon content of 85.86% (dmmf) is 0.24. The distribution of aromatic and non-aromatic carbon is presented in Figure 6.11. The XRD data (Cartz and Hirsch, 1960) is debatable, as Brooks and Stephens (1965) question Hirsch's method of analysing the X-ray spectra. Aromaticity values obtained by Hirsch are consistently below those reported by most other investigators. As can be seen, the average size of condensed aromatic systems increases steeply at carbon percentages greater than 95%. From measurements of electron mobility in anthracities, Van Krevelen (1961) offers the following average cluster sizes for anthracites:

% C	Average Number of Atoms per Aromatic Cluster (\bar{N})
91.7	40
93.7	45
94.2	50
95.0	55
96.0	> 60

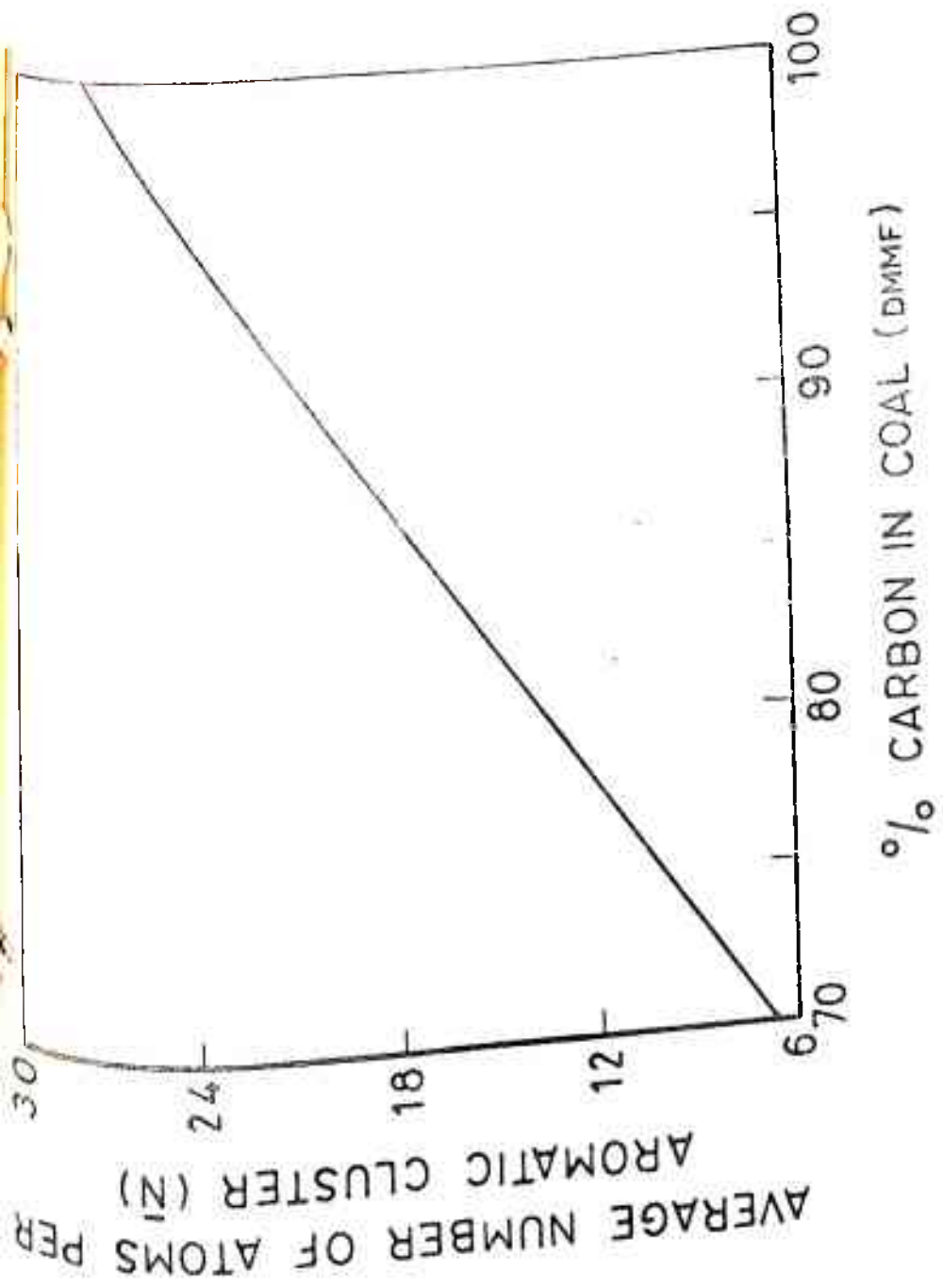


FIGURE 6.11 VARIATION OF \bar{N} WITH RANK (CARTZ AND HIRSCH, 1960 ; VAN KREVELEN, 1961)

From Figure 6.11, the average number of atoms per aromatic cluster (\bar{N}) for an hvAb of 85.86% C (dmmf) is 18. The value for the anthracite is taken to be ~ 55 corresponding to Van Krevelen's (1961) data.

Then, the carbon atoms per average structural unit.

$C = \bar{N}/f_a = 21.43$ for hvAb. The total number of rings for an average structural unit, R is obtained from the Ring Condensation Index data in Figure 6.12. It should be noted that for the hvAb and mvb coals, a weighted average of RCI values obtained from the micrinite and vitrinite curves has been calculated, relative to micrinite and vitrinite maceral fractions in the coal. When this approach is followed for the low rank coals, R values so calculated appear to be higher than is likely for such carbon percentages. For the anthracite, all three curves converge. It needs to be emphasized again, that there are inherent dangers in visualizing monomers comprising an "average" condensed structure; these have been discussed in Chapters 2.2 and 2.3.

Thus, RCI for the hvAb coal = 0.382 and $R = \frac{C}{2} (RCI) + 1 = 5.09$. Since $\bar{N} = 18$ implies 4 ring aromatic structures, the conclusion is that the hvAb has some non-aromatic ring content.

The aliphatic and phenolic hydrogen contents are obtained from Figure 6.13 and for the hvAb coal of 85.86% C (dmmf), work out to 0.477 H/C and 0.043 H/C respectively. The aromatic hydrogen content is then given by

$$\frac{H_{ar}}{C} = \frac{H_{total}}{C} - \left(\frac{H_{al}}{C} + \frac{H_{OH}}{C} \right) = 0.836 - (0.477 + 0.043) = 0.316 \quad (6.1)$$

By catalytically dehydrogenating hydroaromatic structures in coal the number of hydrogen atoms liberated per carbon atom

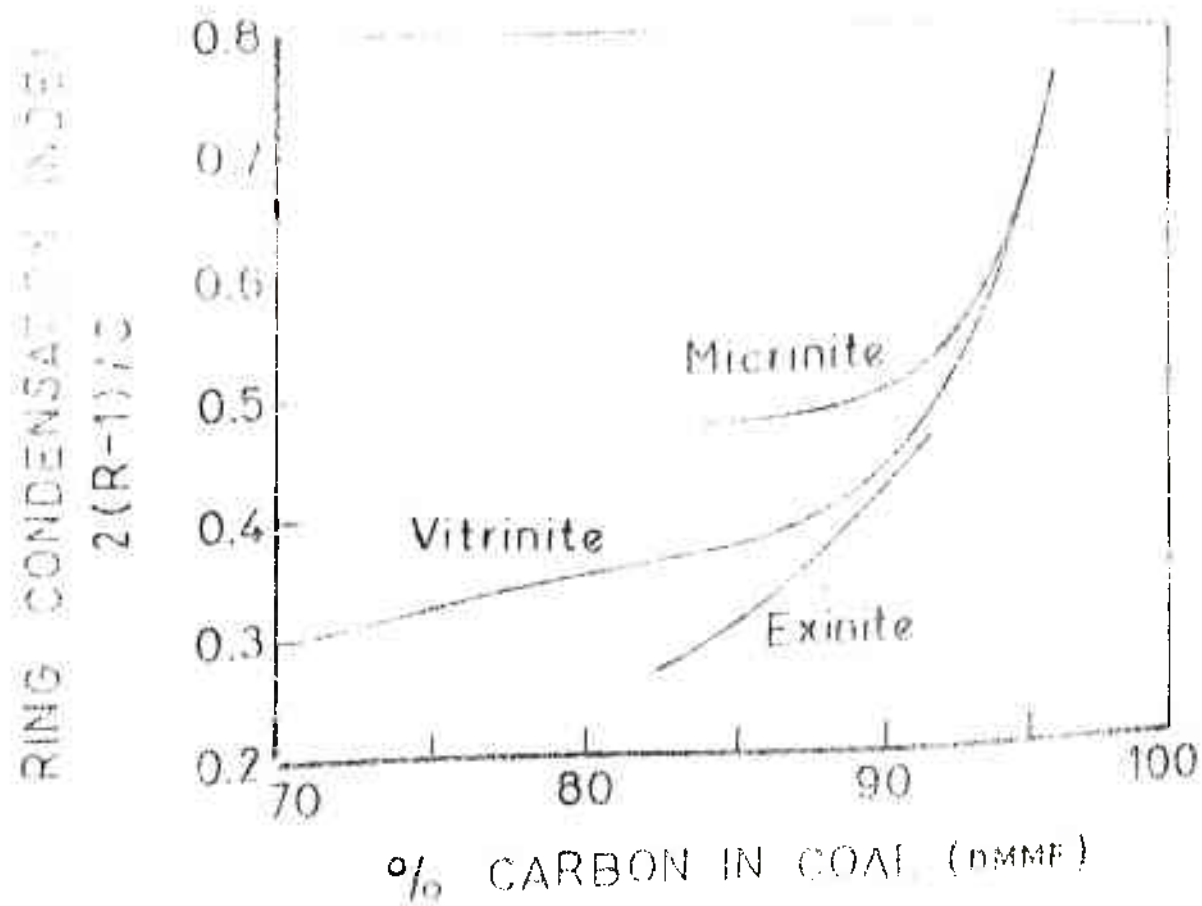


FIGURE 6.12 RING CONDENSATION INDEX VERSUS RANK
(VAN KREVELEN, 1961)

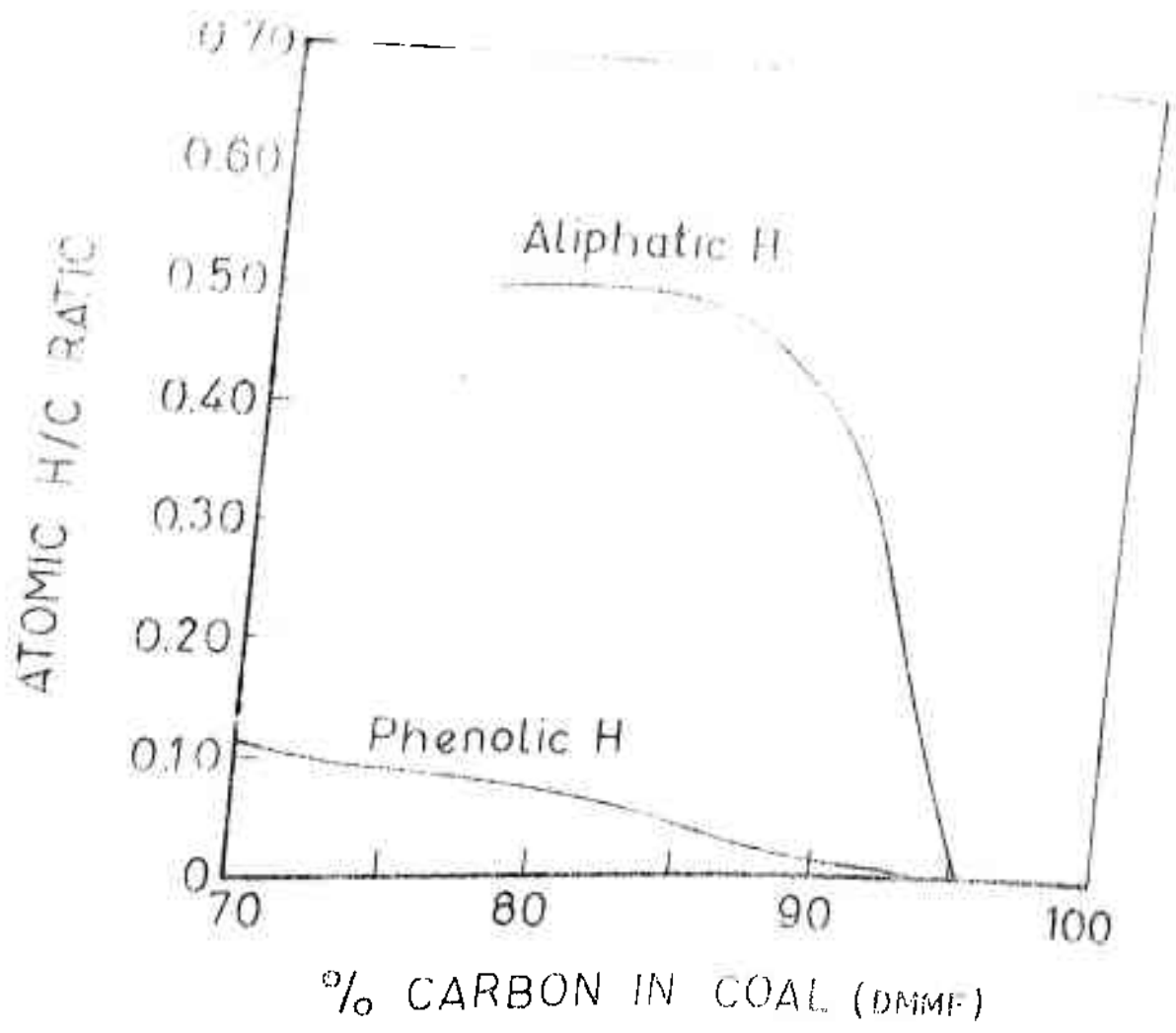


FIGURE 6.13 VARIATION OF ALIPHATIC AND PHENOLIC HYDROGEN WITH RANK (TSCHAMLER AND de RUITER, 1962)

has been obtained (Mazumdar et al, 1962; Reggel et al, 1968), and is plotted in Figure 6.14. From this plot, a value of $\frac{H_{HA}}{C} = 0.213$ is obtained, implying that roughly 4 to 5 hydrogen atoms would be released per average structural unit, for the hvAb coal.

The distribution of aliphatic hydrogen between CH, CH₂ and CH₃ groups is of interest to ascertain the number of bridges. This distribution data is obtained from Figures 6.15 and 6.16 and is roughly as follows:

$$\frac{H_{CH_2}}{C} = 0.254 \quad , \quad \frac{H_{CH_3}}{C} = 0.10$$

$$\begin{aligned} \therefore \frac{H_{CH}}{C} &= \frac{H_{al}}{C} - \left(\frac{H_{CH_2}}{C} + \frac{H_{CH_3}}{C} \right) \\ &= .477 - (.254 + .100) = 0.123 \end{aligned} \quad (6.2)$$

It may be assumed that methylene hydrogen represents that present only in bridges. It is then seen that the number of methylene hydrogens for the Pittsburgh hvAb is 5 to 6. This implies that there may be 2 to 3 methylene-type bridges in each cluster.

Coal has been found to contain small proportions of oxygen, primarily in the form of phenolic hydroxyl, carboxylic acid (salt), carbonyl (such as quinone-type) and ether groups. These are estimated from Figures 6.17 and 6.18.

The various parameters which have been calculated are presented in Table 6.1. From this table it can be seen that the number of aromatic rings in each repeating unit or "monomer" increases during the coal formation process. The lignite "monomer" has one to two rings, the subbituminous two to three, the high

(e) IN COAL BANK (M. D. 1950)

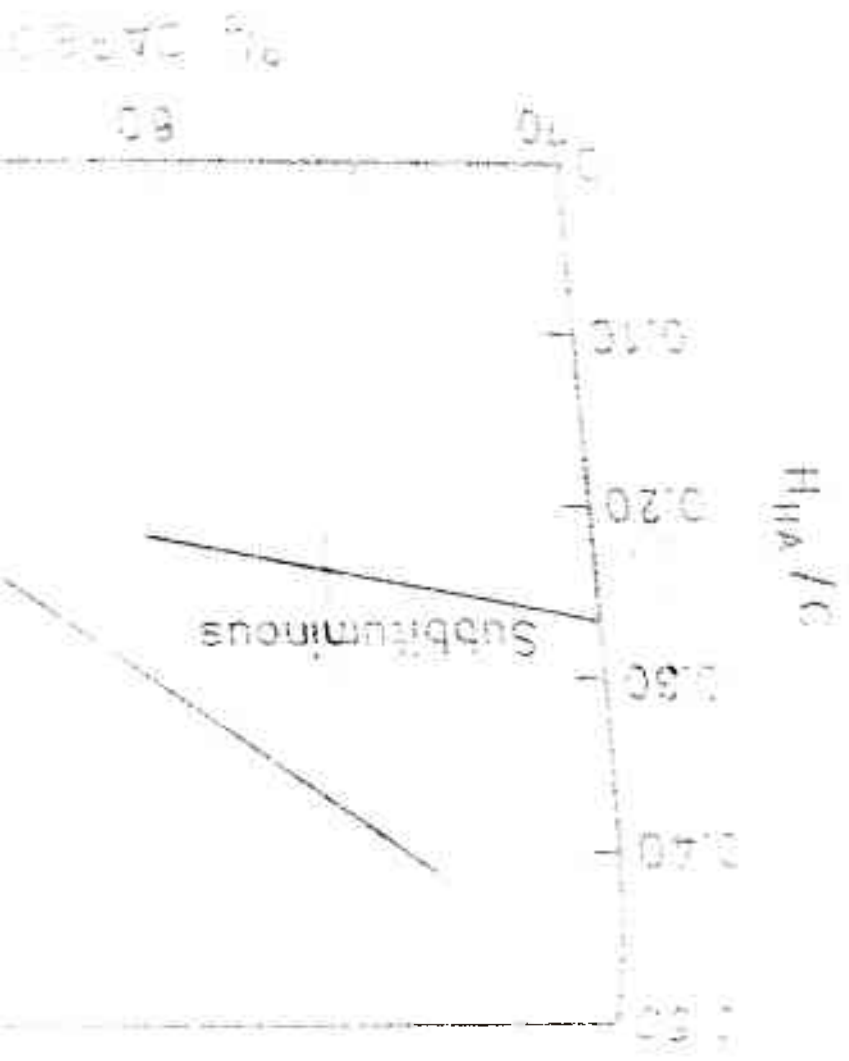
IN COAL BANK (M. D. 1950)

100 50

Bituminous



FIGURE 5.14 HYDROGRAPHIC PROFILES FOR BECKETT CREEK



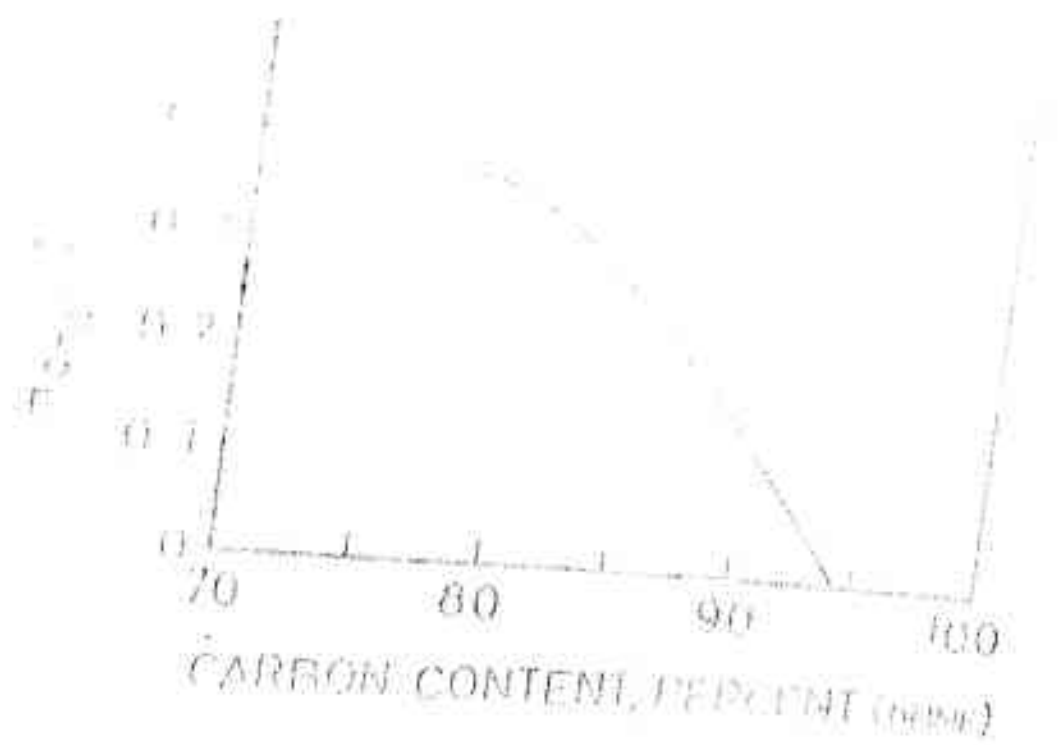


FIGURE 6.15 METHYLENE HYDROGEN CONTENT VERSUS RANK (LADNER AND STACEY, 1963, 1964)

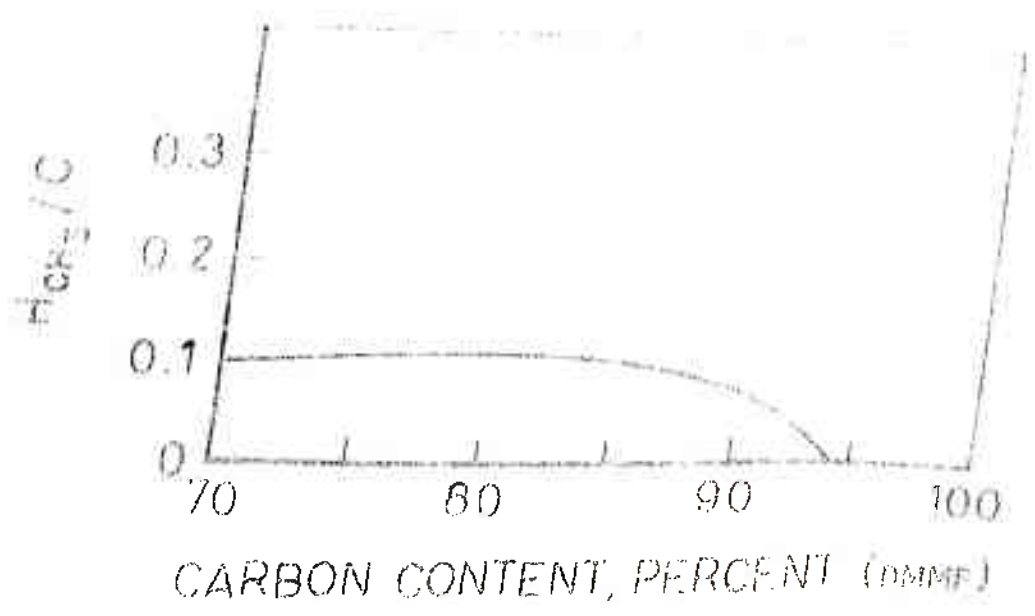


FIGURE 6.16 METHYL HYDROGEN CONTENT VERSUS RANK (MAZUMDAR et al., 1966)

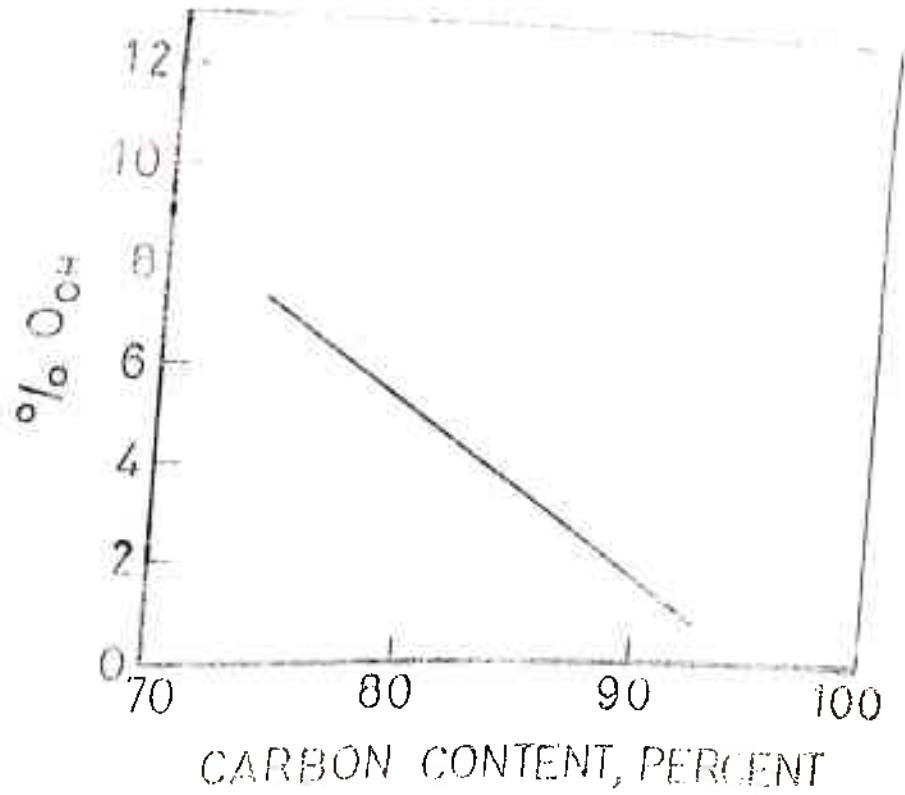


FIGURE 6.17 HYDROXYL OXYGEN CONTENT
VERSUS RANK (GIVEN, 1976)

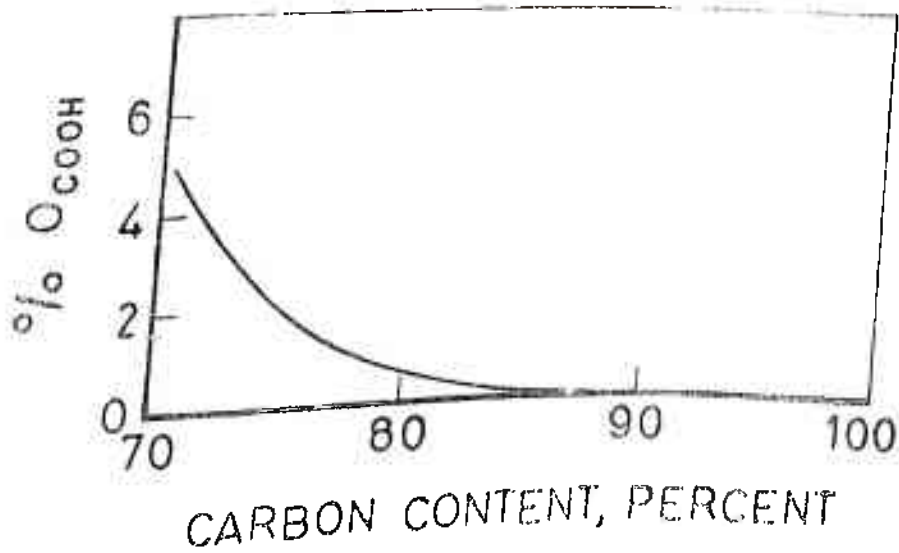


FIGURE 6.18 CARBOXYLIC OXYGEN CONTENT VERSUS
RANK (VAN KREVELEN, 1961)

TABLE 6.1

Structural parameters for coals studied

No.	Parameters	H.L.	M.R.	hvAb	mvb	an
1.	Aromaticity, f_a	.589	.706	.840	.923	.977
2.	Aromatic carbons/ cluster, \bar{N}	7	12	18	21	55
3.	Carbon atoms/average structural unit, C ($C = \bar{N}/f_a$)	11.88	17.00	21.43	22.75	56.29
4.	Ring Condensation Index, RCI ($RCI = \frac{2(R-1)}{C}$)	.300	.340	.382	.475	.710
5.	Total rings/average structural unit, \bar{R}	2.80	3.90	5.10	6.40	20.98
6.	No. of rings/average structural unit	2-3	3-4	5-6	6-7	20-21
7.	Aromatic rings/average structural unit	1-2	2-3	4	4-5	14
8.	H_{al}/C (Aliphatic)	.55	.50	.477	.31	0.00625
	a) H_{CH_2}/C	.381	.369	.254	.092	0
	b) H_{CH_3}/C	.110	.110	.100	.058	0
	c) H_{CH}/C	.059	.021	.123	.160	0
9.	H-hydroaromatic (H_{HA}/C)	.265	.230	.213	.117	0
10.	Phenolic, H_{OH}/C	.113	.087	.043	.013	0
11.	Aromatic, H_{ar}/C (by diff)	.428	.167	.316	.246	.21575

TABLE 6.1 (contd.)

No.		N.L.	M.R.	hvAb	mvb	en
12.	H/C	1.091	.754	.856	.569	.222
13.	Hydroxyl oxygen, % diamf	9%	6%	3%	1%	0
14.	Carboxyl oxygen, % diamf	5%	1%	0	0	0
15.	Carbonyl oxygen \emptyset \emptyset by diff.	5%	4.4%	1.2%	0.8%	0.65%
16.	Ether oxygen \emptyset	5%	4.4%	1.2%	0.8%	0.65%
17.	O/C	.242	.157	.054	.026	.013
18.	No. of oxygen atoms/ cluster	2.87	2.67	1.16	0.6	0.73

volatile bituminous four and the medium volatile bituminous four to five. The anthracites with aromaticity values greater than 0.97 approach the highly condensed structure of graphite.

A reasonable assumption may then be made that coals of different ranks should evolve different types of PAH under conditions which favour thermal cracking of the parent structure. Thus low-rank coals should evolve PAH with at most two to three fused aromatic rings whereas high-rank coals such as bituminous would liberate PAH containing four rings or more.

PAH and soot yields are plotted versus the percentage of carbon (dmmf) present in the coal in Figures 6.19 and 6.20. A representative analysis of PAH identified by GC-MS is presented in Table 6.2. Two distinct conclusions may be drawn. The chemical types of PAH evolved from different coals is very similar. However, the total concentration of PAH and soot formed shows a distinct trend, in the following descending order:

High volatile bituminous > medium volatile bituminous >
subbituminous > lignite > anthracite.

This trend can be observed pictorially by examining the gas chromatographic spectra of the PAH evolved during the pyrolysis of various coals at 1100 K and 300 ms (Figure 6.21).

It is thus evident that the PAH evolved are not simply as a result of bridge cleavage in the coal structure. There is free radical synthesis taking place, resulting in a product spectrum of two to seven ring compounds. This conclusion is strengthened if one examines the theories of PAH formation from simple fuels in flame systems. As already discussed in Chapter 3.1, it is very unlikely that ring fragmentation of aromatic



FIGURE 3.15 PAVE FIELD AREA, PERCENT CARBON IN CEMENT PASTE

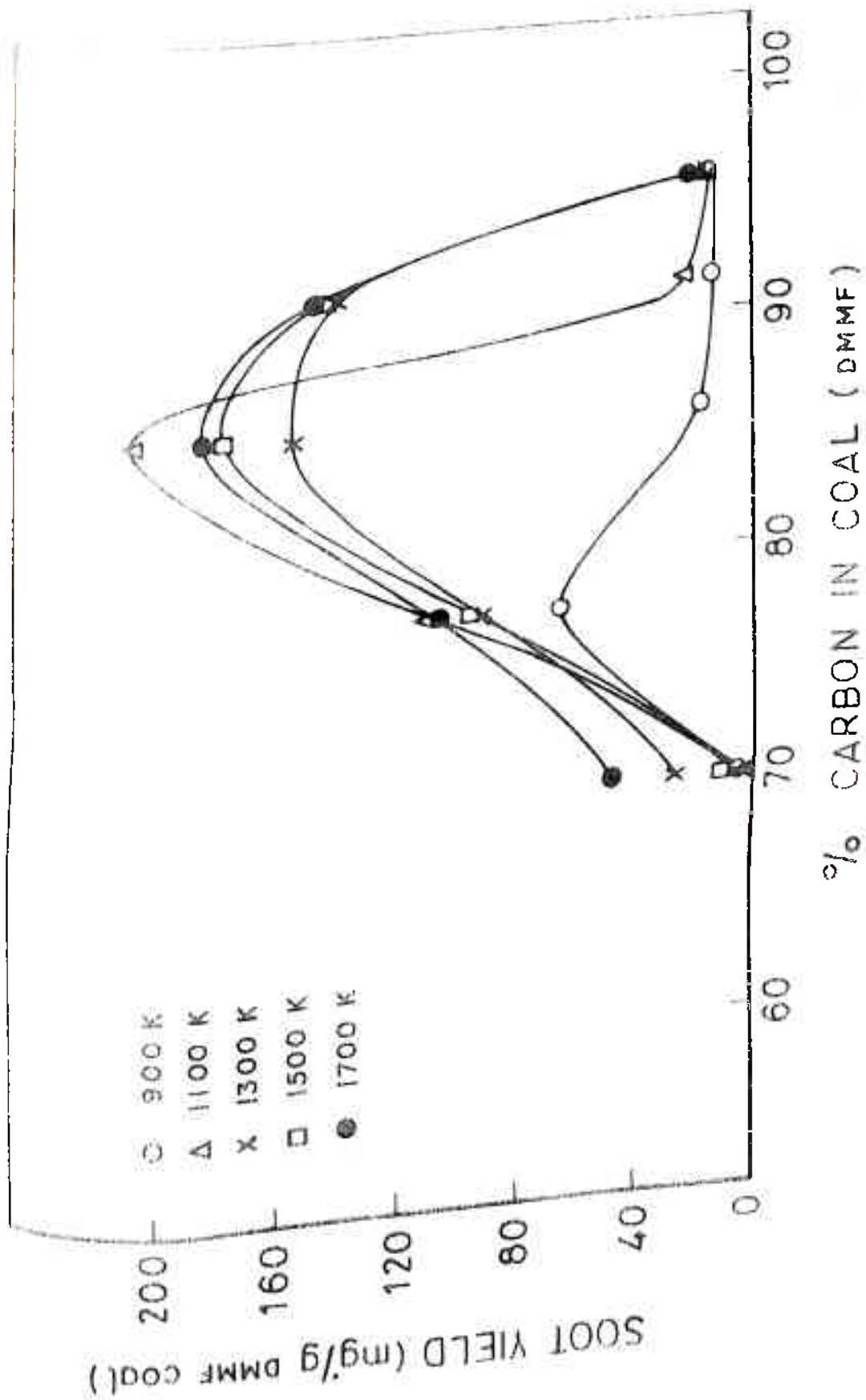


FIGURE 6.20 SOOT YIELDS VERSUS RANK (300MS)

TABLE 6.2

Polycyclic aromatic hydrocarbons evolved (mg/g coal)
during coal pyrolysis at 1250 K, 300 ms

	PSOC 997 Pittsburgh hvAb	M.L. Montana Lignite	PSOC 869 Primrose Anthracite
1. Tetralin	.1487		
2. Naphthalene	1.4360	.6512	.1109
3. Benzo(b) thiophene	.1341	.1928	
4. 2-methylnaphthalene	.8571	.0223	.1238
5. 1-methylnaphthalene	.8260	.0167	.0613
6. Biphenyl	.1192	.0363	.0917
7. 2,3-dimethylnaphthalene	.4954		
8. Acenaphthylene	.8850	.1091	
9. Dibenzofuran	.1579	.0224	.0139
10. Fluorene	.3870	.0556	.0343
11. 9-methylfluorene		.1220	
12. 2-methylfluorene	.3767		
13. Dibenzothiophene	.2902	.0884	.0768
14. Phenanthrene	.4308	.1241	
15. Anthracene	.1439		
16. 2-methylanthracene	.1776	.0464	.0361
17. 1-methylphenanthrene		.0555	
18. Cyclopenta(def)phenanthrene	.3065	.1731	
19. Fluoranthene	.1907	.1173	
20. Benz(j)acenaphthylene	.1953	.1600	.0230
21. Pyrene	.3526	.0897	
22. Cyclopenta(cd)pyrene		.0851	
23. Chrysene		.2485	
24. Benzo(e)pyrene	.0805		
25. Benzo(a)pyrene	.2029		
26. Dibenz(ah)anthracene			

SOOT

GAS-PHASE

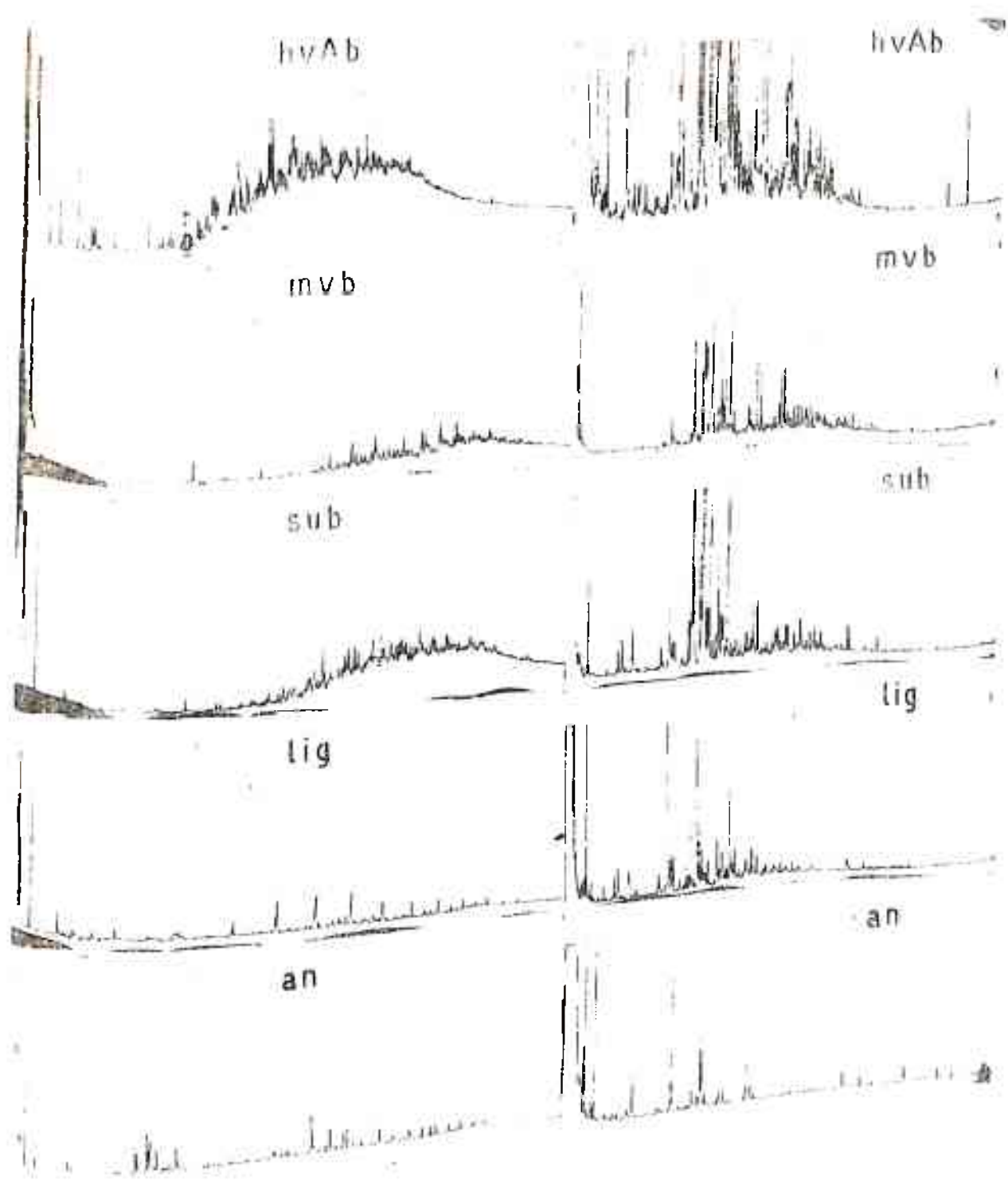


FIGURE 6.21 GC SPECTRA: COAL PYROLYSIS AT 1100 K, 300 MS

fuels is taking place in flames specially when the fuel contains two or more aromatic rings. Ring fragmentation appears even more improbable for the case of coal, where the weak aliphatic bonds linking the resonance stabilised aromatic "monomers" would be likely to break first.

An important difference exists between the types of PAH evolved during coal pyrolysis and those emitted by other fuels. Coal PAH have a greater proportion of alkyl substituents, specially methyl and ethyl groups. Simple gaseous fuels and liquid fuels such as tetradecane (Vranos and Liscinsky, 1983) primarily evolve non-alkylated PAH. This further strengthens the hypothesis that during coal pyrolysis, PAH are evolved as a result of free radical synthesis from smaller fragments (analogous to flame processes) and also as a consequence of bridge cleavages.

Flame studies have also shown that the greater the aromaticity of the parent fuel, the greater its tendency to evolve PAH and soot. The aromaticity of the coals studied increases monotonically from 0.589 for the Montana lignite to 0.977 for the Primrose anthracite. However, PAH and soot yields do not follow this order, as can be seen from Figures 6.19 and 6.20. Instead, PAH evolution peaks at an intermediate value of about 86% carbon, corresponding to the high volatile bituminous coal.

Solomon (1984) established a direct relationship between tar yield and the aliphatic hydrogen content of the coal, for conditions of vacuum pyrolysis. However, such a relationship does not appear to hold for the condition of pyrolysis in an inert atmosphere. As Solomon's (1984) studies also indicate, the ability of a coal to yield volatile hydrocarbon species is the most

important factor governing the evolution of PAH. A distinction needs to be made here between volatile matter (VM) commonly given as a property of coals according to standardised ASTM procedures and the volatile yield. The volatile yield comprises that fraction of the volatile matter which is of a hydrocarbon nature. This fraction is manifested as tars and PAH. Low rank coals such as the lignite and subbituminous exhibit low levels of PAH emission, since a high fraction of the volatile matter consists of low molecular weight hydrocarbons and oxygenated species such as water, carbon monoxide and carbon dioxide (Suuberg et al, 1978). High rank coals such as anthracites are extremely resistant to thermal breakdown, presumably because of the extensive crosslinking in their highly aromatic structures. The greatest yields of PAH and soot occur from the bituminous coals, where a major fraction of the volatile species is known to be present in the form of high molecular weight tars (Suuberg et al, 1978; Solomon, 1984).

6.3 Mutagenic Activity

Together with chemical characterization of the pyrolysis products of coal, it is important to determine their health effects. Assessing the biohazardous activity of coal pyrolysis products is not a major emphasis of this thesis; the primary interest is to ascertain whether or not mutagenic activity shown by coal pyrolysis products can be accounted for by the presence of known mutagenic PAHs in the samples.

Results from the bioassays conducted on the total methylene chloride extractable materials from the pyrolysis of Montana lignite and Primrose anthracite are presented in Tables 6.3 to 6.5

TABLE 6.3

Mutagenicity of polycyclic aromatic hydrocarbons evolved during the pyrolysis of Montana Lignite coal (1250 K) (With PMS)

Montana Lignite, 1250 K, 300 ms

	Soot + Char 100µg/ml	Wt. %	µM	Mutation x 10 ⁵
1.	3-methylbenzoquinoline	2.1	1	-
2.	fluoranthene	3.6	15	45.0
3.	Pyrene	2.4	11	-
4.	Cyclopenta(cd)pyrene	1.9	8	17.0
5.	Chrysene	1.8	8	2.0
6.	Benzo(e)pyrene	5.3	21	2.0
7.	3-methylcholanthrene	3.0	13	1.0
8.	Dibenz(ac)anthracene	6.6	32	30.0
				<hr/>
Sum Mutagenicity				97 x 10 ⁵
Observed Mutagenicity				77 x 10 ⁵

	XAD-2 100µg/ml	Wt. %	µM	Mutation x 10 ⁵
1.	Quinoline	.29	2.5	-
2.	1-methylnaphthalene	.26	1.9	-
3.	Acenaphthene	.45	3.0	1.0
4.	1-methylphenanthrene	.73	3.8	1.0
5.	Pyrene	.74	3.7	-
				<hr/>
Sum Mutagenicity				2 x 10 ⁵
Observed Mutagenicity				9 x 10 ⁵

Montana Lignite, 1250 K, 225 ms

	XAD-2 100µg/ml	St. %	µM	Mutation x 10 ⁵
1.	Quinoline	1.3	10	1.0
2.	1-methylnaphthalene	.9	6	1.0
3.	Acenaphthene	.2	1	1.0
				<hr/>
Sum Mutagenicity				3 x 10 ⁵
Observed Mutagenicity				3 x 10 ⁵

TABLE 6.4 (contd.)

Montana Lignite, 1500 K, 75 ms

<u>Char</u>	100 $\mu\text{g/ml}$	Wt. %	μM	Mutation $\times 10^5$
1. Benzo(b)fluorene		9.7	47	14
2. Benz (a) anthracene		2.9	12	4
				<hr/>
				18 $\times 10^5$
				5 $\times 10^5$

<u>Soot</u>	150 $\mu\text{g/ml}$	Wt. %	μM	Mutation $\times 10^5$
1. 1-methylphenanthrene		2.2	17	4
2. Fluoranthene		.9	6	-
3. Pyrene		2.1	16	1
				<hr/>
				5 $\times 10^5$
				10 $\times 10^5$

TABLE 6.5

Mutagenicity of polycyclic aromatic hydrocarbons evolved during the pyrolysis of Primrose Anthracite coal (1250 K)

PSOC 869 (Primrose Anthracite), 1250 K, 300 ms

XAD-2	100 µg/ml	Wt. %	µM	Mutation x 10 ⁵
1. Quinoline		.22	1.8	-
2. 1-methylnaphthalene		.722	5.1	1.0
3. Acenaphthene		.62	5.4	1.0
4. 1-methylphenanthrene		.42	2.2	0.5
5. Pyrene		.27	1.3	-
6. 1-methylpyrene		.14	.7	-
7. Chrysene		.34	1.5	-
				<hr/> 2.5 x 10 ⁵
				21 x 10 ⁵
				Sum Mutagenicity
				Observed Mutagenicity

PSOC 869 (Primrose Anthracite), 1250 K, 225 ms

XAD-2	300 µg/ml	Wt. %	µM	Mutation x 10 ⁵
1. Quinoline		.71	15.6	1.0
2. 1-methylnaphthalene		.79	16.0	1.0
3. Acenaphthylene		.27	5.3	2.0
4. Acenaphthene		.22	4.3	1.0
5. 2-methylphenanthrene		.54	8.5	1.5
6. Pyrene		.50	7.5	-
				<hr/> 6.5 x 10 ⁵
				39 x 10 ⁵
				Sum Mutagenicity
				Observed Mutagenicity

PSOC 869 (Primrose Anthracite), 1250 K, 150 ms

XAD-2	100 µg/ml	Wt. %	µM	Mutation x 10 ⁵
1. Quinoline		.93	7.3	-
2. Acenaphthylene		.59	3.9	1.5
3. Acenaphthene		.24	1.6	-
4. Pyrene		.71	3.5	-
5. Chrysene		.62	2.7	1.0
				<hr/> 2.5 x 10 ⁵
				14 x 10 ⁵
				Sum Mutagenicity
				Observed Mutagenicity

PSOC 869 (Primrose Anthracite), 1250 K, 75 ms

XAD-2	100 µg/ml	Wt. %	µM	Mutation x 10 ⁵
1. Quinoline		.43	3.3	-
2. 2-methylphenanthrene		.60	3.1	1.0
3. Pyrene		7.00	2.9	-
				<hr/> 1.0 x 10 ⁵
				10 x 10 ⁵
				Sum Mutagenicity
				Observed Mutagenicity

(Mitra et al, 1982). An expected mutagenic activity is computed by summing the individual mutagenic activities of known mutagenic PAH present in the sample. In the majority of cases, this tallies very well with the experimentally observed mutagenicity. The mutagenicity was accounted for mainly by fluoranthene, cyclopenta (cd) pyrene, acenaphthylene, acenaphthene, quinoline, pyrene, chrysene, alkylated naphthalenes and phenanthrenes. Significantly, benzo (a) pyrene, reported as the primary mutating PAH in several earlier studies, contributes insignificantly to total mutagenic loadings.

The attempt was to look for any unusual mutagenicity in the pyrolysis samples. This would be manifested by an unusually large discrepancy between the expected and the experimentally observed mutagenicities, for example, where the observed mutagenicity is much larger than the expected value. This has not yet been observed in the samples tested so far.

Specific mutagenicities have been plotted versus pyrolysis temperature for the five coals studied (Figures 6.22 to 6.31). The specific mutagenicities have been calculated per unit mass of coal (m_{coal}) and per unit mass of tar (m_{tar}) and are defined in equations 6.4 and 6.5 (Braun, 1984).

The mutant fraction is plotted as a function of the concentration of the pyrolysis sample and levels determined for significant mutation at the 99% confidence level. Procedures for measuring mutant fractions have been discussed earlier.

The maximum slope of the dose-response curves is then obtained,

$$\text{Maximum slope} = \frac{\text{Mutant fraction (MF)}}{\text{concentration of sample } (\frac{\mu\text{g sample}}{\text{ml}})} \quad (6.3)$$

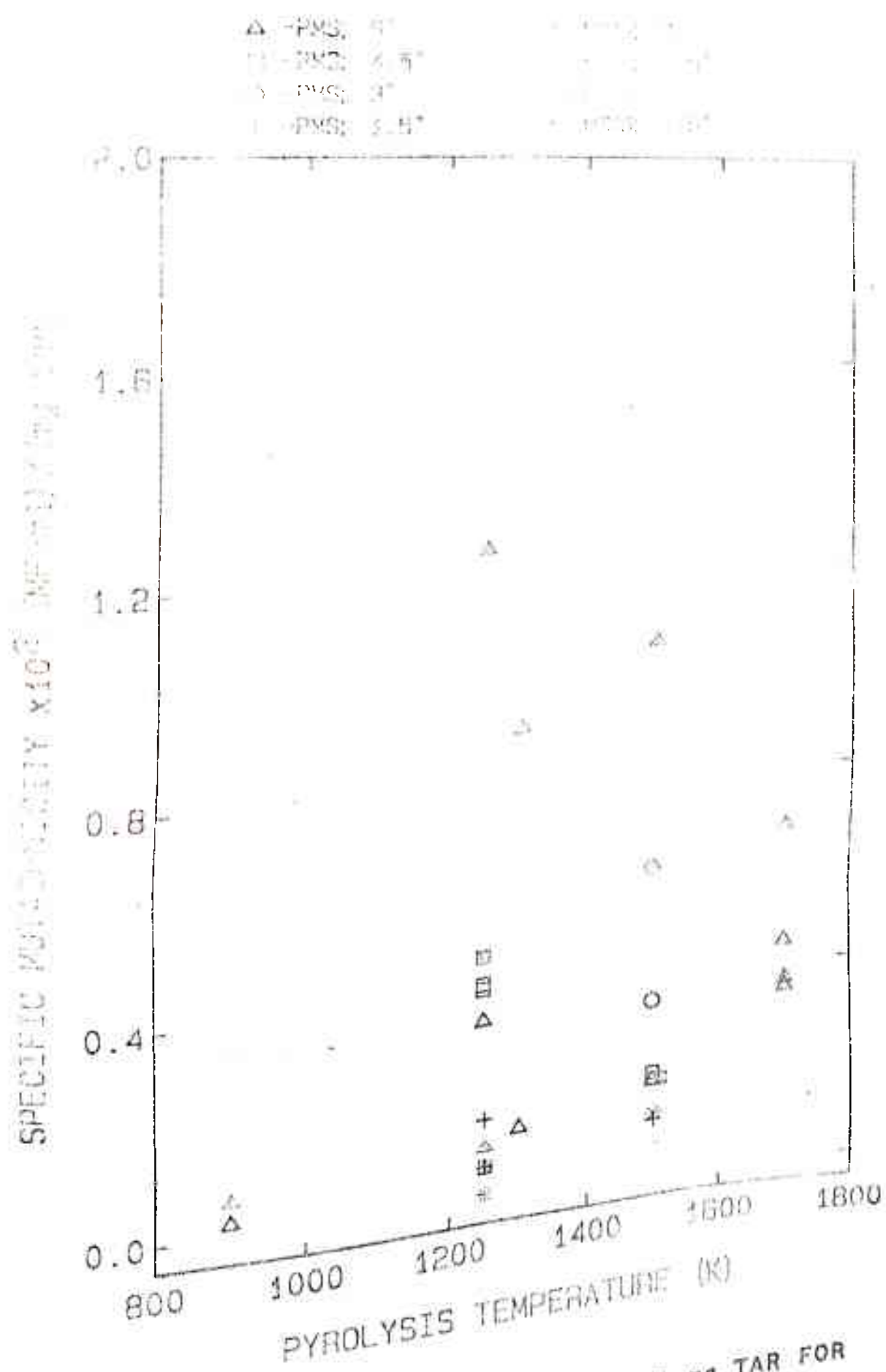


FIGURE 6.22 PAH MUTAGENICITY PER mg TAR FOR MONTANA LIGNITE COAL

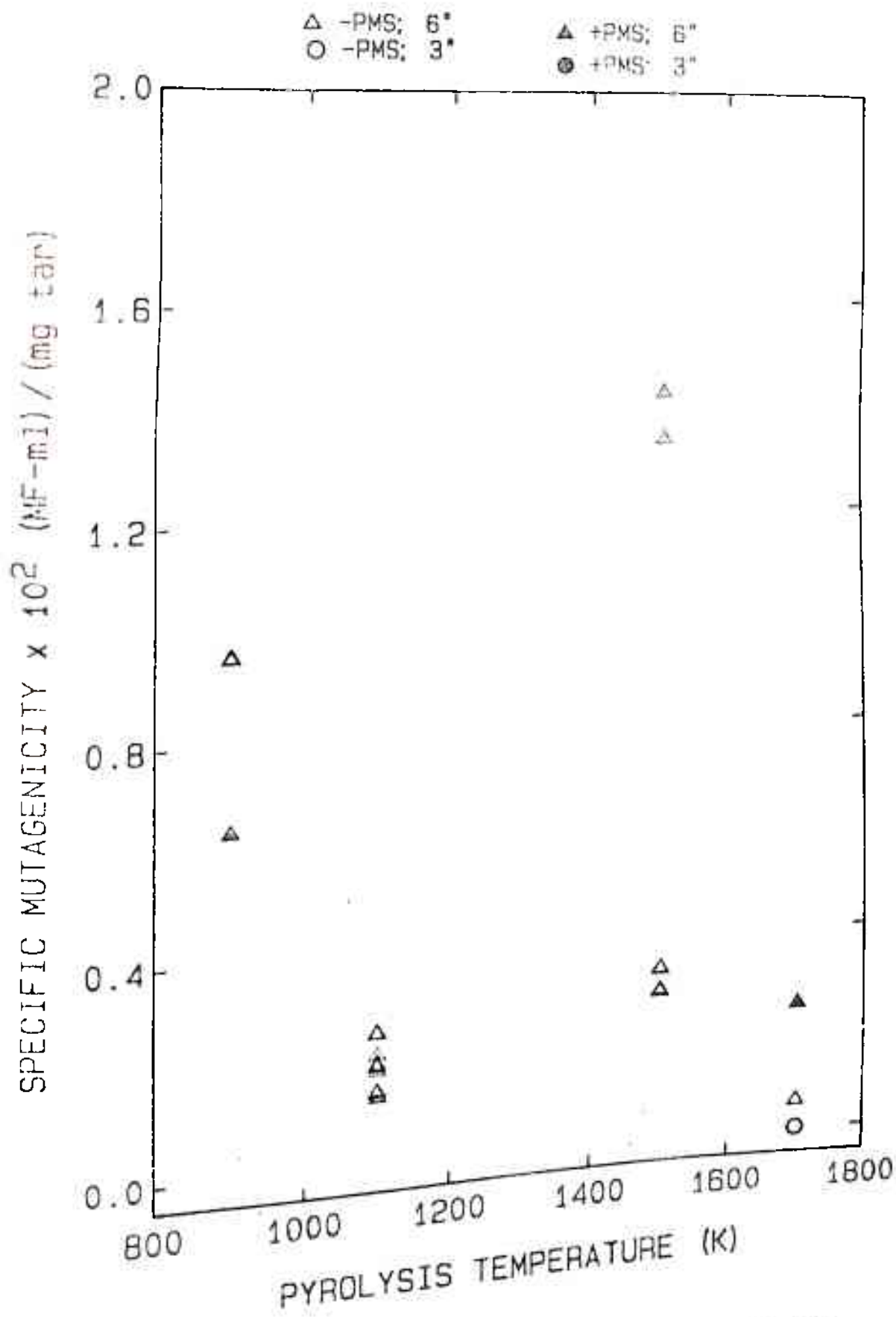


FIGURE 6.23 PAH MUTAGENICITY PER mg TAR FOR MONTANA ROSEBUD SUBBITUMINOUS COAL

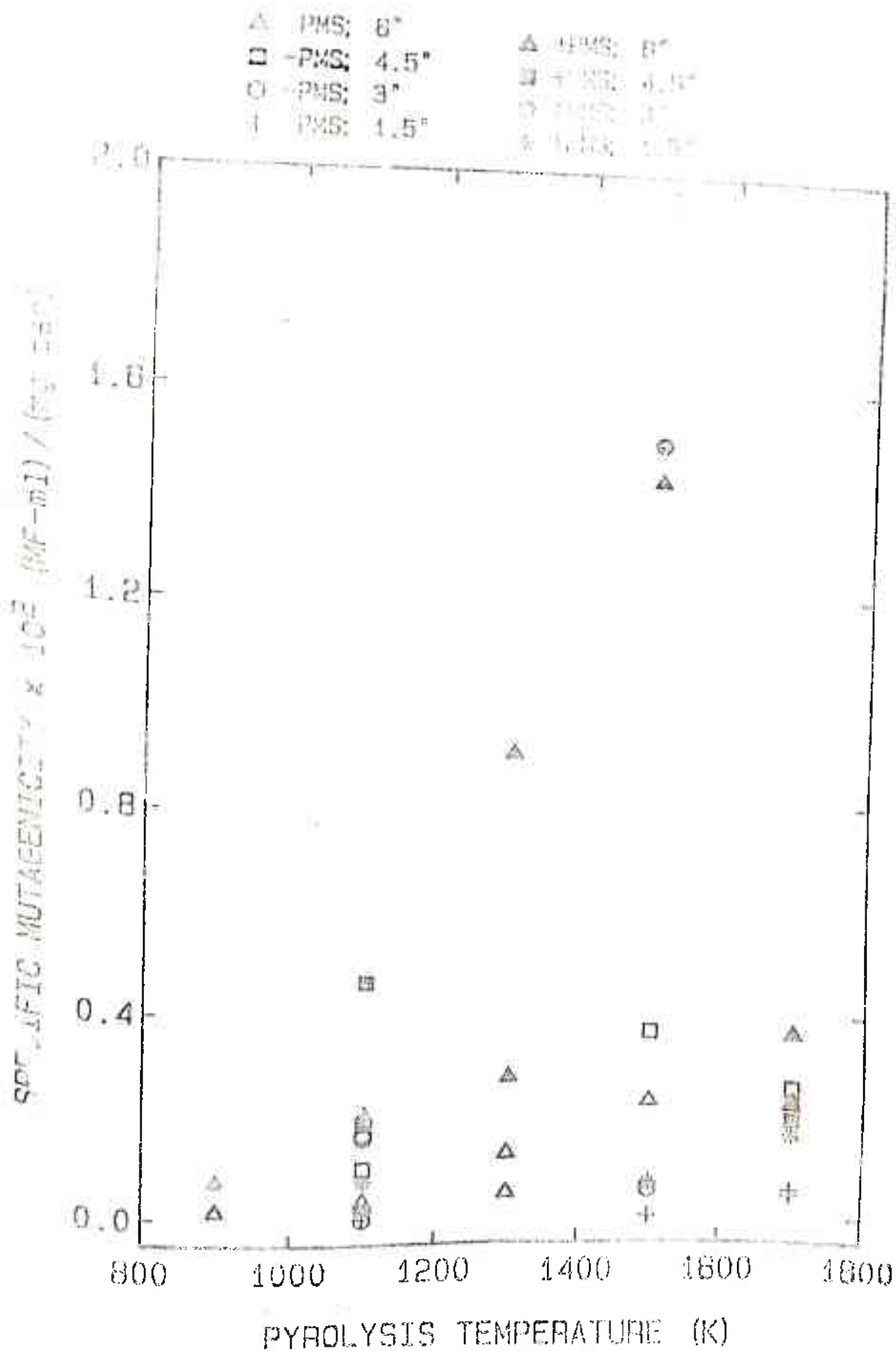


FIGURE 6.24 PAH MUTAGENICITY PER mg TAR FOR PITTSBURGH HIGH VOLATILE-A BITUMINOUS COAL

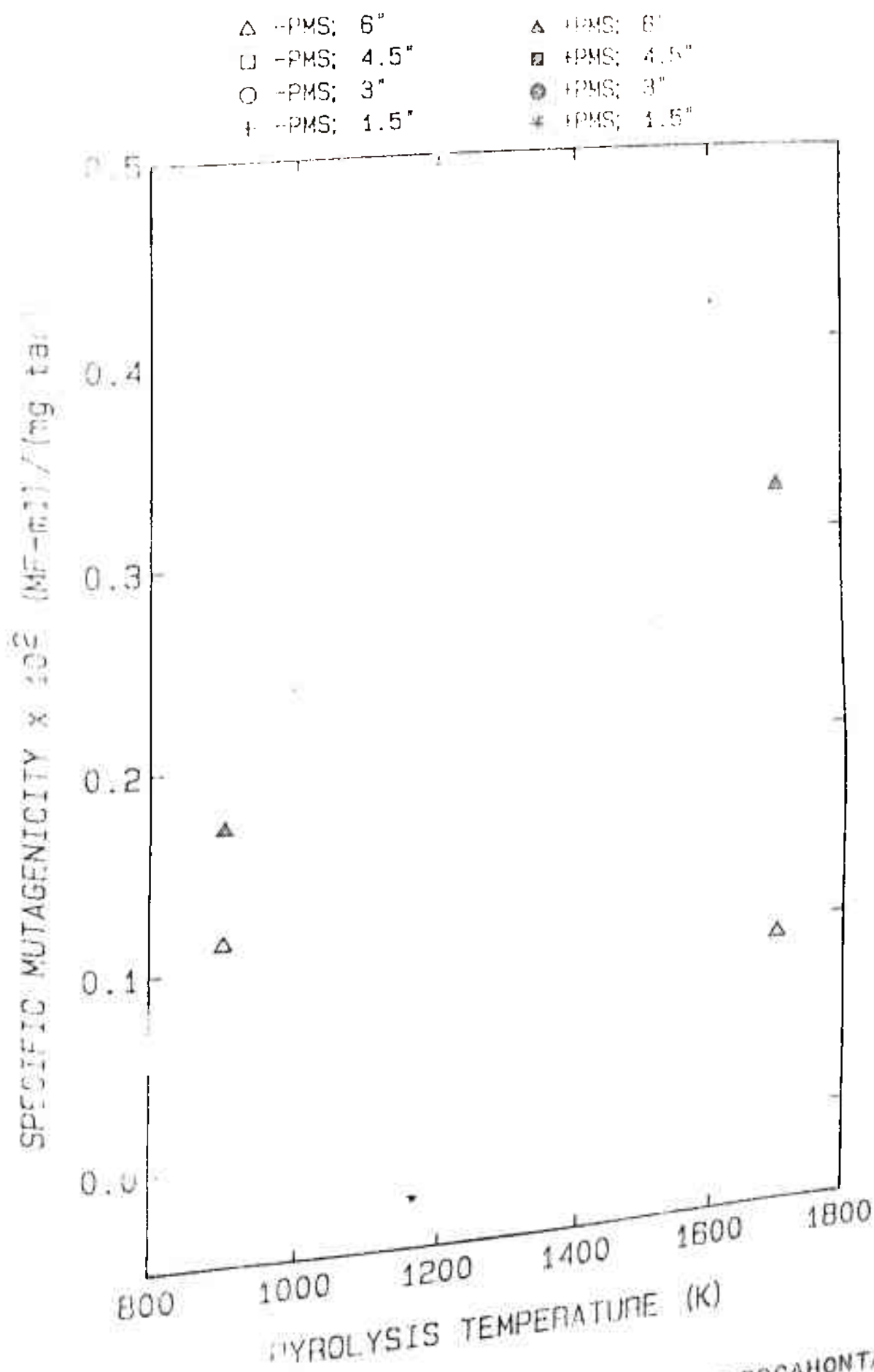


FIGURE 6-25 PAH MUTAGENICITY PER mg TAR FOR POCAHONTAS MEDIUM VOLATILE BITUMINOUS COAL

△	PM5	1.5	△	PM5	4.5
□	PM5	3.0	●	PM5	4.5
○	PM5	3.0	⊙	PM5	3.0
○	PM5	1.5	○	PM5	1.5

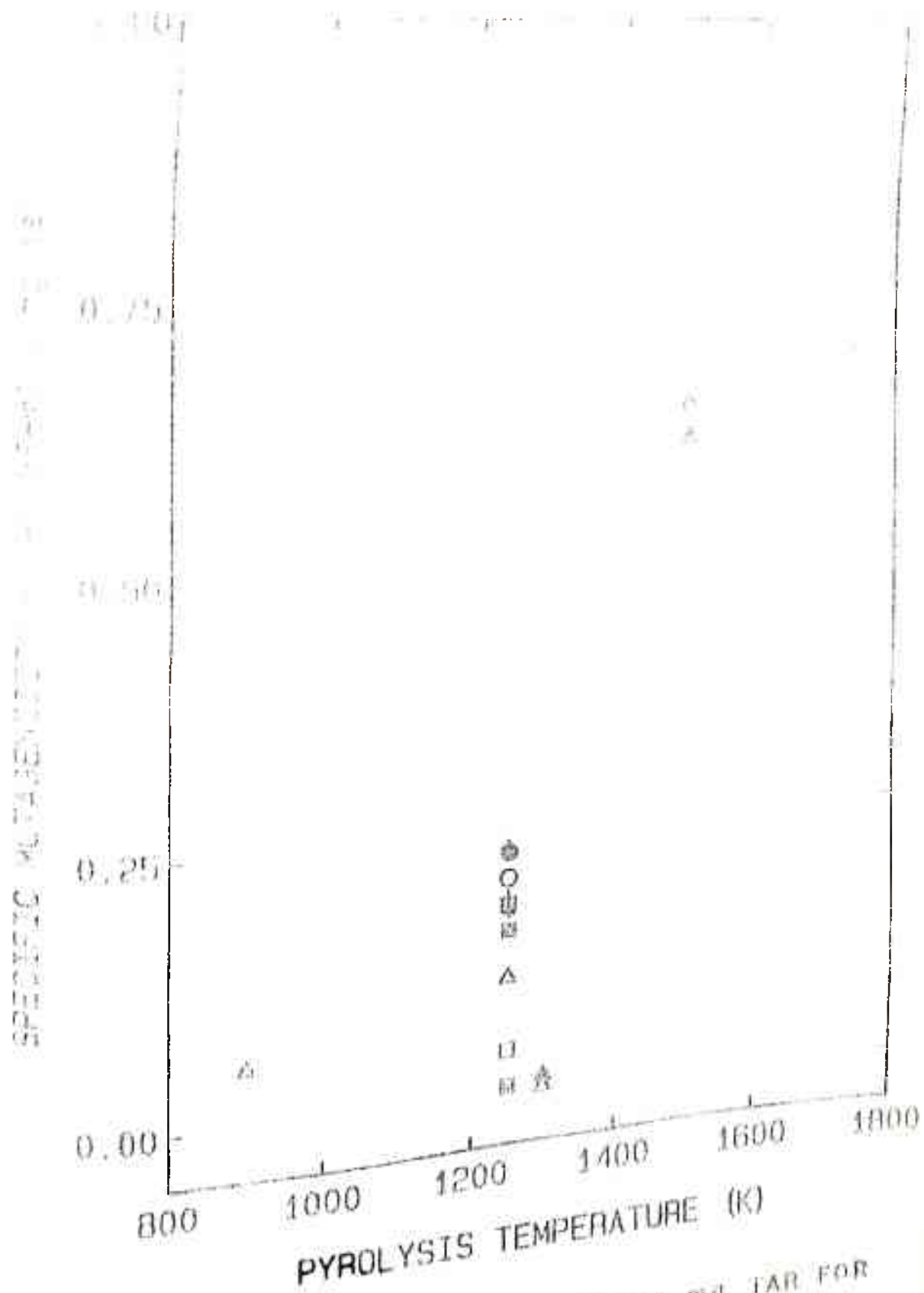


FIGURE 6.26 PAH MUTAGENICITY PER mg TAR FOR PRIMROSE ANTHRACITE COAL

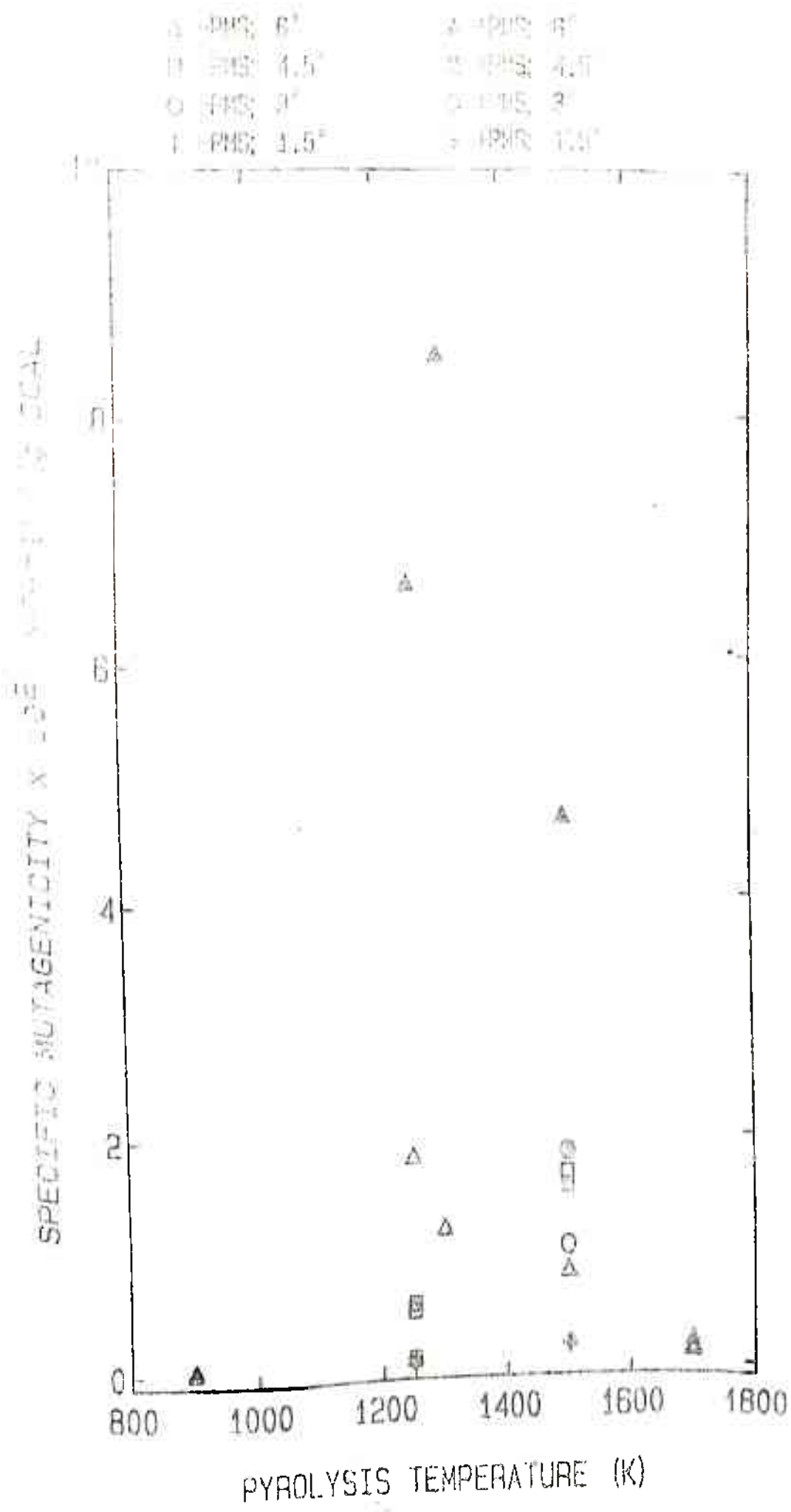


FIGURE G 27 PAH MUTAGENICITY PER g COAL FOR MONTANA LIGNITE COAL

Δ -PMS; 6"
 Δ +PMS; 6"
 \circ -PMS; 3"
 \bullet +PMS; 3"

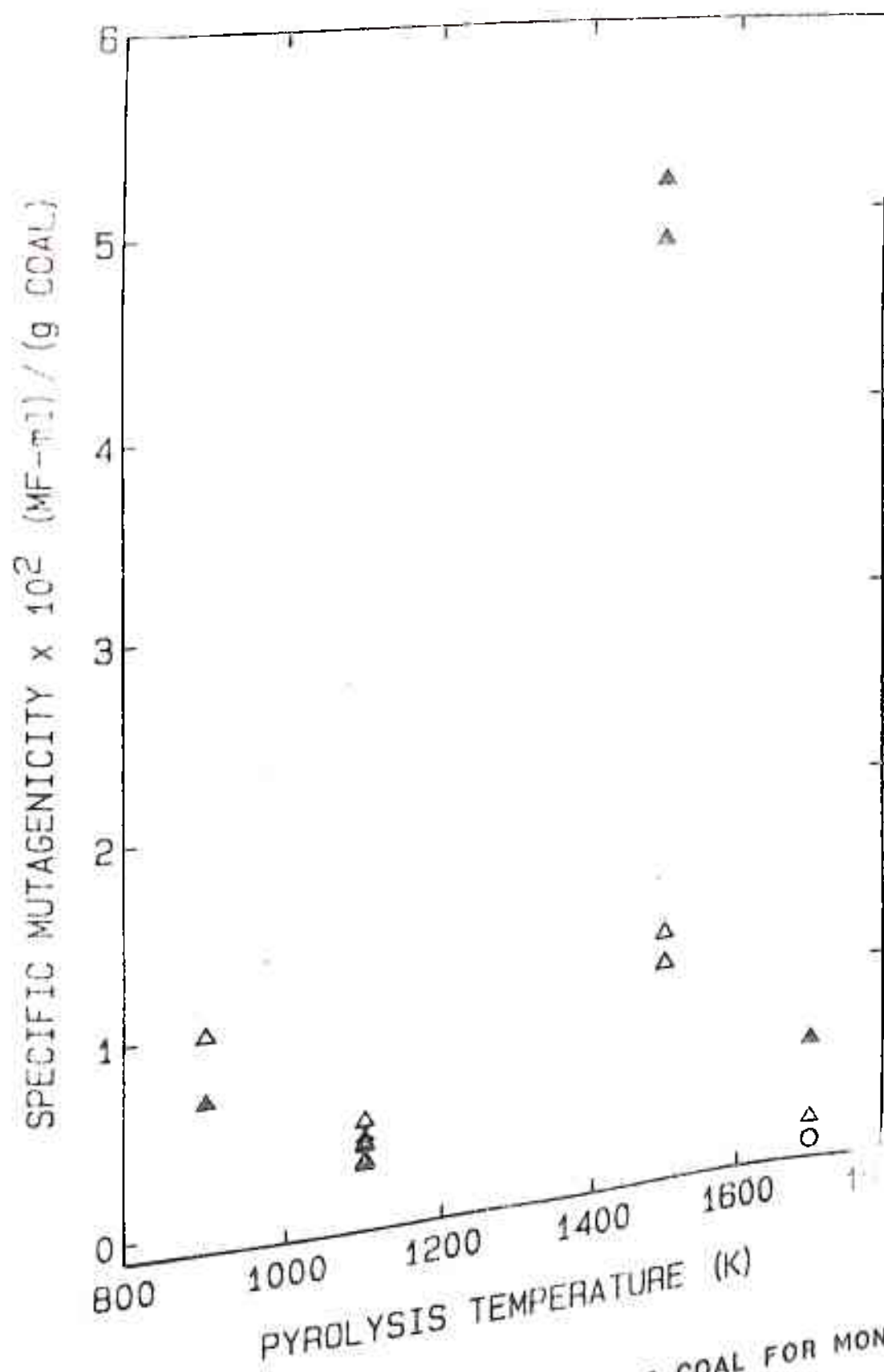


FIGURE 6.28 PAH MUTAGENICITY PER g COAL FOR MONTANA ROSEBUD SUBBITUMINOUS COAL

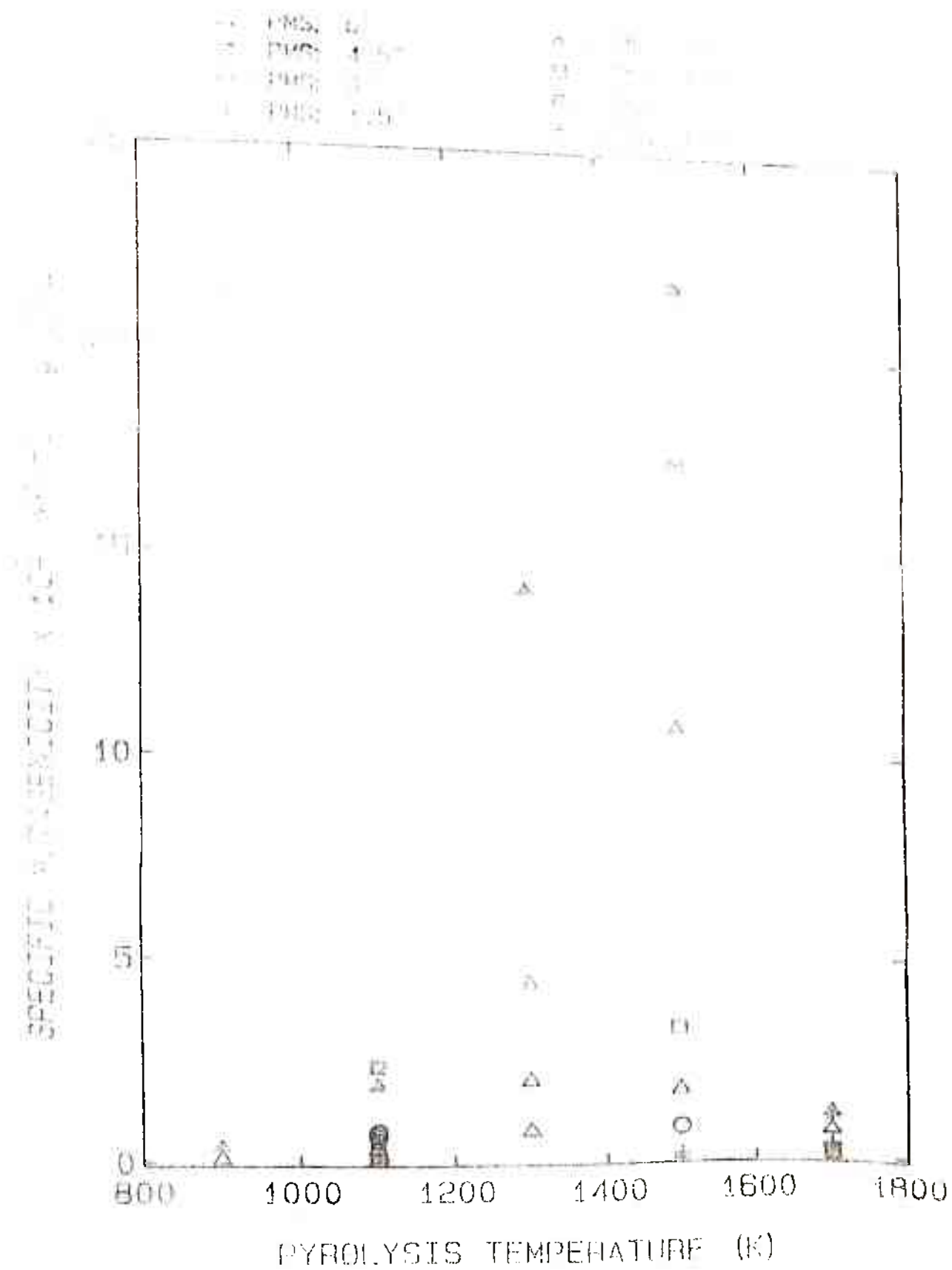


FIGURE 6.29 PAH MUTAGENICITY PER g COAL FOR PITTSBURGH HIGH VOLATILE-A BITUMINOUS COAL

△ -PMS; 6*

▲ -PMS; 6*

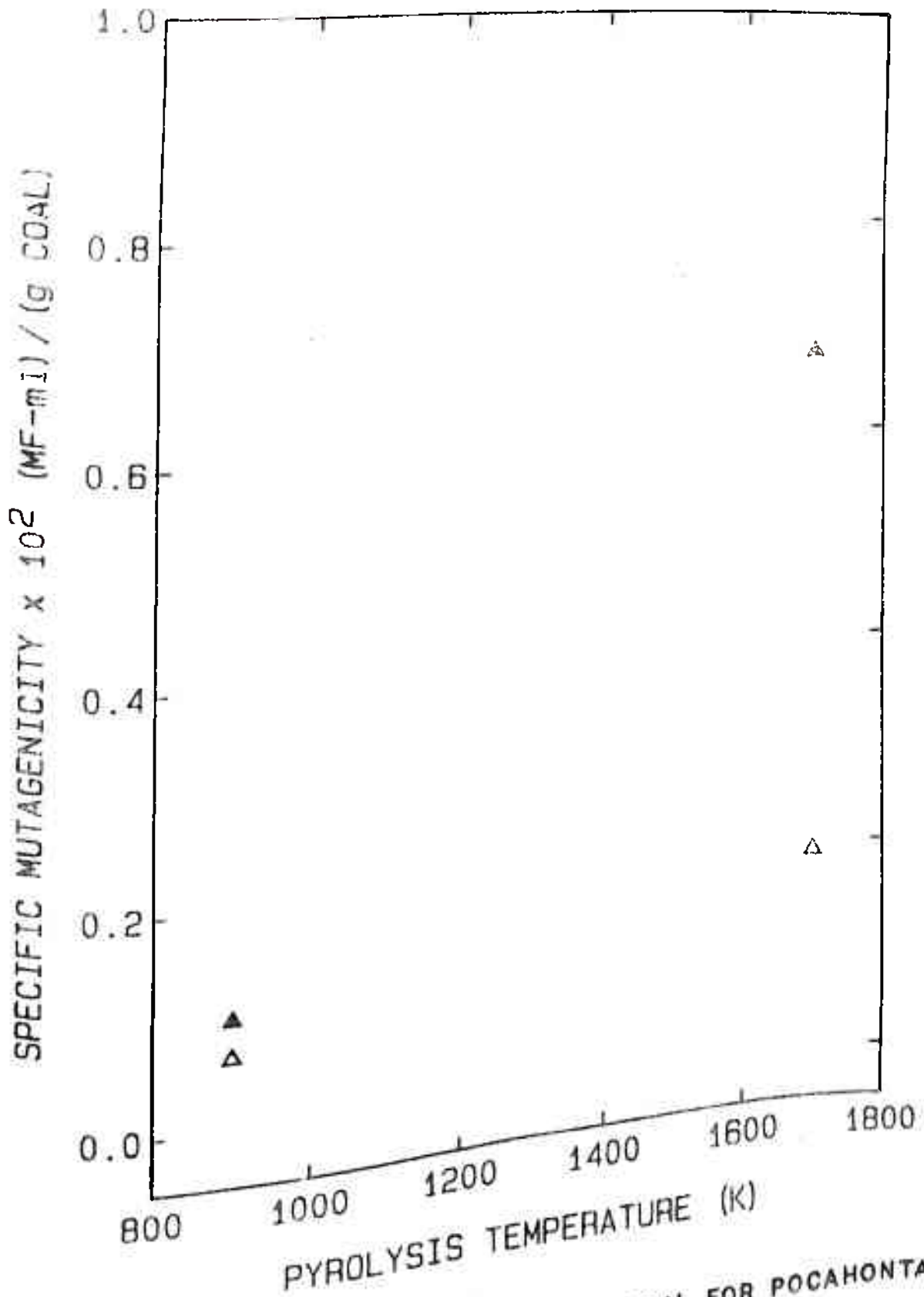


FIGURE 6.30 PAH MUTAGENICITY PER g COAL FOR POCAHONTAS MEDIUM VOLATILE BITUMINOUS COAL —

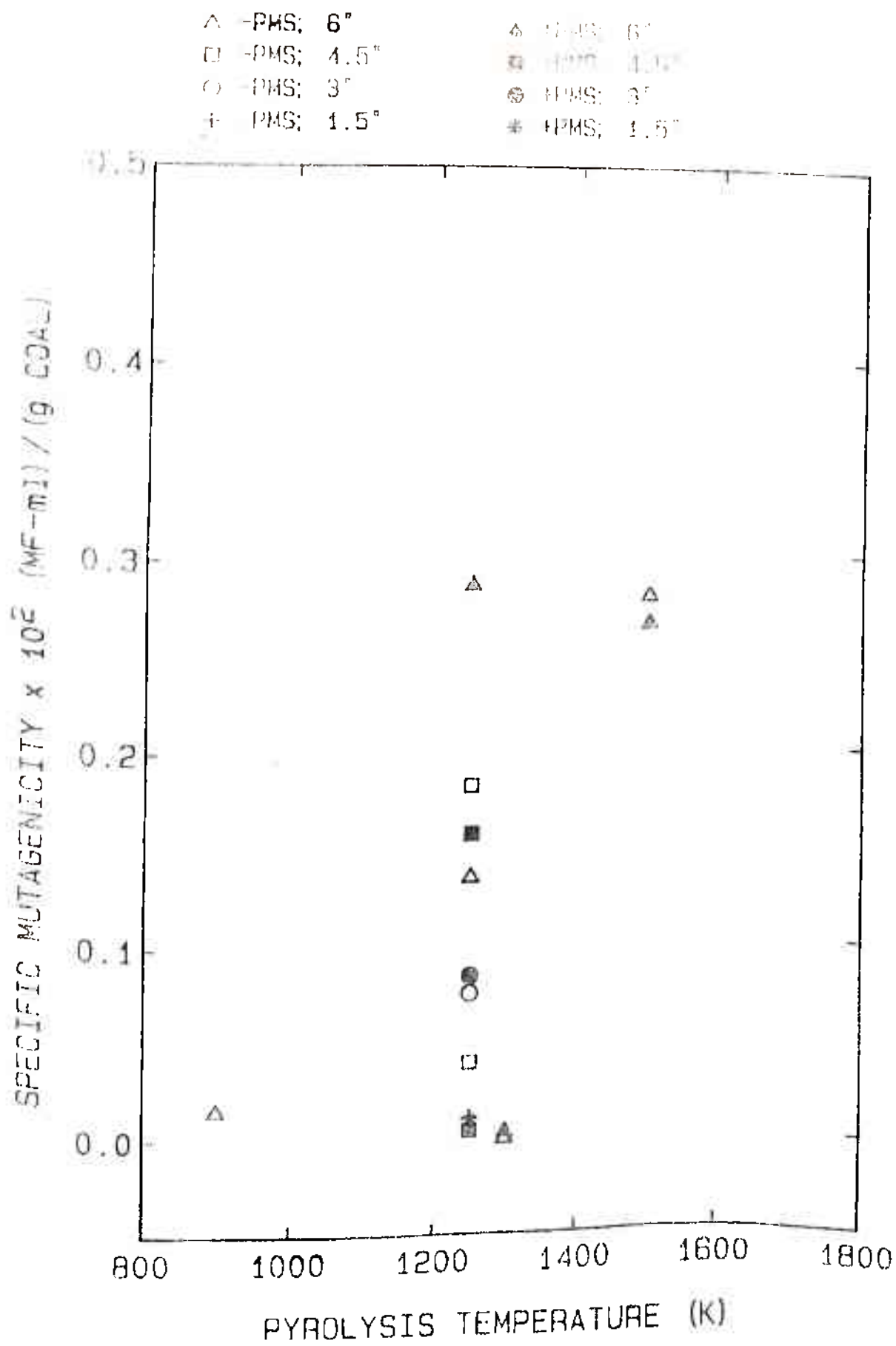


FIGURE 6.31 PAH MUTAGENICITY PER g COAL FOR PRIMROSE ANTHRACITE COAL

(a) Maximum slopes are obtained for both gas-phase PAH and for PAH condensed onto soot particulates. The two slopes are weight-averaged (Wornat, 1984) for a given coal sample to obtain a specific mutagenicity.

Thus, for ma_{tar}

$$\begin{aligned}
 \text{specific mutagenicity} & \quad \left(\frac{MF - ml}{mg \text{ tar}} \right) \\
 &= \frac{\frac{MF}{\mu g \text{ tar}} \text{ (} \mu g \text{ tar)}_g + \frac{MF}{ml} \text{ (} \mu g \text{ tar)}_s}{(\mu g \text{ tar)}_g + (\mu g \text{ tar)}_s} \\
 &= \frac{MF - ml}{g \text{ tar}} \left(\frac{1000 \mu g}{mg} \right) \tag{6.4}
 \end{aligned}$$

where the subscripts 'g' and 's' denote gas-phase and soot-phase PAH respectively.

(b) To obtain specific mutagenicities per unit weight of coal fed () the specific mutagenicity per weight of tar is multiplied by the appropriate PAH yields. Thus, ma_{coal}

$$\begin{aligned}
 \text{specific mutagenicity} & \quad \left(\frac{MF - ml}{g \text{ coal fed}} \right) \\
 &= \frac{MF - ml}{mg \text{ tar}} \times \frac{mg \text{ tar}}{g \text{ daf coal fed}} \tag{6.5}
 \end{aligned}$$

Certain observations may be made from the mutagenicity curves (Figures 6.22 to 6.31) concerning the mutagenic activity of the coal pyrolysis tars:

(1) Effect of Pyrolysis Temperature

In general, at a particular furnace temperature, activated pyrolysis products (+ PMS) exhibit greater specific mutagenicities

than direct-acting mutagens (-PMS). +PMS is for more temperature-sensitive than -PMS and the difference between +PMS and -PMS is greatest at temperatures where peak evolution of PAH has been observed to occur. For ma_{coal} , the peak temperature is in the range of 1300 K to 1500 K. Further the trend in ma_{coal} and ma_{tar} with temperature closely parallels the trends exhibited in PAH yield versus temperature (Figures 6.6 to 6.10). ma_{tar} is observed to peak at about 1500 K.

(ii) Effect of Residence Time

Though the data here is not complete, it is observed that in general both ma_{coal} and ma_{tar} are higher at longer residence times. However, for the hvAb coal, the maximum ma_{coal} and ma_{tar} are obtained at a residence time of about 225 ms at 1100 K whereas PAH yields are observed to peak at 300 ms at the same temperature. At 1500 K, the trend in ma_{tar} and ma_{coal} is similar to that for PAH yields; both specific mutagenicities and PAH concentrations attain a maximum at 150 ms.

(iii) Coal Type Effect

Both ma_{coal} and ma_{tar} exhibit the following order of descending values:

hvAb >> lignite > subbituminous > anthracite.

Data on ma is scant for the mvb coal, but would appear to lie between the hvAb and the lignite. The above order is roughly the same as that observed for PAH and soot yields (per weight of coal fed), the exception being that sub-bituminous has higher yields than lignite.

It is interesting to note that the order of specific mutagenicities roughly parallels the levels of nitrogen present in the coals and their aerosols. It has been predicted earlier (Longwell, 1977) that higher nitrogen levels in fuels could lead to greater mutagenicities.

(iv) Direct-acting Mutagens

These are defined as mutagenic species which do not require activation by PMS and are denoted by '-PMS' in Figures 6.22 to 6.31. Till now such mutagens have been observed in diesels, oil burners and from toluene combustion in a JSR (Nenniger, 1983). It is clear, that direct acting mutagens are produced from the five coal pyrolysed, though at differing ratios to the +PMS activity. Tars evolved from the low rank subbituminous coal show greater direct activity than when activated by PMS. It would appear that the direct-acting mutagens are detoxified by the PMS, together with a simultaneous activation of the PAH (Nenniger, 1983). For the lignite, the difference between -PMS and +PMS mutagenic activities is very little under conditions of short residence times at both low and high pyrolysis temperatures. Both these coals have considerably higher oxygen contents than the other three high rank coals. Thus, it appears that such low rank coals would be capable of emitting direct acting mutagens such as oxygenated PAH, which would not need to be activated in human systems.

The high correlation observed between trends in specific mutagenicity and in PAH yield with pyrolysis temperature, is remarkable, considering the experimental uncertainties inherent

In both the chemical analysis as well as the biological assays, the mutagenic assays thus clearly offer an independent check for the accuracy of the results discussed earlier in Chapters 6.1 and 6.2.

It has also been observed that higher molecular weight compounds condense preferentially onto the soot during the cooling and collection steps in sampling, especially at lower temperatures (Figure 6.32). The majority of the lighter species (< 3-ring) are gasborne and are collected on the XAD-2 though some of the more volatile high molecular weight PAHs are also found on the XAD-2 (Figure 6.33). This stratification of PAH size is significant, since a majority of the highly mutagenic species are found adsorbed on the soot, which can be respired and can lodge in the lungs. The sharp transition from compounds with less than 3-rings condensed into the XAD-2, to those of 3 to 7 rings on the soot, confirm expectations that a sequential condensation of PAH will occur on the soot, with an outer layer of lighter molecular weight PAH condensed onto the heavier and more mutagenic PAH.

6.4 Comparison with Field Studies

Data obtained on coal pyrolysis studies are compared with PAH emissions reported from residential stoker coal-fired boilers, chain-grate stokers, a coal-fired power plant, wood-fired fireplace and baffled stove. PAH measured in earlier studies using the liquid fuels solvent-refined coal (heavy and 2.9:1 blend), Indo-Malay fuel oil and H-coal (Mitra et al, 1981) are also compared with PNA emissions from an oil-fired power plant and two sampling locations on the 1MW M.I.T. CRF oil burner.

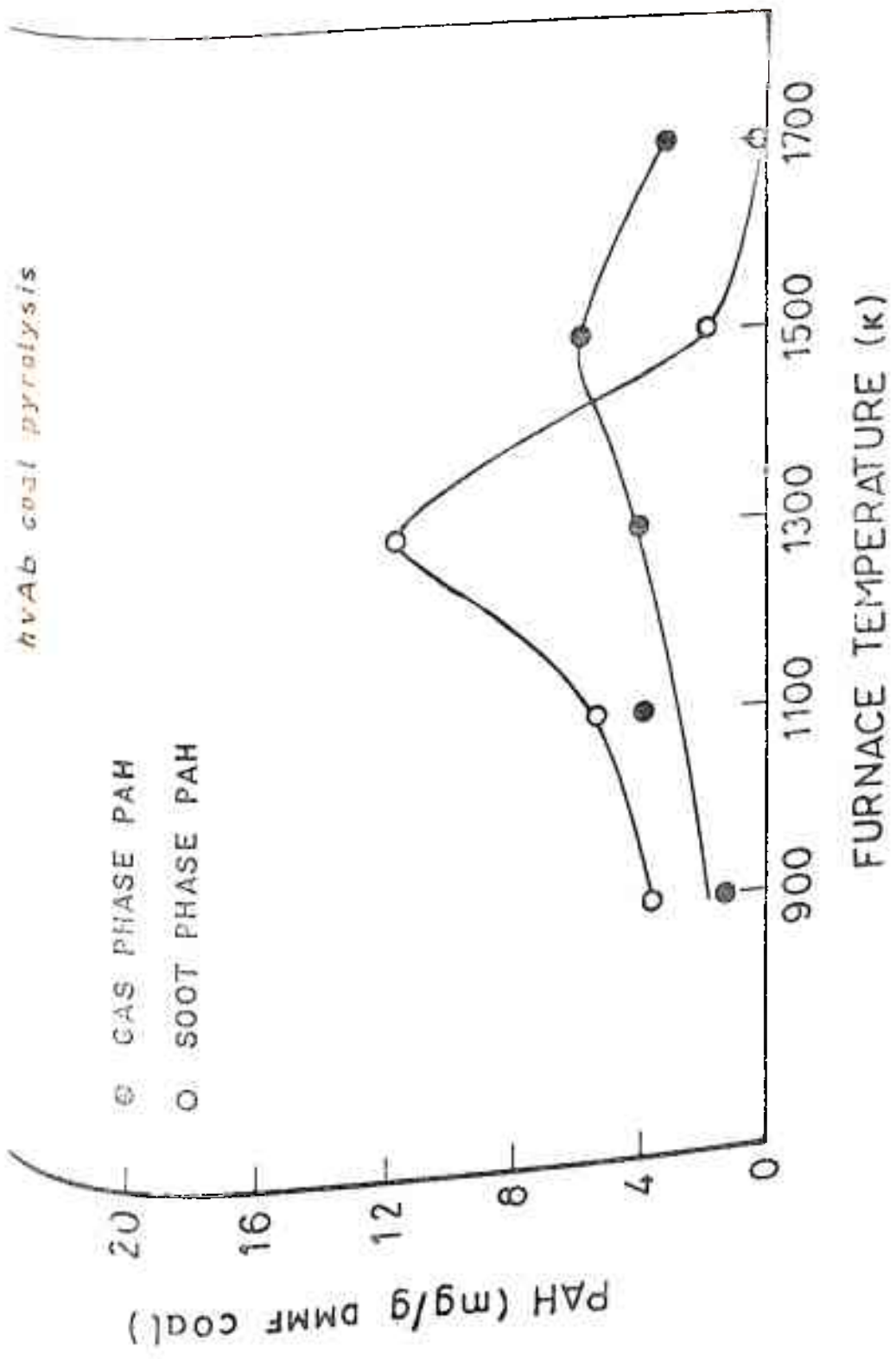


FIGURE 6.32 MOLECULAR WEIGHT DISTRIBUTION OF PAH IN THE GAS PHASE AND DEPOSITED ON SOOT

Pyrolysis of Montana lignite, 1500K, 225 ms

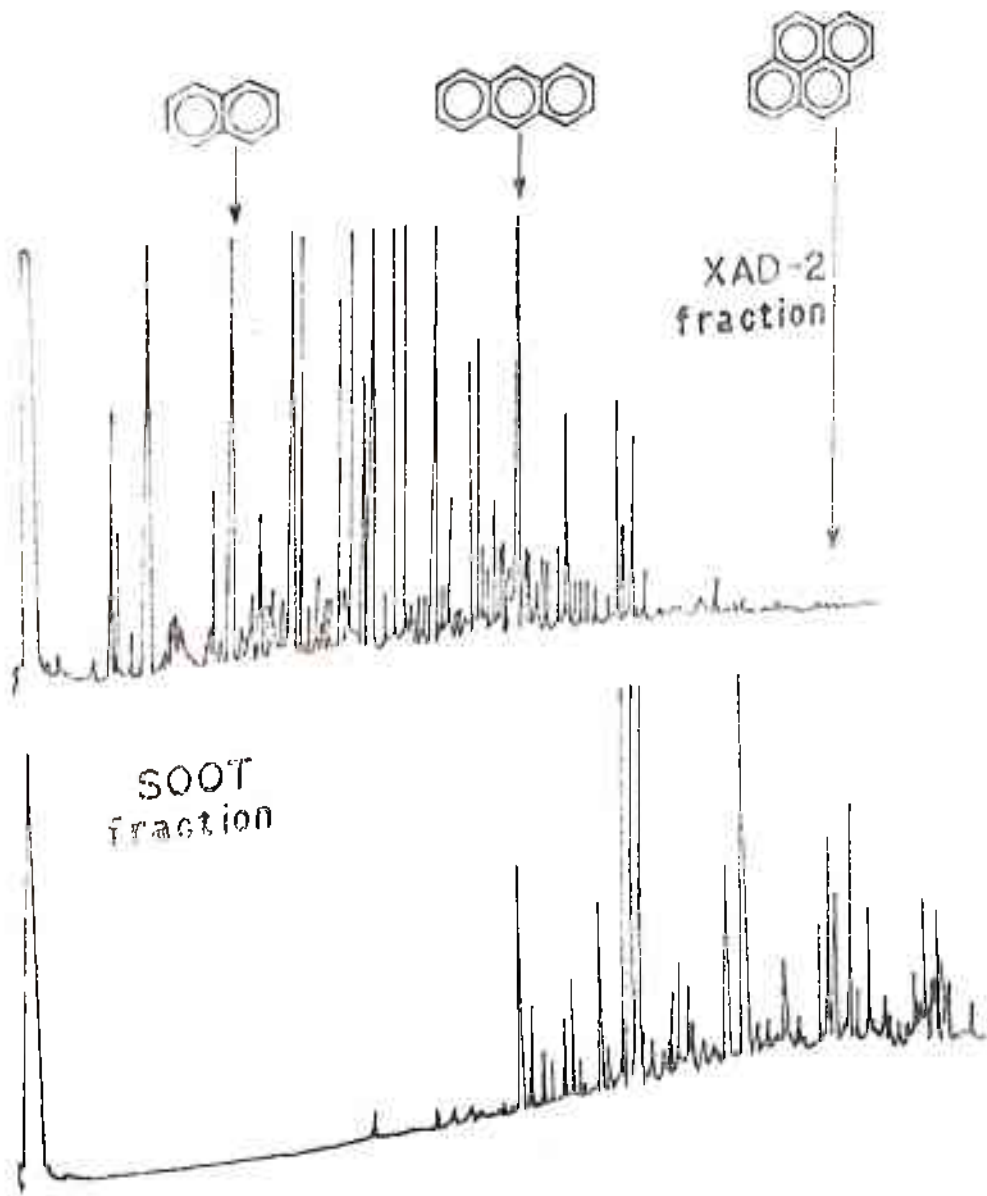


FIGURE 6.33 STRATIFICATION OF PAH DEPOSITED ON SOOT AND IN THE GAS PHASE

In general (Table 6.6) the production of PAH during coal pyrolysis is 2 to 10 times greater than that reported for small hand-stoked residential boilers (Giammar, 1976), 10^3 times greater than an industrial stoker, and 10^5 times than a large utility boiler (Zelenski et al, 1980). From the pyrolysis of fuel oils, PAH production is about 10^3 times greater than that reported in exhaust emissions from the 1 M.W. M.I.T. C.R.F. (Beer, 1980) and about 10^4 to 10^7 times greater than a large oil-fired power plant (Table 6.7).

This establishes the importance of the burnout process in establishing emission levels from the field units and confirms the validity of choosing the pyrolysis stage for detailed study on PAH emissions.

Comparison of TMA evolved (ng/J) during the pyrolysis of Montana Lignite and Pittsburgh High Volatile-A Bituminous coals with that emitted by various sources

	Methyl Anthra- cenes/ Phenen- threnes	Fluoran- thene	Pyrene	Phenan- threne/ Anthra- cene	Chrysene/ Triphe- nylene/ Benz(a)- anthracene	Bap/ BeP	Cyclo- penta (c d) pyrene
A. Residential Stoker Coal- fired Boiler, 200 KW							
1. High-volatile Bitumi- nous (Elkhorn # 3)	3.16	3.12	2.12	5.16	1.43	1.12	-
2. Western Subbituminous (Colorado)	0.37	0.096	0.132	0.72	0.08	0.159	-
3. Low-volatile Bituminous (Pocahontas Seam 3)	0.264	0.152	0.092	0.36	0.175	0.088	-
4. Processed Lignite Char	0.052	0.056	0.052	0.07	0.050	0.026	-
5. Anthracite (#1 Buck- wheat Pennsylvania)	0.061	0.009	0.008	0.035	0.025	0.049	-
B. Chain-grate Stokers	-	0.015	0.011	0.011	-	0.007	-
C. Pyrolysis							
1. Montana Lignite	-	1.72	2.71	10.95	1.06	0.61	0.73
2. Pittsburgh High- Volatile-A Bituminous	5.89	6.32	11.68	19.04	-	2.67	-
D. Coal-fired Power Plant	0.50x10 ⁵	0.07x10 ⁵	0.4x10 ⁻⁵	7.6x10 ⁻⁵	0.22x10 ⁻⁵	0.0935x10 ⁵	
E. Wood-fired							
1. Fireplace	0.09	<0.05	<0.05	0.27	<0.05	<0.05	<0.05
2. Baffled stove	0.70	0.60	0.52	2.47	0.41	0.28	0.16

TABLE 6.7

Comparison of PNA evolved (ng/J) during the pyrolysis of some liquid fuels with that emitted by field sources

PNA (ng/J)	M.I.T. CRF (1MW)		OIL FIRED POWER PLANT	PYROLYSIS		
	Distance from Burner	from Nozzle		SRC-II (2.9:1)	INDO-MALAY *	SRC-II (Heavy)
Phenanthrene/Anthracene	5.02	4.8x10 ⁻³	7.45x10 ⁻⁴	7.78	10.9	9.24
Methylphenanthrenes/Anthracenes	-	-	0.735x10 ⁻⁴	-	24.4	-
Fluoranthene	1.16	2.98x10 ⁻³	0.34x10 ⁻⁴	2.62	16.83	1.38
Pyrene	2.16	3.29x10 ⁻³	0.18x10 ⁻⁴	3.38	6.30	2.88
Methylpyrenes/Fluoranthenes	0.92	1.98x10 ⁻³	0.21x10 ⁻⁴	-	-	-
Chrysene/Triphenylene/Benz(a)anthracene	-	-	0.35x10 ⁻⁷	3.55	-	0.25
Benzo(e)pyrene/Benzo(a)pyrene	0.39	7.48x10 ⁻³	0.7x10 ⁻⁷	3.71	-	0.12

*includes PNA present in residual fuel

CHAPTER 7

CONCLUSIONS AND RECOMMENDATIONS

The major results are summarised below:

(a)

The complexity of the PAH obtained and the amounts of PAH and soot produced reflect the complexity of the parent fuel. Thus the concentration of PAH evolved, in descending order is:

High volatile-A bituminous > Medium volatile bituminous > Subbituminous > Lignite > Anthracite

(b)

The production of PAH is determined by the competition between evolution during the primary pyrolysis of coal and destruction via secondary pyrolysis in the gas phase. As a consequence, the total PAH yield peaks at a temperature of about 1300 K, regardless of the type of coal being pyrolysed.

(c)

Soot yields tend to increase with temperature, finally approaching asymptotic values. A fraction of the PAH act as precursors for soot formation.

(d)

The primary production of PAH during pyrolysis is a factor 2^{10} times greater than that reported for small hand-stoked combustors and 10^5 times that obtained from large coal-burning utility boilers. This establishes the importance of the burnout process in determining levels of emission from field units.

(e)

The mutagenic activity of most samples could be correlated well with the sum of the contributions of the individual compounds, with fluoranthene, methyl-phenanthrenes and cyclopenta(cd)pyrene being the major contributors.

benzo(a) pyrene, generally reported to be one of the primary mutagenic species, contributes insignificantly to the total mutagenic loading.

- (f) Higher molecular weight compounds condense preferentially onto the soot during sampling. The difference in composition of the soot extracts and gas-phase constituents is reflected in the mutagenic activity.

The processes that lead to PAH emissions are shown schematically in Figure 7.1. The PAH may be formed by the thermal breakdown of the coal molecule during pyrolysis (the top branch) or by the pyrosynthesis from low molecular weight hydrocarbons (the bottom branch). PAH produced may undergo transformations during further heating in an oxygen deficient atmosphere (secondary pyrolysis) or via oxidative reactions. The amount and composition of PAH emitted will be a mixture of the species produced by all the paths shown, with weightages that depend on the temperature and mixing history experienced by the volatile products.

Though it has been established that PAH burns out in the presence of oxygen, it would still be of interest to study the formation of heterocyclic PAH evolved during partial oxidation and quenching of the coal pyrolysis products. Some of these heterocyclic PAH are direct-acting mutagens and do not require any enzyme activation. The conditions under which such PAH are formed are those in which air and fuel are mixed at temperatures insufficient to cause ignition, conditions encountered in small combustors and near cold surfaces. The studies of their formation could involve two approaches.

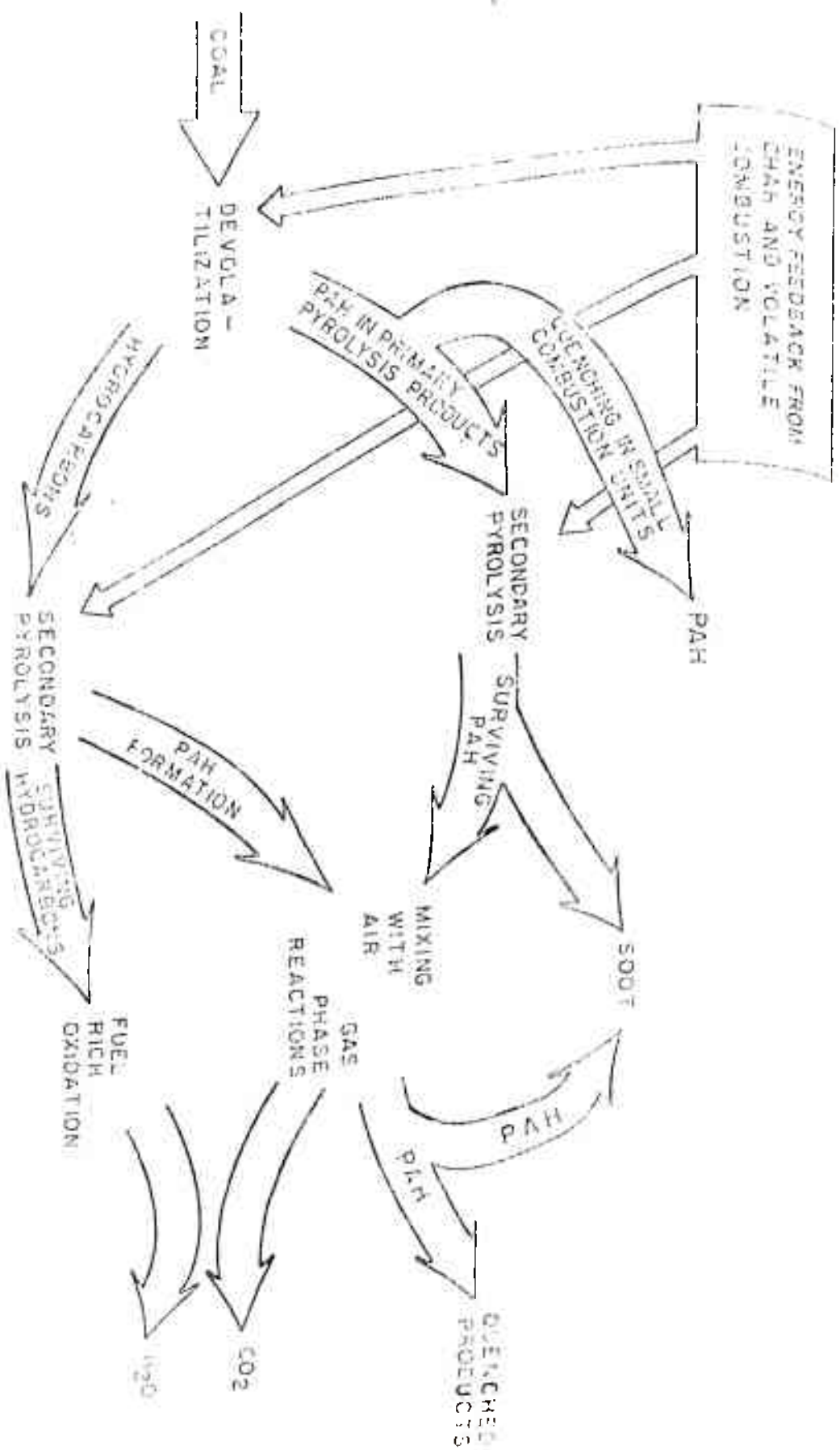




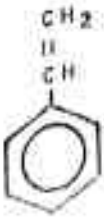
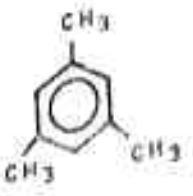





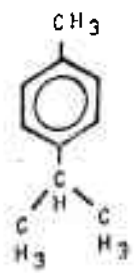
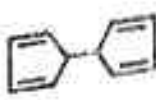
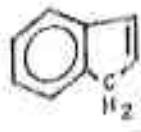
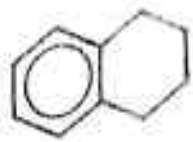

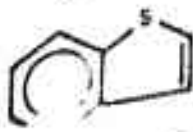
FIGURE 7.1 SCHEMATIC DIAGRAM OF PAH EMISSION DURING THE SERIES OF PROCESSES IN COAL COMBUSTION.

In the first, small amounts of oxygen would be introduced with the inert gas steam in the pyrolysis experiments, and the products quenched and analysed. In the second approach, products of pyrolysis in an inert atmosphere would be quenched with a gas stream containing varying amounts of oxygen and preheated to different temperatures. The pyrolysis products would be exposed to oxygen concentrations increasing linearly with time as the temperature decreases at a controlled rate. This approach would simulate the quenching of pyrolysis products in a practical system as a consequence of localised cooling by the entrainment of air.



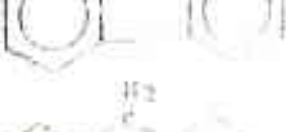
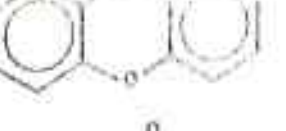
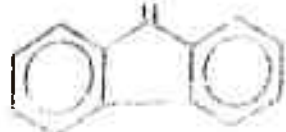








APPENDIX A

CHEMICAL STRUCTURES OF PAH
IDENTIFIED FROM COAL PYROLYSIS

No	Name	Structure	Mutagenic species
1.	Benzene		
2.	Toluene		
3.	para-Xylene		
4.	Cumene		
5.	Styrene		
6.	Thesitylene		

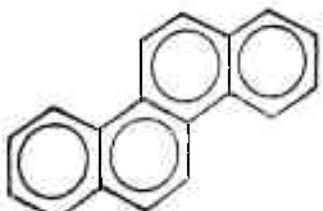
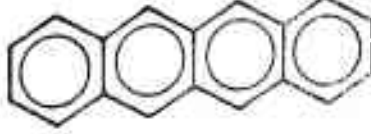
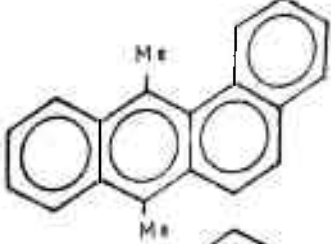
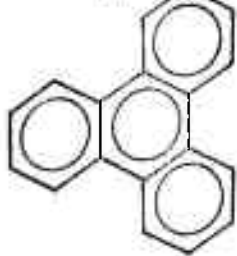

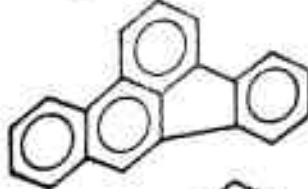
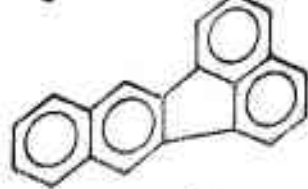

No.	I.U.P.A.C. Name	Structure	Mutagenic species
7.	para-Toluidine		
8.	Phenol		
9.	para-Cresol		
10.	para-Cymene		
11.	Dicyclopentadiene		
12.	Indene		
13.	Tetralin		
14.	Naphthalene		
15.	Benzo(b) thiophene		



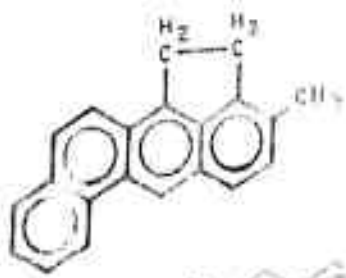


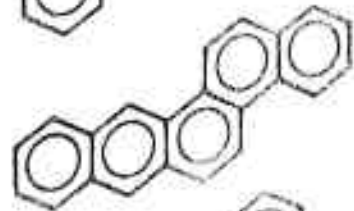

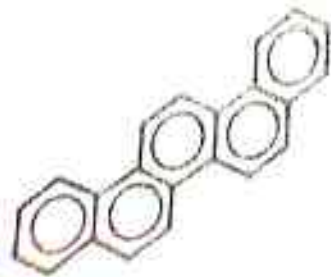
No.	I.U.P.A.C. Name	Structure	Mutagenic species
16.	Quinolene		H
17.	Indole		
18.	Quinoxaline		
19.	Biphenyl		
20.	Isoquinoline		
21.	1,4-naphthoquinone		
22.	1-methyl naphthalene		M
23.	Acenaphthylene		M
24.	Acenaphthene		M
25.	Dibenzofuran		




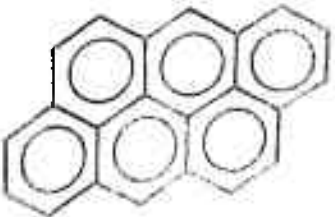


	IUPAC Name	Structure	Mutagenic species
19.	N-methyl guanine		b1
21.	Fluorene		
22.	Fluorenone		
23.	Fluorene		
24.	9-Fluorenone		
30.	Dibenzo thiophene		
31.	Phenanthrene		
32.	Anthracene		
33.	Acridine		
34.	Phenanthridine		
35.	Acridine		
36.	Acridine		
37.	Acridine		

No.	IUPAC Name	Structure	Mutagenic species
41	Benzene (h) quinoline		M
42	Benzene (i) quinoline		M
43	1-methyl anthracene		M
44	1-methyl phenanthrene		M
45	Cyclopenta (def) phenanthrene		M
46	1-methyl anthracene		M
47	2-methyl phenanthrene		M
48	Cyclopent (l,g) acenaphthene		
49	Cyclopent (f,g) acenaphthylene		

No	I.U.P.A.C. Name	Structure	Mutagenic species
45.	Fluoranthene		M
46.	Pyrene		M
47.	Benzo(a) fluorene		
48.	1,1'-binaphthyl		
49.	1-methyl pyrene		M
50.	Benzo(b) fluorene		M
51.	Cyclopenta(cd) pyrene		M
52.	Benz(a) anthracene		M

No	I.U.P.A.C. Name	Structure	Mutagenic species
53	Chrysene		M
54	Naphthacene		
55	7,12-dimethyl benz (a) anthracene		M
56	Triphenylene		M
57	Benzo (j) fluoranthene		
58	Benzo (b) fluoranthene		
59	Benzo (k) fluoranthene		
60	Benzo (e) pyrene		M

Sl. No.	IUPAC Name	Structure	Mutagenic species
61	Benzo(a)pyrene		M
62	Perylene		M
63	3-methyl cholanthrene		M
64	Pentocens		
65	Dibenz(ah)anthracene		M
66	Benzo(b)chrysene		
67	Dibenz(ac)anthracene		M
68	Picene		

No.	IUPAC Name	Structure	Mutagenic species
69	3,3'-difluorenyl		
70	3,3'-bifluorenylidene		
71	Benz(a)ghi perylene		M
72	Dibenzo (def, mno) chrysene		
73	Coronene		
74	Ben(a)acrylene		

APPENDIX BAN ASSESSMENT OF ENVIRONMENTAL SOURCES OF PAH

Polycyclic aromatic hydrocarbons are ubiquitous in the environment. They are evolved during any mode involving combustion and are a result of both man-made and natural processes. They are usually observed in the atmosphere as adsorbates on soot, flyash and other particulates generated in combustion processes.

Hangebrauck (1967) surveyed the contributions by various sources to the total environmental loading of benzo(a) pyrene in a comprehensive study which still remains a major reference point. The primary source of BaP identified was the inefficient combustion of coal in residential and small industrial coal-fired furnaces. PNA loadings due to coal combustion were of the order of 87% of the sources listed. Though concentrations of other PNAs such as pyrene, benzo (ghi) perylene, anthracene, coronene, anthanthrene, phenanthrene and fluoranthene were measured and estimated in specific situations, overall atmospheric loadings due to these species were not tabulated. However, as observed in this thesis, yields of BaP are quite low and those of other mutagenic species, such as fluoranthene considerably higher. From Hangebrauck's data, emission factors have been estimated for all the PNA identified and total PAH emissions determined. These are presented in Table B.1. As can be seen, the estimated annual yield of PAH is roughly thirteen times that of BaP alone. It is also clear that many other PAH types, especially the alkylated phenanthrenes

TABLE B.1

Emission factors ($\mu\text{g}/10^6 \text{ BtU}$) for Benzo(a) Pyrene and total PAH emitted by a variety of environmental sources in U.S.A.

Source	Estimated BaP Emission rate ($\mu\text{g}/10^6 \text{ BtU}$)	Estimated total PAH emission rate ($\mu\text{g}/10^6 \text{ BtU}$)	Total PAH BaP
<u>Heat Generation</u>			
Coal			
Residential			
a) Hand-stoked	1,400,000	17,111,130	12.2
b) Underfeed	44,000	696,249	15.8
Commercial	5,000	6,250	1.25
Industrial	2,700	3,309	1.23
Electric generation	90	991	11.0
	200	1462	7.3
Oil			
	100	2964	29.64
Gas			
	($\mu\text{g}/\text{ton}$)	($\mu\text{g}/\text{ton}$)	
<u>Refuse Burning</u>			
Incineration			
a) Municipal	5,300	74,672	14.1
b) Commercial	310,000	8,632,473	27.8
<u>Open Burning</u>			
a) Municipal refuse	310,000	4,096,184	13.2
b) Grass, leaves	310,000	3,558,257	11.5
c) Auto Components	26,000,000	2.2×10^8	8.6

TABLE B.1 (Contd.)

Source	Estimated BaP emission rate	Estimated total PAH emission rate	Total PAH BaP
	($\mu\text{g}/\text{bbL}$)	($\mu\text{g}/\text{bbL}$)	
<u>Industries</u>			
Petroleum Catalytic Cracking Process (catalyst regeneration)			
FCC			
a) No CO boiler	240	28,382	118.3
b) With CO boiler	14	233	16.6
HCC			
a) no CO boiler	218,000	1,134,902	5.2
b) with CO boiler	45	436	9.7
TCC (Air Lift)			
a) no CO boiler	90,000	735,137	8.2
b) with CO boiler	< 45	-	-
TCC (Bucket Lift)			
a) no CO boiler	31	458	14.8
b) with CO boiler	< 31	-	-
Asphalt road mix	50/ $\mu\text{g}/\text{ton}$	3733/ $\mu\text{g}/\text{ton}$	75
Asphalt air blowing	10 ⁴ / $\mu\text{g}/\text{ton}$	3.808x10 ⁶ $\mu\text{g}/\text{ton}$	381
	($\mu\text{g}/\text{gal}$)	($\mu\text{g}/\text{gal}$)	

Mobile Sources

Gasoline	170	4,811	28.3
Automobiles	7460	25,300	55
Trucks	690	-	> 55 (assumed)
Diesel			

and anthracenes, acenaphthylene, acenaphthene, cyclopenta (cd) pyrene and chrysene which have been identified in this thesis (Mitra et al, 1983) and by several other workers have not been accounted for. Thus the annual emissions of PAH estimated by Hangebrauck (1967) are definitely on the low side. Nevertheless, the study is still one of the best comparative assessments of several diverse sources.

More recently, Peters et al (1980) have estimated annual total POM emissions by source type. Their projections, based on Hangebrauck's catalogue of sources and additional data from several EPA-sponsored projects studying a particular POM source, are presented in Table B.2. The results are startling. Residential wood combustion may turn out to be the largest single contributor of PAH emissions. It is much higher than other residential heating sources and is of the same order of magnitude as open burning. More recently an article in the "New Scientist" (Allaby & Lovelock, 1980) has reinforced this conclusion and states that 'Wood-burning stoves are fashionable, beautiful and friendly. They are also astonishingly dirty'. The authors go on to state that 'the wood-burning stove is one of the most highly and most dangerously polluting domestic devices known to modern man'!

In Peters et al 's (1980) test program on residential wood burning, and in the data from the EPA reports on point sources, twenty two POMS and various other organic species have been identified. Thus the earlier criticism against Hangebrauck's (1967) numbers is invalid here. Further, more powerful and precise GC-MS techniques have been employed in

TABLE B.2

Estimates of annual POM emissions by source type

source type	Estimated annual POM emissions, metric tons (1980)	Percent of total POM emissions from all sources (1980)	Estimated annual POM emissions, metric tons (1967)	Percent of total POM emissions from all sources (1967)
Residential heating				
• Wood-fired total	3,837	38.2		
• primary heating	1,383			
• auxiliary heating	2,376			
• fireplaces	78			
• Coal-fired	102	1.0	5033	77.9
• Oil-fired	7.4	< 0.1	75	1.2
• Gas-fired	9.8	< 0.1	14.5	.2
Open burning sources				
• Agricultural open burning	1,190	1.9		
• Prescribed burning	1,071	10.7	108	2.6
• Forest wildfires	1,478	14.7		
• Coal refuse piles	28.5	0.3		
• Land clearing waste burning	171	1.7		
• Structural fires	86	0.9		
Mobile sources				
• Autos-gasoline	2,160.8	21.5	243.4	3.8
• Autos-diesel	1.2	< 0.1	110	1.7
• Trucks-diesel	103.5	1.0	550	8.5
• Trucks-gasoline				
	632	6.3		
Coke production				
			7.1	.11
Industrial boilers				
• Coal	69.0	0.7	7.1	.11
• Oil	1.3	< 0.1	3.1	.05
• Gas	2.1	< 0.1		
• Wood/bark	1.2	< 0.1		
• Bagasse	0.3	< 0.1		
Incinerators				
			1.41	.02
• Municipal	0.3	< 0.1	133.4	2.06
• Commercial	55.8	0.6		

TABLE B.2 (Contd.)

Source type	Estimated annual POM emissions, metric tons (1980)	Percent of total POM emissions from all sources (1980)	Estimated annual POM emissions, metric tons (1967)	Percent of total POM emissions from all sources (1967)
Utility boilers				
. Coal	12.9	0.1		
. Oil	0.3	< 0.1		
. Gas	0.3	< 0.1		
Carbon black	3.1	< 0.1		
Charcoal manufacturing				
. uncontrolled batch kilns	0.8	< 0.1		
. continuous furnace production	0.7	< 0.1		
Asphalt production				
. Saturators	0.2	< 0.1	.01829	
. Air blowing	0.2	< 0.1	.00075	
. Hot road mix	3.9	< 0.1		
Barium chemicals (black ash rotary kiln)	0.3			
			161.2	2.5
Petroleum cat cracking			6,464	
Total	10,037.4			

the later study, as compared to UV spectrophotometry earlier.

A comparison between the 1967 and 1980 projected total emissions of PAH is presented in Table B.2. There is a remarkable shift in the estimations from residential heating sources. Coal-fired sources dominated in 1967, whereas wood-fired units appear to be the more important source now.

It is clear from both the above estimations that contributions from potentially important sources including natural sources, future energy sources (for example, coal gasification), aircraft, motorcycles, coal tar production etc. have not been made.

An important contribution is that from cigarette smoke. From studies on GC-MS and proton NMR of tobacco smoke condensates (Lee et al, 1976), it is observed that the total emissions of PAH are 1.922 mg/100 cigarettes. Thus, an average smoker who goes through 20 cigarettes a day can expect to take in 0.4 mg of PAH, not to mention other mutagens such as aza-arenes and NO_x . If one assumes a heating value for tobacco similar to that for wood (~ 4300 Btu/kg) one gets an emission factor for PAH of roughly $5 \times 10^5 \mu\text{g PAH}/10^6$ Btu. This is a figure of the same order of magnitude as the emission rates observed in highly polluting residential hand-stoked coal-fired units! Since a small fraction of the total PAH produced by a burning cigarette would escape into the atmosphere cigarette smoke may well turn out to be a major 'dark horse' in the PAH sweepstakes.

The development of techniques for the identification of sources of PAH, by measuring concentrations of tracer species in the environment is of considerable importance. A proper understanding of the role played by various sources in the atmospheric loading of PAHs could lead to a clearer picture of the origins, reactions and fate of these species and thus facilitate control of PAH emissions.

The methods used in determining source I.D.S. may be classified into the following broad categories (Daisey et al, 1979):

- (a) Enrichment factor methods which study the concentrations of various aerosol elements relative to their concentrations in natural materials.
- (b) The chemical element balance method by which mass balances are made for the total emission mass and measured emission ratios of observable tracer elements.
- (c) The use of elemental ratios from a point source to estimate the contribution of that source to the total suspended particulates.
- (d) Statistical models which attempt to correlate various parameters, such as individual PAH concentrations and trace metals, by pairwise correlations and factor analysis.

Enrichment factor methods have been used by Lee et al (1977) to compare the distribution of PAH obtained from the combustion of coal, wood and kerosene with that of airborne PAH from Indianapolis, a high coal consuming area and Boston, where home heating is primarily by wood and fuel oil. A similarity was observed between alkyl homolog distribution plots for coal-soot PAH and Indianapolis aerosol, as well as

between the kerosene-soot PAH and Boston air particulates. The coal used in the laboratory studies was a Pittsburgh seam bituminous. Further, coal generated PAH had a greater relative concentration of alkylated species whereas wood and kerosene generated PAH had a predominance of higher molecular weight species (6-ring and larger). Ratios of PAHs as that of benzo(a) pyrene/benzo(ghi) perylene have been used by various workers to estimate contributions from different sources (Sawicki, 1962; Hangebrauck et al, 1967). Daisey et al (1979) have estimated from such ratios that in the summer of 1976, PAH compounds may have been transported into New York City under certain meteorological conditions.

The chemical element balance method and statistical correlations further indicate that automobiles contributed over 60% of ambient benzo(a) pyrene concentrations in New York City during the same period. Colucci and Begeman (1970) have also used factor analysis techniques to relate PAH with both automotive and non-automotive sources in Los Angeles air. Species such as carbon monoxide and lead are assumed to be emitted only by cars, vanadium is taken as an index of pollution from the combustion of petroleum based fuel oils and sulfate is taken as an indication of pollution due to combustion of non-automotive fuels. On this basis, it is observed that automotive sources are mainly responsible for ambient PAH loadings in Los Angeles. In a more recent study, Daisey et al (1982), samples of TSP were collected in the summer of 1976 and 1977 and during winter in 1977 and 1978 in New York City. From factor analysis studies it was observed that 50% to 75% of the POM in winter could be attributed to oil-burning for space heating.

REFERENCES

1. Albright, L.F. and Yu, Y.C., "Thermal Hydrocarbon Chemistry", Adv. in Chem. Series 183, ACS, 193 (1979)
2. Allaby, K. and Lovelock, J., "Wood Stoves: the trendy pollutant", New Scientist, 420, November 13 (1980)
3. Anthony, D.B., "Rapid Devolatilization and Hydrogasification of Pulverized Coal", Sc.D. Thesis, M.I.T. (1974).
4. Anthony, D.B. and Howard, J.B., A.I.Ch.E. Journal, 22, 625 (1976)
5. Anthony, D.B., Howard, J.B., Hottel, H.C. and Meissner, H.P., 15th Symposium (International) Combustion, The Combustion Institute, Pittsburgh, 1303 (1975)
6. Asaba, T. and Fujii, N., 13th Symposium (International) Combustion, The Combustion Institute, Pittsburgh, 155 (1971)
7. Badger, G.M., National Cancer Inst. Monograph No. 9, presented at Symposium on The Analysis of Carcinogenic Air Pollutants, Cincinnati, Ohio, pp. 1-16 (1962)
8. Badger, G.M. and Spotswood, T.M., J. of the Chemical Society (London), 4420 (1960)
9. Badger, G.M. and Spotswood, T.M., J. of the Chemical Society (London), 4431 (1960a)
10. Badger, G.M., Kimber, R.W.L. and Spotswood, T.M., Nature, 187, 663 (1960b)

- Indger, A., Lewis, G.E. and Miller, I.H., J. of the Chemical Society (London), 2825 (1960c)
13. Berenski, V.J., Maciel, G.E., Schaffer, J. and Stejskal, S.O.,
 "13C NMR studies of Solid Coal Samples", Preprint of the Coal Chem. Workshop, Menlo Park, CA., 26 (1976)
14. Pecker, H.A. and Yamazaki, S., 16th Symposium (International) Combustion, The Combustion Institute, Pittsburgh, 521 (1977)
15. Beer, J.M., Centre for Health Effects of Fossil Fuels Utilization, 2nd Annual Report, Centre Grant No. 5 P30 ESO2109-02 (1980)
16. Beer, J.M., Toqan, M., Farmayan, W., Jacques, M.T. and Prado, G.P., 19th Symposium (International) Combustion, The Combustion Institute, Pittsburgh, (1983)
17. Bittner, J.D. and Howard, J.B., Presented at the General Motors Research Symposium, 'Particulate Carbon Formation During Combustion', pp. 1-46, October (1980)
18. Bittner, J.D. and Howard, J.B., 18th Symposium (International) Combustion, The Combustion Institute, Pittsburgh, 1105 (1981)
19. Blazowski, W.S., 16th Symposium (International) Combustion, The Combustion Institute, Pittsburgh, 1631 (1977)
20. Blazowski, W.S., Comb. Sc. and Tech., 21, 87 (1980)

21. Bonne, U., Homann, K.H. and Wagner, H.GG., 10th Symposium (International) Combustion, The Combustion Institute, Pittsburgh, 503 (1965)
22. Braun, A., Personal Communication (1984)
23. Brooks, J.D. and Stephens, J.F., Carbon, 2, 379 (1965)
24. Brown, J.K. and Hirsch, P.B., Nature, 175, 229 (1955)
25. Brown, R.D., J. Chem. Soc., 691, 2731 (1950)
26. Burgoyne, J.H., Proc. Roy. Soc. London, A 175, 539 (1940)
27. Butze, H.F. and Ehlers, R.C., NASA TM X-71789, pp. 1-14 (1975)
28. Calcote, H.F., 8th Symposium (International) Combustion, Williams and Wilkins Co., Baltimore, 184 (1962)
29. Calcote, H.F., "Ionic Mechanisms of Soot Formation in Flames", Presented at the Fall Technical Meeting, Eastern States Section of Combustion Inst., Miami, FL. (1978)
30. Calcote, H.F., Comb. and Flame, 42, 215 (1981)
31. Calcote, H.F. and Manos, D.M., Comb. and Flame, 49, 289 (1983)
32. Calcote, H.F., and Olson, D.B., Comb. Sc. and Tech., 28, 315 (1982)
33. Cartz, L., and Hirsch, P.B., Phil. Trans. Roy. Soc. London, 252A (1019), 557 (1960)

34. Chakrabartty, S.K. and Berkowitz, N., Fuel, 53, 240 (1974)
35. Chakraborty, B.B. and Long, R., Comb. and Flame, 12, No. 3, 226 (1968)
36. Chakraborty, B.B. and Long, R., Comb. and Flame, 12, No. 3, 237 (1968 a)
37. Chow, R.H., "Formation of Polycyclic Aromatic Hydrocarbons During Coal Pyrolysis and Oxidation", S.M. Thesis, M.I.T. (1979)
38. Clark, A.E., Hunter, T.G. and Garner, F.H., J.Inst. Petroleum, 32, 627 (1946)
39. Cole, J.A., S.M. Thesis, Dept. of Chem.Eng., M.I.T. (1983)
40. Colucci, J.M. and Begeman, C.R., "Polynuclear Aromatic Hydrocarbons and other Pollutants in Los Angeles Air", Proceedings of the Second International Clean Air Congress, 28 (1970)
41. Crittenden B.D. and Long, R., Env. Sc. and Tech., 7, No.8, 742 (1973)
42. Crittenden, B.D. and Long, R., Comb. and Flame, 20, 359 (1973a)
43. Cyprés, R. and Bredael, P., Fuel Processing Technology, 3, 297 (1980)
44. Daisey, J.M., Hershman, R.J. and Kneip, T.J., Atmospheric Environment, 16(9), 2161 (1982)

45. Daisey, J.M., Leyko, M.A. and Kneip, T.J., "Source Identification and Allocation of Polynuclear Aromatic Hydrocarbon Compounds in the New York City Aerosol: Methods and Applications" in Polynuclear Aromatic Hydrocarbons, ed. P.W. Jones and P. Leber, Ann Arbor Science Publishers, Ann Arbor, MI., 201 (1979)
46. D'Alessio, A., DiLorenzo, A., Sarofim, A.F., Beretta, F., Masi, S. and Venitozzi, C., 15th Symposium (International) Combustion, The Combustion Institute, Pittsburgh, 1427 (1975)
47. Davies, R.A. and Scully, D.B., Comb. and Flame, 10, 165 (1966)
48. Depp, E.A., Stevens, C.M. and Neuworth, M.B., Fuel, 35, 437 (1957)
49. DiLorenzo, A., D'Alessio, A., Cincotti, V., Masi, S., Menna, P. and Venitozzi, C., 18th Symposium (International) Combustion, The Combustion Institute, Pittsburgh, 485(1981)
50. Donnet, J.B., Lahaye, J., Voet, A. and Prado, G., Carbon, 12, 212 (1974)
51. Donovan, J., Unpublished UROP Project, Dept. of Chem. Eng., M.I.T., (1978)
52. Dryden, I.G.C., "Chemical Constitution and Reactions of Coal", Ch.6 in Chemistry of Coal Utilization, Supplementary Volume, H.H. Lowry ed. John Wiley & Sons, N.Y. (1963)

53. Essenhigh, R.H., "Coal Combustion", Ch.3 in Coal Conversion Technology, ed. by C.Y. Wen and E.S. Lee, Addison-Wesley Publishing Company, Mass. (1979)
54. Evelyn, J., "Fumifugium", (1661), Reprinted in The Smoake of London, Maxwell Reprint Co. (1969)
55. Fenimore, C.P. and Jones, G.W., Comb. and Flame, 12, No.3, 196 (1968)
56. Fenimore, C.P., Jones, G.W. and Moore, G.E., 6th Symposium (International) Combustion, Reinhold Publishing Corp., New York, 242 (1957)
57. Feugier, A., Rev. Gen. Therm., 105, 1045 (1970)
58. Fields, E.K. and Meyerson, S., Accounts of Chemical Research, 2(9), 273 (1969)
59. Franceschi, A., Gerbaz, G.P. and Mangolini, S., Comb.Sc. and Tech., 4, 33 (1976)
60. Frazee, J.D. and Anderson, R.C., Proc. 3rd Conf. Carbon, Pergammon Press, 405 (1959)
61. Freihaut, J.D., Zabielski, M.F. and Seery, D.J., 19th Symposium (International) Combustion, The Combustion Institute, Pittsburgh, (1983)
62. Frenklach, M., Taki, S. and Matula, R.A., Comb and Flame, 49, 275 (1983)
63. Fuchs, W. and Sandhoff, A.G., Ind. Eng. Chem., 34, 567 (1942)

64. Garner, F.H., Long, R. and Thorp, N., Fuel, 32, 116 (1953)
65. Giammar, R.D., Engdahl, R.B. and Barrett, R.E., "Emissions from Residential and Small Commercial Stoker-Coal-Fired Boilers under Smokeless Operation", EPA-600/7-76-029 (1976)
66. Given, P.H., Fuel, 39, 147 (1960)
67. Given, P.H., "The Organic Chemistry of Coal Macerals", Penn. State Short Course on Coal, The Pennsylvania State Univ., June (1976).
68. Glassman, I., Dept. of Mechanical and Aerospace Eng. Report 1450, Princeton Univ., pp. 1-39 (1979).
69. Glassman, I. and Yaccarino, P., Comb. Sc. Tech., 24, 107 (1980)
70. Glassman, I. and Yaccarino, P., 18th Symposium (International) Combustion, The Combustion Institute, Pittsburgh, 1175 (1981)
71. Graham, S.C., 16th Symposium (International) Combustion, The Combustion Institute, Pittsburgh, 663 (1977)
72. *Graham, S.C., Homer, J.B. and Rosenfeld, J.L.J., Proc. Roy. Soc. London, A344, 259 (1975)*
73. Graham, S.C., Homer, J.B. and Rosenfeld, J.L.J., 10th International Shock Tube Symp., Kyoto, 621 (1975a)
74. Grosjean, D., Anal. Chem., 47, 797 (1975)

75. Gross, G.P., SAE Transactions # 720210, 81, 830 (1972)
76. Grovenstein, E. and Mosher, J., J. of A.C.S., 92(12), 3810 (1970)
77. Hangebrauck, R.P., von Lehmden, D.J. and Meeker, J.E., "Sources of Polynuclear Hydrocarbons in the Atmosphere", U.S. Department of Health, Education and Welfare, Public Health Service Publication No. 999-AP-333, pp. 1-44 (1967)
78. Haynes, B.S., Jander, H. and Wagner, H.G.G., 17th Symposium (International) Combustion, The Combustion Institute, Pittsburgh, 1365 (1979)
79. Heredy, L.A., Kostyo, A.E. and Neuworth, M.B., Fuel, 44, 125 (1965)
80. Heredy, L.A. and Wender, I., "A Model Structure for a Bituminous Coal" (1979)
81. Herlan, A., Comb. and Flame, 31, 297 (1978)
82. Hill, G.R. and Lyon, L.N., Ind. Eng. Chem., 54, 36 (1962)
83. Hirsch, P.B., Proc. Roy. Soc. London, A226, 143 (1954)
84. Holden, C. and Thring, M.W., "Emissivity and Radiation of Steam and Air-atomized Liquid-fuel Flames" in Proceedings of the Residential Conf. on Major Dev. in Liq. Fuel Firing, The Institute of Fuel, London, 60 (1959)
85. Holliday, D.K., "The Radiation from Turbulent Jet Diffusion Flames of Liquid Hydrocarbons", Ph.D. Thesis, Univ. of Sheffield (1955)

86. Homann, K.H., Comb. and Flame, 11, 265 (1967)
87. Homann, K.H., Angew. Chem. International Edit., 7, No. 6, 414 (1968)
88. Homann, K.H., Mochizuki, M. and Wagner, H.G.G., Z. Phys. Chem. N.F., 37, 299 (1963)
89. Homann, K.H. and Wagner, H.G.G., 11th Symposium (International) Combustion, The Combustion Institute, Pittsburgh, 371 (1967)
90. Homann, K.H. and Wagner, H.G.G., Proc. Roy. Soc., London. A, 141 (1968)
91. Howard, J.B. and Essenhigh, R.H., Ind. Eng. Chem., Process Des. Dev., 6, 74 (1967)
92. Hunt, R.A., Ind. Eng. Chem., 45, No. 3, 602 (1953)
93. Jagoda, I.J., Prado, G. and Lahaye, J., Comb. and Flame, 37, 261 (1980)
94. Johnson, G.L. and Anderson, R.C., Proc. of 5th Conf. on Carbon, Buffalo, 1, 395 (1962)
95. Jüntgen, H. and Van Heek, K.H., Fuel, 47, 103 (1968)
96. Kaden, D.A., Hites, R.A. and Thilly, W.G., Cancer Research, 39, 4152 (1979)
97. Kausch, W.J., Clappitt, C.M., Prado, G.P., Hites, R.A. and Howard, J.B., 18th Symposium (International) Combustion, The Combustion Institute, Pittsburgh, (1981)

98. Kessler, T., Raymond, R. and Sharkey Jr., Z.G., Fuel, 48, 179 (1969)
99. Kimber, G.H. and Gray, M.D., Comb. and Flame, 11(4), 160 (1967)
100. Kinney, C.R. and DelBel, E., Ind. and Eng. Chem., 46, No.3, 548 (1954)
101. Kobayashi, H., "Devolatilization of Pulverized Coal at High Temperature", Ph.D. Thesis, M.I.T. (1976)
102. Kobayashi, H., Howard, J.B. and Sarofim, A.F., 16th Symposium (International) Combustion, The Combustion Institute, Pittsburgh, 411 (1977)
103. Kozlov, G.I. and Knorre, V.G., Comb. and Flame, 6, 253 (1962)
104. Ladner, W.R. and Stacey, A.E., Fuel, 42, 75 (1963)
105. Ladner, W.R. and Stacey, A.E., Fuel, 43, 13 (1964)
106. Lahaye, J. and Prado, G., Ch.3 in Chemistry and Physics of Carbon, 14, P.L. Walker and P.A. Thromer, ed. Marcel Dekker, N.Y. (1978)
107. Lee, M.L., Novotny, M. and Bartle, K.D., Anal. Chem., 48(2), 405 (1976)
108. Lee, M.L., Prado, G.P., Howard, J.B. and Hites, R.A., Biomedical Mass Spectrometry, 4(3), 182 (1977)

109. Lee, M.L., Vassilaros, D.L., White, C.A. and Novotny, M., Anal.Chem., 51(6), 768 (1979)
110. Lewis, I.C. and Edstrom, T., Proc. of the Fifth Carbon Conf., 2, Pergamon Press, 413 (1963)
111. Lewis, I.C. and Edstrom, T., J.Org.Chem., 28, 2050 (1963a)
112. Lodge, J.P., The Smoake of London, Maxwell Reprint Co. (1969)
113. Loison, R. and Chauvin, R., Chem. Ind., 91(3), 269 (1964)
114. Longwell, J.P., 16th Symposium (International) Combustion, The Combustion Institute, Pittsburgh, 1 (1977)
115. Longwell, J.P., 19th Symposium (International) Combustion, The Combustion Institute, Pittsburgh (1982)
116. Macfarlane, J.J., Holderness, F.H. and Witcher, F.S.E., Comb. and Flame, 8, 215 (1964)
117. Marsh, H., Preprints Symposia, ACS, Div. Pet. Chem. Inc., 20, 389 (1975)
118. Mazumdar, B.K., Chakrabartty, S.K. and Lahiri, A., Fuel, 41, 129 (1962)
119. Mazumdar, B.K., Ganguly, S.K., Sanyal, P.K. and Lahiri, A., in Coal Science, Advances in Chemistry Series, 55, ACS (1966)

120. Michaud, F., Delfau, J.L. and Barassin, A., 18th Symposium (International) Combustion, The Combustion Institute, Pittsburgh, 443 (1981)
121. Miller, W.J. and Calcote, H.F., "Ionic Mechanisms of Carbon Formation in Flames", Presented at the Eastern Section of the Combustion Inst. Fall Meeting, UTRC, Conn. (1977)
122. Milliken, R.C., J. Phys. Chem., 66, 734 (1962)
123. Mitra, A., Shuck, R.D. and Sarofim, A.F., Centre for Health Effects of Fossil Fuels Utilization, 3rd Annual Report, Centre Grant No. 5 P30 ES02109-02, M.I.T. (1980)
124. Mitra, A., Nenniger, R.D. and Sarofim, A.F., Centre for Health Effects of Fossil Fuels Utilization, 3rd Annual Report, Centre Grant No. 5 P30 ES02109-03, M.I.T. (1981)
125. Mitra, A., Nenniger, R.D., and Sarofim, A.F., Centre for Health Effects of Fossil Fuels Utilization, 4th Annual Report, Centre Grant No. 5 P30 ES02109-04, M.I.T. (1982)
126. Mitra, A., Bar-Ziv, E. and Sarofim, A.F., "Evolution of Polycyclic Aromatic Hydrocarbons During the Pyrolysis of Coal", Presented at the 8th International Symposium on Polynuclear Aromatic Hydrocarbons, Battelle, Ohio, October (1983)
127. Nakanishi, K., Kadota, T. and Hiroyasu, H., Comb. and Flame, 40, 247 (1981)

128. NMS, "Particulate Polycyclic Organic Matter", National Academy of Sciences (1972)
129. Nenniger, J., "Polycyclic Aromatic Hydrocarbon Production in a Jet Stirred Combustor", Sc.D. Thesis, M.I.T. (1983)
130. Nenniger, R.D., Ph.D. Thesis, M.I.T. (1984)
131. Olson, D.B. and Calcote, H.F., 18th Symposium (International) Combustion, The Combustion Institute, Pittsburgh, 453 (1981)
132. Olson, D.B. and Calcote, H.F., "Ionic Mechanisms of Soot Formation in Pre-mixed Flames", Particulate Carbon Formation during Combustion, Plenum Press (1981a)
133. Oro, J. and Han, J., J.of Gas Chrom., 480 (1967)
134. Padia, A.S., "The Behaviour of Ash in Pulverized Coal under Simulated Combustion Conditions", Sc.D. Thesis, M.I.T. (1976)
135. Painter, P.C., Coleman, M.M., Jenkins, R.G. and Walker Jr., P.L., Fuel, 57, 124 (1978)
136. Palmer, H.B., Voet, A. and Lahaye, J., Carbon, 6, 65 (1968)
137. Parker, W.G. and Wolfhard, H.G., J. Chem. Soc., 2038 (1950)
138. Pasternak, M., Zinn, B.T. and Browner, R.F., 18th Symposium (International) Combustion, The Combustion Institute, Pittsburgh, 91 (1981)

139. Pasternak, M., Zinn, B.T. and Browner, R.F., Comb. Sc. and Tech., 28, 263 (1982)
140. Peters, J.A., Deangelis, D.G. and Hughes, F.W., "An Environmental Assessment of POM Emissions from Residential Wood Fired Stoves and Fireplaces", presented at the 5th International Symposium on Polynuclear Aromatic Hydrocarbons, Battelle, Ohio (1980)
141. Peters, W.A. and Penberthy, W.G., M.I.T. Energy Lab. In-house Report (1980)
142. Pines, A., Gibby, M.G. and Waugh, J.S., J. Chem. Phys., 59(2), 569 (1973)
143. Pines, A. and Wemmer, D.E., ACS Preprints, Div. of Fuel Chem., 23(2), 15 (1978)
144. Pott, P., London, Printed for L. Hawes, W. Clarke, and R. Collins (1775)
145. Prado, G., D.Sc. Thesis, Centre University, Haut Rhin and Louis Pasteur University, Strasbourg (1972)
146. Prado, G.P. and Howard, J.B., "Evaporation - Combustion of Fuels", J.T. Zung, ed., ACS, Advances in Chemistry Series 166, Wash., D.C., 153 (1978)
147. Prado, G., Jagoda, J., Neoh, K. and Lahaye, J., 18th Symposium (International) Combustion, The Combustion Institute, Pittsburgh, 1127 (1981)

148. Prado, G.F., Lee, M.L., Hites, R.A., Hoult, D.F. and Howard, J.B., 16th Symposium (International) Combustion, 649 (1977)
149. Ray, S.K. and Long, R., Comb. and Flame, 8, 139 (1964)
150. Ray, S.K. and Long, R., Comb. and Flame, 12(3), 226 (1968)
151. Reggel, L., Wender, I. and Raymond, R., Fuel, 47, 373 (1968)
152. Reidelbach, H. and Summerfield, M., ACS, Div. of Fuel Chem. Preprints, 20(1), 161 (1975)
153. Retcofsky, H.L., Stark, J.M. and Friedel, R.A., Anal. Chem., 40(11), 1699 (1968)
154. Santoro, R.J. and Glassman I., Comb. Sc. and Tech., 19, 161 (1979)
155. Sawicki, E., "Analysis for Airborne Particulate Hydrocarbons: Their relative proportions as affected by different types of pollution", Nat. Cancer Inst. Monograph, 9, 201 (1962)
156. Schalla, R.L. and Hubbard, R.R., NACA Report 1300 (1959)
157. Schalla, R.L. and McDonald, G.E., Ind. Eng. Chem., 45, No. 7, 1497 (1953)
158. Schalla, R.L. and McDonald, G.E., 5th Symposium (International) Combustion, Reinhold Publishing Co., N.Y., 316 (1955)
159. Schalla, R.L. and McDonald, G.E., 6th Symposium (International) Combustion, Reinhold Publishing Co., New York, 316 (1957)

160. Schug, K.P., Manheimer-Timnat, Y., Yaccarino, P. and Glassman I., Comb. Sc. and Tech., 22, 235 (1980)
161. Scully, D.B., and Davies, R.A., Comb. and Flame, 9, 185 (1965)
162. Shirmer, R.M., Proceedings of the Symp. on Emissions from Continuous Comb. Systems, GM Research Labs., Warren, MI., 189 (1971)
163. Sjogren, A., 14th Symposium (International) Combustion, The Combustion Institute, Pittsburgh, 919 (1973)
164. Skopek, T.R., Liber, H.L., Kaden, D.A., Hites, R.A. and Thilly, W.G., JNCL, 63(2), 309 (1979)
165. Smith, R.D., Comb. and Flame, 35, 179 (1979)
166. Smith, R.D., Comb. and Flame, 83, 1553 (1979a)
167. Smith, R.D., J. of Phys. Chem., 83, No.12, 1553 (1979b)
168. Smyth, K.C., Lias, S.G. and Ausloos, P., Comb. Sc. and Tech., 28, 147 (1982)
169. Solomon, P.R., ACS Div. of Fuel Chem., Preprints, 24(2), 184 (1979)
170. Solomon, P.R., "Characterization of Coal and Coal Thermal Decomposition", Ch.3 in Pulverized Coal Combustion: Pollutant Formation and Control to be published by EPA (1984)

171. Solomon, P.R. and Hamblen, D.G., "Understanding Coal using Thermal Decomposition and Fourier Transform Infrared Spectroscopy", Presented at the Conference on the Chemistry and Physics of Coal Utilization, Morgantown, W.Va., June (1980)
172. Speight, J.G., Applied Spectros. Reviews, 2(2), 211 (1971)
173. Sprouse, K.M. and Schuman, M.D., Comb. and Flame, 42, 265 (1981)
174. Stehling, F.C., Frazee, J.D. and Anderson, R.C., 6th Symposium (International) Combustion, Reinhold Publishing Co., New York, 247 (1957)
175. Stehling, F.C., Frazee, J.D. and Anderson, R.C., 8th Symposium (International) Combustion, Williams and Wilkins Co., Baltimore, 774 (1962)
176. Stein, S.E., J. of Phys. Chem., 82, No.5, 566 (1978)
177. Stein, S.E., Golden, D.M. and Benson, S.W., J. of Physical Chem., 81, 4, 314 (1977)
178. Street, J.C. and Thomas, A., Fuel, 34, 4 (1955)
179. Suuberg, E.M., "Rapid Pyrolysis and Hydrolysis of Coal", Sc.D. Thesis, M.I.T. (1977)
180. Suuberg, E.M., Peters W.A. and Howard, J.B., Symp. on Thermal Hydrocarbon Chemistry, Divns. of Petroleum Chem. and Fuel Chem., A.C.S., Anaheim, CA March (1978)

181. Thiessen, R., Coal Age, 18, 1183-89, 1223-28, 1275-79 (1920)
182. Thiessen, R., Sprunk, G.C. and O'Dourell, H.J., U.S. Bur. Mines Inf. Circ., 7021, pp. 1-8 (1938)
183. Thomas, A., Comb. and Flame, 6, 46 (1965)
184. Thorp, N., Long, R. and Garner, P.H., Fuel, 30, 266 (1951)
185. Tompkins, E.E. and Long, R., 12th Symposium (International) Combustion, The Combustion Institute, Pittsburgh, 625 (1969)
186. Tsai, S.C., "Chemical Structure and Chemical Reactions of Coal," Ch.2 in Fundamentals of Coal Benefication and Utilization (1982)
187. Tschamler, H. and deRuiter, E., Brennstoff-Chemie, 43, 16 (1962)
188. Van Krevelen, D.W., Coal, Elsevier Publishing Co., Amsterdam (1961)
189. Van Krevelen, D.W., Fuel, 42, 427 (1963)
190. Vranos, A. and Liscinsky, D.S., to be published in Comb. Sc. and Tech. (1983)
191. Wagner, H.GG., 17th Symposium (International) Combustion, The Combustion Institute, Pittsburgh, 3 (1979)

192. Wang, T.S., Matula, R.A. and Farmer, R.C., 18th Symposium (International) Combustion, The Combustion Institute, Pittsburgh, 1149 (1981)
193. Wen, C.Y. and Chen, L.H., "A Model for Coal Pyrolysis", Presented at ACS National Meeting, Washington, D.C. Sept. 9-14 (1979).
194. Wender, I., ACS Div. Fuel Chem. Prepr., 20(4), 16 (1975)
195. Wender, I., Heredy, L.A., Neuworth, M.B. and Dryden, I.G.C., "Chemical Reactions and the Constitution of Coal", Ch. 8 of Chemistry of Coal Utilization, 2nd Supplementary Volume, ed. M.A. Elliott, John Wiley & Sons, New York, (1981)
196. Wersborg, B.L., Howard, J.B. and Williams, G.C., 14th Symposium (International) Combustion, The Combustion Institute, Pittsburgh, 929 (1973)
197. Wersborg, B.L., Yeung, A.C. and Howard, J.B., 15th Symposium (International) Combustion, The Combustion Institute, Pittsburgh, 1439 (1975)
198. Wiser, W.H., in Wolk, R.H., Stewart, N.C. and Silver, H.F., ACS, Div. Fuel Chem. Prepr., 20(2), 116 (1975)
199. Wornat, J., Personal Communication (1984)
200. Wright, F.J., 12th Symposium (International) Combustion, The Combustion Institute, Pittsburgh, 867 (1969)

201. Wright, F.J., Comb. and Flame, 15, 217 (1970)

202. Wright, F.J., 15th Symposium (International) Combustion,
The Combustion Institute, Pittsburgh, 1449 (1975)

203. Yokono, T., Miyazawa, K, Sanada, Y. and Marsh, H.,
Fuel, 58, 692 (1979)

204. Zaghini, N., Mangolini, S., Cornetti, G., Salvatori, T.
and Rizzi, G., Comb. Sc. and Tech., 5, 225 (1972)

205. Zelenski, S.G., Pangaro, N. and Hall-Enos, J.M.,
"Inventory of Organic Emissions from Fossil Fuel
Combustion for Power Generation", EPRI EA-1594/TPS
78-820 (1980)

206. Zilm, K.W., Pugmire, R.J., Grant, O.M., Wood, R.E. and
Wiser, W.H., Fuel, 58, 1 (1979)